The University Of Sheffield.

NEUROANATOMICAL EVALUATION OF THE OUTCOME OF PERIPHERAL NERVE REPAIR USING 3D PRINTED BIODEGRADABLE CONDUITS

By

Emad Ali Albadawi

Academic Unit of Oral and Maxillofacial Medicine and Surgery,
School of Clinical Dentistry,
Claremont Crescent,
Sheffield, S10 2TA, UK

A thesis submitted to the Faculty of Medicine, Dentistry and Health of the University of Sheffield for the degree of Doctor of Philosophy

January 2018

DECLARATION

I hereby declare that this thesis entitled ‘‘Neuroanatomical Evaluation of the Outcome of Peripheral Nerve Repair Using 3D Printed Biodegradable Conduits’’ has been composed by myself and has not been submitted to any other university or institute for any degree. The work reported in this thesis has been done by myself and all sources of information have been particularly acknowledged by means of references.

EMAD ALBADAWI

SUMMARY

Peripheral nerve injuries are commonly seen in society, and are often associated with loss of function and development of neuropathic pain. Enhancing nerve regeneration following injury is challenging, especially if damage to the nerve results in tissue loss. The overcome aim of this study is to investigate the ability of different nerve conduit designs to support nerve regeneration, and assess their potential to influence the development of neuropathic pain.

This literature review gives an overview of the peripheral nervous system including the anatomical features of nerves, classification of injuries, and events and processes occur during nerve regeneration after injury. Moreover, it highlights the current strategies and methods to repair injured peripheral nerves, particularly the role of using nerve conduits. It also briefly describes neuropathic pain, including the pathophysiology that is involved in nerve injury-induced neuropathic pain, particularly in relation to glial cells. Finally, it mentions some strategies for improving peripheral nerve regeneration.

This thesis describes an initial study that focused on developing a methodology to quantify spinal glial activation following nerve/conduit repair, this activation is strongly associated with the development of neuropathic pain. Using common fibular and sciatic nerve repair models in *thy-1-YFP-H* mice, several designs of potential nerve conduit were evaluated; Nylon, polycaprolactone (PCL) and polyglycerol sebacate (PGS).

Some approaches to enhance the level of regeneration were mentioned in this thesis. Mannose-6-Phosphate (M6P), a potential scar-reducing agent, was evaluated as it has a role in reducing the amount of intra-neural scarring by inhibition of latent TGF-β activation. Etanercept (a decoy receptor for tumour necrosis factor-alpha) was also investigated as it has a role in reducing the inflammation and scarring at the site of injury which results in enhancing the regeneration.

A novel method to investigate the functional recovery of injured nerves using genetically modified mice with fluorescent axons has recently been developed in our laboratory, this method will be used in this thesis, and is also described.

ABSTRACT

Introduction: Nerve guide conduits are an alternative to autografts for peripheral nerve repair. Many studies have investigated the ability of conduits to support regeneration; however, their likely impact on neuropathic pain has not been investigated. Spinal glial activation has been reported as a key regulator of neuropathic pain and could reveal important differences in potential neuropathic pain development between novel conduit designs. The materials and methods used in producing nerve conduits influence the potential for nerve regeneration following repair.

Aims: The overall aim was to investigate the effect of applying different conduit designs, M6P and Etanercept on nerve regeneration and spinal glial activation following nerve repair.

Methods: The common fibular or sciatic nerve of *thy-1-YFP-H* mice was transected, and a 3.0mm (common fibular) or 4.0mm (sciatic) gap was repaired using conduits made from nylon, PCL (with or without Etanercept) or PGS, or a nerve graft (with or without M6P). The nerve ends and graft/conduit were aligned and secured using fibrin glue. After 2, 3 or 5 weeks, spinal cords were harvested and prepared for immunohistochemistry to label microglia and astrocytes. The nerves also were harvested for analysis. Electrophysiology and CatWalk gait were performed in the sciatic repair model.

Results: Nylon conduit repairs produced high levels of glial activation and low levels of nerve regeneration, while grooved PCL conduit repairs produced low glial activation and better levels of nerve regeneration (Chapter 3). No significant differences were observed when using M6P incorporated within fibrin glue [Chapter 4]. PCL conduit plus Etanercept repairs produced significantly lower glial activation in the spinal dorsal horn, improved regeneration (as indicated by CatWalk analysis) and lower axon disruption compared to the PCL conduit repair plus vehicle [Chapter 5]. Although similar levels of glial activation was observed following repair with PGS conduit and nerve graft, PGS repair was inferior to nerve graft in overall nerve regeneration [Chapter 6].

Conclusion: Better nerve regeneration after repair reduces glial activation that may help to reduce the potential development of neuropathic pain. PCL conduits appear to elicit the best response in terms of improve nerved regeneration and reduced glial activation while nylon conduits appear less suitable. Etanercept appears to evoke reduced microglial activation, which may decrease neuropathic pain development; and enhances functional recovery of the nerve. PGS conduits may provide an alternative repair method to nerve graft repair, in terms of the likelihood of neuropathic pain development following repair. Further investigation may be warranted in order to optimise dosage, administration route of M6P and determine any effect.

ACKNOWLEDGEMENTS

Lots of people, both professionally and personally, should to be mentioned for their supports which made this thesis comes into being. Listing each person and their assistance would require an acknowledgements chapter; so for those of you who do not get a particular mention here, I apologize and thank you for your assistance.

Amongst my colleagues I must thank my supervisor, Professor Fiona Boissonade, for the aspiring guidance, advice and encouragement she has provided throughout my PhD journey. I have been extremely lucky to have a supervisor who cared so much about my work, and who responded to my queries and questions so promptly. I sincerely thank, Dr. Adam Harding, for teaching me the technical skills related to the surgeries, axon analysis and the usage of the fluorescent microscope. I am indebted to Dr. Mario Vettore, Dr. Emma Bird, Dr. Simon Atkins, Dr. Hisham Shembesh, Dr. Matthew Worsley, Dr. Claire Morgan and Mrs. Susan Spriggs for their unlimited supports. In particular, Dr. Milena De Felice, for sharing her skill and knowledge on the use of the CatWalk system. Also, Dr. Nicola Green for teaching me the usage of the confocal microscope. I would like to thank, Professor John Haycock, Dr. Frederik Claeyssens and their research groups for their assistance. Specifically, Jonathan Field and Dharaminder Singh for their work on the artificial nerve guide conduits discussed in chapters 5 and 6 of this thesis.

On a personal note, I would like to thank my parents, Ali Albadawi and Safiah Aljuhani, who have constantly prayed to Allah for my success and have forgiven my shortcomings towards them during my study. I could not have achieved this without their help and encouragement. My older brother, Eng. Mohammed Albadawi, should be mentioned for consistently driving me to endeavor to prove I am the best person in the family. Also grateful thanks to, Professor Mahroos Alghabban, for his ultimate support, things get a lot easier by having him beside me. And definitely I would not have made it without the understanding and love of my two children, Rose and Yazan. Most importantly, I must express my gratitude to my beloved wife, Dr. Hadel Ghaban, who has supported me during my educational journey, shared my intellect and hopes, lived my suffering and accompanied me in a strange land. This work would not have been possible without her presence in my life.

I would like to thank Saudi Arabia Ministry of Higher Education for funding this thesis. Finally, and most of all, I am extremely grateful to Allah without whom nothing is possible.

PUBLICATION AND PRESENTATIONS

The following paper has been submitted for publication:

Dharaminder Singh, Adam Harding, **Emad Albadawi**, Fiona Boissonade, JohnHaycock, Frederik Claeyssens**. In vivo investigation of Additive Manufactured Biodegradable Poly (glycerol sebacate methacrylate) (PGSm) Nerve Guidance Conduits.**

The following communications have been presented at meetings of scientific societies**:**

Emad Albadawi, Adam Harding, Frederik Claeyssens, Neil Hopkinson, John Haycock and Fiona Boissonade. **The Influence of novel nerve conduit design on development of neuropathic pain following nerve repair**. poster presentation at 5th International Congress on Neuropathic Pain; Nice, France. May 2015.

Emad Albadawi, Adam Harding, Frederik Claeyssens, Neil Hopkinson, John Haycock and Fiona Boissonade. **The Influence of novel nerve conduit design on development of neuropathic pain following nerve repair**. poster presentation at the ABAOMS conference; Sheffield, UK. November 2015.

Emad Albadawi, Adam Harding, Frederik Claeyssens, Neil Hopkinson, John Haycock and Fiona Boissonade. **A Comparison between the influence of three nerve conduit designs on development of neuropathic pain following common-fibula nerve repair**. Poster presentation at the 9th Saudi Students Conference, Birmingham. UK. February 2016.

Emad Albadawi, Adam Harding, and Fiona Boissonade**. The Effects of Mannose-6-Phosphate on development of neuropathic pain following nerve repair.** poster presentation at the 16th World Congress on Pain; Yokohama, Japan, September 2016.

Emad Albadawi, Adam Harding, Frederik Claeyssens, Neil Hopkinson, John Haycock and Fiona Boissonade. **A Comparison between the influence of three nerve conduit designs on development of neuropathic pain following common-fibula nerve repair**. poster presentation at the sheffield Pain Network meeting; Sheffield, UK. May 2016.

Dharaminder Singh, Adam Harding, Emad **Albadawi**, Fiona Boissonade, JohnHaycock, Frederik Claeyssens. **Novel PGSm nerve guidance conduits for peripheral nerve repair in vivo**. Oral presentation at the Tissue and Cell Engineering Society Annual Conference; London, UK, July 2016.

Emad Albadawi, Adam Harding, and Fiona Boissonade. **The Effects of Mannose-6-Phosphate on development of neuropathic pain following nerve repair.** Oral presentation at the Glial Symposium; Sheffield, UK, November 2016.

Dharaminder Singh, Adam Harding, **Emad Albadawi**, Fiona Boissonade, John Haycock, Frederik Claeyssens. **In vivo implantation of novel PGSm 3D printed NGCs for nerve repair**. Poster presentation at the TERMIS-America conference, San Diego, USA, December 2016.

Emad Albadawi, Adam Harding, Dharaminder Singh, Frederik Claeyssens, John Haycock and Fiona Boissonade. **Glial activation following nerve repair with novel 3D-printed poly-glycerol sebacate conduits versus nerve grafts.** Poster presentation at the Challenge of Chronic Pain conference, Cambridge, UK, March 2017.

Emad Albadawi, Adam Harding and Fiona Boissonade. **Glial activation following nerve graft repair and local administration of Mannose-6-phosphate.** Poster presentation at the BNA2017: Festival of Neuroscuence; Birmingham, UK, April 2017.

Dharaminder Singh, Adam Harding, **Emad Albadawi**, Fiona Boissonade, JohnHaycock, Frederik Claeyssens. **In vitro, ex vitro and in vivo analysis of novel 3D printed PGSm nerve conduits**. Poster presentation at the TERMIS-EU conference, Davos, Switzerland, June 2017.

Emad Albadawi, Adam Harding, Dharaminder Singh, Frederik Claeyssens, John Haycock and Fiona Boissonade. **Glial activation following nerve repair with novel 3D-printed poly-glycerol sebacate conduits versus nerve grafts.** Poster presentation at the Sheffield Neuroscience, Sheffield, UK, July 2017.

Emad Albadawi, Hisham Shembesh, Adam Harding, Jonathan Field, Simon Atkins, Emma Bird, Frederik Claeyssens, John Haycock and Fiona Boissonade.**The effect of Local administration of Etanercept on nerve regeneration Following Poly-caprolactone Conduits Repair.** Poster presentation at the 3rd Annual Neuroscience R&D Technologies Conference, London, UK, September 2017.

TABLE OF CONTENTS

LIST OF FIGURES

LIST OF TABLES

CHAPTER 1

LITERATURE REVIEW

ABBREVIATIONS

µSL	Micro-Stereolithography
ANOVA	Analysis of variance
BDNF	Brain-derived neurotropic factor
CAMS	Cell adhesion molecules
CAP	Compound action potential
CCI	Chronic constriction injury
CCL2	Chemokine (C-C motif) ligand 2
CD 14	Cluster of differentiation 14
CD-M6PR	Cation-dependent MPR
CF nerve	Common fibular nerve
CGRP	Calcitonin-gen related peptide
CNS	Central nervous system
CSPGs	Chondroitin sulphate proteoglycans
CV	Conduction velocities
Cy3	Cyanine dyes 3
DMD	Digital Micro-mirror Device
DPCs	Dental pulp cells
DRG	Dorsal root ganglions
FB	Fibroblasts
FDA	Food and drug administration
GABA	Gamma-aminobutyric acid
GAG	Sulphated glycosaminoglycan
GC	Growth cone
GFAP	Glial fibrillary acidic protein
GFAP	Glial fibrillary acidic protein
GFP	Green fluorescent protein
G-PCL	Grooved poly-caprolactone
IASP	International Association for the Study of pain
Iba1	Ionized calcium binding adaptor molecule 1
IFN	Interferon ɣ
IGF-II	Insulin-like growth factor-II
IL-1	Interleukin-1
ip	Intraperitoneally
LAP	Latency-associated protein
LN	Lymph node
M6P	Mannose-6-Phosphate
MAG	Myelin-associated glycoprotein
MAPK	Mitogen-activated protein kinase
MC	Mast cells
mGluR	Metabotropic glutamate receptor
NA	Neutralising antibody
NDS	Normal Donkey serum
NF-ƘB	Nuclear factor-ƘB
NGC	Nerve guide conduit

NGF	Nerve growth factor
NMDA	N-methyl-D-aspartate
NO	Nitric oxide
NP-PGS	Non-porous PGS
Nylon NGC	3D Printed nylon conduit
O Mgp	Oligodendrocyte myelin glycoprotein
OCT	Optimal Cutting Temperature compound
PBS	Phosphate Buffer Saline
PBS-T	Phosphate Buffer Saline-Triton
PCL	Poly-caprolactone
PGS	Poly-ethylene glycol
PGA	Poly glycolic acid polymer
PGS	Polyglycerol Sebecate
PGSm	Poly-Glycerol Sebacate methacrylate
PK	Protein kinase
PLCL	Poly actide-carpolactone polymer
PLGA	Poly-DL-lactide-co-glycolide
PLLA	Poly (L-lactic acid*)*
PNI	Peripheral nerve injury
PNS	Peripheral nervous system
P-PGS	Porous PGS
PSCL	Partial spinal cord ligation
PSNL	Partial sciatic nerve ligation
RFP	Red fluorescent protein
ROS	Reactive oxygen species
SC	Subcutaneously
SCS	Spinal cord stimulation
SD	Standard deviation
SEM	Standard error of the mean
SIS	Small intestinal submucosa
SLS	Selective laser sintering
SNI	Spared nerve injury
S-PCL	Smooth poly-caprolactone
TGF-β	Transforming growth factor *beta*
TNF-α	Tumour necrosis factor alpha
TTX-R	Tetrodotoxin resistance
TTX-S	Tetrodotoxin sensitive
UV	Ultraviolet
VEGF	Vascular endothelial growth factor
WT	Wild-type
YFP	Yellow fluorescent protein

1.1 INTRODUCTION

Peripheral nerve injury (PNI) is a historical problem. 3500 years ago, PNI was reported in the Bible, when the Biblical patriarch Jacob fought with the angel. During the battle, he appears to suffer from a neurological injury to the sciatic nerve with a temporal limping gait caused by a traumatic hip dislocation. It is suggested that Jacob suffered from a type of peripheral nerve injury called neurapraxia (section 1.3.1.1). Although there were neither radiographs nor pathological specimens at that time, the suggestion is based on the description of Jacob's injury in the original Hebrew text found in the book of Genesis in the Bible (Chapter 32:25-33) (Cornwall and Radomisli, 2000, Hoenig, 1997).

Peripheral nerve injury is common across society. In Europe, it has been reported that over 300,000 patients per annum suffer from such injuries each year, and approximately 200,000 surgical nerve repairs are performed per annum in the United States (Gaudin, 2016, Ichihara et al., 2008). Thirty percent of war injuries are associated with peripheral nerve injuries. It has been reported that blast injuries caused by shrapnel are the most common cause of peripheral nerve injury in wars (Campbell, 2008, Maricevic and Erceg, 1997). During the American Civil War, S. Weir Mitchell, a neurologist, was the first person to study PNIs systematically (Zuniga and Radwan, 2013). War injuries and the physicians who treated the soldiers greatly enhanced our understanding of peripheral nerve injuries, due to the high incidence of these injuries during battle (Roganovic and Petkovic, 2004, Seddon, 1943).

In everyday life PNIs are caused mainly by traumatic accidents, but can also occur as a side effect of surgical procedures (Atkins et al., 2006a, Ichihara et al., 2008). The most common types of PNI include crush, traction, ischemia, and penetrating injury; less common causes include trauma from electrical shock, percussion, radiation, vibration and thermal injury (Campbell, 2008, Robinson, 2000, Robinson, 2004).

The upper extremities are more likely to be affected than the lower extremities (Robinson, 2000). The majority of nerve injuries in the upper limbs involve the radial

nerve, with injuries to the ulnar and median nerves also common. In lower limb injuries, the sciatic nerve is the most commonly affected nerve, followed by the common fibular and then the tibial or femoral nerves (Robinson, 2000). In a 16-year retrospective study on 557 PNIs, Kouyoumdjian (2006) reported that injuries of the upper limbs accounted for 73.5% of cases, and the ulnar nerve injuries were presented among all, either alone or in combination with the median nerve (Kouyoumdjian, 2006). Nobel et al. (1998) reported that out of 200 peripheral nerve injuries, 121 were in the upper extremity. Also they reported that radial nerve was the most frequently injured (58 injuries), while common fibular nerve was the most commonly injured (29 injuries) in lower extremity (Nobel et al., 1998).

Most peripheral nerve injuries (especially in nerves supplying the upper limbs) have a large effect on the quality of the patients' life (Bailey, 2009). There is a major impact on the physical and psychological qualities of patients' lives due to chronic pain, problems carrying out daily activities, substantial long-term disability, or dependence on others for assistance. In addition, these injuries increase the chance of clinical depression or post-traumatic stress) (Aktins et al., 2006, Baily, 2009).

The sequence of regeneration of PNIs has been extensively studied in a large number of laboratory investigations. This has furthered our understanding and allowed some enhancement to the level of recovery (Aktins et al., 2006b). However, the outcomes following nerve repair are far from perfect, even with advanced technology in neurosurgical instrumentation, and use of surgical microscopes and diagnostic imaging in the management of transected peripheral nerves (Artico, 1996, Robinson, 2000).

1.2 ANATOMICAL FEATURES OF PERIPHERAL NERVES

To better classify and treat nerve injuries, it is important to understand the anatomy and structure of the nervous system. Unlike many cells in the body adult neurones cannot replicate, making them unique (Heath and Rutkowski, 1998, Osbourne, 2007). The nervous system is divided into two components, central and peripheral, which differ in function and physiology. The peripheral nervous system (PNS) receives information

coming from the external environment and carries signals to and from the spinal cord and then to the brain via central nervous system (CNS) (Heath and Rutkowski, 1998). The spinal and cranial nerves form the PNS. The spinal nerves consist of 31 pairs, and the cranial nerves of 12 pairs (Osbourne, 2007). All the spinal nerves are mixed in function, which means they include both sensory (afferent) and motor (efferent) fibres, while some of the cranial nerves have both sensory and motor fibres others have either pure sensory or motor fibres (Heath and Rutkowski, 1998, Osbourne, 2007).

1.2.1 Microstructure of Peripheral Nerves

Description of internal structures of peripheral nerves has been widely reported in a large number of publications dating back to 1945 (Sunderland, 1973). A cross-sectional diagram of the peripheral nerve is very useful to distinguish and illustrate the components of a nerve. The peripheral nerve is formed of connective tissue and neural and glial components (neurones and Schwann cells). The connective tissue consists of outer, medial and inner layers; epineurium, perineum and endoneurium, consecutively (Dagum, 1998, Flores et al., 2000, Sunderland et al., 1990). Generally, these layers form the framework of the nerve, and play an essential role in organisation and protection of the nerve fibres and axons (Figure 1.1) (Dagum, 1998, Flores et al., 2000, Weber and Dellon, 2004).

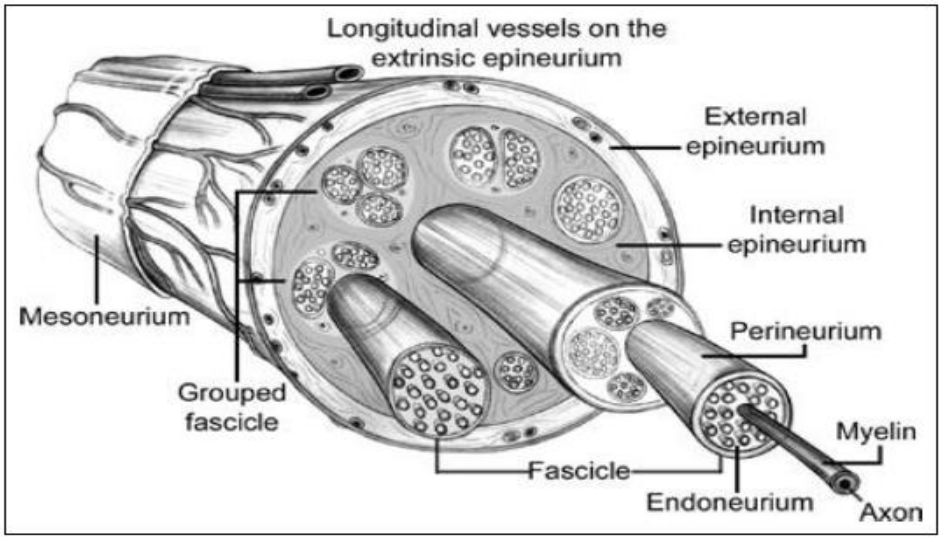

Figure 1.1: A cross-section diagram showing the structures of a nerve; epineurium, perineum, endoneurium, Schwann cells and axon (Weber and Dellon, 2004).

1.2.1.1 Epineurium

The epineurium is a connective tissue, which forms the outer (covering) layer of the nerve. It is divided into two parts; external and internal epineurium (Figure 1.1). The external part is tougher than the internal. The thickness of the epineurial tissue varies from nerve to nerve and even in some regions of the same nerve (Dagum, 1998, Sunderland, 1973). It makes up approximately 30-75% of the total nerve area, and is mainly composed of type 1 collagen and elastic fibres (Flores et al., 2000, Zochodne, 2008). This layer plays a critical role in the protection of the fascicles.

1.2.1.2 Perineurium and Endoneurium

The perineurium is a thin, dense, fibrous, multi-layered, strong sheath made up of collagen and elastic fibres. It forms the middle layer of the nerve (Figure 1) (Dagum 1998, Flores et al., 2000). Two or more fascicles form a fascicular group which is surrounded by the perineurium. A pseudo-intraneural plexus (known as the plexus of Sunderland) is formed from the interconnecting of these individual fascicles (Dagum, 1998, Sunderland, 1973). The perineurium plays an important role in preserving the intrafascicular pressure. The endoneurium (also named endoneurial tube, endoneurial sheath, endoneurial channel or Henle's sheath) is a layer of connective tissue surrounding the myelin sheath of each myelinated nerve fiber (Dagum, 1998, Flores et al., 2000). In the endoneurial microvessels, the endothelial cells act with the perineurium as the blood-nerve barrier, which in turn helps to control the local environment of the endoneurial space (Dagum, 1998, Geuna et al., 2009, Sunderland, 1973). In addition, the perineurium also helps to prevent infections from spreading into the nerve fibres (Flores et al., 2000).

1.2.1.3 Nerve Fibres

The smallest functional unit of a nerve is a nerve fibre (axon). Any major peripheral nerve trunk has larger myelinated axons (α motor and Aα sensory axons), small myelinated axons (Aβ and Aδ sensory axons and γ motor axons) and unmyelinated axons (C sensory and autonomic axons) (Zochodne, 2008). Myelination is the formation

of a fatty layer by Schwann cells that isolates the axon and allows salutatory conduction in a nerve. A Schwann cell is a type of glial cell found in the peripheral nervous system, and supports all types of axon (Zochodne, 2008). From the embryological aspect, Schwann cells are derived from neural crest cells (Bhatheia and Field, 2006). Myelinated fibres are composed of a single axon surrounded by a number of Schwann cells and their associated myelin sheaths. The gap between Schwann cells is called the node of Ranvier, in this region the axon is not myelinated (Flores et al., 2000). Unmyelinated fibres are grouped together in units containing a number of nerve axons surrounded by a number of Schwann cells. The Schwann cells isolate these axons by a layer of cytoplasm forming a structure named a Remak bundle (Flores et al., 2000, Geuna et al., 2009).

1.3 CLASSIFICATION OF PERIPHERAL NERVE INJURIES

The classification of peripheral nerve injuries assists clinicians to grade the severity and degree of the injury. This, in turn, helps in the choice of treatment and informs the prognosis (Dagum, 1998, Osbourne, 2007). Currently, the two classifications that are used widely are those described by H. J. Seddon and S. Sunderland. Both these classifications are based on the degree of the injury and not on the injury's cause (as the same agent can cause any type of nerve injury) (Sunderland, 1973, Sunderland et al., 1990).

1.3.1 Seddon's Classification

In 1943, the first classification of nerve injuries was described and published by Herbert Seddon. His classification includes three broad categories of nerve injury based on severity; neurapraxia, axonotmesis and neurotmesis (Burnet and Zager, 2004, Zuniga and Radwan, 2013). In general, the three categories were inserted to cover conduction block (neurapraxia), loss of axon continuity (axonotmesis), and loss of the continuity of nerve trunk (neurotmesis) (Sunderland et al., 1990). The full details of this classification are found in Seddon's publication; however, here are some essential descriptions of these three terms of injury.

1.3.1.1 Neurapraxia

Neurapraxia (not neuropraxia) is the mildest injury category in this classification (praxia= to do) (Campbell, 2008, Osbourne, 2007, Seddon, 1943, Sunderland, 1973). This type of injury is characterised by interruption of the conduction in the axon at the injury site, while axon continuity remains intact. Although the axon remains undamaged, segmental demyelination may be present (Figure 1.2) (Dagum, 1998, Osbourne, 2007, Sunderland, 1973, Zuniga and Radwan, 2013). Acute compression is the major cause of this injury, for example, Saturday night palsy, carpal tunnel syndrome and crutch palsy. Some patients with this injury complain of paralysis due to losing motor and sensory functions of the nerve. In this category of injury, recovery is spontaneous, complete and very rapid, and there is no Wallerian degeneration (Section 1.5.1) after the injury, unlike in the other two categories (Dagum, 1998, Osbourne, 2007, Seddon, 1943, Sunderland 1973). Full recovery can take up to 12 weeks (Dagum, 1998).

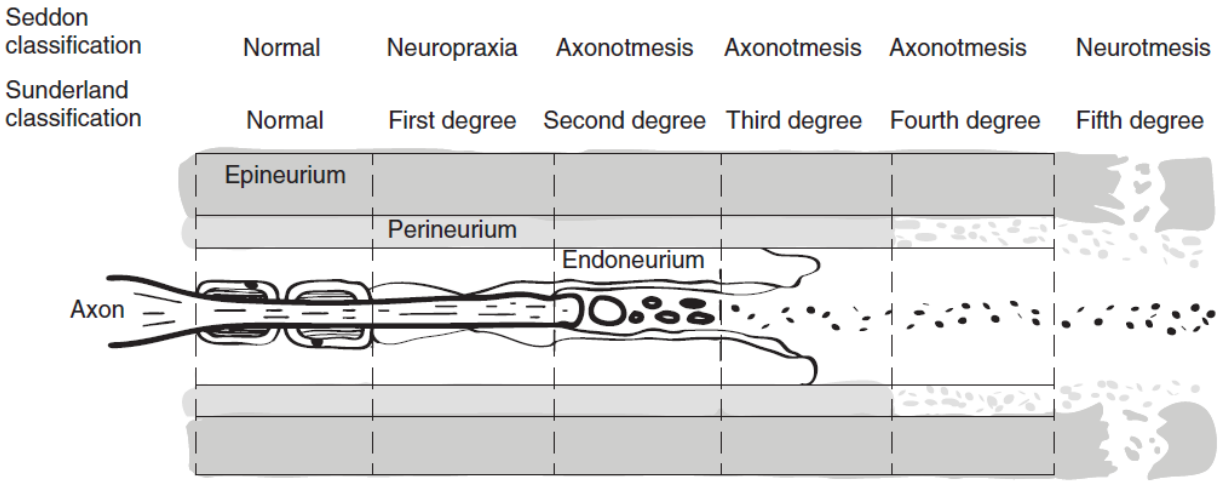

Figure 1.2: Scheme illustrates the categories of nerve injury in Seddon and Suderland classifications (Zuniga and Radwan, 2013, pp.18).

1.3.1.2 Axonotmesis

A more severe category in the Seddon's classification is called axonotmesis (tmesis= to cut). In this category, the nerve axon is completely interrupted as well as its myelin

sheath, while the supporting structures are preserved (helping the nerve to recover) (Figure 1.2) (Campbell, 2008, Dagum, 1998, Seddon, 1943, Sunderland, 1973, Zuniga and Radwan, 2013). An example of this category of injury is birth-related brachial plexus injury, and the major causes of this category are stretch, crush and percussion injuries (Osbourne, 2007, Robinson, 2000, Seddon, 1943). Clinically, the recovery process is the only point that can distinguish this type from neurotmesis, because in axonotmesis it is a spontaneous process (Sunderland, 1973). The prognosis of axonotmesis depends on the severity of the injury (Osbourne, 2007).

1.3.1.3 Neurotmesis

The most severe category in Seddon's classification is neurotmesis. In this type of injury all the essential structures of the nerve are severely damaged and disconnected, which means the two ends of the nerve (proximal and distal) are no longer connected (Figure 1.2) (Burnett and Zager, 2004, Dagum, 1998, Osbourne, 2007, Sunderland, 1973, Zuniga and Radwan, 2013). This results in the total loss of sensory, motor, and sympathetic functions. The most common causes in this category are sharp, percussion, or traction injuries. Spontaneous recovery is unlikely and the prognosis is very poor without surgical intervention. The level of functional recovery is increased by re-connecting the two ends; however, the outcome may still be poor (Dagum, 1998, Robinson, 2000, Seddon, 1943, Sunderland, 1973,).

Although Seddon's classification greatly clarifies nerve injuries and it is used more than Sunderland's in a clinical setting, it has some limitations (Osbourne, 2007, Sunderland, 1973). An example of these limitations is using some Greek language, which makes it hard to remember. Another limitation is the gap between axonotmesis and neurotmesis, as he defined axonotmesis as a lesion in which only the axon and its myelin sheath are completely interrupted while neurotmesis is a lesion in which the entire nerve is completely disconnected. So, he did not classify whether the perineurium and endoneurium layers are both intact or if only one or neither of them is intact, and these factors influence the prognosis (Sunderland 1973).

1.3.2 Sunderland's Classification

Due to the aforementioned limitations, in 1952, S. Sunderland decided to expand Seddon's classification based on changes in the nerve's normal anatomy. This classification is formed of five different degrees of nerve injuries arranging from lowest to highest severity. According to Seddon's classification, neurapraxia is essentially equivalent to 1st degree injury, axonotmesis corresponds to 2nd, 3rd and 4th degrees injury (with the difference in the severity determined by the level of mesenchymal damage and the recovery process), while neurotmesis is equivalent to 5th degree injury (Dagum, 1998, Osbourne, 2007, Sunderland, 1973, Sunderland et al., 1990).

1.3.2.1 First-degree Injury

In 1876, Erb described the first-degree injury as 'intermediate form', this was followed by Seddon in 1943 describing it as neurapraxia (Section 1.3.1.1) (Seddon, 1943, Sunderland, 1973).

1.3.2.2 Second-degree Injury

In this type of injury, the axon is severed, and the continuity is compromised due to disorganisation of the axonal mechanisms, causing the distal part to fail to survive. The endoneurium surrounding the axon is preserved as well as the axon's general arrangement (Figure 1.2). In the distal component, Wallerian degeneration (Section 1.5.1) occurs due to loss of axon continuity and damage to the axonal myelin sheath. The recovery time for this type of injury is longer than for first degree and may lead to signs of atrophy in the muscle supplied by the affected nerve. However, overall recovery seems to be good as the axon is confined inside its original endoneurial tube, which allows the axon to reach the end-organ that was originally innervated by it (Sunderland, 1973).

1.3.2.3 Third-degree Injury

The essential change in the 3rd degree injury is disorganisation of the internal components of fascicles (loss of the endoneurial tube continuity), in addition to the presence of Wallerian degeneration and axonal disintegration (Figure 1.2) (Section 1.5) (Sunderland, 1973, Zuniga and Radwan, 2013). Although the perineurium is preserved and the general arrangement of the fascicle is retained, loss of endoneurial tube continuity leads to the axon being no longer confined inside its original endoneurial tube. This leads to a greater chance that the regenerating axon to enter an incorrect endoneurial tube or to fail reaches one at all, which in turn results in an increase in the recovery time and makes the recovery functionally worse than the 2nd degree (Sunderland, 1973). Loss of motor or sensory function, distributed or in a localised area depends on the type of affected axon and level of severity (i.e. intra- fascicular damage including all the fascicles leads to complete loss of motor and sensory in area that supplied by the nerve, while in partial lesions the defect ranges from localised paralysis or sensory impairment, caused by affected axons within the fascicles responsible for motor or sensory function, respectively) (Sunderland, 1973).

1.3.2.4 Fourth-degree Injury

In 4th degree injury, the entire perineurium and fascicle continuity is affected (Figure 1.2). Although the nerve trunk continuity remains intact, the involved section is transformed into a strand of tissue formed of connective tissue, regenerating axons and Schwann cells, which in turn may enlarge and distribute to form a neuroma (Sunderland 1973). The Wallerian degeneration in 4th degree is the same of that recorded in 2nd and 3rd degree; however, the regeneration is more complicated. Spontaneous recovery may occur; however, excision of the affected segment and surgical repair are highly recommended for a better outcome (Dagum, 1998, Sunderland, 1973).

1.3.2.5 Fifth-degree Injury

A 5th degree nerve injury is equal to the most severe injury type in the Seddon's classification, neurotmesis (Section 1.3.1.3).

The two classification systems are briefly summarised in Table 1.1 (Robinson, 2000).

Table 1.1: Classification systems of peripheral nerve injury (Modified from Robinson, 2000, pp. 864).

Seddon classification	Sunderland classification	Pathology	Prognosis
Neurapraxia	**First degree**	Myelin injury or ischemia	Excellent recovery in weeks to months
Axonotmesis		Axon loss Variable stromal disruption	Good to poor, depending upon integrity of supporting structures and distance to muscle
	Second degree	Axon loss Endoneurial tubes intact Perineurium intact Epineurium intact	Good, depending upon distance to muscle
	Third degree	Axon loss Endoneurial tubes disrupted Perineurium intact Epineurium intact	Poor Axonal misdirection Surgery may be required
	Fourth degree	Axon loss Endoneurial tubes disrupted Perineurium disrupted Epineurium intact	Poor Axonal misdirection Surgery usually required
Neurotmesis	**Fifth degree**	Axon loss Endoneurial tubes disrupted Perineurium severed Epineurium severed	No spontaneous recovery Surgery required Prognosis after surgery guarded

1.3.2.6 Mixed Lesion

In 1988, Mackinnon inserted a new injury pattern in the nerve injury classification, known as 6th-degree injury. This classification includes multiple degrees of nerve injury previously described in Sunderland's classification. It means that there are both axon loss and conduction block occurring in some fibres with viable degrees of the outcome and recovery (Mackinnon, 1988, Robinson, 2000, Zuniga and Radwan, 2013).

1.4 DIFFERENCES IN CNS AND PNS REGENERATIONS

Following an injury to both the peripheral (PNS) and central (CNS) nervous systems, a cascade of events occurs. Examples of these events are: increase of the vascular permeability followed by hyperaemia and oedema formation, and an increase of the pressure of the endoneurial fluid. Finally, permanent nerve dysfunction leads to intraneural ischemia (LaBanc, 1992). The ability of the peripheral nervous system to undergo regeneration spontaneously or after surgical intervention (in severe cases) and then to reinnervate its original tissue, is better than that in the central nervous system (Figure 1.3) (Strittmatter, 2010). In the past, it was believed that axons in the central nervous system did not have the ability to regenerate, this was disproved in later studies (Aguayo, 1981, Clark, 1943, Richardson, 1980). Nowadays, several studies have focused on factors that prevent the regeneration in the CNS, and have attempted to enhance regeneration but with little success. The environment of the CNS after injury is believed to be the essential factor that affects regeneration, as well as some other factors such as pathological changes and the type and nature of the cells involved. The environmental effect on regeneration was examined in two experimental studies mentioned by Santiago Ramon Cajal (1991) [updated translation] and Aguayo et al., (1982). In the first study, a segment of CNS tissue was transplanted inside a peripheral nerve. The study reported that the regeneration of peripheral nerve axons stopped when they contacted the CNS tissue (Cajal, 1991). While Aguayo et al., (1982) did the opposite experiment, in which a section of PNS nerve was transplanted into the CNS. They recorded that CNS axons showed an ability to regenerate when they made contact with the PNS nerve (Aguayo et al., 1982).

The nature of the process of demyelination and regenerative potential of oligodendrocytes are shown to be factors that affect regeneration of the CNS (Ludwin, 1988). Demyelination and remyelination in the PNS is prompt, efficient, and the number of active Schwann cells is superior to the required number for adequate remyelination. So, Schwann cells play an important role for ensheathing peripheral axons, while oligodendrocyte cells ensheath the central axons. The mitotic capacity of

oligodendrocyte cells is lower than that of Schwann cells (Benson et al., 2005, Ludwin 1988).

It has been reported that Myelin-associated inhibitors are the main obstacles preventing regeneration in the CNS (Chen et al., 2007). These inhibitors include oligodendrocyte myelin glycoprotein (O Mgp) (Chen et al., 2007, Kottis et al., 2002), myelin-associated glycoprotein (MAG) (Chen et al., 2007, McKerracher et al., 1994) Ephrin B3 (Benson et al., 2005), Nogo (Strittmatter, 2010), and repulsive guidance molecule A (Grados-Munro and Fournier, 2003). In addition to these inhibitors, the extra-cellular matrix of the CNS includes some molecules that prevent axon regeneration. One of these molecules is called chondroitin sulphate proteoglycans (CSPGs). They are composed of a glycoprotein core and sulphated glycosaminoglycan (GAG) sugar chains, and the CNS extra-cellular matrix is richly populated with CSPGs (Rhodes and Fawcett, 2004). The mechanism of action of CSPGs to inhibit axonal regeneration is not fully understood (Schmalfeldt et al., 2000). However, some studies detected that these molecules are found inside the glial scar formed by reactive astrocytes following CNS injury and is associated with failure of regeneration of axons (Rudge and silver, 1990).

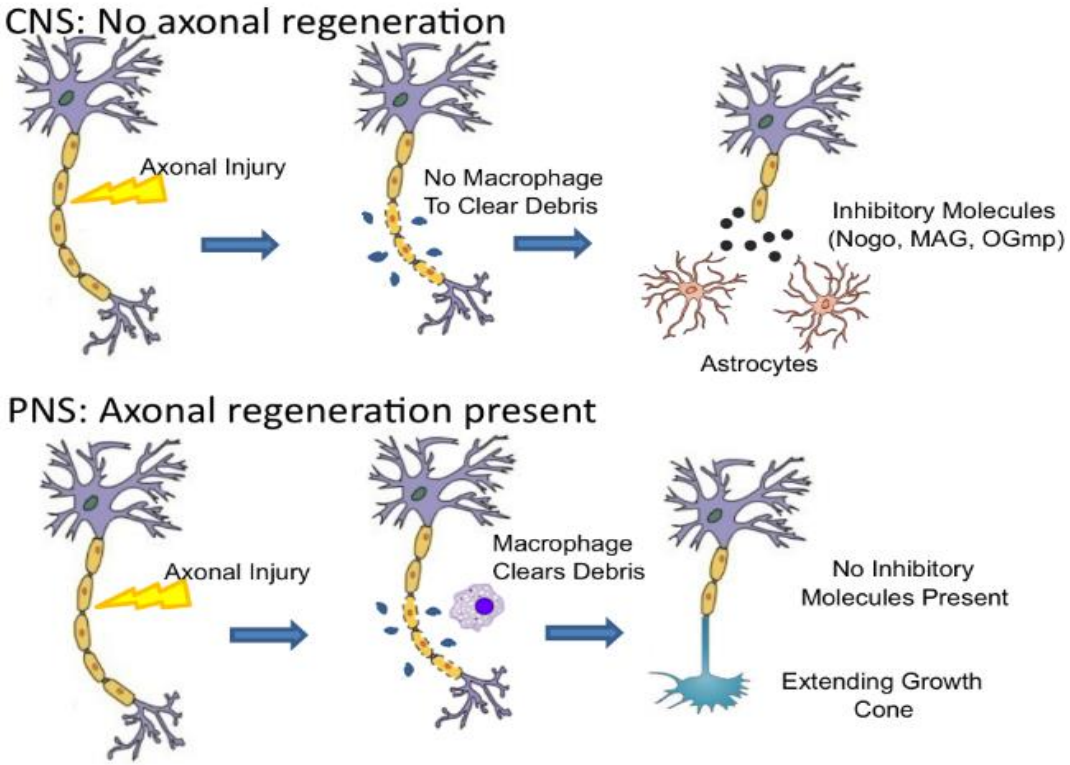

Figure 1.3: A diagram showing the differences in nerve regeneration between CNS and PNS. In the CNS, there are no macrophages to clear the debris, while they are present in the PNS. There are inhibitory molecules in the CNS, whereas these are not found in the CNS (Strittmatter, 2010, pp.56).

1.5 DEGENERATION AND REGENERATION OF PERIPHERAL NERVE INJURY

Under natural circumstances, peripheral nerves maintain normal connections between the axons and their targets. Following injury, these stable connections are lost (Fawcett and Keynes, 1990). In peripheral nerve injuries, there are two essential components: the axon and the Schwann cells together with their myelin sheaths (Stoll and Müller, 1999, Waller, 1850). In the mildest forms of neurapraxia and axonotmesis, a complete recovery is predictable. In contrast, in more advanced cases there is an interruption of the axon integrity followed by several processes that take place in the proximal and distal stumps (Osbourne, 2007, Stoll and Müller, 1999, Terenghi, 1999).

1.5.1 Wallerian Degeneration

In 1850, Waller published a paper describing events following nerve injury including axon and myelin degeneration below (distal to) the level of injury, known as Wallerian degeneration (Waller, 1850). This process also occurs in a small area of the immediately proximal stump as some axons may retrogradely degenerate as far as the 1st node of Ranvier. Waller explained all these changes and processes in the hypoglossal and glossopharyngeal nerves of the frog (Dagum, 1998, Osbourne, 2007, Terenghi, 1999, Waller, 1850). The principle of the Wallerian degeneration process is to remove and recycle the axonal and myelin-derived material in order to prepare a suitable environment for the axons to regenerate through (Fawcett and Keynes, 1990). Many events take place during Wallerian degeneration such as axon degeneration, myelin sheath degradation, macrophage secretion, and Schwann cell stimulation and proliferation (Ngeow, 2010, Osbourne, 2007, Terenghi, 1999, Salzer et al., 1980).

Axonal continuity and the conduction of impulses at the distal part of the nerve will be lost by 48-96 hours post-injury, and Wallerian degeneration starts with quick degradation of axons and myelin that is induced by the activation of Ca^{2+} influx and axonal proteases released by Schwann cells (George et al., 1995, Osbourne, 2007, Stoll and Müller, 1999, Terenghi, 1999). Normal axons regulate a low intracellular calcium concentration; however, the concentration is significantly increased following nerve transection. This leads to activation of Ca^{2+} sensitive proteases (LoPachin et al., 1990, Ngeow, 2010). A comparable process happens in unmyelinated nerve fibres (Fawcett and Keynes, 1990). Schwann cells have an important role in Wallerian degeneration as they work together with macrophages, providing them with the cell debris to phagocytose (Acheson et al., 1991, Hall, 1997, Osbourne, 2007, Terenghi 1999). For many years, the roles of Schwann cells and macrophages in clearing out the degenerating debris were unclear until experiments done by Friede and companions answered this question (Beuche and Friede, 1984, Scheidt and Friede, 1987). In their experiments, sections of mouse nerve were put inside Millipore diffuse chambers with a pore size of 0.22µm for the purpose of ingress prevention. Then they implanted the sections into the peritoneal cavity of mice. Eight weeks later, the Schwann cells hadn't

proliferated. In addition, the myelin was not phagocytosed, although it was discarded. In contrast, when they used a chamber with a larger pore size (5µm), the macrophages engulfed the myelin. They concluded that macrophages are necessary to trigger the removal of myelin and the myelin debris is ingested by macrophages (Beuche and Friede, 1984, Fawcett and Keynes, 1990, Scheidt and Friede, 1987). This opened a pathway for the removal of the myelin (Crang and Blakemore, 1987, Fawcett and Keynes, 1990).

Starting on the 2nd day and with a peak between the 4th and the 7th day post-injury, the permeability of the blood-nerve-barrier becomes high. This results in haematogenous macrophages moving from the circulation into the distal region of the injured nerve (Stoll et al., 1989, Stoll and Müller, 1999). Within 14 days, macrophages will have totally cleared out the myelin debris (Brück, 1997, Stoll and Müller, 1999).

It has been reported that the myelin and axonal membrane debris stimulate the mitosis of Schwann cells (Perry et al., 1981, Salzer et al., 1980). The Schwann cells divide and proliferate inside their basal lamina tubes, persisting for approximately 2 weeks and reach their peak by the 3rd to 4th day (Clemence et al., 1989, Son and Thompson, 1995, Stoll and Müller, 1999, Terenghi, 1999). Macrophage cells are mitogenic and participate with Schwann cells, spreading from the distal stump to cross the site of injury in order to form a conduit, known as the bands of Büngner, providing nutrient (trophic) and guidance (tropic) factors for the regenerating axons from the proximal stump to reach their targets (Reynolds and Woolf, 1993, Stoll and Müller, 1999, Terenghi, 1999). Contact with the neurotrophic factors with the regenerating axons stimulates a second phase of the proliferation of Schwann cells. In cases where the axonal regeneration process is delayed, the numbers of Schwann cells decrease gradually and the response to axonal regeneration will become reduced (Li et al., 1997, Terenghi et al., 1999).

There are a number of mediators that play an important role in Wallerian degeneration, such as histamine and serotonin. These mediators are released by mast cells and their function is to improve macrophage migration, resulting in enhanced Wallerian degeneration.

The end stage of Wallerian degeneration is a shrinking of the nerve due to vesicular breakdown. In some cases, the presence of vigorous oedema and inflammation, coupled with fibroblast proliferation leads to the production of dense fibrous scar tissue (Osbourne, 2007, Stoll et al., 1989).

1.5.2 Axonal Regeneration

The regeneration response depends on several factors, and among these factors is the severity of the injury (Burnett and Zager, 2004). The axons start to regenerate only after the course of Wallerian degeneration is carried out. The axonal regeneration is a concert of activity which occurs in different anatomical zones, beginning at the neuronal cell bodies, then the proximal stump (axonal process between the neuronal cell body and the site of injury), the injury site itself, the distal stump (severed axonal process between the site of injury and the end organ), finally finishing at the end organ itself (Burnett and Zager, 2004, Cambell, 2008, Dagum, 1998, Osbourne, 2007). Unsuccessful or delayed regeneration may impede the normal processes at one or more of these zones (Burnett and Zager, 2004).

The first changes that happen following nerve injury occur in the cell body (Burnett and Zager, 2004). The axons and cell body are interdependent in recovery. The cell body responds with an increase in protein metabolism and synthesis of lipids. Within the first 6 hours post-injury, the nucleus moves to the periphery of the cell where Nissl substance disperses as a result of the disintegration of rough endoplasmic reticulum. This morphological event is named chromatolysis. It is believed that it works as a signal for glial cells, with the purpose of extending the processes of the injured neurone in addition to breaking away synaptic connections. This, has the effect of isolating the affected neurones to allow for recovery (Burnett and Zager, 2004, Lundborg and Sweden, 2000, Osbourne, 2007, Terenghi, 1999).

A complicated and not fully understood interaction happens between the cell body and the tip of regeneration axons. Axoplasm arises from the area between the cell body and the proximal axon segment. Axoplasmic transport consists of both fast and slow

components and they supply and move protein, lipid, and other materials from the cell bodies through the cytoplasm of its own axon (axoplasm) toward the injury site in a process called anterograde transport (Burnett and Zager, 2004). In cases where the affected area is more proximal, the cell body degenerates (as seen in a severe trauma). This may result in Wallerian degeneration of the entire proximal stump, which is then phagocytosed, resulting in no axonal regeneration (Burnett and Zager, 2004, Dagum, 1998).

A structure called the growth cone is formed at the top of the regenerating axon (terminal edge), consisting of finger-like filopodia built around actin filaments emerging from web-like lamellipodia (Figure 1.4) (Dagum, 1998, Lundborg and Sweden, 2000, Terenghi, 1999, Zochodne, 2008).

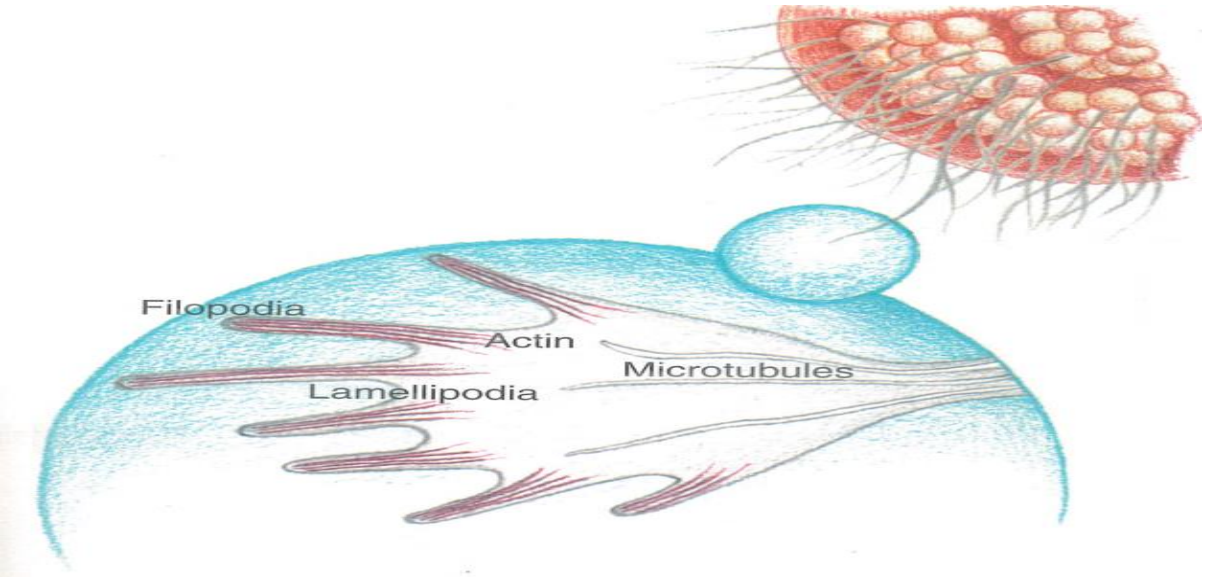

Figure 1.4: Diagram showing the axon sprouts and a growth cone (Zochodne, 2008).

The growth cone responds to contact guidance cues, and contacts with basal lamina of the Schwann cell through its filopodia in order to use it as a guide (Burnett and Zager, 2004, Terenghi et al., 1998). The growth cone grows distally across the site of the injury, and it actively searches for an appropriate matrix and environment to assist the axon to grow (Figure 1.5) (Lundborg and Sweden, 2000, Rutishauser, 1993, Terenghi,

1999). The sprouts that contact via the filopodia to the distal stump (Schwann cell basal lamina) continue to grow inside the endoneurial tubes. The lamina acts as contact guidance to the filopodia. Growth cones have been studied in detail as they are specialised structures that have an essential role, and are responsible for many steps in regeneration including growth, path-finding and identifying targets (Ide, 1996, Landis, 1983).

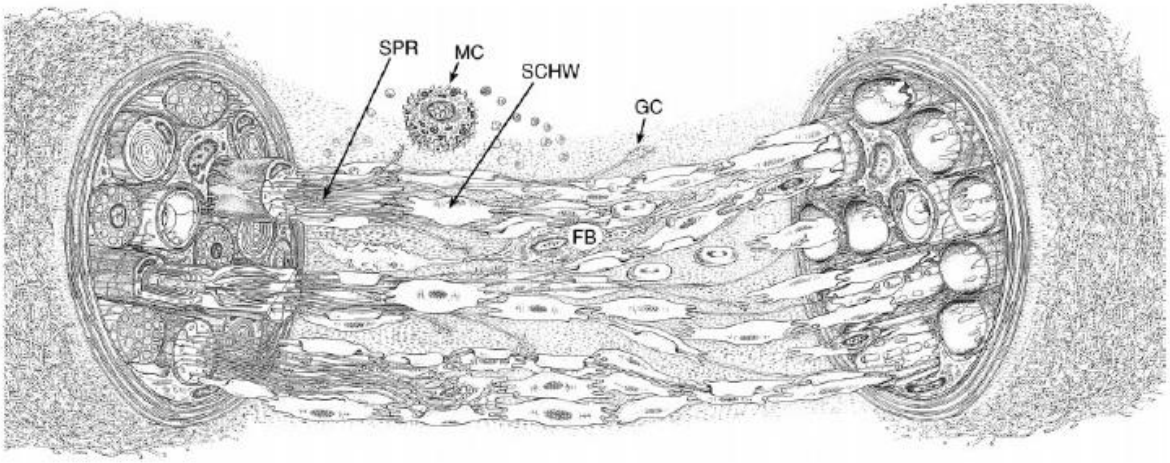

Figure 1.5: Scheme shows cellular response to nerve transection. Sprouting occurs at the proximal nerve stump (left). Sprouts (SPR) projecting from myelinated axon and form a regenerating unit that enclosed by common basal lamina. A growth cone (GC) found on the tip of each sprout. Sprouts pass over the site of injury and associated with Schwann cells (SCHW). At the site of injury there are fibroblasts (FB), mast cells (MC), macrophages, and blood corpuscle elements. Finally, the sprouts attach the band of Bügner at the distal stump (Lundborg and Sweden, 2000, pp. 394).

In myelinated axons, the first sprouts are seen coming from the 1st node of Ranvier proximal to the injury site, though some may come from the 2nd node of Ravier (Fawcett and Keynes, 1990, Friede and Bischhausen, 1980, Meller, 1987, Osbourne, 2007); the growth rate of unmyelinated axons is equal to that in myelinated axons. In addition, the myelinated axons may regrow inside an endoneurial tube that previously contained unmyelinated axons, and vice versa (Burnett and Zager, 2004). Due to the number of neuronal sprouts being higher than the number of axons originally found in the nerve, it is believed that this phenomenon is for the purpose of maximising the chance of each

single neuronal cell to reach its target organ. However, scant survival signals coming from the target organ causes ‘die back’ of some of these sprouts via ‘axonal pruning’ (Brushart, 1993, Ngeow, 2010, Terenghi, 1999). The axonal sprouts that cannot make contact with supportive factors will undergo degeneration along with the muscle tissue if it is not reinnervated within 1-2 months (Dagum, 1998).

The interaction between the growth cone and Schwann cells is mediated by cell adhesion molecules (CAMS) (Rutishauser, 1993, Terenghi, 1999). Some evidence suggests that neuronal CAMS expression is up-regulated by nerve growth factor (NGF) (Friedlander et al., 1986, Terenghi, 1999).

Motor and sensory fibres have the same ability to grow and maturate (Osbourne 2007). Motor fibres will search and innervate a motor distal axonal region (Rath and Green, 1991, Terenghi, 1999). This ability is believed to be dependent on the L2 epitope, expressed by myelinating Schwann cells that relate to motor axons (Martini et al., 1994, Terenghi, 1999).

The rate of axonal regeneration is controlled by many factors, such as changes occurring within the neural cell body and the activity of the growth cone at the axon sprout tip (Burnett and Zager, 2004). While the distal regeneration rate is affected, and becomes slow if the endoneurial tubes have been torn, because the axons can’t find their way inside the tube before advancing (Burnett and Zager, 2004).

In the late stages of peripheral nerve regeneration, Schwann cells have another role when they act together with fibroblasts, as they are a considerable source for endoneurial expression of cytokines (Taskinen et al., 2000).

Figures 1.6 and 1.7 illustrate the differences in regeneration between mild (crushed) and server (transected) nerve injury levels (Holland and Robinson, 1998).

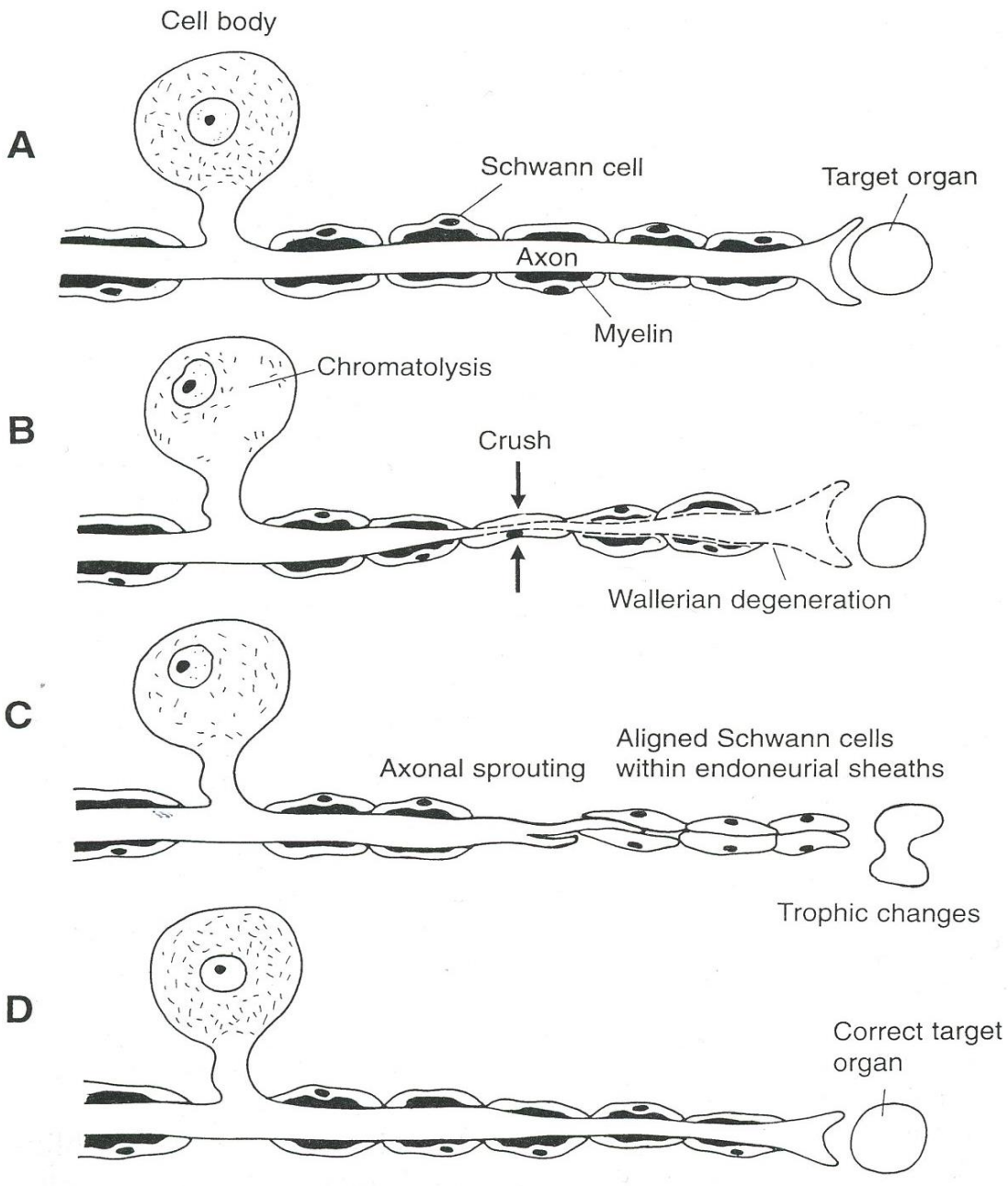

Figure 1.6: Regeneration following crushed axon. A) Uninjured nerve. B) Crush injury to the nerve. C) Axonal sprouting and regenerating within the original endoneurial sheaths. D) Successful regeneration (Holland and Robinson, 1998, pp.279).

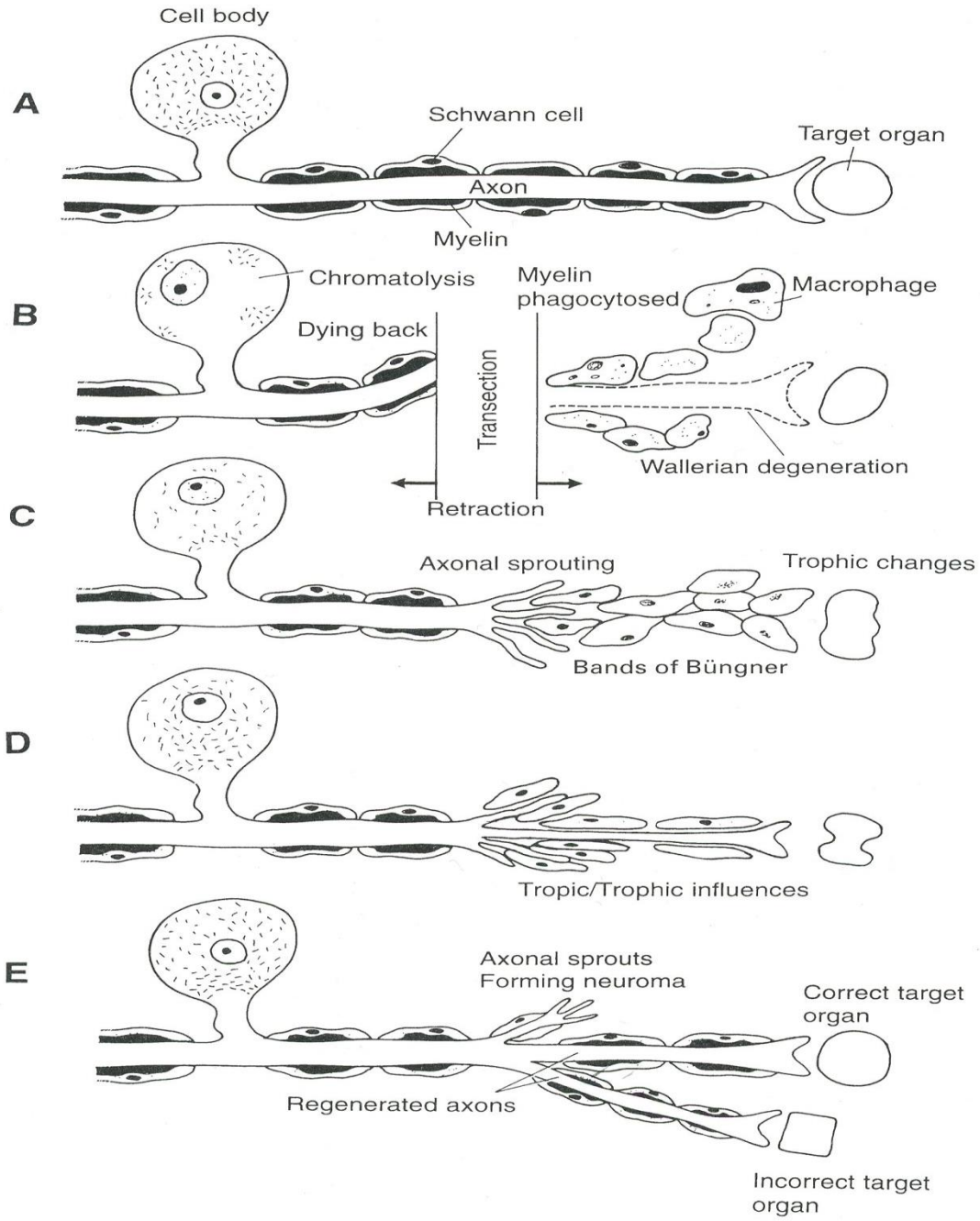

Figure 1.7: Regeneration following transected axon. A) Uninjured nerve. B) Transection injury to the nerve. C) Axonal sprouting attempts to find original endoneurial tube. D) Tropic/Trophic influences encouraging growth in one sprout E) Some of regenerating axons find the original endoneurial tube and then innervate the original target, while others enter incorrect endoneurial tube and then fail to innervate the original target, and the rest fail to find and enter any endoneurial tube, in turn forming a neuroma (Holland and Robinson, 1998, pp.280).

1.6 PERIPHERAL NERVE REPAIR

The surgical repair of PNIs can be traced back to the 13th century. At that time, as reported by Browne (1967), surgical knowledge of the peripheral nerve was primitive and depended on rudimentary attempts by Avicenna at direct nerve suturing (reviewed in Artico et al., 1996). During the 13th century, Guglielmo da Saliceto, an Italian pioneer of anatomy, suggested some types of nerve suture; however, his exact technique is unknown (reviewed in Artico et al., 1996). After that, Guido Lanfranchi, Guglielmo's pupil, attempted to perform a direct suture at the two ends of nerve. Although Guido Lanfranchi, Guglielmo da Saliceto and Avicenna reported some efforts of direct suturing of the nerve, the information provided was sketchy (reviewed in Artico et al., 1996). In 1596, Gabriele Ferrara, a Milanese surgeon, published his book which includes a clear description and much more details of direct nerve suturing. At that time, he became the first to provide a lucid and precise description of the direct suture in the field of peripheral nerve injury, and he is now named the ''father'' of peripheral nerve reconstruction (reviewed in Artico et al., 1996). His description was of suturing the retracted stumps of the nerve by using a special needle and suture that had been immersed and treated in a concoction of rosemary, red wine and rose. A mixture of hypericum and spruce oils were applied. Finally, the patient was later confined to bed for the purpose of immobilisation of the limb to avoid any damage to the suture. The use of rosemary, red wine and rose is believed to be comparable to alcoholic disinfection. The procedures of identification of nerve stumps, disinfection, correct technique and immobilisation of the affected limb after the operations are highly similar to the surgical protocol of modern medicine (reviewed in Artico et al., 1996).

In the late 17th century, Robert Hooke and Antonio van Leeuwenhoek, pioneers of microscopy, were interested in the discovery and manufacture of microscopes. Leeuwenhoek discovered that the optic nerve is composed of many filamentous particles and is not just a hollow tube, as he was interested in using microscopy to explore nerve fibres (reviewed in Wade, 2004). The first explanations of end-to-side peripheral nerve repair, allograft and autograft, and nerve guide conduit were issued

and published in the 19th century (reviewed in Artico et al., 1996, reviewed in Battiston, 2009).

1.6.1 Different Repair Methods for Peripheral Nerve Injury

Making a decision on the repair technique and method of repair depends on many factors, such as the severity or type of nerve injury and tension at the injury site (Matsuyama et al., 2000). There are several repair techniques to treat a peripheral nerve injury, and the following sections will talk briefly about direct suture (End-to-End), nerve grafts, and provide details of currently available nerve guide conduits.

1.6.1.1 Direct Suture (End-to-End)

Direct suture intervention is the preferred technique in nerve injuries with a simple transection and without severe nerve tissue damage (Sunderland, 1973). The idea of applying the suture is to align the corresponding fascicular elements of both proximal and distal ends (Lundborg and Sweden, 2000). Direct suture can be subdivided into epineural, grouped fascicular and fascicular repair techniques. By careful examination of the proximal and distal stumps, the surgeon can opt for the most appropriate type of repair (Matsuyama et al., 2000).

The simplest direct repair technique is the epineural repair. It can be used when the nerve transection is clean or partial with easily alignment of the fascicles possible (Figure 1.8A). The technique is performed by suturing the proximal and distal ends together with suture passing through the epineurial sheath (Figure 1.8B) (Rowshan et al., 2004, Lundborg and Sweden, 2000, Matsuyama et al., 2000).

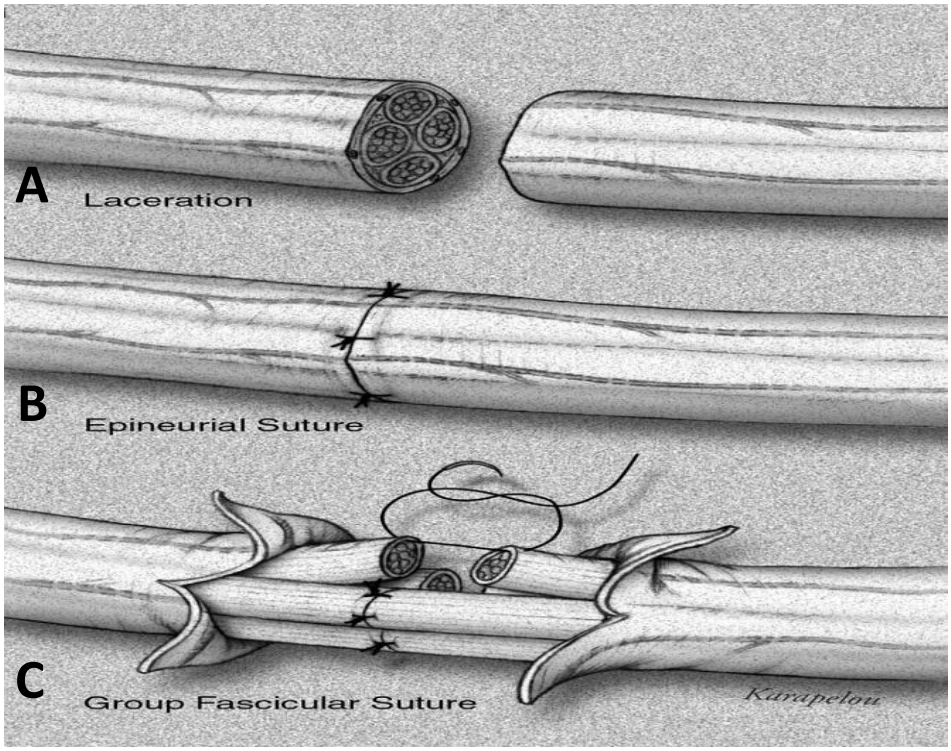

Figure 1.8: Schematic diagram of different direct suture repair techniques. A) A clear cut in a nerve. B) Epineurial suture, sutures are passed via the external and internal epineurium of proximal and distal ends. C) A group fascicular suture, epineural tissue has been resected and fascicular groups are coaptated with single sutures passing through the interfascicular epineurium (Rowshan et al., 2004, pp.164).

A more accurate technique, relative to epineural repair, is grouped fascicular repair. The technique is performed by suturing the interfascicular epineurium of both nerve ends (Figure 1.8C) (Rowshan et al., 2004, Lundborg and Sweden, 2000, Matsuyama et al. 2000). It is appropriate in the repair of nerve injuries such as partial injury in large nerves, nerves having two major fascicular groups which can be easily identified, and nerves having both mixed sensory and motor fibres (Matsuyama et al., 2000).

Fascicular repair is the most difficult and complicated direct suture technique for repairing nerve injury. It is performed by suturing each perineurium and reconnection of corresponding fascicles in both ends to get an optimal alignment (Matsuyama et al., 2000).

Several experimental and clinical studies have investigated the superiority of one of these techniques relative to the others. However, there is no study reporting that any type is better than the others (Lundborg and Sweden, 2000, Matsuyama et al., 2000).

In some situations, using sutures can lead to irritation and increase the possibility of scar tissue formation. For that reason, some experimental studies use fibrin glue in nerves that won't undergo any tension/strain during joint movement instead of suture to avoid these disadvantages (Ornelas et al., 2006). A study by Menovsky and Beek (2001), reported that using CO_2 laser nerve welding is equal to use of either microsurgical suture repair or fibrin glue repair at the site of the injury. Hence, laser nerve repair with soldering is believed to be an excellent alternative to both suture and fibrin glue repairs. However, the use of laser nerve welding requires complicated equipment and is expensive (Menovsky and Beek, 2001).

When a nerve injury is associated with a loss of tissue and the two ends of the nerve cannot be joined together without undue tension, an alternative to direct repair is required. The reason behind avoiding undue tension after repair is because excessive tension leads to the development of ischemia at the repair site and this results in prevention of the regeneration process and a decrease in functional recovery (Matsuyama et al., 2000, Siemionow and Brzezicki, 2009). In cases where a gap will be formed at the site of an injury, it can be bridged and repaired by using either a nerve graft or conduit.

1.6.1.2 Nerve Graft

When a direct suture repair causes considerable tension at the site of the nerve repair, a graft repair is recommended (Matsuyama et al., 2000). Clinically, the gold-standard method for bridging nerve gaps is an autologous nerve graft (autograft) (Ichihara et al., 2008, Lundborg and Sweden, 2000, Zhu et al., 2011). The sural and the greater auricular nerve are specifically well-suited for grafting. The nerve grafting technique is similar to end-to-end suturing, but with the presence of transplanted nerve tissue (Figure 1.9) (Hausamen and Schmelzeisen, 1996).

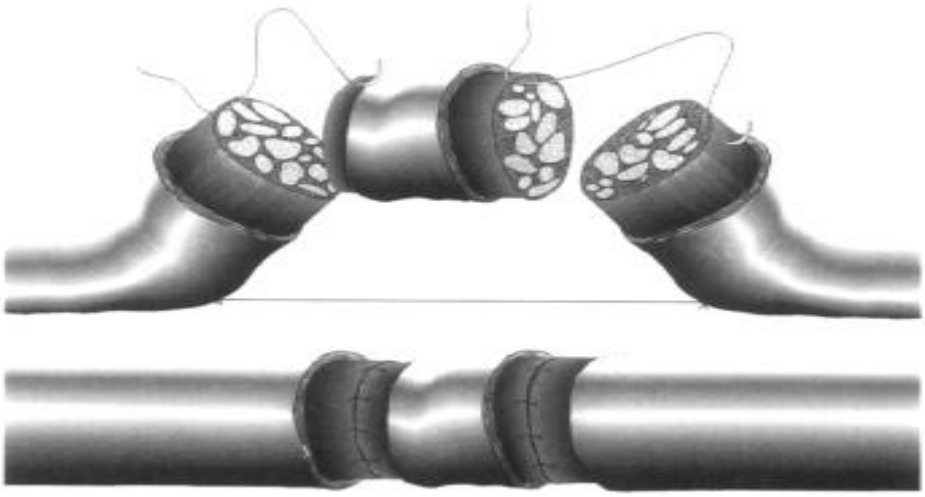

Figure 1.9: Microsurgical suturing technique. Graft interposition between proximal and distal stumps, graft and gap of identical size (Hausamen and Schmelzeisen, 1996, pp. 147).

In many nerve injuries the use of autograft is not preferential, either because a large number of nerves need repair or the large length of the nerve gap; therefore, nerve allografts can be an alternative choice (Siemionow and Brzezicki, 2009). The essential drawback of using nerve allografts is that heavy immunosuppression is mandatory in order to avoid rejection of the nerve (Matsuyama, 2000, Ray and Mackinnon, 2010). To avoid this downside, cadaveric allograft decellularization was developed. Avance (AxoGen) are commercially available decellularized nerve allografts. The Avance graft

is produced by processing human nerve through a combination of detergent decellularization, chondroitin sulfate proteoglycans degradation, enzyme treatment, and γ-irradiation sterilization (Shanti and Ziccardi, 2011, Wood et al., 2014). In theory, a decellularized allograft allows Schwann cells to quickly repopulate the allograft tissue by giving a more biologically pertinent microenvironment. Another benefit of the decellularized grafts is the removal of neurite inhibitory chondroitin sulphate proteoglycans from the basal lamina, leading to an increase in axonal regeneration (Krekoski et al., 2001, Shanti and Ziccardi, 2011). Whitlock et al. (2009) compared the use of Avance allograft and NeuraGen®, a type I collagen NGC (see section 1.7.3.2.i), on short (14mm) and long (28mm) nerve gaps. They reported that Avance allograft had higher robust reinnervation than NeuraGen in gaps longer than 10mm. They concluded that in cases with large nerve gaps, a decellularized allograft is considered to be a suitable alternative material (Whitlock et al., 2009).

In small diameter nerves, it is possible to use a single similar sized graft for bridging, while in large diameter nerve it is necessary to use two or more small diameter nerve grafts for bridging the gap, due to limited availability of thicker nerves (Figure 1.10) (Hausamen and Schmelzeisen, 1996).

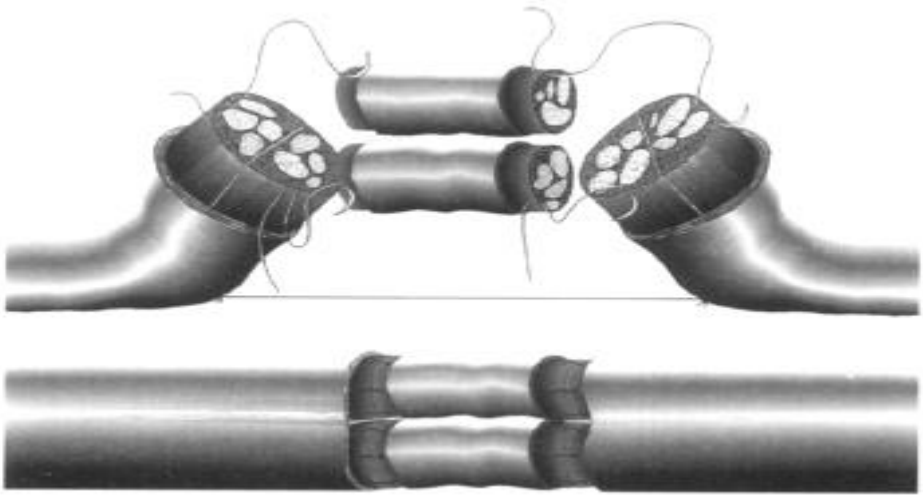

Figure 1.10: Microsurgical suturing technique. Two small diameter nerve grafts interposition between proximal and distal stumps of a large diameter nerve (Hausamen and Schmelzeisen, 1996, pp. 147).

Although autografting shows acceptable outcomes, there are some disadvantages such as multiple surgeries required, scarified of an intact nerve, limited availability, loss of sensation, neuroma formation (donor site), with the potential for neuropathic pain (Shanti and Ziccardi, 2011). The use of nerve guide conduits (NGCs) can remove these problems.

1.7 NERVE GUIDE CONDUITS

Although nerve graft techniques have some advantages, such as serving as a physical guide for regenerating axons, they have many disadvantages such as: sensory and motor dysfunction at the donor site, additional (secondary) surgery, sacrifice of uninjured nerve, mismatches of nerve size, lack of availability or suitability, and donor site scarring and morbidity (Kim et al., 2008, Moore et al., 2009, Taras et al., 2005, Zhu et al., 2011). Within the last three decades the use of an alternative technique, nerve guide conduits, to bridge nerve gaps has been established and developed to overcome these disadvantages (Figure 1.11) (Cui et al., 2018, Lundborg and Sweden, 2000, Oh et al., 2018, Zhu et al., 2011).

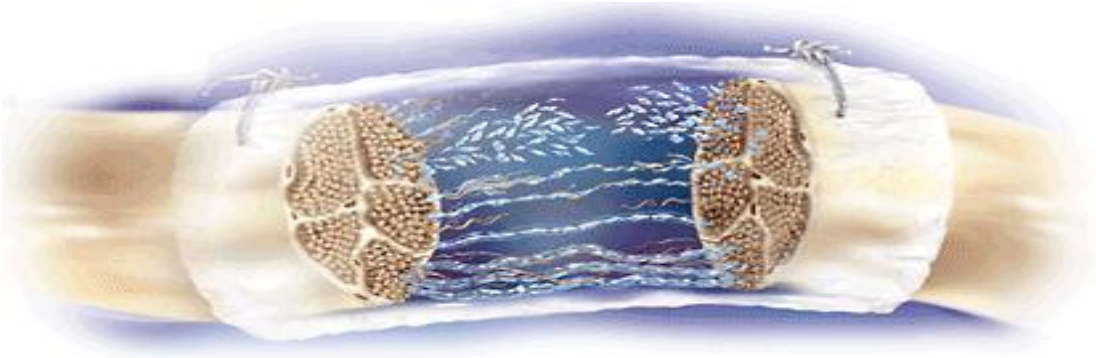

Figure 1.11: Diagram of conduit repair. The conduit fitted between the two ends and secured by sutures (http://www.whichmedicaldevice.com/by-manufacturer /235/ 581/neuragen-nerve-guide).

1.7.1 Basic Concepts of Nerve Guides

Use of mesothelial tubes for bridging nerve gaps was first reported in 1979 (Lundborg and Hansson, 1979, Lundborg and Sweden, 2000). In the early 1880s, Gluck applied decalcified bone to use as a conduit (reviewed in Taras et al., 2005). Following that, a variety of substances have been examined including blood vessels and fallopian tubes with varying success level (Evans et al., 1999, Taras et al., 2005).

Nerve conduit material is either natural, such as collagen (Archibald et al., 1991, Farole and Jamal, 2008) or synthetic, such as silicone (Matsumoto et al., 2000, Waitayawinyu et al., 2007). Silicone was the first reported synthetic conduit material that was developed in the early 1980s because of its elastic and inert properties (Ichihara et al., 2008, Lundborg et al., 1982). Many studies have reported that first generation non-degradable conduits composed of silicon and poly (2-hydroxyethel methacrylate-co-methyl methacrylate) may lead to chronic inflammation, nerve compression (nerve collapse), foreign body reaction, and scar formation (Moore et al., 2009, Zhu et al., 2011).

For the next generation conduits, three key mechanical properties have been added to enhance them. First, the conduits should supply the regenerating axons with an adequate scaffold. If the nerve conduits are too soft, they may not resist any pressure from the external tissue. On the other hand, if they are too hard, they will damage the surrounding tissues (Ichihara et al., 2008, Sivak et al., 2017, Taras et al., 2005). Second, they must be semi-permeable to allow the greater interaction and exchange with the surrounding environment (Aebischer et al., 1988, Li et al., 2014, Ichihara et al., 2008). Third, the conduits degradation must be at an appropriate speed to avoid the formation of fibrous tissue inside the conduit and mechanical damage to the regenerating axons (Ichihara et al., 2008, Wang et al., 2017). Other properties preferential for the ideal conduit are that they must have a suitable diameter for axon regeneration, the conduits should require minimal effort to implant, and they must be sterilisable (Gonzalez-Perez et al., 2017, Taras et al., 2005). Figure 1.12 illustrates some methods to enhance the role of conduits in peripheral nerve repair.

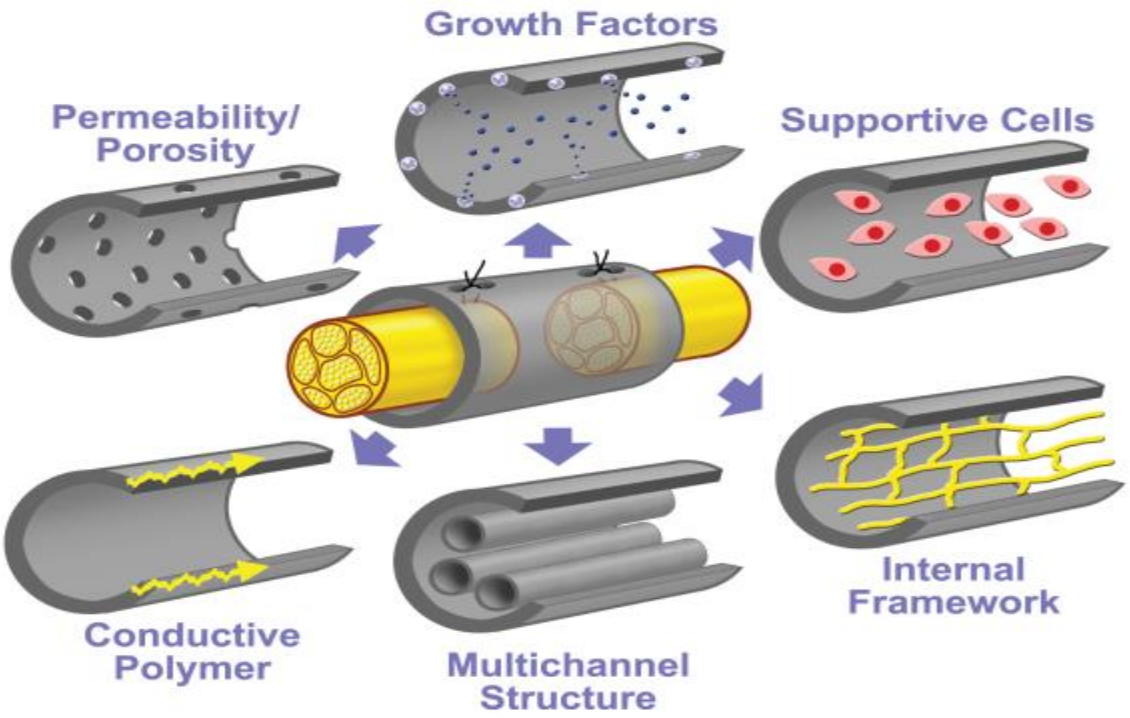

Figure 1.12: Strategies to enhance the internal lumen of nerve conduit (De Ruiter, et al. 2009).

1.7.2 The Use of Conduits in Animal Studies

Biological conduits such as collagen, fibronectin, and laminin have been demonstrated to enhance nerve regeneration (Taras et al., 2005). A variety of natural absorbable materials have been investigated for peripheral nerve regeneration. Many types of biological collagen conduits have been utilised experimentally and clinically, and some of them demonstrated good results in rats, mice (Gomez et al., 1996, Kim et al., 1993), and rabbits (Kim et al., 1993). In addition, Archibald et al 1995 reported on the effectiveness of using type I bovine collagen conduit in a 5 mm nerve gap in monkeys (nonhuman primate) (Archibald et al., 1995, Taras et al., 2005).

On the other hand, a lot of experiments have examined synthetic absorbable materials including the polymers: polyglycolic acid (PGA), polylactide-caprolactone (PLCL), and *poly (L-lactic acid*) (PLLA) (Ichihara et al., 2008, Li et al., 2014). In rat nerve repair,

Polyglactin conduits lead to poor nerve regeneration (Ichihara et al., 2008, Gibson et al., 1991) but better outcomes were mentioned with poly (organo) phosphazine, polyglactin acid, poly-(L-lactide-co-caprolactone) conduits, and polyglycolic acid polymer coated with cross-linked collagen (PGA-c) (Ichihara et al., 2008, Siemionow and Brzezicki, 2009).

1.7.3 Current FDA Approved Nerve Guidance Conduits and Materials

The use of conduits in the clinical field is not as common as nerve grafts; however, there are a number of conduits that are commercially available and are approved by The Food and Drug Administration (FDA) for clinical repair of peripheral nerve injuries (Table 1.2) (Arslantunali et al., 2014 Kehoe et al., 2012, Pabari et al., 2014).

Table 1.2: Current FDA approved nerve guide conduits.

Product Name	Material	Type	FDA Clearance Date	Company	Degradation Time	Length (cm)	Diameter (mm)
Neurotube®	Polyglycolic acid (PGA)	Synthetic	22/03/1999	Synovis Micro Companies, Inc.	3 months	2-5	2.3-8
NeuraGen®	Type I collagen	Natural	22/06/2001	Integra Life Sciences Corp.	36-48 months	2-3	1.5-7
Neuroflex™	Type I collagen	Natural	21/09/2001	Collagen Matrix, Inc	4-8 months	2.5	2-6
Neuromatrix™	Type I collagen	Natural	21/09/2001	Collagen Matrix, Inc	4-8 months	2.5	2-6
Surgisis® Nerve Cuff (AxoGuard™)	Porcine small intestinal submucosa	Natural	15/05/2003	Polyganics BV	3 months	10	1.5-7
Neurolac®	Poly $_{D,L}$ lactide-co-ε-carprolacton (PDLLA/CL)	Synthetic	04/05/2005	Cook Biotech Products	16 months	3	1.5-10
SaluTunnel™	Polyvinyl alcohol (PVA) hydrogel	Synthetic	05/08/2010	SaluMedica, LLC	Non-absorbable	6.35	2-10

1.7.3.1 Synthetic Non-absorbable

1.7.3.1.i Polyvinyl Alcohol Hydrogel (SaluTunnel™)

The SaluTunnel™ is used for nerve injuries without loss of tissue. It remains the only approved synthetic non-absorbable material. No data have been published for this device neither pre-clinical nor clinical studies (Kehoe et al., 2012, Pabari et al., 2014).

Advantages: SaluTunnel has similar properties to human tissues as they contain water. They are easily sterilised

Limitations: As they are non-absorbable (permanent), they may cause nerve compression and tension at the site of suture. There are no pre-clinical or clinical studies published yet to support the efficacy of these materials (Kehoe et al., 2012 Pabari et al., 2014).

1.7.3.2 Natural Absorbable

Natural materials decrease the toxicity, increase the biocompatibility, and improve support cell migration compared to synthetic materials (Schmidt and Leach, 2003).

1.7.3.2.i Type 1 Collagen (NeuraGen®, Neuroflex™, and NeuromatrixTM)

The major component of the extra-cellular matrix is collagen, which makes it superior to the other natural materials (Kehoe et al., 2012).

NeuraGen® was the first semi-permeable type I collagen to receive FDA approval in 2001. Some of the pre-clinical studies to investigate the efficiency of NeuraGen® are summarised in Table 1.3.

Table 1.3: Experimental data on NeuraGen® (Modified from Kehoe et al., 2012, pp. 558).

First author	Animal	Gap size	Groups	Control	Results
Tyner (2007)	Rat	20 mm	8 NeuraGen® 8 sham animals 8 distal autograft	8 control (neurectomy)	7/8 (88%) of the control (neurectomy) animals developed moderate to severe autotomy. 1/8 (13%) of NeuraGen group developed autotomy
Archibald (1995)	Nonhuman primate (monkey)	20 mm	5 NeuraGen® 5 suture	5 autograft	Reinnervation of Pacinian corpuscles and thenar muscles in all animals
Archibald (1991)	Rat & Nonhuman primate (monkey)	40 mm	NeuraGen®	Direct suture Autograft	At 4-week, the direct suture repair group illustrated a greater MAP compared to the other groups. However, at 12-week all repair groups showed similar levels of recovery.

In the Archibald et al. (1995) study, NeuraGen® was compared to direct suture and autograft in repairing peripheral nerve transection of nonhuman primate (monkey). They reported that nerve regeneration outcome using this type of conduit is equal to that of autograft repair (Kehoe et al., 2012, Li et al., 2014). Some of the clinical published cases of using NeuraGen® are summarised in Table 1.4.

Table 1.4: Clinical data on the use of NeuraGen® (Modified from Kehoe et al., 2012, pp. 560).

First author	Numbers	Gap size (mm)	Complications	Results
Schmauss (2014)	20 repairs, 16 patients	<26	None	Sensibility at 12-month: 13 cases improved 3 cases same value 4 cases had worsened
Wangensteen (2010)	126 repairs, 96 patients	Range: 2.5-20; mean:11.7-12.8	Two minor and one case of Pulmonary embolism. All Postoperative	40/126 lost to follow-up. 26/126 quantitative testing: 35% mentioned improvement and 31% need revision. 60/126 qualitative testing: with 45% mentioned improvement and 5% need revision
Lohmeyer (2009)	15 repairs, 14 patients	Mean: 12.5-3.7	None	4/12 (33%) excellent; 5/12 (42%) good; 1/12 (0.08%) poor; 2/12 (0.17%) none.
Bushnell (2008)	12 repairs	<20	None	4/9 excellent; 4/9 good; 1/9 fair.
Farole (2008)	5 repairs	15	None	4/9 good; 4/9 some; 1/9 none
Ashley (2006)	9 repairs	≤20	None	4/5 good (1 year follow-up); 3/5 excellent (2 years follow-up).
Taras (2005)	73 repairs	<20	None	1/5 poor Ongoing clinical study

In 2001, and after the approval of NeuraGen®, two devices of type I collagen were approved by the FDA; Neuroflex™, Neuromatrix™. To date, Neuroflex™ is the only flexible and up to 140^{O} kink resistance type I collagen conduit. Neuromatrix™ is similar

to Neuroflex™ in material composition, but it does not have the properties of Neuroflex™ with regards to flexibility and resistance. Although all of these three type I collagen conduits are approved by the FDA, NeuraGen® is the only conduit that has featured in published animal and clinical studies (Kehoe et al., 2012; Pabari et al., 2014).

Advantages:

Collagen Type 1 is an abundant material, easily isolated, encourages cell adhesion, prolong's survival and procreation, and it was reported that NeuraGen® can bridge gaps up to 4cm (Kehoe et al., 2012).

Limitations:

Long time for complete biodegradation (NeuraGen® = up to 48 months, Neuroflex™, Neuromatrix™ = 8 months) and the requirement to use immunosuppression drugs as unwanted immune responses were reported (Kehoe et al., 2012).

1.7.3.2.ii Porcine Small Intestinal Submucosa (Surgisis® Nerve Cuff (AxoGuard™))

Porcine small intestinal submucosa is a flexible, strong, and cell-free collagen matrix (Jernigan et al., 2004, Kehoe et al., 2012). Initial studies have suggested that small intestinal submucosa (SIS) may act as a neural guide material for nerve regeneration (Smith et al., 2004). The Surgisis® SIS Nerve Cuff is marketed as AxoGuard™ Nerve Connector (Kehoe et al., 2012).

Advantages:

Produced in a xenogeneic host, offers suitable biomechanical support, and accelerates cell proliferation.

Limitations:

No pre-clinical or clinical studies have been published yet to support the efficacy of this material, high cost, and immune response in some cases.

1.7.3.3 Synthetic Absorbable

1.7.3.3.i Polyglycolic Acid (PGA) (Neurotube®)

PGA is a highly crystalline, rigid thermoplastic polymer. Because of its high crystallinity, it has perfect mechanical properties that help in regeneration. PGA starts to lose strength in 1-2 months and loses total mass in 6-12 months (Kehoe et al., 2012; Pabari et al., 2014; Rai et al., 2012). Neurotube® is the first synthetic absorbable with highly porous nerve guide conduit that has received FDA approval. The results of two published animal studies using Neurotube® are summarised in Table 1.5 (Kehoe et al., 2012).

Due to the quantity and quality of clinical results and well as suitable cost, length, and availability, in addition to Meek and Coert's (2008) review, Neurotube® is considered the optimal synthetic conduit amongst surgeons (Kehoe et al., 2012, Meek and Coert, 2008). The results of most recent published clinical cases using this type of conduit are summarised in Table 1.6 (Kehoe et al., 2012).

Table 1.5: Experimental data on Neurotube® (Modified from Kehoe et al., 2012, pp. 562).

First author	Animal	Gap size	Groups	Control	Results
Waitayawiny (2007)	Rat	10mm	15 NeuraGen® 15 Neurotube®	15 autografts	NeuraGen® and nerve graft groups demonstrated obvious differences in the isometric muscle, axonal counts, contraction force, and wet muscle weights compared to Neurotube®.
Dellon (1988)	Monkey	30mm	8 graft 16 Neurotube® (8 rigid/ and 8 mesh)	Sural graft	Electromyographic evidence of intrinsic muscle recovery in 5/6 monkeys. No difference in electrophysiology or electron microscopy between groups.

Table 1.6: Clinical data on the use of Neurotube® (Modified from Kehoe et al., 2012, pp. 563).

First author	Numbers	Gap size	Complications	Results
Rosson (2009)	6 repairs	Range: 15-40mm	None	100% return to useful motor function.
Donoghoe (2007)	2 patients; 4 repairs	30mm	None	By 2 years following the nerve reconstruction reported discrimination with good localisation in the thumb, index, and middle finger. Both patients recovered abductor pollicis brevis function.
Dellon (2006)	1 patient; 2 repairs	25mm	None	The cutaneous pressure threshold for 1-point static touch was 0.7g/mm2.
Battiston (2005)	13 patients received muscle-vein combined NGCs. 17 patients (19 repairs) PGA	Range: 10-40mm	None	77% displayed very good results, and 18% displayed good results in the PGA group. 76.9% displayed very good results, while only 23.1% displayed good results in the muscle vein- combined group. Regarding functional recovery, there was no difference between the groups.
Navissano (2005)	7 repairs	Range: 10-30mm	None	1/7 very good, 4/7 good, 2/7 poor

Advantages: A large body of clinical data, reported to have comparable efficiency to autograft (gold standard) in bridging up to 20 mm nerve gaps, high cell viability levels, and initial mechanical properties are good.

Limitations: High rate of degradation, acidic degradation products, and low solubility.

1.7.3.3.ii Poly $_{D,L}$ lactide-co-ε-caprolactone (PLCL) (Neurolac®)

Poly $_{D,L}$ lactide-co-ε-caprolactone (PLCL) is a hydrophobic semi-crystalline polyester. Neurolac® is the only transparent nerve guide conduit approved by FDA (Kehoe et al., 2012). Copolymerization with Poly ($_{D,L}$-lactide) offers better acceleration of degradation rate. The results of published experimental studies using Neurolac® are summarised in Table 1.7 (Kehoe et al., 2012, Pabari et al., 2014).

Table 1.7: Experimental data on the use of Neurolac® (Modified from Kehoe et al., 2012, pp. 563).

First author	Animal	Gap size	Groups	Control	Results
Meek (2009)	Rat	10mm	8 Neurolac®	Not stated	At 5 weeks, no betterment in nerve regeneration was observed or even axon and myelin degradation. The walls of NGC were swollen which in turn blockage and cracks happened. At 8 weeks, few myelinated nerve fibres were observed distal to NGC. After 12 weeks, some myelinated nerve fibres were observed. Proximal to the NGC, Neuromas had occurred with fragmentation.
Meek (2009)	Rat	15mm	5 Neurolac®	Non-operated Nerve	Nerve regeneration was evident in all rats after two years. Biomaterial fragments with a 15mm maximum diameter. Due to severe automutilation, the functional analysis was impossible.
Luis (2007)	Rat	10mm	Direct suture Neurolac®	Non-operated injured nerves	No significant difference in comparative functional assessment. No statistical difference was observed for the number of regenerated myelinated fibres between the groups. A different pattern of tube degradation did not influence the degree of nerve regeneration.
Jansen (2004)	Rat	15mm	8 PDLLA-e-CL NGC 8 non-operated nerves (control)	Sciatic, right nerve of the same animal (non-operated contralateral side)	Little fragments of material remained, results a secondary foreign body reaction. The structure of the nerve and buildup of ECM proteins without extensive scar tissue formation recovered long term.

An experimental study by Shin et al. (2009) compared three types of conduits (NeuraGen®, Neurotube®, Neurolac®) against autografts. The study reported that Neurotube® had the poorest results for motor functions compared to the others (Kehoe et al., 2012, Shin et al., 2009). A recent study by Reid et al. (2013) reported similar numbers of myelinated axons at 18 weeks following sciatic nerve repair between both autografts and PCL nerve conduits repairs in rat (Reid et al., 2013).

Advantages:

Easy fabrication, low cost, highly soluble in many organic solvents, non-toxic degradation products (less acidic than PLA), randomised clinical trials report that Neurolac® has comparable efficiency to autograft in bridging up to 20 mm nerve gaps, and has the majority of pre-clinical data among FDA approved conduits (Kehoe et al., 2012).

Limitation:

High rigidity (breakage of the conduits during suturing due to its rigidity has been reported), inflexible, complications such as tissue reaction, swelling, fragmentation, and collapse (Kehoe et al., 2012). Slow degradation, up to 4 years in some conditions (Rai et al., 2012).

1.7.4 FDA Approved Materials

1.7.4.1 Polycaprolactone (PCL)

PCL is a synthetic biodegradable polyester that has great promise for clinical use as a nerve guide conduit (Reid et al. 2013). It has shown good outcomes in many experimental studies. In Reid et al's 2013 study, PCL conduit was used to repair a 1cm gap in sciatic nerve injury model of rat. The results of PCL repairs were similar to autograft repairs in term of the volume of regenerated axons at 18 weeks postoperative. Based on these reported data, PCL was used in this thesis using a promising manufacturing process, Micro-Stereolithography [µSL]. More details on PCL and µSL can be found in Chapters 2, 3 and 5.

1.7.4.2 Polyglycerol Sebacate (PGS)

Polyglycerol Sebacate (PGS) is a novel biodegradable polymer, first mentioned in 2002 as a good synthesised polyester for soft tissue engineering (Ameer et al., 2002, Rai el at., 2012). The material was recently developed and used as a nerve guide conduit because it has mechanical properties similar to those observed in the peripheral nerve. PGS material has a Young's modulus of 0.28 MPa which is very close to the peripheral nerve (approximately 0.45 MPa). Also, it has a greater than 0.5 MPa ultimate tensile strength and a fast degradation rate (complete resorption) was observed at day 60 (Sundback et al., 2005). In addition, PGS is inexpensive, translucent, and not rigid (possible to use suture through it).

In a study by Sundback et al. (2005), PGS was compared to poly-lactide-co-glycolide (PLGA) implanted in the sciatic nerve. Although the results demonstrated that PGS and PLGA caused the same early tissue responses, the inflammatory responses evoked by PGS continued to reduce while in the PLGA group it spiked later. Also PGS had significantly lower fibrosis and without notable swelling during the time of degradation (Sundback et al., 2005). More details on PGS can be found in Chapter 6.

1.8 NEUROPATHIC PAIN

One of the big challenging in the peripheral nerve injuries is the development of neuropathic pain even after repair. The sense of pain is extremely valuable for survival as it has a protective role; it tells us of any actual injury and keeps the damage to a minimum level through actions such as avoidance of use or seeking help. However, this is changed when the pain becomes chronic, which is considered to be a disease (Dworkin et al., 2010, Mika et al., 2013, Monkhouse and Ali, 2013, Woolf and Mannion, 1999). In cases where the tissue damage is sudden, reversible pain hypersensitivity is established in the affected tissues and surrounding areas (Woolf and Mannion, 1999). This process acts as a guard for the affected area because it prevents any contact with it until healing has occurred. On the other hand, persistent pain syndromes have no

biological function, which in turn leads to suffering and distress. Such pain commonly occurs due to damage to the nervous system (PNS, dorsal root ganglion/dorsal root, or CNS), and is termed neuropathic pain (Woolf and Mannion, 1999). Neuropathic pain was defined by the International Association for the Study of Pain (IASP) as ‘‘pain initiated or caused by a primary lesion or dysfunction in the nervous system’’ (Treede et al., 2008, pp. 1630). This definition is useful to distinguish neuropathic pain from other types of pain; however, the definition has some limitations as it lacks both anatomic precision and diagnostic specificity. For that reason, the definition of neuropathic pain was replaced and redefined as ‘‘pain arising as a direct consequence of a lesion or disease affecting the somatosensory system’’ (Treede et al., 2008, pp. 1631). Neuropathic pain leads to extreme secondary changes in the whole nervous system (Mika et al., 2013). It has been described as ‘‘the most terrible of all tortures which a nerve wound may inflict’’ (Jaggi and Singh, 2011). Chronic pain is either neuropathic or nociceptive in origin, and it is considered to be maladaptive (Monkhouse and Ali, 2013) (Table 1.8).

Table 1.8: IASP pain definitions (Monkhouse and Ali, 2013, pp.426).

Pain	An unpleasant sensory and emotional experience associated with actual or potential tissue damage or described in terms of such damage
Acute pain	Awareness of noxious signalling from recently damaged tissue, complicated by sensitisation in the periphery and within the central nervous system
Chronic pain	Pain without biological value that has persisted beyond the normal tissue healing time (usually taken to be 3 months). This may be nociceptive or neuropathic in origin
Neuropathic pain	Pain caused by a lesion or disease of the somatosensory nervous system. It is a clinical description (not a diagnosis) which requires a demonstrable lesion or a disease that satisfies established neurological diagnostic criteria
Nociceptive pain	Pain that arises from actual or threatened damage to non-neural tissue and is due to the activation of nociceptors (high-threshold sensory receptors of the peripheral somatosensory nervous system that are capable of transducing and encoding noxious stimuli)

Girlon et al. predicted that the prevalence of neuropathic pain is approximately 3% of the population (Gilron et al., 2006). It is believed that it is multi-factorial with many mechanisms working at multiple sites; one mechanism could be responsible for many different symptoms. Furthermore, one symptom may result from more than one mechanism. Lastly, the same symptom in two different patients could be caused by different mechanisms, and these mechanisms could change over time (Monkhouse and Ali, 2013, Woolf and Mannion, 1999). This results in the development of a great variation in the degree, type, and duration of pain in patients with the same clinical diagnosis (Monkhouse and Ali, 2013). Thus, it is impossible to predict which mechanism is responsible for causing pain in patients with neuropathic pain based on the aetiology of the neuropathy or nature of the symptoms. In addition, it is hard to select the proper management without knowing the responsible mechanisms (Woolf and Mannion, 1999).

Neuropathic pain is classified depending on either the aetiology that affects the nervous system or the anatomical allocation of the pain. Although this classification is used as a differential diagnosis of the neuropathy, it has no role in the clinical management of the pain (Woolf and Mannion 1999). A patient with neuropathic pain suffers from a stabbing, sharp, electric shock or shooting pain characterised by one or more positive/negative features of neuropathic pain (Tables 1.9 and 1.10) (Monkhouse and Ali, 2013, Nickle et al., 2012). Although neuropathic pain may be diagnosed and classified solely on the basis of history, clinical examination is required as in other neurological diseases (Treede et al., 2008).

Table 1.9: Definition of common positive symptoms of neuropathic pain (from Monkhouse and Ali, 2013, pp.427).	
Hyperalgesia	Increased perceived pain from a stimulus which is normally painful.
Allodynia	Pain resulting from a stimulus that would not normally provoke pain. There is an implicit change in the sensory quality of the stimulus.
Dysaesthesia	Unpleasant abnormal sensations, whether spontaneous or evoked (includes allodynia and hyperalgesia) .
Paraesthesia	An abnormal sensation, but not unpleasant or painful, whether spontaneous or evoked.
Hyperaesthesia	Increased sensitivity to stimulation (includes hyperalgesia and allodynia)
Hyperpathia	Abnormal pain response (i.e. explosive, unusual radiation, extreme severity) to stimuli (often repetitive) applied to an area of decreased sensitivity (i.e. denervated).

Table 1.10: Definition of common negative symptoms of neuropathic pain (from Monkhouse and Ali, 2013, pp.428).	
Hypoaesthesia	Decreased sensitivity to stimulation.
Hypoalgesia	Decreased sensitivity to painful stimuli.

1.8.1 Mechanisms of Neuropathic Pain

Although several mechanisms of neuropathic pain have been elucidated during recent years, the complete picture has not resolved yet. Here is an explanation of 4 classes of maladaptive changes that occur following nerve injury.

1.8.1.1 Sensitization of Nociceptors

Nociceptors are receptors with stimulus-specific variant modalities that located at the nerve endings of both thin myelinated Aδ and un-myelinated C fibres (Cohen and Mao, 2014, Meacham et al., 2017, Nickel et al., 2012). They are activated and modulated by exogenous or endogenous substances. The endogenous substance includes inflammatory mediators (prostaglandins and bradykinin), growth factor (nerve growth factor) and neurotransmitters (histamine, serotonin and noradrenalin) (Figure 1.13A) (Liu and Yuna, 2014, Meacham et al., 2017, Nickel et al., 2012).

After axonal damage, pro-inflammatory cytokine mediators (interleukins and tumour necrosis factor α), prostaglandins, bradykinin, and nerve growth factor (NGF) are released. It is believed that hyperalgesia is associated with increased NGF levels (Nickel et al., 2012, Tsuda et al., 2017). Neuropathic pain is associated with increased activation of a number of intracellular signalling pathways including protein kinases (e.g. mitogen-activated protein kinase, MAPK), nitric oxide, and 2^{nd} messenger (e.g. cyclic AMP). These signalling pathways initiate structural and functional changes that are linked to the development of persistent pain (Nickel et al., 2012).

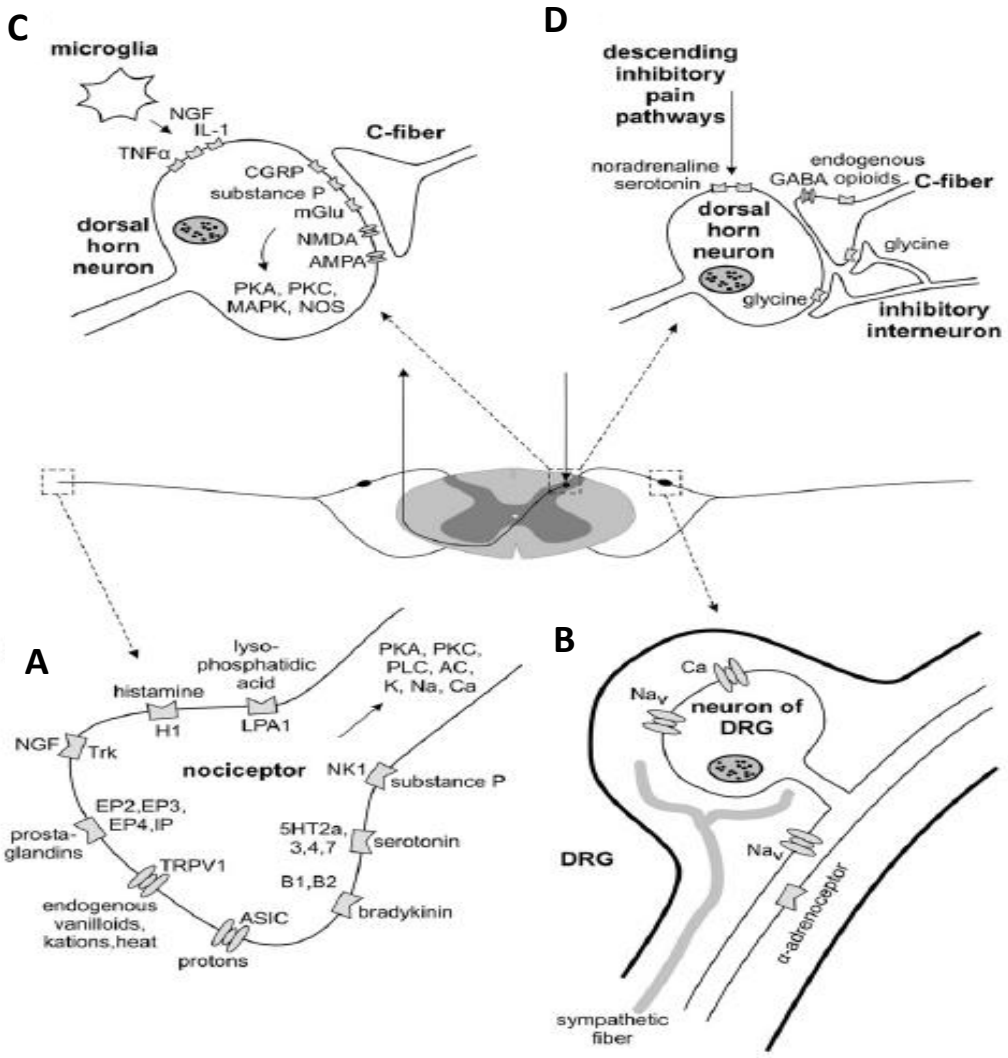

Figure 1.13. Synopsis of mechanisms contributing to neuropathic pain. A) Sensitization of nociceptor. B) Abnormal ectopic excitability of afferent neurons. C) Facilitation of pronociceptor at the spinal dorsal horn. D) Disinhibition of nociceptors (see text for details) (Nickel et al., 2012, pp. 83).

1.8.1.2 Abnormal Ectopic Excitability of Afferent Neurons

Positive symptoms of neuropathic pain are caused by abnormal excitability of afferent neurones (Meacham et al., 2017). The mechanisms leading to the development of this activity are complex and a wide range of molecules have been implicated, some examples are described below.

Sensory neurones express two classes of sodium channels; the first class is sensitive to tetrodotoxin (TTX-S), and is responsible for the initiation of the action potential. These channels are fast acting and found in all sensory neurones. The second type is insensitive/resistant to tetrodotoxin (TTX-R), and has slower activation and inactivation kinetics than TTX-S. TTX-R channels exist only in nociceptor sensory neurones and they are implicated in pathological pain (Nickel et al., 2012, Novakovic et al., 1998, Patel and Dickenson, 2016).

Following nerve injury, the concentration of both sodium channel types will increase at the site of the injury and along the axon length, which in turn leads to foci of hyperexcitability and production of ectopic action potential discharge in both cell body and axon of the affected sensory neurons (Nickel et al., 2012, Woolf and Mannion, 1999). Another type of channel involved in the development of neuropathic pain is Ca^{++} channels (Figure 1.13B). They are expressed at a high level following neural damage, leading to increased excitability and sensitization. Activation of voltage-gated Ca^{++} channels leads to the release of neurotransmitters and neuropeptides for example Glutamate and substance P. Development of allodynia correlates with increased expression of the α2δ subunit of voltage-gated Ca^{++} channels in dorsal root ganglia (DRG). Blockage of Na^{+} or Ca^{++} channels is believed to reduce neuropathic pain (Nickel et al., 2012).

1.8.1.3 Pronociceptive Facilitation at the Spinal Dorsal Horn

Primary afferent Aδ and C fibres terminate at spinal projection neurones and interneurons, types of spinal dorsal horn neurones. The thalamus and parabrachial area are innervated by spinal projection neurones, while interneurons serve many functions. These interneurons provide a polysynaptic connection between primary afferent fibres and lamina I projection neurones. In addition, they modify synaptic transmission at the spinal dorsal horn (Meacham et al., 2017, Nickel et al., 2012) (Figure 1.13C).

The main excitatory transmitter in the CNS is glutamate. Glutamate receptors can be classified into three types implicated in the transmission of signals in peripheral pain.

One metabotropic G-protein coupled glutamate (mGluR) receptors, and two ionotropic receptors; α-amino-3-3hydroxyl-5-methyl-4-isoxazeloproprionoc acid (AMPA) and N-methyl-D-aspartate (NMDA) (D'Mello and Dickenson, 2008, Nickel et al., 2012). mGluRs are subdivided into three classes. Receptors in group I, which includes mGluR1 and 5, activate phospholipase leading to enhance the synaptic transmission as well as neural discharge. On the other hand, Receptors in group II, which includes (mGluR2 and 3), and group III, which includes (mGluR4, 6, 7 and 8), inhibit the adenylyl cyclase and decrease transmission of nociceptive signals (Pan et al., 2008). Activation of AMPA receptors mediates the basic respond to acute painful stimuli. NMDA receptors can be blocked by Mg^{++}. This blockage can be released by repetitive depolarization caused by amplification and prolongation of noxious input into the spinal dorsal horn. Disinhibition of NMDA is also caused by the neuropeptides substance P and calcitonin-gene related peptide (CGRP), which are found in C fibre terminals. Moreover, activation of nitric oxide synthetase (NOS), mitogen-activated protein kinase (MAPK) pathway and protein kinase A and C (PKA, PKC) may induce synaptic plasticity (D'Mello and Dickenson, 2008, Woolf and Salter, 2000). These mechanisms lead to increased excitability of nociceptive central neurones, which in turn become activated not only by C and Aδ fibres but also by Aβ fibres. This explains the extension in the receptive field of nociceptor fibres in the periphery and increased stimulus-evoked painful sensation (Meacham et al., 2017, Nickel et al., 2012). Several recent studies have also described a significant role for spinal glial cells in the pathogenesis of neuropathic pain (see section 1.8.2.1).

1.8.1.4 Disinhibition of Nociceptors

The activation of neurones in the dorsal horn projecting into the central system has an important role in pain perception. It is depended on a number of inhibitory factors, such as descending inhibitory noradrenergic and serotonergic pathways (Figure 1.13D). Glycinergic and GABAergic synapses exert inhibitory effects at the spinal dorsal horn. Inhibitory synaptic transmission by glycine and GABA has been shown to reduce in neuropathic pain. This leads to disinhibition of nociceptive input which in turn increases

the pain sensation. Expression of dynorphin, an endogenous opioid peptide, in inhibitory interneurons could decrease their activity. It is reported that dynorphin acts on bradykinin receptors. The use of spinal cord stimulation (SCS) therapy is believed to improve inhibitory GABAergic signalling (Nickel et al., 2012). Following nerve injury, the balance of excitatory and inhibitory control is shifted and excitatory mechanisms are strengthened while inhibitory mechanisms are weakened in neuropathic pain (Trang et al., 2012).

1.8.2 Glial Activation in Neuropathic Pain

Although the mechanisms underlying the maintenance and persistence of neuropathic pain are still unclear, spinal glial activation has been reported and implicated as a key regulator in many recent studies (Mika et al., 2013). Glial activation is a part of the classic immune defence that acts to protect the body (Figure 1.14) (Imamato et al., 2013, Liu and Yuan, 2014, Mika et al., 2013). Glia account for approximately 70% of cells in the nervous system, and can be divided into microglia and macroglia. In the resting condition, glial cells are quiescent. In contrast, following peripheral nerve injury, glial cells become activated and release numerous pro-inflammatory factors (Liu and Yuna, 2014, Mika et al., 2013).

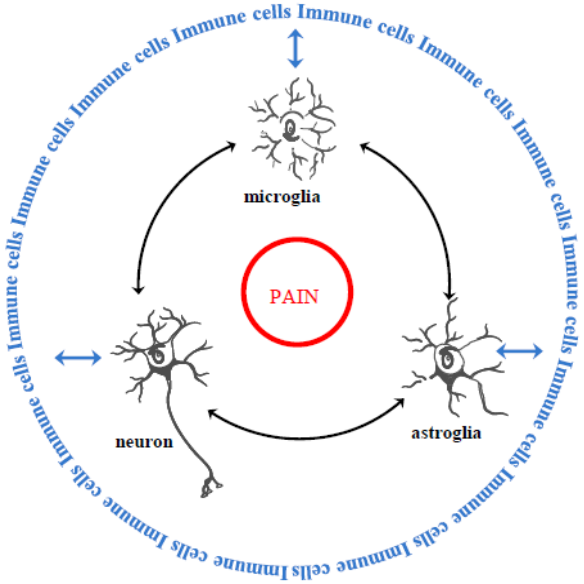

Figure 1.14. Interaction between neuron and glia in neuropathic pain (Mika et al., 2013, pp.107).

1.8.2.1 Role of Microglia in Neuropathic Pain

The immune system is represented at the spinal cord level by the microglial cells. Under normal conditions, microglia account for around 5-20% of all glia cells. Microglial cells can be activated 24 hours after nerve injury at the dorsal horn and remain activated for approximately 12 weeks (Liu and Yuan, 2014, Mika et al., 2013). Following injury, microglia adopt an amoeboid-like structure and undergo proliferation at the ipsilateral spinal dorsal horn (Trang et al., 2012). The onset of pain symptoms (e.g. hyperalgesia and allodynia) is believed to be associated with microglial activation (Coyle, 1998, Liu and Yuan, 2014, Mika et al., 2013, Tanga et al., 2004).

Microglia-neuron interaction mediated via ATP-gated P2-receptors, has an essential role in the pathogenesis of nerve injury-induced neuropathic pain. ATP is an endogenous ligand of the P2 receptor family; these receptors are expressed by activated microglia, and divided into ionotropic (P2X) and metabotropic (P2Y) receptors. Microglial expression of P2Y receptors includes P2Y1, 2, 4, 6, and 12 receptor subtypes, and they are coupled to intracellular 2^{nd} messenger systems via heteromeric G protein. On the other hand, microglial expression of P2X receptors consists of only two receptors subtypes, P2X4 and P2X7, and they are non-selective cation channels permeable to K^+, Ca^{++}, and Na^+ (Liu and Yuan, 2014, Trang et al., 2012).

A number of molecules have been implicated in the upregulation of P2X4Rs including: Fibronectin, Chemokine (C-C motif) ligands (CCL21), interferon γ (IFN), tryptase. ATP stimulation of P2X4Rs leads to influx of extracellular Ca^{++}, which in turn induces the phosphorylation and activation of activation of P38 mitogen-activated protein kinase (p38 MAPK) particularly the β isoform expressed by microglia (Beggs and Salter, 2013, Trang et al., 2012) (Figure 1.15).

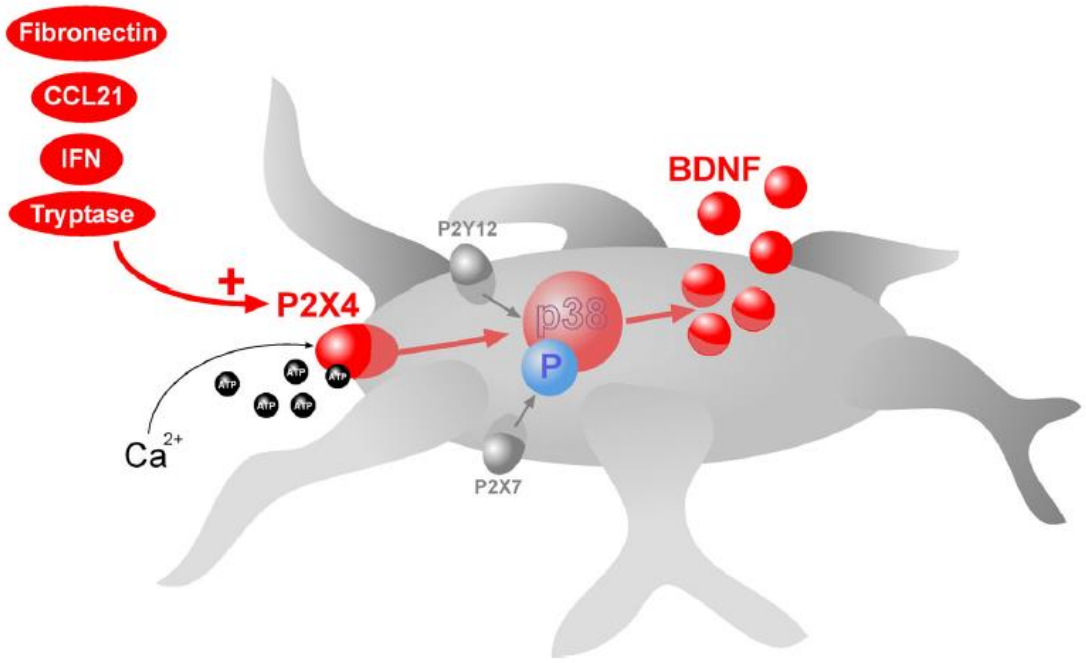

Figure 1.15. The role of P2X4, P2X7, and P2Y12 receptors signaling in activation of p38 MAPK and release of BDNF (Trang et al., 2012, PP. 359).

Activation of p38 MAPK leads to synthesis and release of brain-derived neurotrophic factor (BDNF) by the microglial cell. BDNF is a cellular pain signal between microglia and neurones in the spinal cord, and causes disinhibition of nociceptive dorsal horn neurones by disrupting intracellular Cl^{-} homeostasis (Beggs and Salter, 2013, Trang et al., 2012). Disinhibition of microglia-neuron signalling improves excitatory synaptic transmission at spinal dorsal horn to transform the output of the nociceptive network (Beggs and Salter, 2013, Trang et al., 2012). In addition to P2X4R, activation, both P2X7 and P2Y12 receptors also signal via P38 MAPK. P2X7R-P38 MAPK signalling assists in the releasing of interleukin-1β and cathepsin S, which are involved in the maintenance of mechanical hypersensitivity. Although microglia express many of P2YRs, only the P2Y12R has been reported, so far, to have a role in neuropathic pain. The mechanism of P38 MAPK activation by P2Y12 remains unclear (Liu and Yuan 2014, Trang et al., 2012). Blockage of P2X4R has been reported to decrease the microglial BDNF level, impairing the signalling of BDNF in spinal cord, and preventing the development of mechanical allodynia after nerve injury (Liu and Yuan, 2014).

Implication of microglial activation has been reported in many models of neuropathic pain such as chronic constriction injury (CCI) (Mika et al., 2009), partial sciatic nerve ligation (PSNL) (Coyle 1998), spinal nerve injury (Tsuda et al., 2003), and spared nerve injury (SNL) (Beggs and Slater, 2007).

1.8.2.2 Role of Macroglia in Neuropathic Pain

Astrocytes, star-shaped cells, are the most abundant macroglial cells in the nervous system (Liu et al., 2011, Mika et al., 2013). Increased astrocyte activation on the affected side of the spinal cord following sciatic nerve injury was first observed by Garrison and colleges in rat (Mika et al., 2013, Garrison et al., 1991). As mentioned previously, microglia are implicated in the early stages of the development of pain; activated astrocytes were observed at 3 days and this continues up to 12 weeks post-injury, and is thus proposed to be implicated in the persistence of pain (Liu and Yuan, 2014, Mika et al., 2013, Romero-Sandoval et al., 2008).

Astrocytes act as bridges in the CNS, between microglia, neurones, oligodendrocytes, and astrocytes themselves. Pro-inflammatory cytokines, especially interleukin-1 (IL-1), play an essential role in microglial-mediated activation of astrocytes. IL-1 is characterised by fast release in pathological conditions and the ability to upregulate other inflammatory cytokines (Liu et al., 2011). Is believed that microglia are the only source for IL-1 in the CNS (Herx and Yong, 2001, Liu et al., 2011). Astrocyte activation depends on the endogenous IL-1 (released from microglia) or exogenous administration (Liu et al., 2011).

The main job of astrocytes is the uptake of Gamma-aminobutyric acid (GFAP) and extracellular glutamate found in the synaptic region via astrocytic transporters. Induction and persistence of pain mainly depend on the reduction in uptake activity of glutamate transporters (Mika et al., 2013). IL-1 dose-dependently inhibited the uptake of glutamate by astrocytes, which in turn leads to increase the levels of glutamate that could exert over excitation of neurones. Moreover, free radicals are released from astrocytes activated by IL-1. Besides IL-1, IL-18 also has a role in activation of microglia/astrocytes

(Figure 1.16) (Liu et al., 2011). It has been reported that IL-18 and IL-18R express at the spinal dorsal horn, and were upregulated in hyperactive microglia and astrocyte respectively, after nerve injury. Inhibition of IL-18 signalling pathways suppressed injury-induced tactile allodynia, and decreases the phosphorylation of nuclear factor KappaB in astrocytes (Liu et al., 2011).

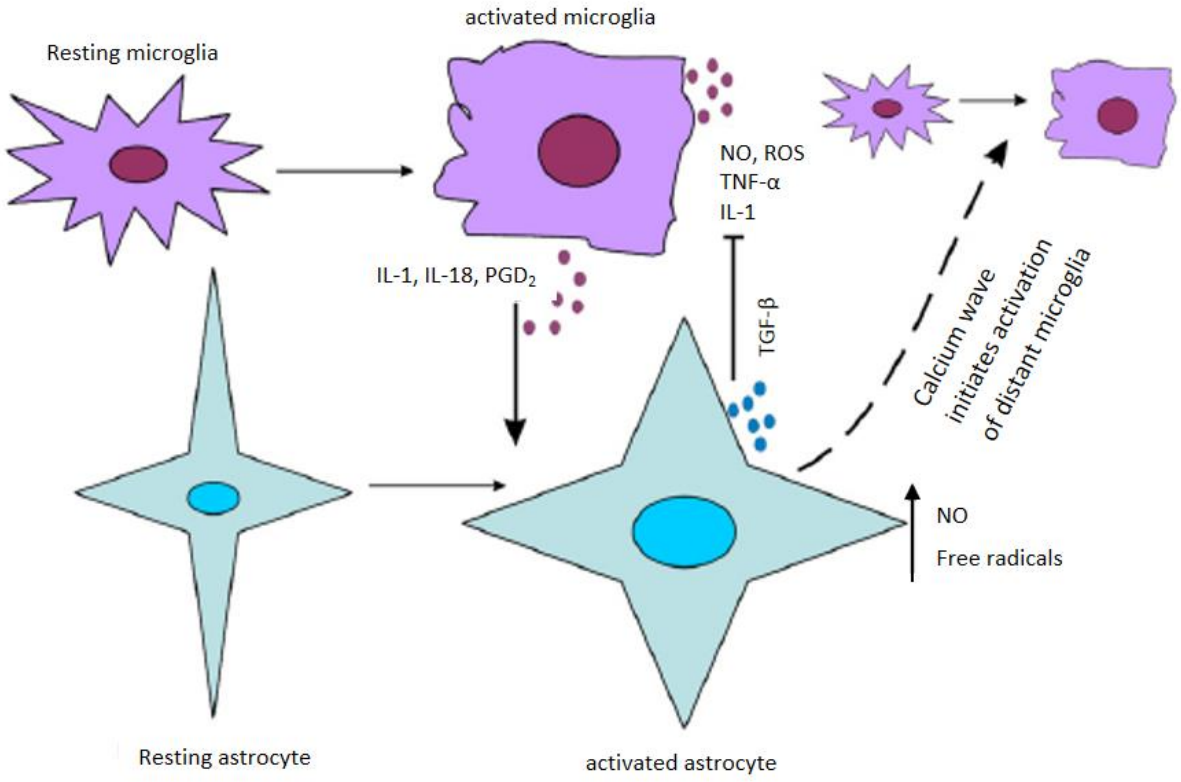

Figure 1.16. Intercommunication between microglia/astrocyte activation. Activated microglia assess facilitates the activation of astrocytes by pro-inflammatory cytokines (such as IL-1). Activated astrocytes promote distant microglial activation through calcium wave, and by downregulating NO, ROS, and TNF-α can also inhibit the activation of microglia at the same time. ATP: adenosine triphosphate; IL-1: interleukin 1; IL-18: interleukin 1; PGD_2: prostaglandin D_2; TGF-β: transforming growth factor beta; NO: nitric oxide; ROS: reactive oxygen species; TNF-α: tumor necrosis factor alpha (Modified from Liu et al., 2011, pp.144).

Activated astrocytes promote distant microglial activation through calcium waves (Figure 1.16) (Liu et al., 2011). Upon the activation of astrocytes, the cytosolic Ca^{++} increased and propagated among astrocytes, called a calcium wave. The main responsible messenger for this is ATP, which could mediate astrocyte-to-microglia communication. Several studies showed that ATP released from activated astrocytes during calcium wave propagation leads to the activation of microglia (Liu et al., 2011). ATP-derived from astrocytes induces vesicle formation in local microglia facilitating microglial phagocytosis. In contrast, ATP-degrading enzyme apyrase and P2X7 receptor antagonists have been shown to inhibit this process. Astrocytic Ca^{++} signalling and the ability of astrocytes to propagate long-distance Ca^{++} waves contribute to the activation of distant microglia (Liu et al., 2011).

Activated astrocytes have an inhibitory effect on microglia by decreasing the production of NO, TNF-α, and reactive oxygen species (ROS) from microglia. It has been reported that transforming growth factor beta (TGF-β), which is predominantly produced by astrocytes, reduces microglial activation. TGF-β inhibits the activation of microglia by downregulating the expression of molecules that are associated with antigen presentation and production of NO, pro-inflammatory cytokines, and oxygen free radicals (Liu et al., 2011). The role of oligodendrocytes and radial cells, types of macroglial cells, in nociceptor transmission is still not established (Mika et al., 2013).

1.9 STRATEGIES FOR IMPROVING PERIPHERAL NERVE REGENERATION

There are currently established several strategies to promote axon regeneration. Some of these strategies include biomolecular based therapies, cellular based therapies such as the use of macrophages to clear debris. Cellular transplantation is another strategy such as modified fibroblasts, Schwann and stem cells (Alovskaya et al., 2007). Reducing the amount of scarring and inflammation at the site of peripheral nerve repair is considered to be an alternative approach to improve the regeneration of peripheral nerves. Some of these strategies have already been used with conduit repairs (Figure 1.12).

1.9.1 Scarring of Injured Peripheral Nerves

Scarring is important for natural wound healing process; however, the presence of scar tissue formation around the site of injury can impede the regeneration process (Graham et al., 1973, Lane et al., 1978; Sunderland, 1978). This applies to the degenerative and regenerative processes described in 1.5.1 and 1.5.2, intraneural scarring leads to increased deposition of collagen that can be detrimental to these two processes and results in an impediment of the regenerating axons and the restoration of the continuity of the nerve.

Proof of this concept was provided by Atkins et al. (2006b) who reported that better recovery is associated with the reduction of scar formation at the site of nerve repair. They compared the regeneration of the sciatic nerve in two transgenic mice strains with an increased propensity for scarring [IL-4L/IL-10 null mice] or decreased propensity for scarring [M6PR/IGF2 null mice] and compared them to normal mice. It was reported that the peripheral nerve regeneration (compound action potential ratio) of IL-4L/IL-10 mice reduced because of increased the scarring when compared to normal mice. In contrast, peripheral nerve regeneration of M6PR/IGF2 mice was enhanced when compared to normal mice (Atkins et al., 2006b).

1.9.1.1 Transforming Growth Factor and its Role in Scarring

Transforming growth factor-β (TGF-β) is a cytokine strongly linked to the repair of damaged tissue. Several cytokines are involved in dermal wound healing, but TGF-β has the widest range of activity among these agents and affects all healing process phases (Harding et al., 2014, Roberts and Sporn, 1996, Shah et al., 1992, Shah et al., 1995). TGF-β has many pivotal roles in nerve regeneration after injury, such as acting as a stimulator for chemotaxis of monocytes (macrophages after entering tissue), which helps in Wallerian degeneration. Also it turns Schwann cells from an inactive state to a proliferative state, this may encourage neurite outgrowth (Einheber et al., 1995).

TGF-β is produced in three iso-forms, named TGF-β1, TGF-β2 and TGF-β3. As TGF-β is a multifunctional cytokine, each iso-form has special biological abilities and actions. TGF-β1 is the most abundant type that is found in most tissues. It is chemotactic to fibroblasts and macrophages, causes angiogenesis and formation of granulation tissue, and reduces degradation of extracellular matrix (Roberts and Sporn 1996, Williams et al., 1992). TGF-β2 is found mainly in bodily fluid and may act interactively with TGF-β1. TGF-β3 is implicated in the migration of cells and the restoration of natural dermal appearance (Ferguson and O'Kane., 2004).

It has been reported that the ratio of TGF-β iso-forms is different between adult and embryonic wounds. It is reported that adult wounds, healed with scar tissue formation, contain high levels of TGF-β1 and TGF-β2 with low levels of TGF-β3. On the other hand, embryonic wounds healed with an absence of scarring as well as lower inflammatory and cytokines response, contain low levels of TGF-β1 and TGF-β2 with high levels of TGF-β3 (Ferguson and O'Kane, 2004, Whitby and Ferguson, 1991). All three iso-forms are found in Schwann cells in uninjured and injured peripheral nerve, and their ratios in injured nerve are comparable to that found in injured dermal tissue (Rufer et al., 1994).

1.9.1.2 Manipulation of TGF-β

Investigations have suggested that manipulation of TGF-β in adult wounds may mimic embryonic wounds and result in a reduction of scarring (Ferguson and O'Kane, 2004, Shah et al., 1992, Shah et al., 1995). Our raised understanding of scarring opens a new approach to reduce it by targeting the impact of TGF-β, and this may be achieved by inhibition of TGF-β1 and TGF-β2 and/or exogenous application of TGF-β3.

Exogenous addition of TGF-β3 peptide was mentioned by Ferguson and O'Kane (2004) and Shah et al. (1995) as an approach to reduce scarring in skin via a decrease in the levels of monocytes and macrophages in addition to the deposition of collagen I and III. In contrast, in Atkins et al's 2007 study it did not decrease intra-neural scarring or enhance the nerve regeneration. They concluded that the TGF-β3 concentration used in

the study was not sufficient. Another approach to reduce scarring has been the neutralising of TGF-β1 and TGF-β2 using antibodies. Administration of neutralising antibodies to TGF-β1 and TGF-β2 was reported to reduce skin/intra-neural scarring in many studies. In Shah et al's 1992 study, a group of adult rats were injected with neutralising antibody (NA) to TGF-β and compared to groups injected with TGF-β, irrelevant antibody, and non-injected group. Their results showed that the skin wounds healed without scarring in treated-NA group, while in the other groups the skin wounds healed with scar tissue formation. In addition, the results also reported that the level of macrophage, collagen, blood vessels were lower in the NA-treated group. However, more natural dermal architecture and similar tensile strength compared to other groups were present. They concluded that early manipulation of TGF-β concentration using relevant antibodies was a novel approach to control the level of scar tissue formation (Shah et al., 1992).

A study by Davison et al. (1999) reported that neutralising antibodies to TGF-β1 helps to reduce the scarring at the site of nerve injury as well as the regeneration was improved. Whereas, the outcomes of a study by Atkins et al. (2006a) mentioned that neutralising antibodies to TGF-β1 and TGF-β2 reduced the scarring but impeded, rather than improved, nerve regeneration.

1.9.1.2.i Neutralising of TGF-β by Addition of Mannose-6-Phosphate

Neutralising of TGF-β in order to decrease the amount of scarring formation at the site of injury by using anti-scarring agent's such as Mannose-6-Phosphate (M6P), is an alternative approach to improve regeneration. There are two identified M6P receptors; ~46-kDa cation-dependent MPR (CD-M6PR) and ~300-kDa cation-independent MPR/insulin-like growth factor-II (IGF-II) receptor (CI-M6PR). M6P is a molecule which binds to CI-M6PR and inhibits the activation of latent TGF-β (Ghosh et al 2003). TGF-β is produced from cells and stored in the extra-cellular matrix as an inactive complex bound to the latency-associated protein (LAP), and unable to bind directly to its receptors (Roberts and Sporn, 1996). CI-M6PR is reported to facilitate the activation of

latent TGF-β as it has several binding sites for LAP (Zhang et al., 2015). Binding of TGF-β-LAP to CI-M6PR leads to separation of TGF-β from LAP. TGF-β can then bind to the TGF-β receptor (Dennis and Rifkin, 1991, Roberts and Sporn, 1996). Hence, M6P is considered a competive inhibitor of latent TGFβ activation (Figure 1.17).

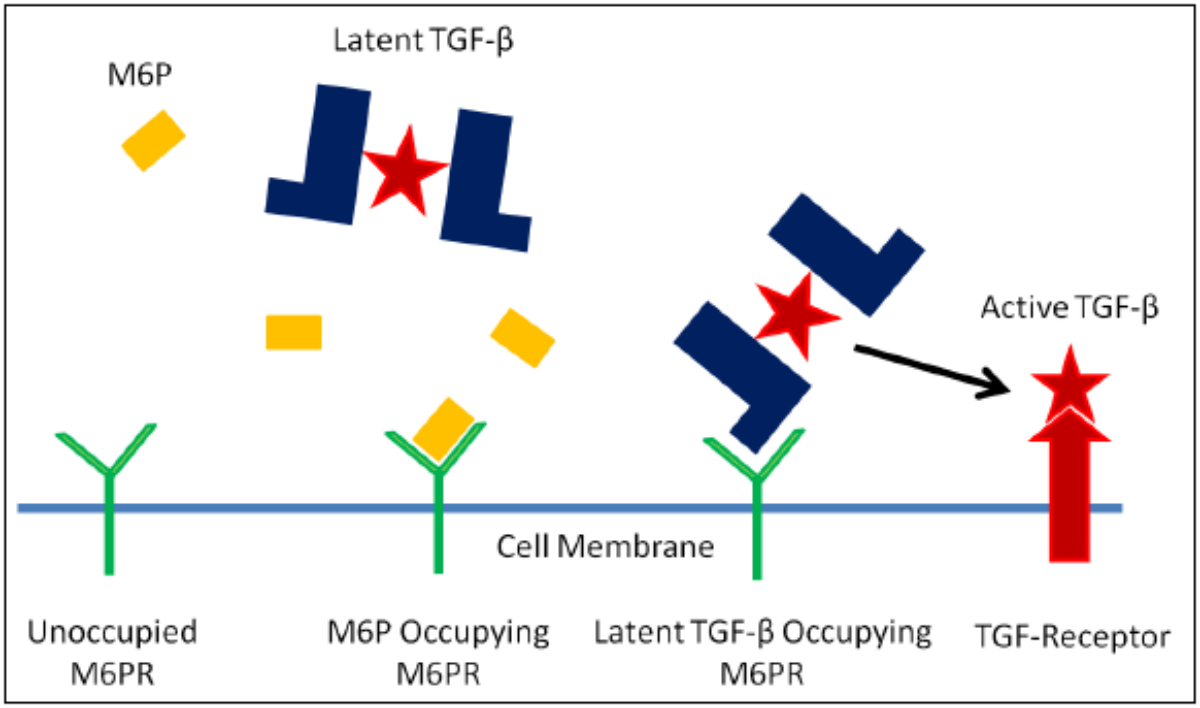

Figure 1.17. Diagram illustrating the role of M6P in preventing the activation of latent TGF-β as it competes with latent TGF-β for access to M6P receptors (Harding, 2014).

A series of studies performed by McCallion and Ferguson (1996) investigated the potential use of M6P as a scar reducing agent and compared it to M1P. Deposition of collagen was observed at an early time point in both groups. At 7-days post-injury, lower macrophage and monocyte infiltration was reported in M6P compared to M1P-treated wounds, in addition to significant reduction of scar formation in M6P-treated wounds. Several mechanisms have been suggested by which M6P might reduce scar formation:

A) Inhibition of latent TGF-β activation

B) Reduction in the cellular sequestration of platelet-released TGF-β by cells at the site of injury.

C) Inhibition of formation of the large latent TGF-β complex by prevention of latent TGF-β binding protein polymerization to the LAP at the M6P receptor.

D) Induction of changes in the number or state of activation of inflammatory cells recruited to the wound site.

Recent studies by Ngeow and colleagues (2010, 2011a) have investigated nerve regeneration following M6P treatment. The results showed a significant improvement of peripheral nerve regeneration at an early stage (6 weeks) following M6P treatment. More details on M6P can be found in Chapter 4.

1.9.1.3 The Effects of Anti-inflammatory Agent in Scarring

The process of wound healing starts with the early inflammatory phase and finishes with scar maturation. Because of this, the use of anti-inflammatory agents as scar reducing agents has been established. Many studies have been carried out in our laboratory to investigate potential nerve injury treatment with therapeutics that help to reduce scar formation at the site of injury via their anti-inflammation effects (Atkins et al., 2007, Ngeow et al., 2011b). Etanercept, a decoy tumour necrosis factor alpha (TNF-α) receptor which binds and removes any TNF-α in the sample, is a new approach that was used and investigated in this thesis (Chapter 5).

1.9.1.3.i Etanercept

TNF-α is a pro-inflammatory cytokine that mediates several immune functions. It is secreted by many cells, especially fibroblasts, monocytes, and activated macrophages (Khan et al., 2005, Weinblatt et al., 1999). TNF-α has an important role in the pathogenesis of many diseases, particularly rheumatoid arthritis (RA) (Weinblatt et al., 1999).

Etanercept is a genetically engineered fusion protein that binds with type II TNF receptors that acts to diminish the effectiveness of TNF-α. It has two human TNF-receptors; TNFR1 (p55) and TNFR2 (p75) that merged with the Fc domain of human IgG1, then binds and inactivates the TNF. Neutralising of TNF-α receptors has been reported to reduce the activity of RA (Mease et al., 2000, Weinblatt et al., 1999). Two

previous studies demonstrated a significant benefit with minimal toxicity when using etanercept in patients with RA, who failed to respond to other drugs (Moreland et al., 1997, Moreland et al., 1998, Weinblatt et al., 1999). Additionally, TNF signals trigger a number of intracellular events resulting in the activation of transcription factor nuclear factor-κB (NF-κB), which is implicated in the suppression of apoptosis of several cells in the inflammatory responses. Hence, blocking of TNF can inhibit the activation of NF-κB and increase apoptosis of inflammatory cells which in turn decreases the inflammatory response (Chan et al., 2000, Khan et al., 2005). There is a considerable potential for the use of etanercept s in enhancing nerve regeneration as they have a significant role in reducing inflammation that has a strong link in reducing scarring, in addition to their minimal toxicity. More details can be found in Chapter 5.

1.9.2 The Use of Genetically Modified Mice in Peripheral Nerve Repair

The use of standard animal model to assess nerve regeneration required the harvested nerve to be cut into thin sections and specific staining performed in order to enable the axons to be visible using the microscope, and even after staining it is impossible to trace the axons as the sectioning process will produce loss in axon continuity. However, when using certain genetically modified animals, axons can inherently fluoresce and the harvested nerve can be directly placed under the fluorescent microscope as the axons are visible without the requirement for additional processing. In addition, fluorescent proteins produce strong fluorescent signals (Unezaki et al. 2009; Yan et al., 2011).

The discovery of the jellyfish green fluorescent protein (GFP) as a vital stain and a valuable marker of gene-expression helped to make it possible to stain specific components of living cells (Feng et al., 2000). A study by Feng et al. (2000) generated transgenic mice expressing green (GFP), yellow (YFP), red (RFP), and cyan (CFP) fluorescent protein (collectively termed XFPs) all incorporating similar regulatory elements [from the *thy1* gene]. All of these four variants satisfactorily label neurons in vivo, and they have no discernible impact for up to 9 months upon synaptic structure. All

strains of the four variants labeled specific neurons entirely, including dendritic spines, dendrites, nerve terminals and axons (Feng et al., 2000).

To be able to generate the transgenic mice, a modified *thy1* vector was used to delete exon 3 and the introns alongside using *Xho1* restriction enzyme for the purpose of replacing the deleted region with a transgene (i.e. YFP) (Figure 1.18) (Caroni 1997, Feng et al., 2000). A fertilised mouse oocyte was injected with the modified *thy1* vector that contained the relevant fluorescent protein transgene. Animals positive for the transgene were then used to found strains (Feng et al., 2000).

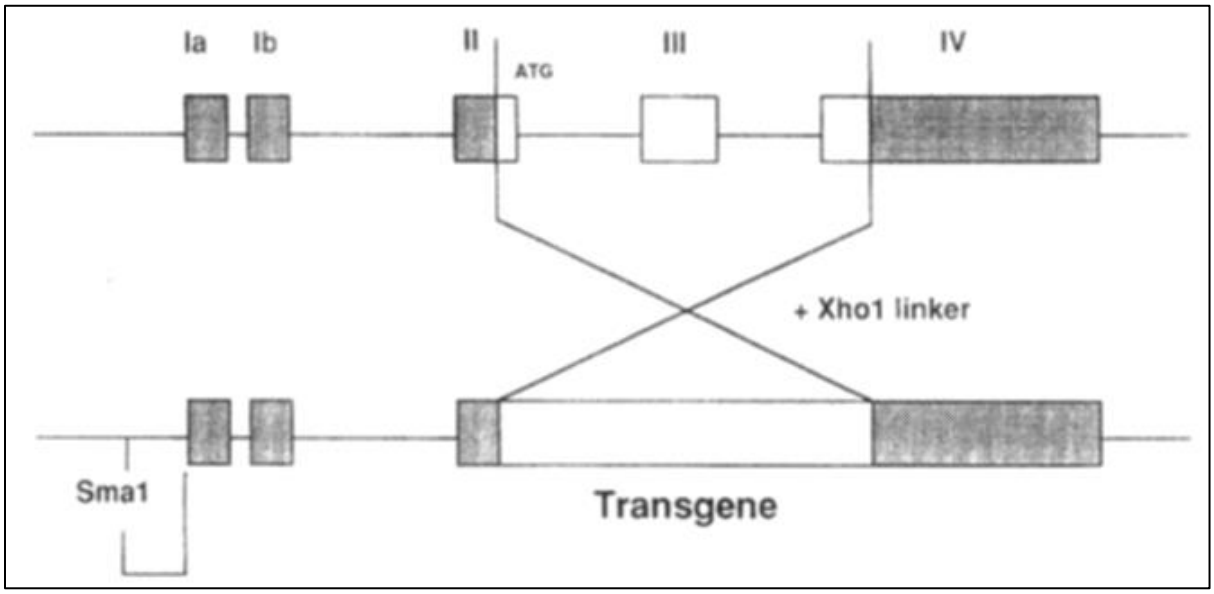

Figure 1.18: Schematic presentation of thy-1 gene modification. Top: thy-1 gene before removal of exon 3 and the introns alongside using *Xho1* restriction enzyme. Bottom: thy-1 gene after replacing deleted region by chosen transgene in place (Caroni, 1997).

Each XFP transgenic mouse strain expresses a unique heritable pattern of fluorescent protein because of the chromosomal integration and/or copy number of the transgene are different. As a result, groups of neurons are labelled by XFP in some lines, allowing analysis of processes (e.g. axonal guidance, neuronal migration, synaptogenesis and dendritic growth). Two factors play a vital role in this variation; the percentage of neurons found in specific tissues and the intensity of the XFP labelling (Feng et al., 2000).

Among all the different colour variants that were used to generate strains of *thy1-XFP* expressing mice, YFP (*thy1-YFP-H*) has proven the most popular in experimental studies compared to the other strains (Feng et al., 2000, Pateman et al., 2015, Sabatier et al., 2008). The *thy1-YFP-H* mice were generated by Feng et al. (2000) and have been used with excellent results in many nerve regeneration studies (Groves *et al.*, 2005, Harding *et al.,* 2014, Pateman et al., 2015). T*hy1* is an immunoglobulin that is expressed by projection neurons in the nervous system as well as non-neuronal cell types (Feng et al., 2000, Morris, 1985). Early transgenic examination discovered that both expression (neural and non-neural) rely on special genomic elements, and that deletion of a specific intron selectively abolishes expression in non-neural cells (for details, Vidal et al., 1990). A construct without this intron has been effectively used to overexpress β-galactosidase and growth-promoting molecules in neurons with lower non-neural expression (Caroni, 1997, Kelley et al., 1994). The *thy1-YFP-H* strain expresses limited yellow fluorescent protein in a subset of axons, and for the entire length of these axons (Figure 1.19) (Feng et al., 2000, Groves et al., 2005). As this strain has limited number of axons expressing YFP, it means that the density of fluorescent axons is reduced in the peripheral nerve. Thus, individual axons are easier to identify and trace in this strain. Approximately 2.6% of all sensory axons are YFP labelled [based on 122.6 YFP labelled axons out of 4625 in the L4 spinal nerve (Lieble et al., 1997)] was calculated by Groves et al (2005). Also, they reported that sensory axons make up around 58% of all labelled axons. Another study by Witze et al. (2005) reported that 72% of YFP labelled axons in the sciatic nerve were sensory axons and 28% were motor axons.

Line	Motor Axon	Retina		SCG		DRG
		RGC	INL	Pre	Post	
YFP-12	All	Many	A	None	None	Many
-16	All	All	A+B	All	Few	All
-21	All	All	A	All	Many	All
-A	Many	Many	A	Many	None	Many
-C	All	All	A+B+M	All	Few	All
-D	All	All	A	All	None	All
-F	All	Many	A	Many	None	All
-G	All	Many	A	All	Few	All
-H	Few	Few	None	Few	Few	Many

Figure 1.19: Patterns of transgene expression in thy-1-YFP lines showing that YFP-H has fewer numbers of labelling than others. All = expression in >80% of neurons; many = expression in 10-80%; few = expression in <10%. RGC = retinal ganglion cells; INL = inner nuclear layer of the retina [A = amacrine cells, B = bipolar cells, M = Muller cells]; SCG = superior cervical ganglion; DRG = dorsal root ganglion. Modified from (Feng et al., 2000).

All the experimental studies reported in this thesis were performed using *thy1-YFP-H* mice model for the following reasons:

A) No staining process is required as the axons are visible under the fluorescent microscope.

B) This strain has proven the most popular and used successfully in several nerve regeneration studies among others XFP. In addition, all similar studies in our laboratory are using this mice strain

C) The labelled axons remain for up to 9 months upon the synaptic structure.

D) Individual axons are easier to identify and trace as the expression of YFP is limited to a subset of axons.

1.10 GENERAL AIMS AND OBJECTIVES

The overall aim of this project is to use *thy1-YFP-H* mice to investigate efficacy of nerve repair, and the potential for the development of neuropathic pain, following a range of different repair methods. The specific aims were:

- To develop methodology to quantify spinal cord glial activation, and to investigate whether the efficacy of different types of conduits, in terms of supporting nerve regeneration, influences the degree of glial activation and therefore the potential development of neuropathic pain [chapter 3].
- To determine whether an anti-scarring agent (M6P) enhances nerve regeneration and/or decreases the potential for development of neuropathic pain using an easy method of application (incorporated within fibrin glue) [chapter 4].
- To determine whether nerve conduit repair in conjunction with an anti-inflammatory agent (etanercept) vs nerve conduit repair alone enhances nerve regeneration and/or decreases the potential for development of neuropathic pain [chapter 5].
- To determine whether nerve conduits constructed from polyglycerol sebacate support nerve regeneration and/or decrease the potential for the development of neuropathic pain compared to graft repairs [chapter 6].

Many of the protocols for these experimental studies were based on previous studies undertaken at the School of Clinical Dentistry, University of Sheffield and have been previously described by Atkins et al. (2006a, 2007) and Harding et al. (2014).

CHAPTER 2

MATERIALS AND METHODS

2.1 INTRODUCTION

My project has investigated the effects of different types of conduits, a scar reducing agent, Mannose-6-Phosphate, (Merck, UK) and anti-inflammatory agent, etanercept (Enbrel® 25mg, Pfizer Limited, Sandwich, UK/Reino Unido) on peripheral nerve regeneration after repair. In order to assess nerve regeneration, a combination of methods including immunohistochemistry, electrophysiology, behavioural methods (CatWalk), and axon counting and tracing analysis were used.

This chapter provides a detailed description of the materials, methodology, and protocols for analysis. Further brief descriptions of the specific methods used will be provided in the subsequent chapters. All experiments were performed under UK Home Office license regulations and approval (UK Animal {Scientific Procedures} Act, 1986), under Project Licence number PPL 70/8194. I was granted a personal license number PIL 36111 in order to undertake the work mentioned in this thesis.

2.2 MATERIALS AND METHODS

2.2.1 Animals

thy1-YFP-H mice, on a C57BL6 background, were used in all experiments (see section 1.9.2). In addition, Wild type mice littermates, from heterozygous breeding, were used as donors for nerve grafts.

All mice used in the experiments described in this thesis were descendants from four breeding pairs purchased in 2009 from JAX® Mice (Maine, USA via Charles River UK Limited, Margate, UK). The YFP-H (Yellow Fluorescent Protein) pairs consisted of one heterozygous YFP-H mouse and one wild-type (WT) mouse [C57BL-6J background] derived from previous YFP-H/WT matings. The purpose of this mating is to provide mixed litters with equal numbers of YFP-H and WT mice. In experiments that required nerve grafts, WT littermates were used as donors to provide the graft material in the experimental YFP-H mouse that required nerve grafting.

The common fibular (CF) nerve, a terminal branch of the sciatic nerve, has been used widely for nerve regeneration experiments in these mice because it has been reported that it contains more YFP-labeled axons (36.03±2.35) than the tibial nerve, the other terminal branch of the sciatic nerve. (Groves et al., 2005). Hence, the CF nerve is more appropriate for tracing of YFP axons. The sciatic nerve is commonly utilised in peripheral nerve regeneration studies; however, has a relatively large number of YFP-labeled axons (±80), which makes YFP tracing analysis more difficult and time consuming than the common fibular nerve. In cases where investigations required assessment of a larger gap injury, the sciatic nerve is more appropriate because it provides an adequate length and space that makes the application of graft or conduit easier. As the sciatic nerve has three branches; CF, tibial and sural nerves, it covers several areas in the hindlimb. So, it provides a robust test to assess recovery following nerve injury. Electrophysiology and behavioural testing (e.g. CatWalk) are commonly used analysis after sciatic nerve injury (Rodriguez et al., 2004).

The mice were housed in a climate-controlled room (between 19 and 21^{o}C) maintained on a 12-hour light/dark cycle in soft-wood-chip-lined plastic cages in a central animal care facility (Biological Services Unit, University of Sheffield) with free access to food (standard rodent chow) and water. During the post-operative recovery period, mice were singly housed in order to reduce the incidence of suture removal. All mice were aged between 8 and 18 weeks old when surgery was performed to reduce any age related differences in outcomes. Mice aged between 12-18 weeks old were used in experiments using the CF nerve (chapters 4 and 6) as there was insufficient space to place conduits in mice <12 weeks old. Mice aged between 8-13 weeks old were used in the artificial nerve guide conduit experiments that were performed in the sciatic nerve (chapter 5).

2.2.2 Methods of Manufacture

All conduits included in this thesis were produced by either: Micro-Stereolithography [µSL], selective laser sintering [SLS] or Ultraviolet [UV] curing manufacturing techniques.

2.2.2.1 Micro-Stereolithography [µSL]

Conduits produced using µSL technique were obtained from the laboratory of Professor John Haycock and Dr. Frederik Claeyssens [Kroto Research Institute University of Sheffield, UK] where this technique developed. These conduits were used in studies described in Chapters 3, 5, and 6.

µSL was chosen because it has several positive properties such as the ability to create complex microstructures, which may enable guidance channels to be incorporated within the conduits in the future.

A pre-polymer solution of PCL was used to produce conduits made by the µSL. PCL material is approved by FDA for several uses (see section1.8.3.2). Its use depends on some factors such as the biological suitability of this material and the ability of using µSL for manufacture conduits. PCL materials have been used previously in many *in vitro* and *in vivo* studies with successful outcomes (Chiono et al., 2008, Chang, 2009a, Chang, 2009b).

A 405 nm µSL setup was used to create conduits used in chapters 3, 5 and 6. The setup comprising of: 100 mW 405nm tunable laser source with associated software (Vortran Laser Technology Inc, Sacramento, CA, USA), a (Texas Instruments Incorporated, TX, USA), motorised z-axis translation stage apparatus attached to a metal stage (Thorlabs Ltd, Cambridgeshire, UK), and a software to control the Z-stage (APT Software, Thorlabs Ltd, Cambridgeshire, UK) (Pateman et al., 2014). The process is illustrated in (Figure 2.1). The 405nm laser was directed to DMD. Bitmap images were created using Microsoft Paint software that initially uploaded onto the DMD to project the laser beam to a desired shaped (i.e a hollow tube) and dimensions. The

laser beam is reflected off the DMD and expanded through an assembly of lenses and mirror (Thorlabs Ltd, Cambridgeshire, UK) which then direct the beam down onto a pre-polymer PCL solution. This leads to curing of the pre-polymer PCL solution at the surface where the Z-stage was located. The Z-stage then proceeded to move down at a rate of 0.01mm/s, allowing the cured pre-polymer layer to drop and a fresh subsequent layer to be cured on top, creating a three-dimensional structure. By creating the final layer and reaching the desired length, the μSL process was complete. The conduit was then carefully removed from the Z-stage and immediately submerged into denatured alcohol (90% ethanol/10% methanol) for 72 hours to allow the removal of any remaining of uncured pre-polymer (Pateman et al., 2014). All conduits were sterilised using UV irradiation before the implantation. To achieve the desired conduit length, laser cutting was used; this gives a clean and accurate cut.

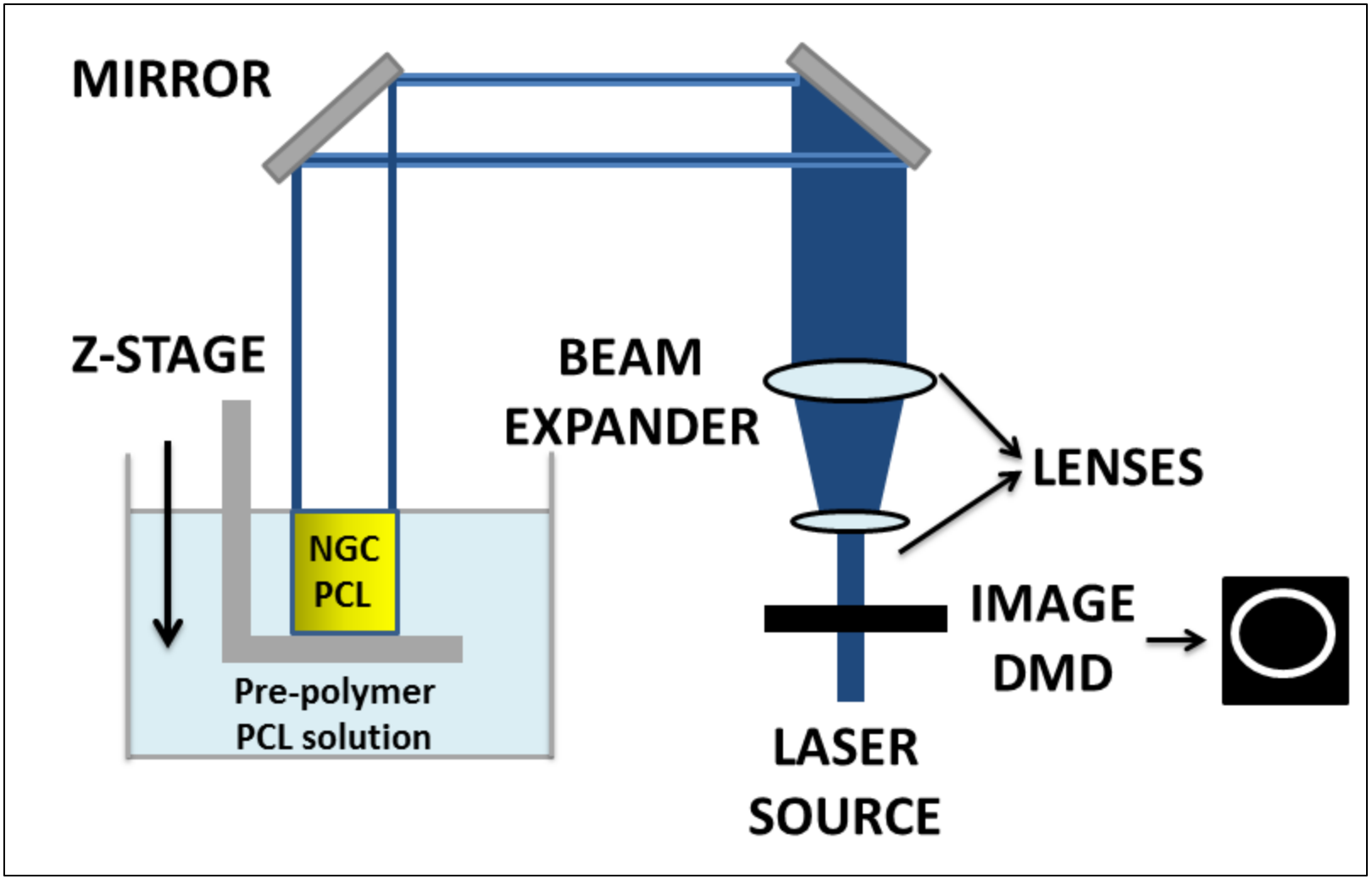

Figure 2.1: Schematic overview of microstereolithography (μSL) process (Modified from Pateman et al., 2014).

2.2.2.2 Selective Laser Sintering [SLS]

The conduits produced by SLS technique were obtained from the laboratory of Professor Neil Hopkinson [Department of Mechanical Engineering, University of Sheffield, UK]. These conduits were only used in studies described in Chapter 3.

SLS is a layer manufacturing process allows creating 3D structures by solidifying layers of powdered material on top of each other (Dotchev and Yusoff, 2009). An EOS Forming P100 was the SLS machine used to produce the Nylon conduits in this study. It uses a scanning system to direct a laser beam at a layer of fine nylon-12 powder [the standard material for this machine (Johnson et al. 2013)]. The powder will sinter (melt) into a pattern adjusted by a CAD image file (Figure 2.2). Once the desired pattern is sintered, the powder's stage moves down by a predetermined distance. On top of the old powder layer, a new layer of Nylon-12 powder will be spread by using a dispensing hopper. This leads to sintering the new pattern layer, and so on until the desired shape is formed. After completion of the process, the formed conduit is removed from the non-sintered powder and the loose powder is removed by pressurised air (Dotchev and Yusoff, 2009).

It was difficult to clear out all the non-sintered powder from the internal surface of the conduits as they have a small inner diameter size. So, in addition to the pressurised air, a hypodermic needle filled with alcohol was used for further removal of the remaining powder out of the conduits. After that, the conduits were soaked in denatured alcohol from 48 hours for the purpose of removing any remaining powder. Finally, the conduits were placed in the autoclave for sterilisation (at 120^{o}C for 20 minutes), ready for implantation.

2.2.2.3 Ultraviolet Curing

The PCL material was cured by UV around a smooth metal rod to form a 3D conduit with a smooth internal surface. Then the samples cut to the desired sizes. It is a molding process rather than a 3D printed process, which form in a layer by layer such as SLS or µSL. These conduits were only used in studies described in Chapter 3.

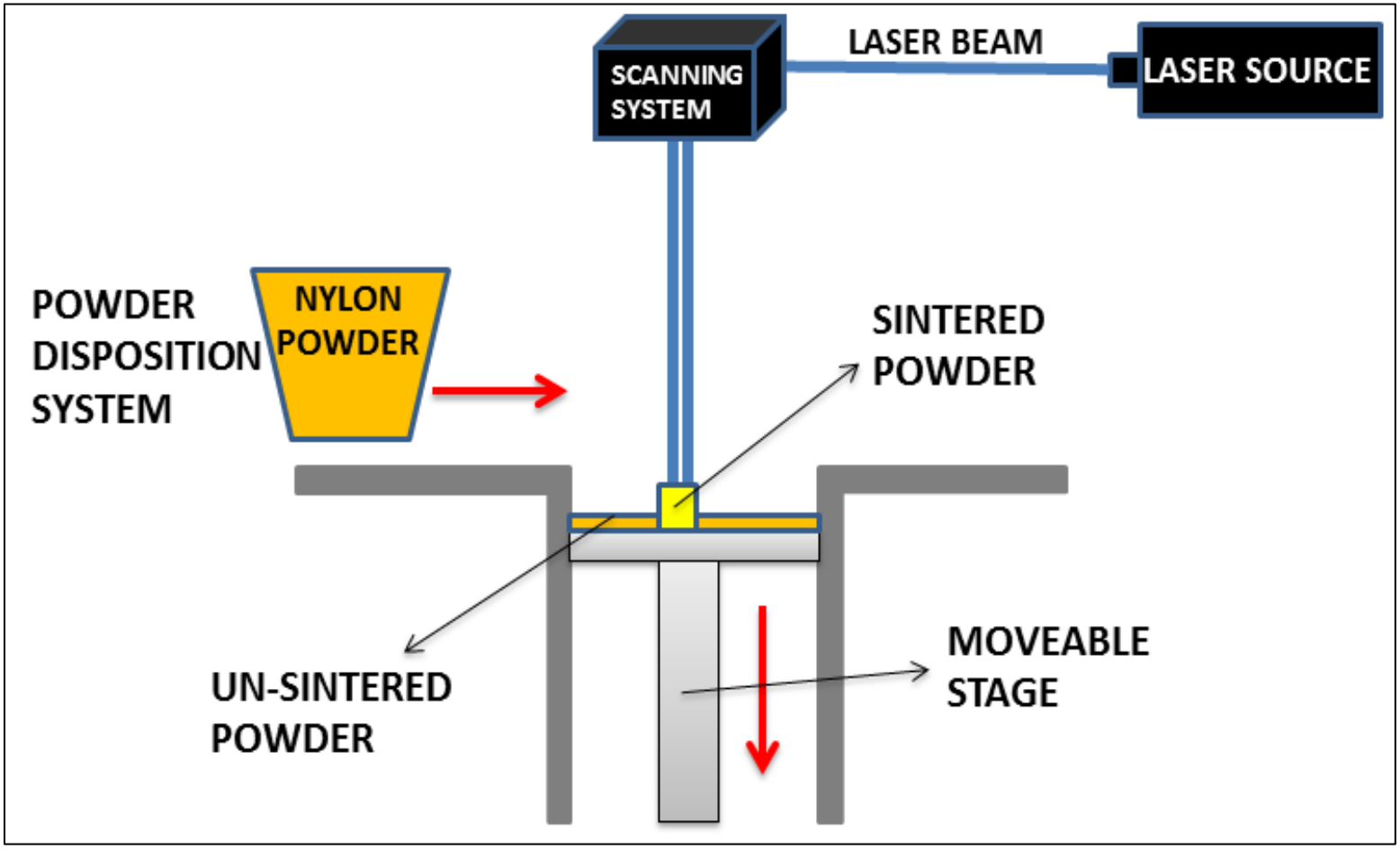

Figure 2.2: Schematic overview of Selective Laser Sintering (SLS) process.

2.2.3 Surgical Procedures

2.2.3.1 Nerve Repair Procedure

Prior to each surgery, all the surgical instruments and devices were sterilised using (Autoclave *Classic;* Prestige Medical Limited, Blackburn, UK). The health of animals was checked carefully and the body weight was measured.

2.2.3.1.i Anaesthesia

Anaesthesia for nerve repair procedures was induced using an isoflurane (Isofli®, Abbott Laboratories, UK) oxygen (BOC, UK) mixture. Induction was initiated by placing the animal in a special transparent box connected to an anaesthetic machine [Harvard Apparatus LTD, Kent, UK] providing a mixture of 4% isoflurane in 100% oxygen at a flow rate of 4L/minute. Once anaesthetised, the animal was placed on a thermostatically controlled blanket [Harvard Apparatus LTD, Kent, UK] in order to maintain body temperature at 37.5 ± 2^{o}C. Maintenance of anaesthesia was achieved by connecting the animal to the anaesthetic machine's vaporizer, via a special nosepiece and providing 1-4L/minute of 1.5-4% isoflurane in 100% oxygen. To keep the depth of the anaesthesia at the correct level, the respiratory rate and reflex responses to paw squeeze were visually checked throughout the procedure.

2.2.3.1.ii Nerve Injury

Once anaesthetised (as described in section 2.2.3.1.i), the animal was placed in the prone position with extended left leg. After shaving the leg and cleaning it with hibitane solution, the leg was secured in place using adhesive tape. Using a surgical microscope (Global Microscope: DP Medical Systems Ltd, Surrey, UK), a longitudinal incision was made on the posterolateral aspect of the thigh. The CF/Sciatic nerve was then carefully exposed and freed from the surrounding tissues by blunt dissection.

2.2.3.1.iii Preparation and Placement of Nerve Graft

The Wild-type littermate of the YFP mouse was anaesthetised using a combination of fentanyl 0.8ml/kg (Hypnorm; VetaPharma Ltd, Leeds, UK) and midazolam 4mg/kg (Hypnovel; Roche Products Limited, Welwyn Garden City, UK), inter-peritoneal (ip) injection. Once anaesthetised, the common fibular nerve was exposed (as described in section 2.2.3.1.ii) and freed from the surrounding tissues, preparing it to be trimmed and removed later. The muscle and skin were placed back over the nerve.

YFP mice were prepared to receive the nerve graft under general anaesthesia (as described in section 2.2.3.1.i). The left common fibula was exposed (as described in section 2.2.3.1.ii), a 5.0mm silicone trough was placed underneath the nerve prior to sectioning, preventing the adhesion of the nerve with the underneath tissues when applying a glue during the surgery. The nerve was then transected transversely with microscissors, forming the required gap between proximal and distal ends. The nerve graft from the wild type was then trimmed and a section of 3.0mm length extracted and placed within the gap of the prepared recipient YFP littermate. The nerve graft and was aligned with the proximal and distal ends and was secured in place by fibrin glue [1:1 ratio blend of 40IU/ml thrombin and 10mg/ml fibrinogen; Sigma Aldrich, UK) that was allowed to set for 5 minutes. When the ends were secured, the silicone trough was removed and the incision closed in anatomical layers using 6-0 Coated Vicryl® suture (Polyglactin; Ethicon, US). Three sutures were used to approximate the muscles, and 7-10 sutures were placed to close the skin.

Following successful completion of the surgery, a single dose of analgesia (0.01ml buprenorphine hydrochloride 0.3mg/ml; Vetergesic®, Alstoe Animal Health, UK) was then administered subcutaneously (sc) before placing the YFP mouse in an incubator (Octagon TL-4 Brooder; Brinsea Products Ltd, Winscombe, UK) to fully recover from the effects of anaesthesia. The wild-type mouse was then culled by dislocation of the neck whilst still under anaesthesia, and the YFP mouse was returned to its cage for the14-day recovery period. The mouse was carefully checked for any sign of excessive pain, bleeding, or infection regularly during the recovery period.

2.2.3.1.iv Implantation of Nerve Guide Conduit

Under general anaesthesia (as described in section 2.2.3.1.i), the left CF or sciatic nerve of the YPF mouse was exposed and freed from the surrounding tissue (as described in section 2.2.3.1.ii). The nerves were then transected transversely forming a 3.0mm gap for the CF and 4mm gap for the sciatic. The proximal and distal nerve ends were inserted approximately 1.00mm for the CF and 0.5mm for the sciatic into the conduit and secured by fibrin glue (1:1 ratio blend of thrombin and fibrin; Sigma, UK) that was allowed to set for 5 minutes. The incision was then closed in anatomical layers using 6-0 Coated Vicryl® suture (Polyglactin; Ethicon, US).

Following the successful completion of the surgery, a single dose of analgesia was then applied subcutaneously before placing the animal in an incubator to fully recover from the effects of anaesthesia. The animal was returned to its cage for a 3 or 5-week recovery period (CF or Sciatic, respectively). The mouse was carefully checked for any sign of excessive pain, bleeding, or infection regularly during the recovery period.

2.2.3.1.v Administration of Mannose-6-Phosphate and Etanercept

M6P was applied incorporated with fibrin glue. The majority of studies load drugs into the fibrinogen to allow them to be distributed throughout the solution before crosslinking with thrombin (Gao et al., 2088 Wong et al., 2003); however, (Woodruff et al., 2077) loaded a drug into thrombin before cleaving fibrinogen to form fibrin glue. M6P was made up to 600mM with dH2O then used to make up the fibrinogen. Some fibrinogen was made up without M6P. M6P+fibrinogen, fibrinogen and thrombin were filled in separate syringes and stored in freezer prior to the application. At the time of surgery, two syringes (M6P±fibrinogen and thrombin) were removed from the freezer to warm up. Fibrinogen was then applied at the site of the nerve ends with the addition of thrombin to form fibrin glue.

Etanercept solution was prepared a few minutes prior to the application. Two very small openings were made in the epineurium (with a 4mm separation) using microscissors. A fine microdialysis needle was connected to a cannula, and was carefully inserted beneath the epineurium and 15µl of the etanercept was then injected in each opening. After placement of the nerve conduit (as described in section 2.2.3.1.iv), another 30µl was injected within the conduit. Finally, 2x20µl were injected beneath muscles surrounding the nerve.

2.2.3.2 Non-recovery Experimental Procedure

2.2.3.2.i Anaesthesia

Following the recovery period, the animals were re-anaesthetised using a combination of fentanyl and midazolam (as described in section 2.2.3.1.iii).

2.2.3.2.ii Harvesting Nerve Tissue for Analysis

Once anaesthetised (as described in section 2.2.3.1.iii), the left CF nerve (chapters 3, 4 and 6) was exposed (as described in section 2.2.3.1.ii). The surrounding skin flaps were raised and sutured to brass ring for the purpose of forming a pool to be filled with 4% (w/v) paraformaldehyde for 30 minutes to allow the nerve to be fixed in situ. The nerve was then dissected free from surrounding tissues and carefully removed. The right CF nerve was also removed as a control, using the same protocol.

The left sciatic nerve (described in chapter 5 with a longer gap repair) was exposed (as described in section 2.2.3.1.iii). A pool filled with paraffin was formed in order to carry out the electrophysiology (as described in section 2.2.6). Following electrophysiology, the pool was filled with 4% (w/v) paraformaldehyde for 30 minutes in order to fix the nerve and harvest it as described above. The right sciatic nerve was also removed as a control, using the same protocol.

Following removal, nerves were placed on a glass slide for more precise dissection to remove the adhered tissues/conduit as much as possible. Following nerve harvesting, the animal was culled by cervical dislocation while under anaesthesia, and the vertebral column was then removed from the animal and immersed in a tube filled with 4% (w/v) paraformaldehyde for 24 hours at 4^{o}C then placed in sucrose 30% (w/v) for 24 hours at 4^{o}C to protect tissue when freezing. The spinal cord was then freed from the vertebral column and cut in half (the lower half was used for this study as it includes L3-L6 spinal segments). The two halves were then embedded in OCT fluid (Thermo Shandon Limited, Cheshire, UK) and frozen slowly using a cryostat (Microm HM 560, Zeiss, UK) as rapid freezing makes the cords more fragile during cutting. Finally, the cords were stored in a -80^{o}C freezer.

2.2.4 Immunohistochemistry

The lower halves of the spinal cords were removed from the -80^{o}C freezer and mounted in the cryostat. Transverse sections were cut until the L4 segment was reached (CF nerve projects to the L2-L6 segments of the spinal cord) (Shuhua *et al*. 1984). After reaching the L4 segment, 8-10 sections (30µm thick) from each sample were collected, and each section was placed in a separate well in a 24 Well Plate filled with Phosphate Buffer Saline (PBS) (Table 2.1). For microglial and astrocyte labelling, the sections underwent immunofluorescence staining using the following protocol: the sections were washed by PBS (2x10 minutes) at room temperature (from this point till the end of the staining process, the plate was placed on a shaker device). Next, the sections were washed by Phosphate Buffer Saline+0.2%Triton (PBS+T) (Triton^{TM} X-100, Sigma-Aldrich, St. Louis, USA) (2x10 minutes) at room temperature. Then the sections were incubated with PBS+T containing 10% Normal Donkey Serum (NDS; Jackson ImmunoResearch Inc, West Grove PA, USA) for 1 hour at room temperature in order to increase the permeability of cell membrane to the antibodies and decrease non-specific background staining. The sections were then incubated with PBS+T containing 5% NDS including the primary antibody (Iba-1 goat polyclonal antibody (1:2500, Abcam, UK) to label microglia, or GFAP rabbit polyclonal antibody (1:2000, Abcam, UK) to label

astrocyte) overnight at 4^{o}C (Table 2.2). The following day, the sections were washed by PBS (2x10 minutes) before they were incubated with the secondary antibody (Donkey anti-goat Cy3 antibody (1:500, Jackson, UK) for microglia, or Donkey ant-rabbit Cy3 antibody (1:500, Jackson, UK) for astrocyte) in PBS+T containing 2% NDS (Table 2.3) at room temperature for 2 hours in the dark. After washing with PBS (1x10 minutes), the prepared sections were then mounted on glass slides (usually 3-5 sections on a slide) and coverslipped with Vectashield® (Vector Lab, Burlingame, CA, US).

Table 2.1: Preparation of used substances.

Substance	Volume	Preparation
Phosphate Buffered Saline	1L	950ml distilled water + 50ml 0.2M phosphate buffer + 8.8g NaCl + 0.2g KCl
Phosphate Buffered Saline+0.2%(w/v)Triton	1L	950ml distilled water + 50ml 0.2M phosphate buffer + 8.8g NaCl + 0.2g KCl + 2.0g Triton^{TM} X-100
0.2M Phosphate Buffer	1L	-Solution A: 5.928g 0.2M $NaH_2PO_4.2H_2O$ + 0.19L distilled water -Solution B: 23g 0.2M HN_2PO_4 + 0.81 distilled water -Solution A + Solution B. (pH 7.4)
30%(w/v) Sucrose Solution	100ml	50ml 0.2M phosphate buffer + 50ml distilled water+30g sucrose.
4%(w/v) Paraformaldehyde	1L	-Heat 400ml distilled water to approx.80^{o}C in a litre flask -Add 40g paraformaldehyde to the water -Add drops of 1N NaOH until the solution see clear -Cover the flask and cool down to approx. 15 ^{o}C -Add 500ml 0.2M Phosphate Buffer -Top up to 1L with distilled water -Filter the solution (End up solution, 4% paraformaldehyde in 0.1M Phosphate buffer).
1N NaOH	100ml	-Dissolve 4.5g NaOH in 100mL distilled water -Add drops of saturated barium hydroxide solution until a precipitate is formed. -Allow for complete precipitation and filter the solution.

Table 2.2: Primary antibody markers for microglia and astrocyte.			
Primary antibody	**Supplier/Catalogue Number**	**Concentration of stock antibody**	**Dilution**
Iba-1 goat polyclonal Microglial marker	Abcam/ab5076	0.5 mg/ml	1:2500 in Normal Donkey serum
GFAP rabbit polyclonal Astrocyte marker	Abcam/ab7260	1-10mg/ml	1:2000 in Normal Donkey serum

Table 2.3: Secondary antibody markers for microglia and astrocyte.			
Primary antibody	**Supplier/Catalogue Number**	**Concentration of stock antibody**	**Dilution**
Donkey anti-goat Cy3 (Microglia)	Jackson/705-165-147	1.5 mg/ml	1:500 in Normal Donkey serum
Donkey anti-rabbit Cy3 (Astrocyte)	Jackson/711-165-152	1.5 mg/ml	1:500 in Normal Donkey serum

2.2.4.1 Control for Immunohistochemistry

Several types of immunohistochemistry controls have been described (Burry, 2011).

2.2.4.1.i Primary Antibody Control

The primary antibody control shows the specificity of primary antibody to bind to the correct epitope that found on the expected antigen. Several methods have been used for the primary antibody control. The first method is a genetic approach to manipulate of the antigen protein expression. The second method is immunoblotting (Western blot), the most common used method to determine the specificity of the primary antibody as it is very reliable, straightaway, and relatively inexpensive. The third method is colocalization with the principle primary antibody with an additional primary to demonstrate that both of them will bind to the same structure. In this method, two primary antibodies bind to different epitopes that are located on the same antigen, labelling of the same structures by antibodies demonstrates that the primary antibody is

specific. The fourth method is absorption controls. This method, which was chosen for this study, depends on mixing the primary antibody with the purified antigen that was used to generate the antibody. The absorbed antibody loses its function and becomes unable to bind to antigen in the sample (Figure 2.3) (Burry, 2011, Saper and Sawchenko, 2003). Specific to the current study, Human Iba-1 peptide (ab23067, Abcam, UK) and Human GFAP peptide (ab48665, Abcam, UK), 100µg at 1 mg/ml were used in the method. 10µl from the peptide was mixed with the primary antibody for 24 hours at 4^{o}c. Following that, the staining protocol was carried out as described in section 2.2.4. The result did not show any labelling of either Iba-1 or GFAP (Figure 2.4B), demonstrating the specificity of the antibodies used.

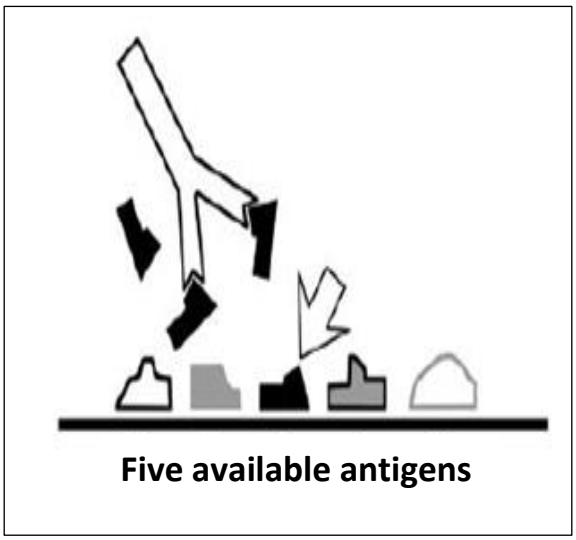

Figure 2.3: Absorption control showing the incubation of the primary antibody with the purified antigen. Incubated of the primary antibody with antigens results in prevent binding it to the antigen in the tissue (arrow) (Modified from Burry, 2011).

2.2.4.1.ii Secondary antibody controls

The secondary antibody control confirms that the observed labelling occurs due to the secondary antibody only binding to the primary antibody. Secondary antibody controls can be performed by either omission of the primary antibody or replacing the primary antibody with normal serum from the same species (Burry, 2011). For the current study, secondary antibody control was performed by omission of the primary antibody (Iba-1 goat polyclonal and GFAP rabbit polyclonal). The result did not show any labelling of either Iba-1 or GFAP (Figure 2.4C).

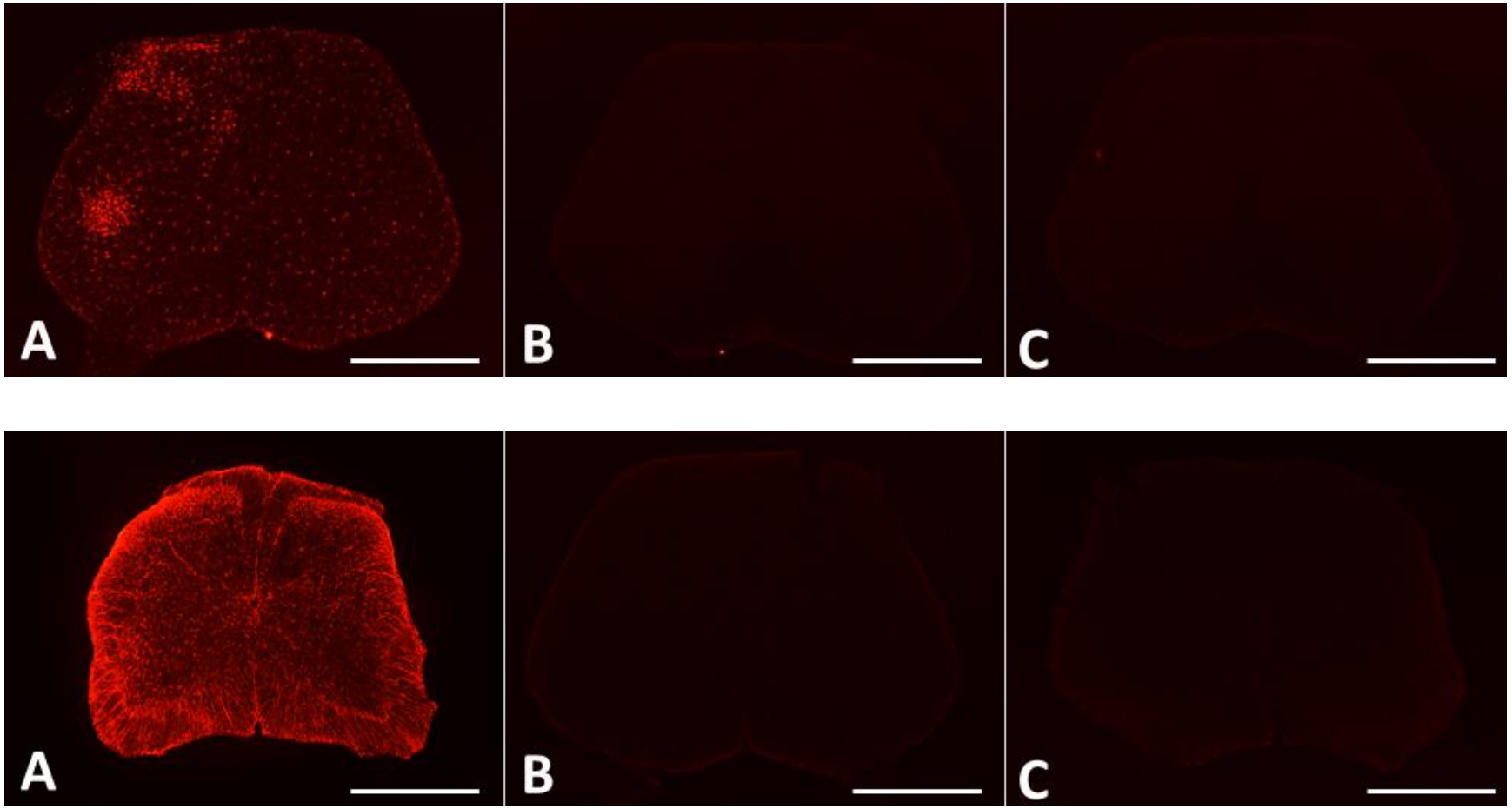

Figure 2.4. Immunohistochemistry staining of spinal cord sections for both Iba-1 (TOP) and GFAP (BOTTOM). A) Staining following a standard protocol. B) Primary antibody control. C) Secondary antibody control. scale bar = 1.0mm.

2.3.3.1 Evaluation of Iba-1 and GFAP Expression in Microglia and Astrocyte

Immunohistochemical images were acquired using a fluorescent microscope (Axioplan2 Imaging; Zeiss, Welwyn Garden City, UK) fitted with Qimaging Retiga 1300R camera, and combination excitation Cy3 filter was used to examine the fluorescent markers. The microscope is linked to a PC running Image-Pro Plus v.7 software (Media Cybernetics, MD, USA). Five pictures from each section were taken; one for the whole section (using 5x magnification), two for a specific area in the dorsal horn on both ipsilateral and contralateral sides (using 40X magnification), and two for a specific area in the ventral horn on both ipsilateral and contralateral sides (using 40X magnification) (Figure 2.5) (Molander *et al.* 1984).

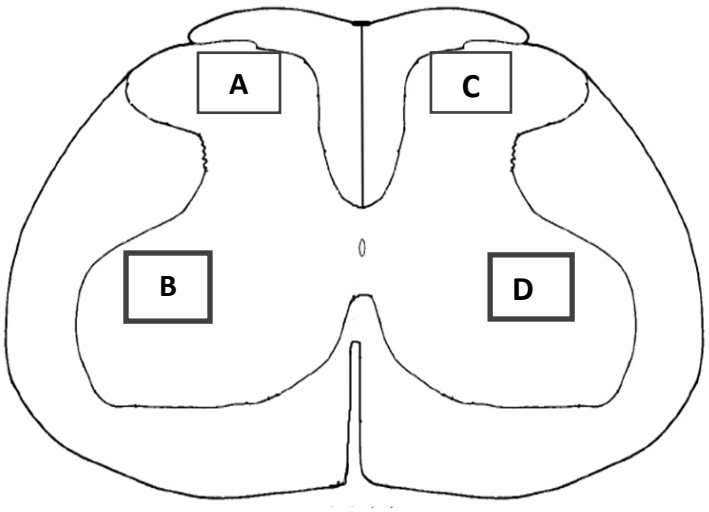

Figure 2.5: Scheme shows L4 segment of the spinal cord. A) Ipsilateral dorsal horn. B) Ipsilateral ventral horn. C) Corresponding contralateral dorsal horn. D) Corresponding contralateral ventral horn (modified from Molander et al., 1984, pp. 139).

2.3.3.2 Data Analysis of Glial Activation at Spinal Cord

To quantify the percentage area of Iba-1 and GFAP labelling, Image-Pro Plus v.7 software was used. This system enables the percentage area of glial labelling to be calculated. The activation areas would be highlighted by pink, while the remaining areas would be highlighted by yellow (Figure 2.6A, B and C). The brightness and contrast of the images were adjusted to make the images similar to that observed in the fluorescent microscope. Each reading was taken three times, and the mean was taken.

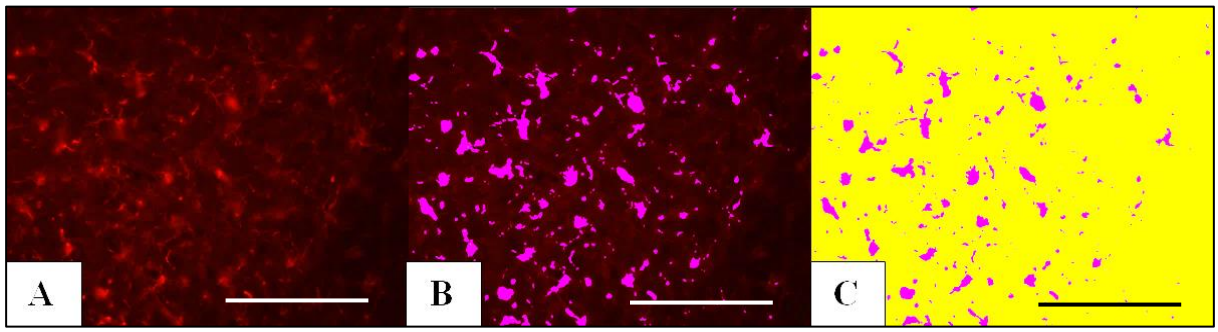

Figure 2.6: Analysis of a region of spinal cord. A) The activation area (the bright dots). B) Highlighted activation area (area of interested by pink). C) Highlighted activation area (pink) and background (yellow). The ratio of activation area (pink) to the entire picture (yellow) is calculated. Scale bar = 0.1mm.

2.2.5 Behavioural Observations

Behavioural observations are non-invasive methods used to investigate function of injured nerves. Behavioural observations include gait analysis, the CatWalk (Noldus Information Technology, Wageningen, Netherlands) gait analysis system is an advanced version which measures a wide range of gait parameters in an automated way by measuring print area (Deumens 2007).

The CatWalk system was used in experiments described in chapter 5. Data was obtained from each animal prior to the nerve injury and repair procedure and at post-operative weeks 1, 2, 3, 4, and 5. The last data collection was obtained immediately before the electrophysiological recordings on week 5. The CatWalk system (Figure 2.7) consists of a translucent glass plate (1.3m long) forming the floor of the walkway, two black parallel walls, two flexible barriers to adjust the space of the walkway and ensure that the animal will move in one direction, a fluorescent tube producing light rays which are entirely reflected internally, and a recording camera which is placed underneath the glass plate (Bozkurt et al., 2011, Gabriel et al., 2007, Vrinten and Hamers, 2003).

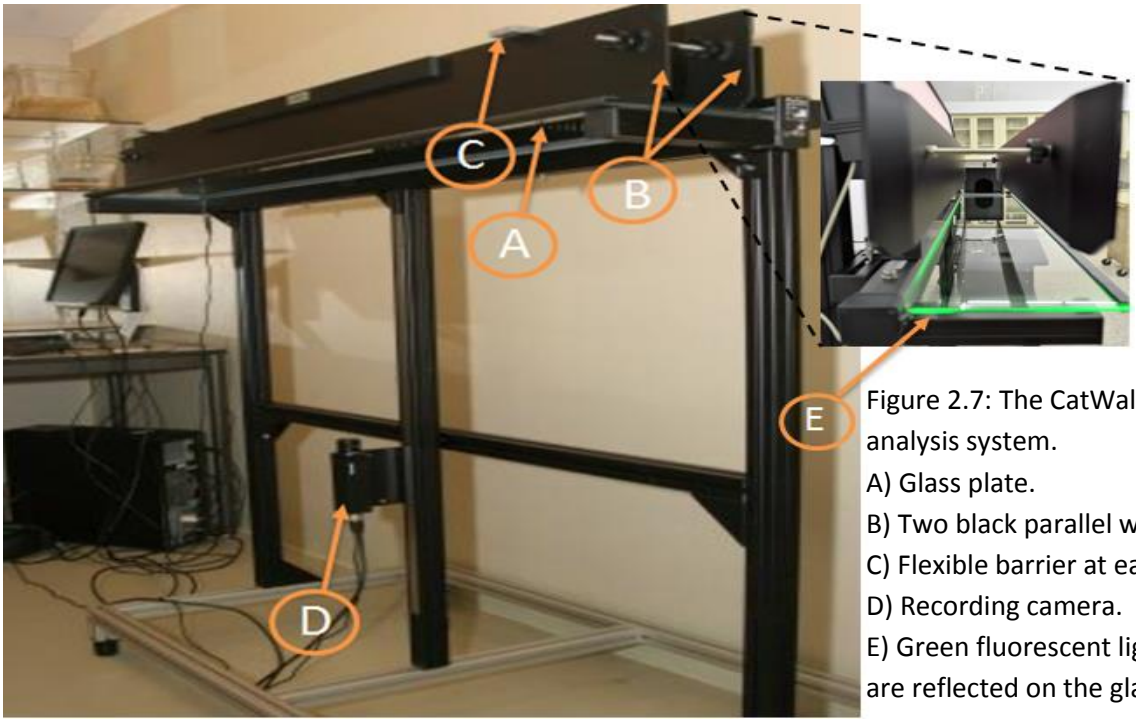

Figure 2.7: The CatWalk gait analysis system.
A) Glass plate.
B) Two black parallel walls.
C) Flexible barrier at each side.
D) Recording camera.
E) Green fluorescent light rays. are reflected on the glass plate.

In a darkened room, the animal was placed on the right side (start zone) of the glass walkway and allowed to walk along the walkway to the left (stop zone). As soon as the animal's paw passes the start zone and touches the glass surface, light rays are reflected downwards where the paws contact the glass plate, producing illuminated areas that correspond to the paw contact. These illuminated areas are copied for the entire walk by the camera (Pulnix, Japan; 50Hz, f = 3.0, variable focus and variable iris), which is equipped with a wide-angle objective and a frame grabber (Matrix Vision SG-board) linked to a computer and image analysis software included in the CatWalk® system. This produces in a sharp image of a bright paw print representing the area of contact (Figure 2.8) (Vrinten and Hamers, 2003). The signal's intensity depends on the pressure applied by the animal paw. Hence, the pixels appear brighter (intensity increases) when more weight was put on the animal paw (Bozkurt et al., 2011, Gabriel et al., 2007, Vrinten and Hamers, 2003).

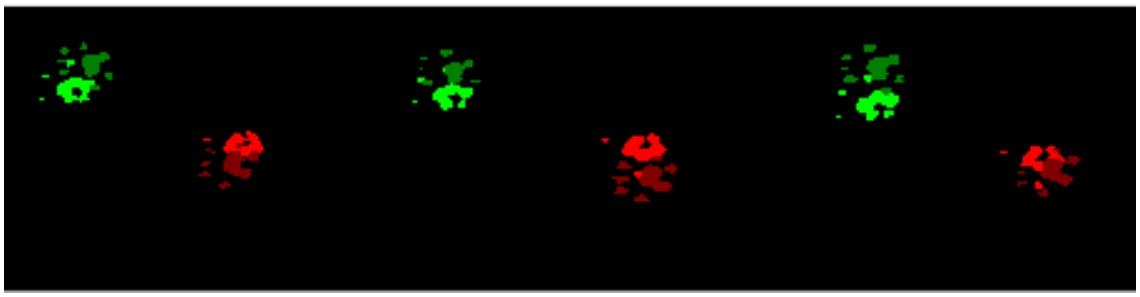

Figure 2.8: Image of paw prints produced by the CatWalk gait analysis system. Light green is right front paw. Dark green is right hind paw. Light red is left front paw. Dark red is left hind paw.

Animals require little training in crossing the walkway, as they generally have no hesitation in doing so with sufficient speed. One run two crossings were done for each animal and averaged data were used in the analysis.

Using the CatWalk software, the threshold was set to 5 arbitrary units (a.u.) in order to define the paw-floor contact areas, thus all areas containing pixels brighter than 5 a.u. were included in the analysis. Coded labels were applied to the prints to indicate

forepaw/hindpaw and left/right. There are many different parameters that could be calculated; however, only two were used in the study:

1)- Intensity of the paw print:

This reflects the mean pressure applied by an individual paw during contacting the glass surface all along crossing the walkway. The intensity is expressed in arbitrary units (a.u.) (Deumens et al., 2007, Vrinten and Hamers, 2003).

2)- The print area

This reflects the total surface area that was contacted during the stance phase of the paw. The print area is expressed in mm^2 (Deumens et al., 2007, Vrinten and Hamers, 2003).

Although CatWalk gait system is used to assess both the pain and recovery function, it does not give any details about the quantification of the overall level of regeneration across an injury site.

2.2.6 Electrophysiology

The electrophysiology technique was used only in the studies described in Chapter 5, and performed by Hisham Shembesh. With the sciatic nerve exposed and freed, it was sectioned as far proximally and distally as possible and raised from the underlying tissues except for a small area kept adhere to the nerve to keep it in healthy condition. The surrounding skin flaps were raised and sutured to an earth brass ring for the purpose of forming a pool that will be filled by warm paraffin solution (BDH Laboratory Supplies, UK). Two platinum wire recording electrodes were placed underneath the proximal end of the nerve. A pair of stimulating electrodes was placed 2mm distally to the conduit while another pair was sited 2mm proximal to the conduit. A piece of parafilm (Parafilm, American National Can, USA) was placed underneath the nerve in order to isolate the electrodes from the surrounding muscle (Figure 2.9) (Atkins et al., 2006b, Ngeow, 2010).

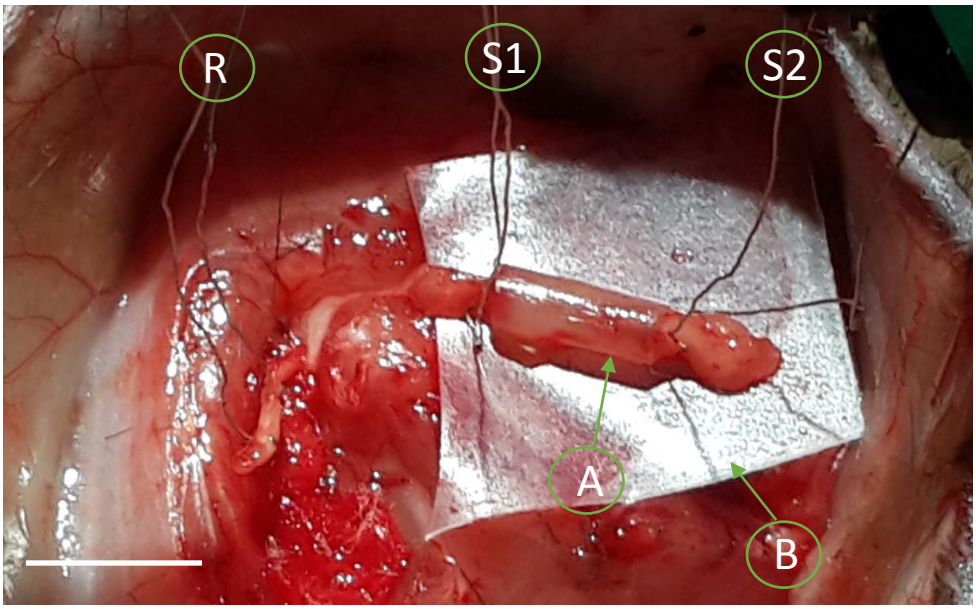

Figure 2.9: A photograph of sciatic nerve repair illustrating the placement of electrodes for the electrophysiological recordings. A) PCL conduit. B) Parafilm. R) Recording electrodes. S1) Proximal stimulation electrodes. S2) Distal stimulation electrodes. Scale bar = 5.0mm.

The electrodes were connected to a headstage designed by Harris and Matthews (1978). Earth leads from the pool holder and the metal recording table were connected to this headstage, then to a preamplifier of a Neurology (NL 104) recording system. The information was then passed from this preamplifier through a low pass filter at 3KHz (NL 135), to a digital storage oscilloscope (TDS 240, UK) and a CED 1401 plus data interface system (Cambridge Electronic Devices, UK). The CED 1401 was then connected to a computer, through a CED 1401 interface card. The CED Spike 2 data recording software (Cambridge Electronic Design, UK) was used to analysis and storage of action potentials (Atkins et al., 2006b, Ngeow, 2010).

Stimuli of 10 Volts and 0.5 milliseconds duration were generated, and were applied through the described electrode for recording the compound action potential (CAP) centrally. An average from 10 responses evoked by stimulation at each site was stored using Spike 2 software. The area underneath the curve (Modulus) was determined and the ratio of stimulations was then calculated (distal modulus ÷ proximal modulus) (Figure 2.10).

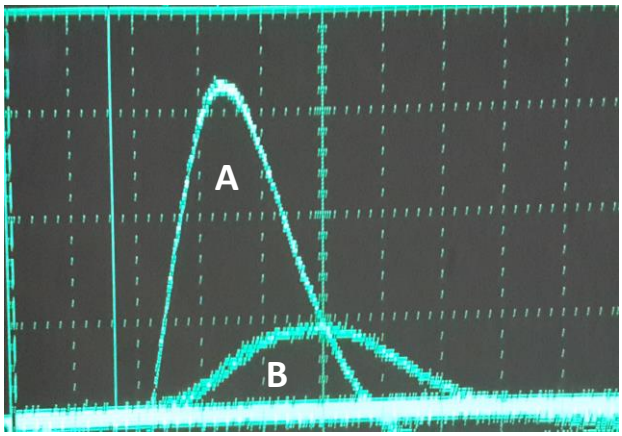

Figure 2.10: An example of a compound action potential after a conduit repair of injured sciatic nerve. A) Proximal modulus. B) Distal modulus.

The ratio gives an expression of the percentage of functional axons that have regenerated across the site of the injury (Atkins et al., 2006b, Ngeow, 2010). Therefore, a higher ratio would be an indication of better regeneration and vice versa (Ashur et al., 1987).

Electrophysiology provides a more in depth analysis of nerve regeneration compared with CatWalk system; however, it still does not explain what is happening at the level of each individual axon. To achieve that, another method is needed.

2.2.7 Axon Counting and Tracing Analysis

2.2.7.1 Nerve Image Acquisition and Processing

Images of CF nerves were obtained using a fluorescent microscope (Zeiss Axioplan2 Imaging microscope, Welwyn Garden City, UK) fitted with QImaging QI Click camera, and combination excitation filter (FITC filter was used) that connected to a computer. Using Image-Pro Plus v.7 software (Media Cybernetics, MD, USA), images were acquired (λex = 467-498nm / λem = 513-556nm) using a 10x objective lens with 30 x 10 µm z-stack sections through the nerve, these z-stack sections were then merged into

single images. Adobe Photoshop software was used to stitch images together to obtain a single image of the entire nerve and enhance the clarity of the axons.

Images of Sciatic nerve were obtained using a confocal microscope (Upright Zeiss LSM 510 META with Axioplan2 Imaging microscope) fitted with FITC filter and using a mercury lamp. Using LSM 510 software, Argon lasers of 458, 477, 488, 514nm was used, images were acquired using a 10x objective lens with 40µm z-stack sections through the nerve, which were then merged into single images. Adobe Photoshop software was used to stitch images together to obtain a single image of the entire nerve and enhance the clarity of the axons.

2.2.7.2 Qualitative observation of regenerated nerve

Investigating the ability of conduits to improve nerve function can be inferred by examining the recovery of the individual axons on the injured nerve. Because the axons of the mouse strain (*thy1-YFP-H*) used in the current study are visible under the microscope (Figure 2.11), a relatively new method (axon counting and tracing analysis) was used to investigate recovery as this method has proven useful in previous, similar studies (Harding et al., 2014, Pateman et al., 2015).

2.2.7.3 Quantification of Nerve Regeneration

Three types of analysis were carried out; counting the number of axons at intervals along the repair (sprouting index), tracing the axons to determine how many unique axons crossed the injury site, and measuring the actual length of the axon's path across the start of the regenerating area. Images were divided into 0.5mm intervals, drawn across the width of the image. Starting with 0.0mm at the first point at which abnormal morphology was present (reference line). Then, 0.5mm intervals were marked, distally to the reference line, plus one more 0.5 interval proximal to the reference line (Figure 2.12). This is shown as -0.5mm interval and was used as the pre-repair interval.

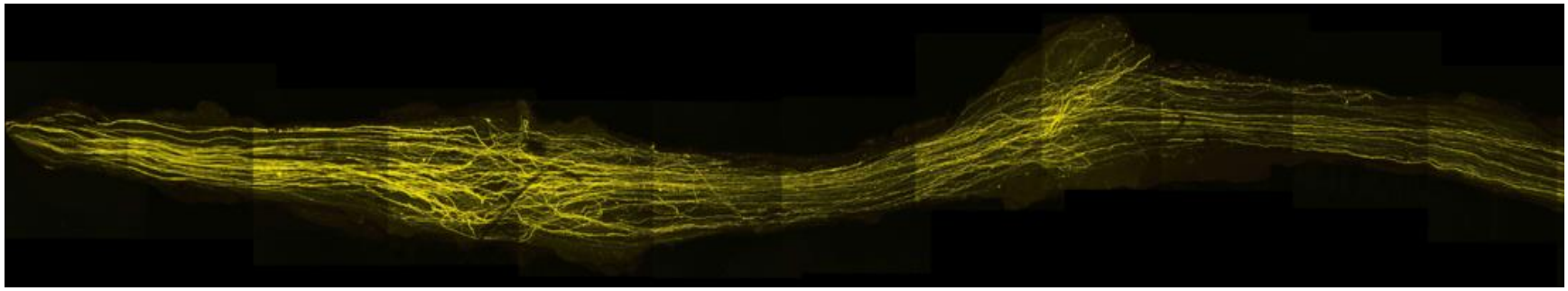

Figure 2.11: Image of entire common fibula nerve after reconstruction.

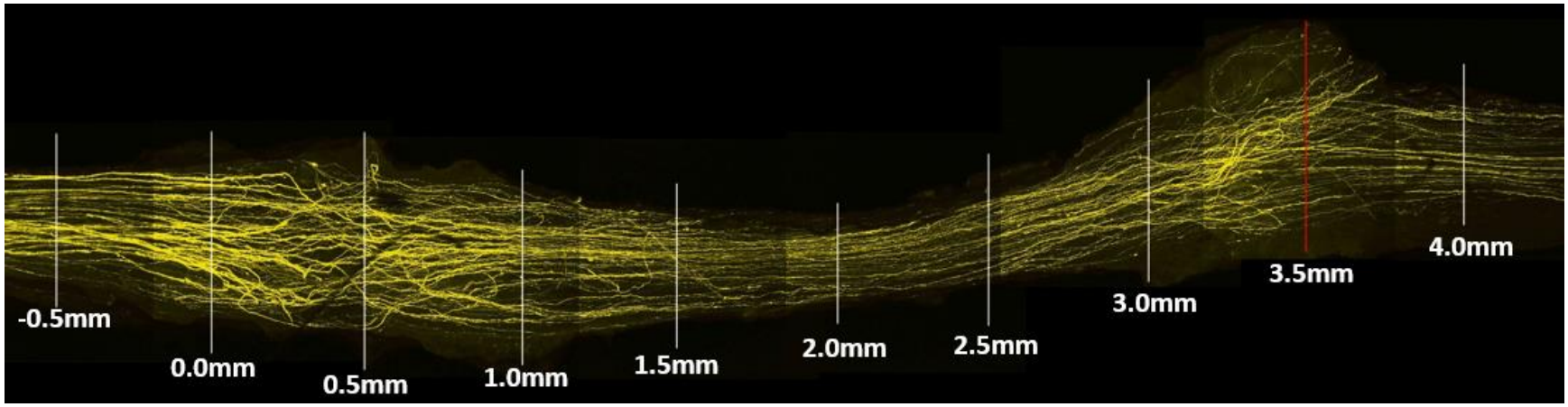

Figure 2.12: Image of entire common fibula nerve after reconstruction shows the 0.5mm intervals marked.

2.2.7.3.i Sprouting Index

Using ImageJ software (National Institutes of Health, Bethesda, MD, USA) the number of axons present at each interval was counted. The sprouting index for each interval was calculated by dividing the number of axons presented at each interval by the number of axons at the -0.5mm interval (Figure 2.12). The sprouting index gives an indication of axon branching at different intervals, but it does not indicate the number of unique axons that successfully regenerate from the repair start to the distal nerve ending. This can be measured by reverse tracing of the axons.

2.2.7.3.ii Axon Tracing

Axon tracing can be done by using Adobe Photoshop or similar software. This software gives an opportunity to trace the axons more clearly by colour, using offset and gamma correction levels, to make the axons more distinguishable. A minimum of 75% (not 100%, as many axons re-crossing intervals) of axons are traced from the final (4.0mm) interval back toward to the 0.0mm interval. Using this method rather than from the 0.0mm interval toward the final interval, allows the percentage of axons at the graft start represented at the 4.0mm interval to be determined - as axons may branch more than once, with some reaching the end while others may fail to (Figure 2.13). A high percentage may indicate better recovery of function.

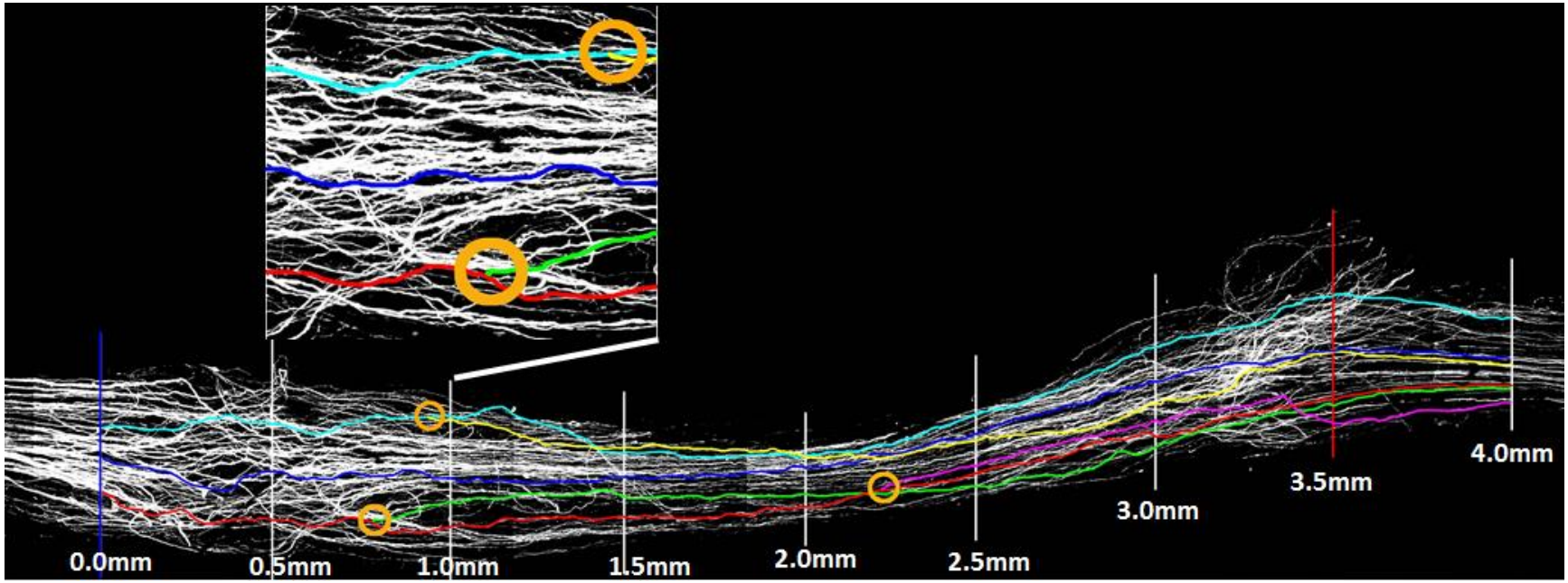

Figure 2.13: Image of some traced axons from 4.0mm interval back toward to the 0.0mm shows some convergence of axons (the orange circles).

2.2.7.3.iii Axon Disruption

The third step is to investigate the actual length of each axon across the initial injury site. Tracing and colouring axons makes following and measuring the actual length of each axon much easier. Measuring can be performed accurately using ImageJ software. Between 0.0mm and 1.5mm intervals the shortest direct path was accurately measured and the lengths of traced axons across the same area were also measured. This helps to determine the average length of axons compared the shortest direct route (Figure 2.14) (Harding et al., 2014, Pateman et al., 2015). Smaller difference between the axon length and the length of the direct path across the injury site indicates less disruption/obstruction during axonal regeneration, and vice versa.

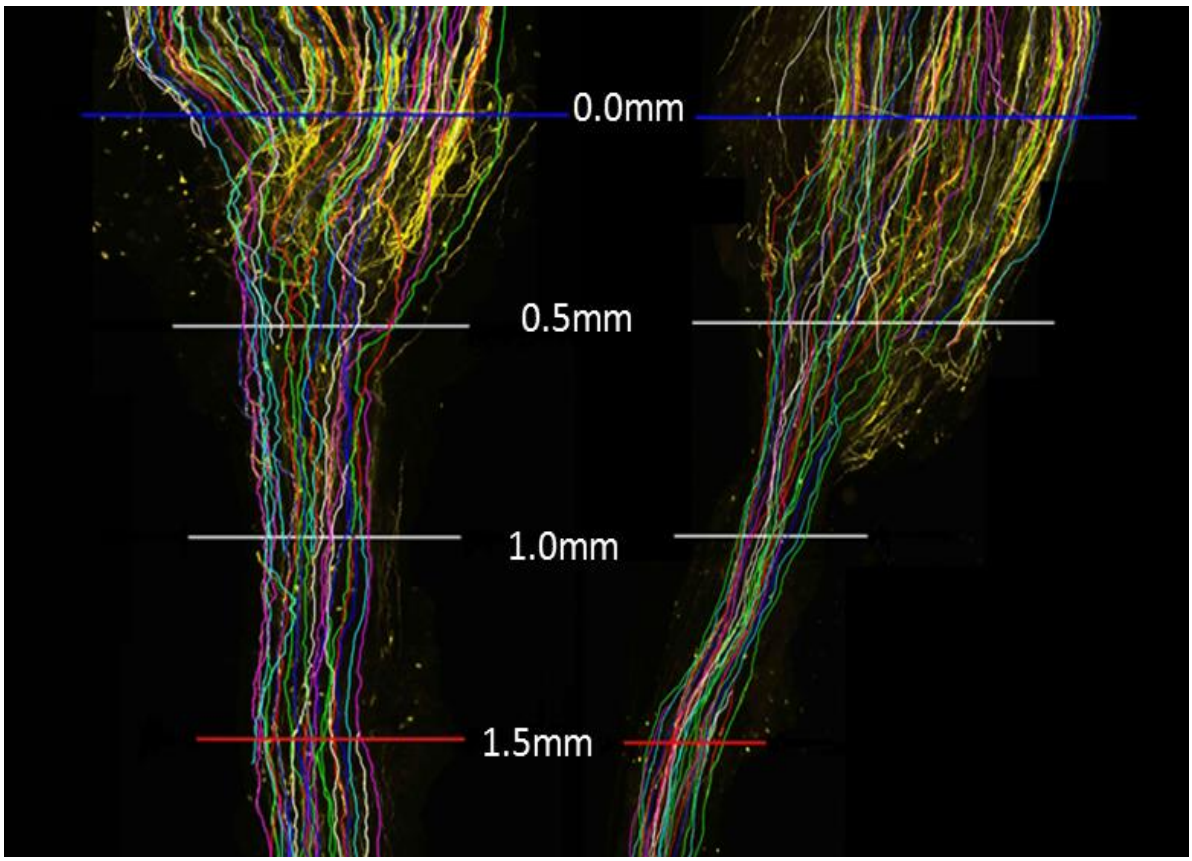

Figure 2.14: Image showing traced axon disruption between two nerve repairs. The example traced axons in the left side have more disruption and took a longer route between 0.0mm (blue line) and 1.5mm (red line) than the axons in the right side.

2.2.8 Statistical Analysis

2.2.8.1 Statistical Analysis of Glial Activation at Spinal Cord

A). Was carried out to illustrate the microglial and astrocyte activation in all groups. In this step, the differences in glial activation between the groups on the ipsilateral and contralateral sides in both ventral and dorsal spinal horns were calculated.

B). It was noted that there was some variation in the background staining between different animals. Thus, in order to allow clearer comparison between the groups, prior to statistical analysis the data was converted so that it could be expressed as the percentage increase of the ipsilateral (injured) side over the contralateral (uninjured) side in each group, ‘‘staining ratio’’. Then comparisons were made between the groups.

All statistical analysis was performed using 1-way ANOVA tests with Bonferroni’s multiple comparisons test or Unpaired t-test (two-tailed) test on GraphPad Prism 7 software (GraphPad Prism Inc, CA, USA). Differences were considered to be significant at a *p* value below 0.05.

2.2.8.2 Statistical Analysis of the Nerves

For sprouting index, axon tracing and CatWalk results a 2-way ANOVA test with Bonferroni’s multiple comparisons test was used, while for axon disruption and electrophysiology results Unpaired t-test (two-tailed) was used in order to detect overall and individual intervals differences between the experimental groups. All statistical analysis was performed using GraphPad Prism 7 software (GraphPad Prism Inc, CA, USA). Differences were considered to be significant at a *p* value below 0.05.

CHAPTER 3

QUANTIFICATION OF SPINAL GLIAL ACTIVATION AFTER NERVE GUIDE CONDUIT REPAIR

SUMMARY

The study described in this chapter was designed to develop methodology to quantify spinal cord glial activation following nerve repair with different types of conduits. This methodology was chosen as several studies have demonstrated that activation of glial cells is highly linked to the development of neuropathic pain. Three types of conduits were used, Nylon, Grooved-PCL (G-PCL) and Smooth-PCL (S-PCL). In addition, intact samples from uninjured mice were also used. The results of this chapter reported that each conduit type influence a different degree and morphology of glial activation. Nerve repair with Nylon conduits produce a high level of glial activation and poor regeneration, which may increase the potential development of neuropathic pain. On the other hand, G-PCL conduit repairs produce lower levels of glial activation and demonstrate good regeneration, which may decrease the potential development of neuropathic pain.

3.1 INTRODUCTION

Nerve regeneration following minor injury such as compression can occur without intervention. However, in case of severe nerve damage or loss of tissue leading to gap formation, nerve regeneration is generally poor without surgical repair. End to end suture can be performed in the case of clear and short gap, but if the gap is longer (approximately >5.0mm), use of direct suture repair causes considerable tension at the site of the nerve repair, and an alternative surgical repair is recommended (Belkas et al., 2004, Matsuyama et al., 2000). The use of nerve grafts is one of the alternative methods, in particular autografts, as allografts can be unsuitable due to the need for immunosuppressants (Battiston et al., 2005, Shanti and Ziccardi, 2011). Autografting, is the gold standard repair method, but it requires the removal of tissue (nerve) from the patients' own body (e.g. sural nerve) to bridge a gap at the site of injury. Although autografting shows acceptable outcomes, there are some disadvantages such as multiples surgical sites, sacrifice of an intact nerve, limited availability, loss of sensation, neuroma formation, and the potential for neuropathic pain at the donor site (Shanti and Ziccardi, 2011). The use of NGCs can remove these problems. A NGC is a biocompatible hollow tube made of natural or synthetic materials. Several approved NGC and materials have been used in peripheral nerve repair as described in section 1.7.3.

As described in the introduction in sections 1.8.2, activation of spinal astrocytes and microglia following peripheral nerve injury has been reported in many models of neuropathic pain (Colburn et al., 1999; Zhang et al., 2003; Zhang and Koninck, 2006). A study by Coly (1998) investigated the development of allodynia following partial sciatic nerve ligation (PSCL). The results showed that following PSCL rats developed significant mechanical allodynia compared to sham or un-operated groups as indicated by increased response to the Von Frey test. This test measures the threshold at which the ipsilateral paw is withdrawn following a mechanical stimulus. The development of allodynia was linked with increased levels of microglial and astrocyte activation seen in nerve injured rats. The study concluded that upon peripheral nerve injury, glial cells are activated and this correlates with the development of allodynic behaviour (Coly, 1998). High levels of glial activation are considered to be an indication of a greater potential to develop neuropathic pain.

Despite numerous studies describing glial activation following nerve injury, to my knowledge very little has been done investigating glial activation following nerve repair procedures, or any attempt made to compare glial activation following repair with different types of nerve conduit. A previous study done in our laboratory by Dr. Adam Harding compared nerve regeneration following repair with three different nerve guide conduits produced using different materials and methods. One from a nylon powder material using a selective laser sintering technique [SLS] (Nylon NGC), and two produced from poly-caprolactone (PCL) material produced by Micro-Stereolithography [µSL] (Grooved-PCL) or ultraviolet [UV] curing (Smooth-PCL). The results of Harding's (2014) study demonstrated that nerve regeneration was poor with both Nylon NGC and S-PCL, while it was very good with G-PCL. However, the effect of these different conduit repairs on glial activation, and thus their potential to influence the development of neuropathic pain was not investigated. The clear difference in nerve regeneration using these conduits provides a good basis for evaluating whether the degree of regeneration has an effect on glial activation.

3.2 AIM OF THIS STUDY

The aims of the study performed in this chapter were to develop methodology to quantify spinal cord glial activation, and to investigate whether the efficacy of different types of conduits, in terms of supporting nerve regeneration, influences the degree of glial activation and therefore the potential development of neuropathic pain.

3.3 MATERIAL AND METHODS

The protocols for this study were based on previous protocols carried out in our laboratory at the University of Sheffield, and have been described in Chapter 2. Additional specific information involved in the present study is described below. All conduits used in this chapter were provided by Christopher Pateman from the laboratories of Prof. John Haycock and Dr. Frederik Claeyssens, Kroto Research Institute, University of Sheffield and laboratories of Prof. Neil Hopkinson, department of mechanical engineering, University of Sheffield, UK.

3.3.1 Animal Numbers and Groups

Spinal cords from 12 *thy-1-YFP-H* mice were used in this chapter, these were harvested from animals in 4 experimental groups: Nylon conduit repair (n=3), Grooved-Walled PCL [G-PCL] conduit repair (n=3), Smooth-Walled PCL [S-PCL] conduit repair (n=3), and intact (uninjured) mice (n=3) (Figure 3.1).

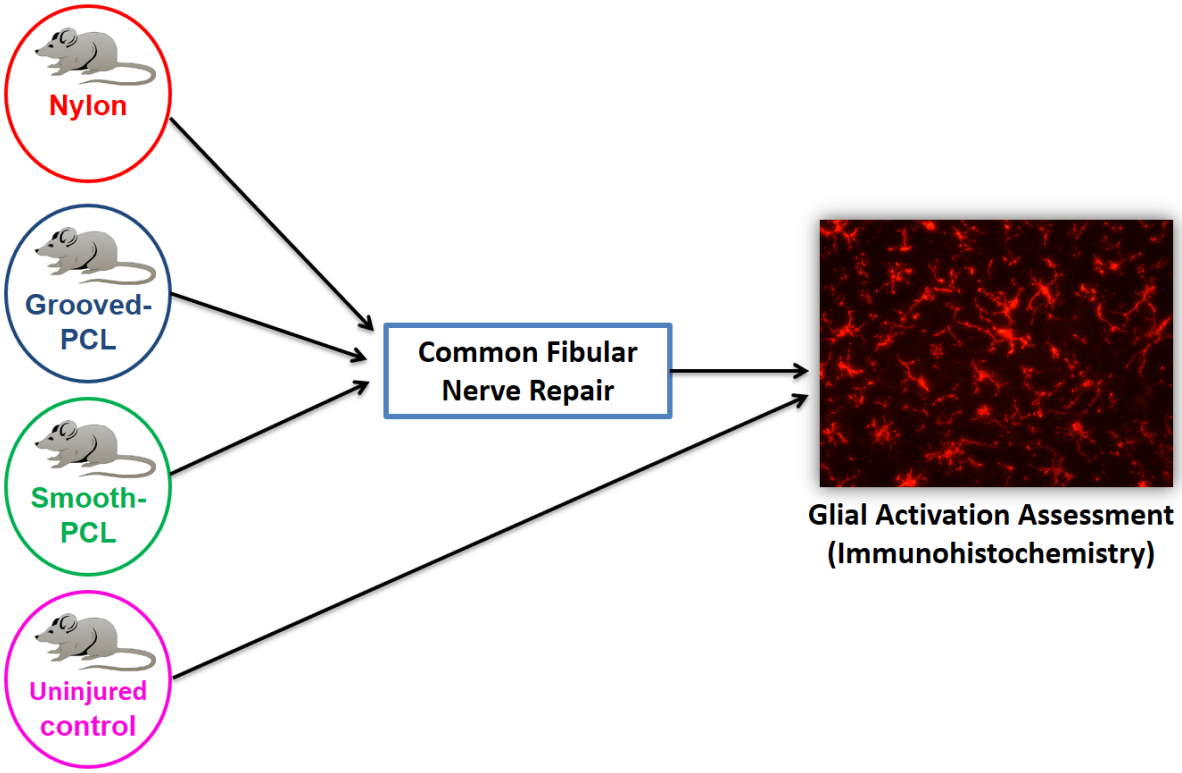

Figure 3.1 Summary of groups for the investigation of the conduits.

3.3.2 Experimental Methods

The nerve repair and tissue harvesting was carried out previously by Dr. Adam Harding, and all the evaluated spinal cords in this chapter were provided by him.

Thy-1-YFP-H mice were anaesthetised (see section 2.2.3.1.i) and the common fibular nerve exposed and transected. A 3-mm gap was made (see section 2.2.3.1.il) and repaired using either Nylon conduits, G-PCL conduits, or S-PCL conduits secured by fibrin glue (see section 2.2.3.1.iv) (Figure 3.2). Animals were allowed to

recover for 21-days to allow the regenerating nerve to gain sufficient strength to remain intact during harvesting.

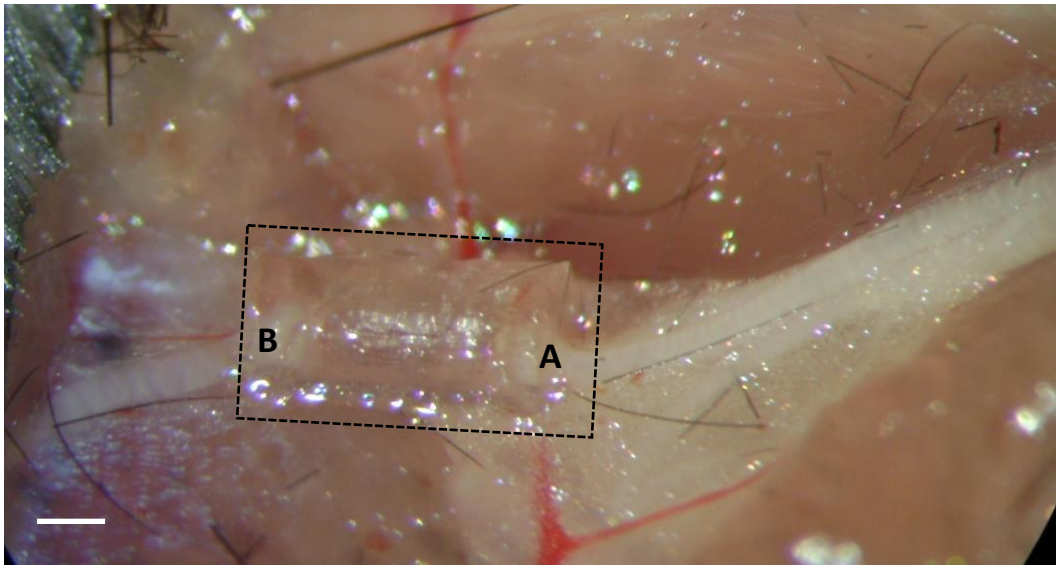

Figure 3.2: Image shows the implantation of a conduit between the two ends of the CF nerve and secured by glue. A) The proximal stump. B) The distal stump. The rectangle is the conduit (Modified from Pateman et al., 2015). Scale bar = 1.0mm.

Following the recovery period, animals were anaesthetised (see section 2.2.3.2.i), the CF nerve was harvested (see sections 2.2.3.2.ii) and prepared for analysis using fluorescent microscope (see sections 2.2.7). In addition, the spinal cord was also harvested (with additional 3 cords from uninjured mice), fixed and prepared for immunohistochemistry using primary antibodies raised in goat against Iba-1 (to label microglia) and in rabbit against GFAP (to label astrocytes) (see sections 2.2.4). Immunohistochemical labelling was quantified as described in Chapter 2. In all cases, analysis was carried out blind.

3.3.3 Statistical Analysis

Statistical comparisons between groups were carried out as stated in section 2.3.7.1. All glial activation data were analysed using 1-way ANOVA with Bonferroni's multiple comparisons test. Differences were considered to be significant when $p<0.05$.

3.4. RESULTS

All animals recovered well from the surgical procedure without any sign of infection. A range of different sizes (length and internal diameter) of nylon conduits were initially produced by SLS technique in order to test the capabilities of the SLS machine, however for the dimensions used for the repairs described here were 5.00mm length, 0.5mm thick walls and 0.8mm internal diameter (giving a 1.8mm outside diameter). While conduits produced by µSL technique (G-PCL and S-PCL) were approximately 5.00mm long, 1.00mm internal diameter and 0.25mm wall thickness (giving a 1.5mm outside diameter).

Only the results of immunohistochemistry investigation and quantitation of glial activation will be fully detailed in this chapter as results for nerve regeneration were carried out by Dr. Adam Harding and have been previously described (Harding 2014).

3.4.1 Assessment of Glial Activation

3.4.1.1 Qualitative Observations of Spinal Cord

Glial activation was apparent in the injured side for all repair groups and the greatest observed immunoreactivity was present in specific areas of grey matter. This represents the region of the spinal cord to which the common fibular nerve projects. The activation was very high in the nylon group, and amoeboid glia were observed (Figure 3.3A). The level of activation was minimal in both G-PCL and S-PCL groups, and some hypertrophied glia were observed in both groups however the degree of hypertrophy appeared greater in the S-PCL group). Ramified glia were seen in the intact group (Figure 3.3B, C and D).

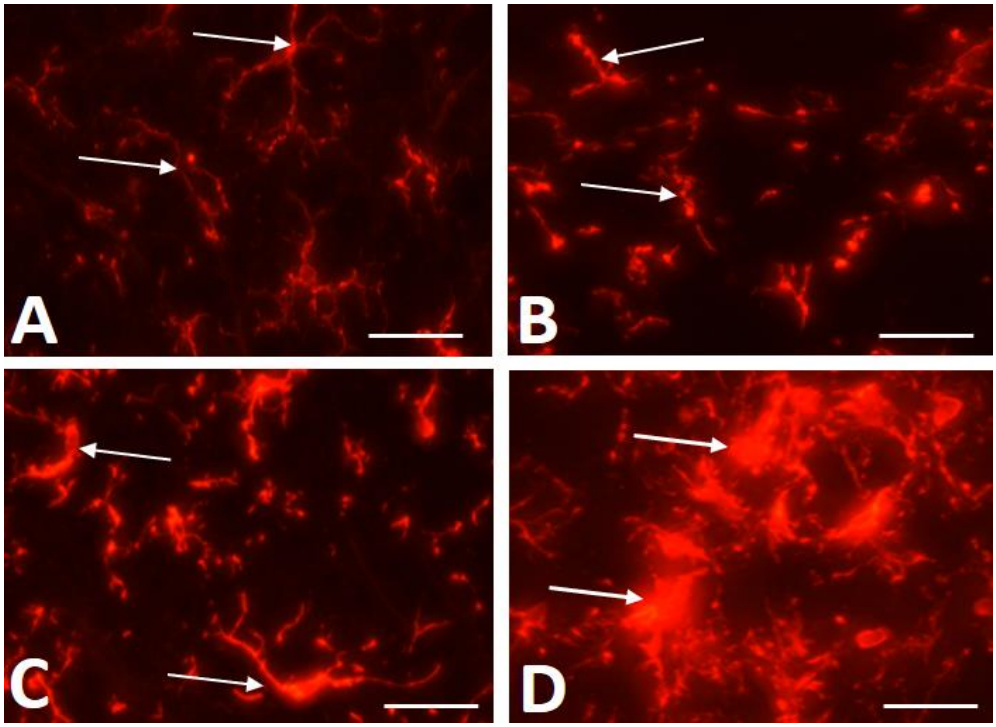

Figure 3.3: Sections of spinal cord after Immunohistocal staining with antibody Iba-1 showing three different morphological phenotypes of microglial cells. A) Intact spinal cord showing the ramified microglia: normal-appearing body with long, thin and radially projecting processes (white arrow). Spinal cords following peripheral nerve injury repair using B) G-PCL and C) S-PCL conduits showing hypertrophied microglia: enlarged body with shorter, thicker processes (white arrows), D) Nylon conduit showing amoeboid microglia: bigger and densely stained body with much fewer processes (white arrows). Scale bar = 0.1mm.

3.4.1.2 Quantitative Analysis of Spinal Cord

As described in section 2.2.8.1(A), the percentage area of labelling for Iba-1 and GFAP was calculated in defined regions of the dorsal and ventral horns of the spinal cord both ipsilaterally and contralaterally to the nerve repair.

3.4.1.2.i Quantification of Iba-1 Expression

Quantification of labelling for microglial activation within the four groups demonstrates that the nylon NGC group had significantly higher levels than other groups in both ipsilateral dorsal (18.8% vs 9.1% [G-PCL; $p<0.01$], 10.6% [S-PCL; $p<0.05$] and 8.5% [intact; $p<0.01$]) and ventral (33.4% vs 9.9% [G-PCL; $p<0.001$], 10.6% [S-PCL; $p<0.001$] and 8.3% [intact; $p<0.001$]) horns (Table 3.1 & Figure 3.8). There were no significant differences in labelling between G-PCL, S-PCL and intact groups (refer to Table 3.1 & Figure 3.8). In the corresponding contralateral side, the percentage area of Iba-1 labelling in the dorsal horn was slightly higher in the Nylon NGC group (9.1%) compared with the G-PCL group (7.8%), S-PCL group (8.6%) and intact group (8.1%). In the ventral horn, the percentage area in the Nylon NGC group was slightly higher (10.1%) compared with G-PCL group (8.1%), S-PCL group (8.2%) and intact group (7.7%) (refer to Table 3.1 & Figure 3.8); these differences in contralateral side (dorsal and ventral horns) were not significant between the groups. The activation areas of Iba-1 in each group are shown in Figures 3.4-3.7.

Nylon Conduit

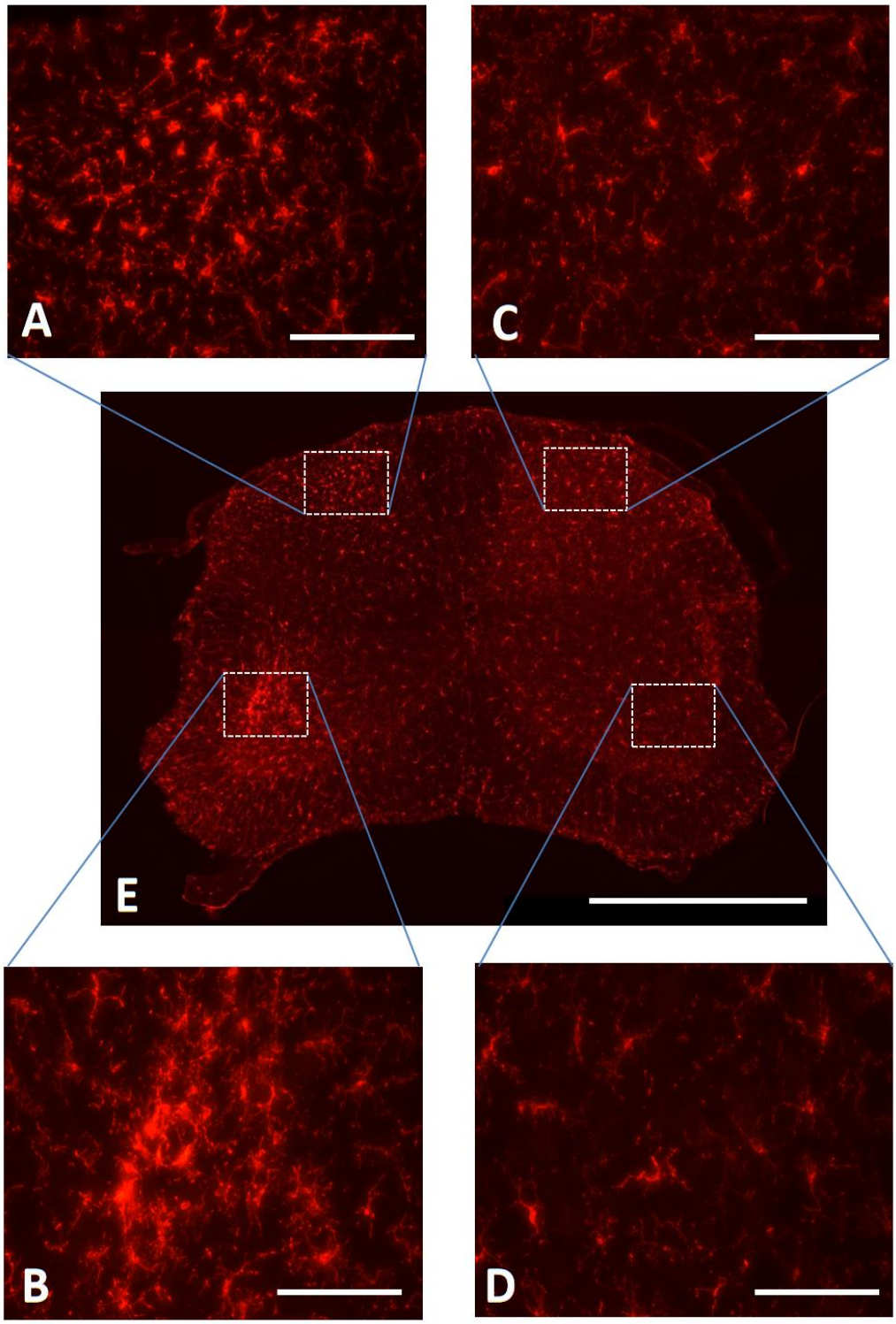

Figure 3.4: A section of spinal cord following nerve repair with a Nylon conduit shows microglial activation (E using 5x magnification). A) Ipsilateral dorsal horn, B) Ipsilateral ventral horn. C) Contralateral dorsal horn. D) Contralateral Ventral horn (A,B,C,D using 40x magnification). Scale bar A,B,C and D = 0.1mm, E = 1.0mm.

Grooved-PCL Conduit

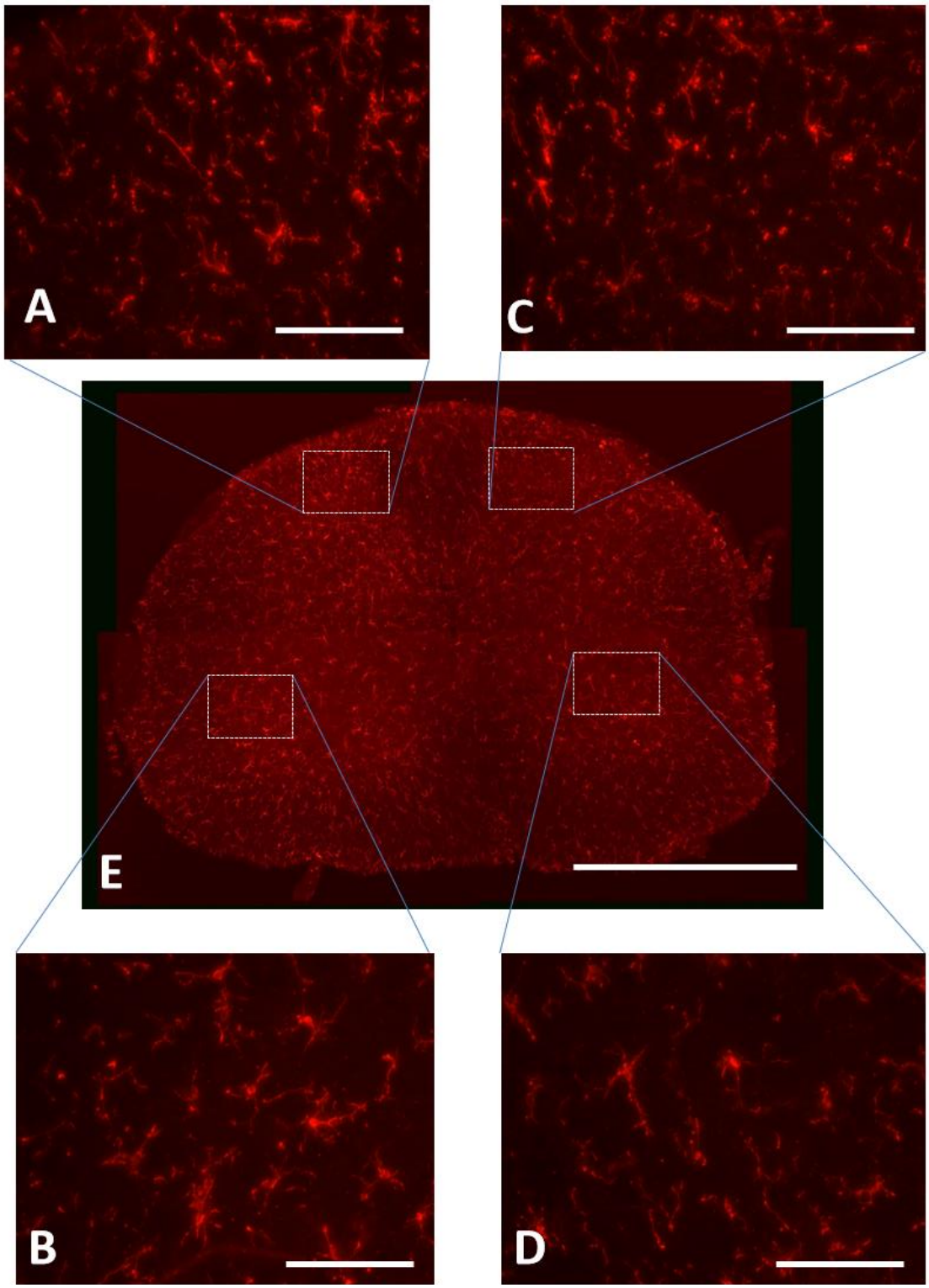

Figure 3.5: A section of spinal cord following nerve repair with a G-PCL conduit shows microglial activation (E using 5x magnification). A) Ipsilateral dorsal horn, B) Ipsilateral ventral horn. C) Contralateral dorsal horn. D) Contralateral Ventral horn (A,B,C,D using 40x magnification). Scale bar A,B,C and D = 0.1mm, E = 1.0mm.

Smooth-PCL Conduit

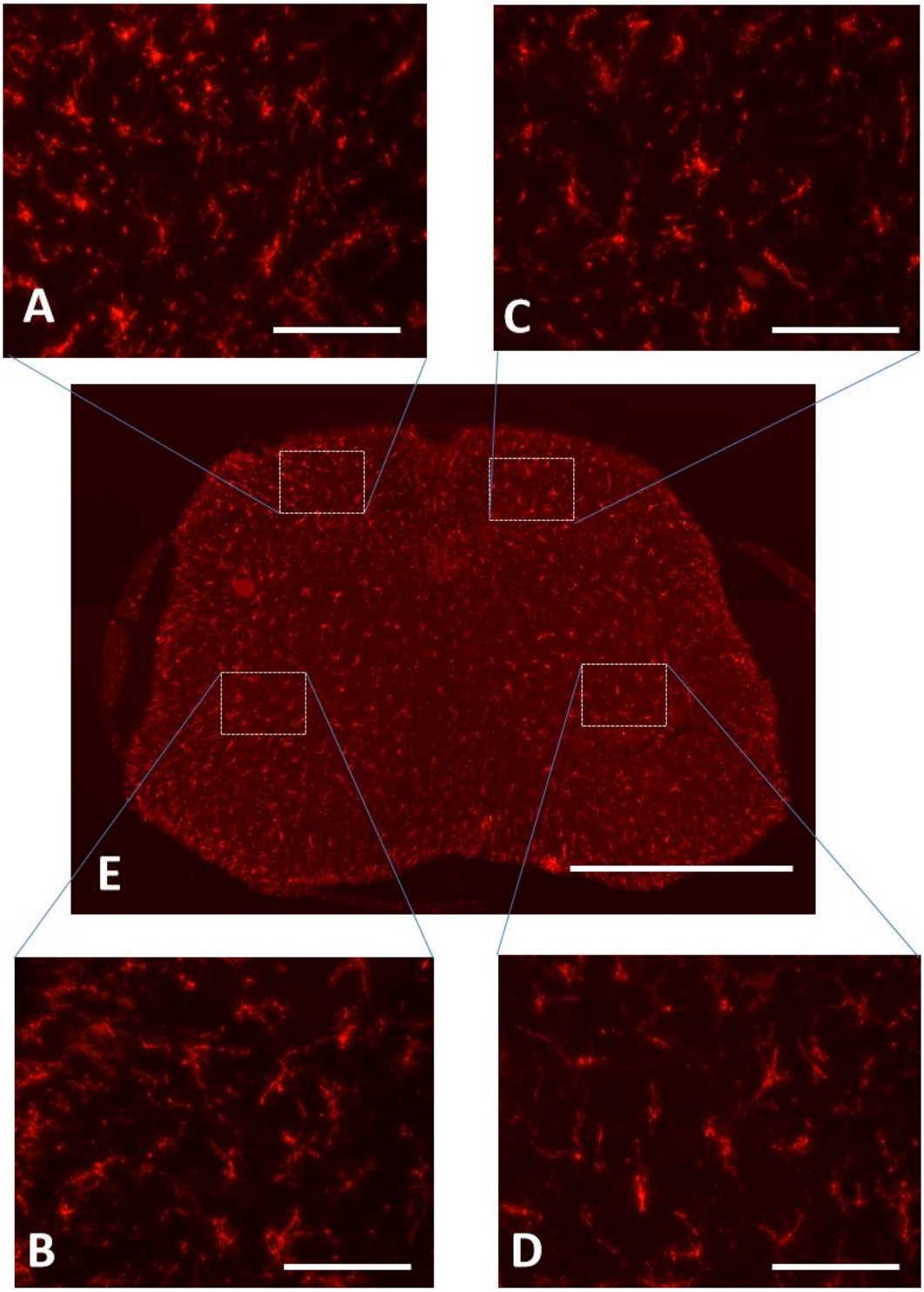

Figure 3.6: A section of spinal cord following nerve repair with a S-PCL conduit shows microglial activation (E using 5x magnification). A) Ipsilateral dorsal horn, B) Ipsilateral ventral horn. C) Contralateral dorsal horn. D) Contralateral Ventral horn (A,B,C,D using 40x magnification). Scale bar A,B,C and D = 0.1mm, E = 1.0mm.

Intact Cord

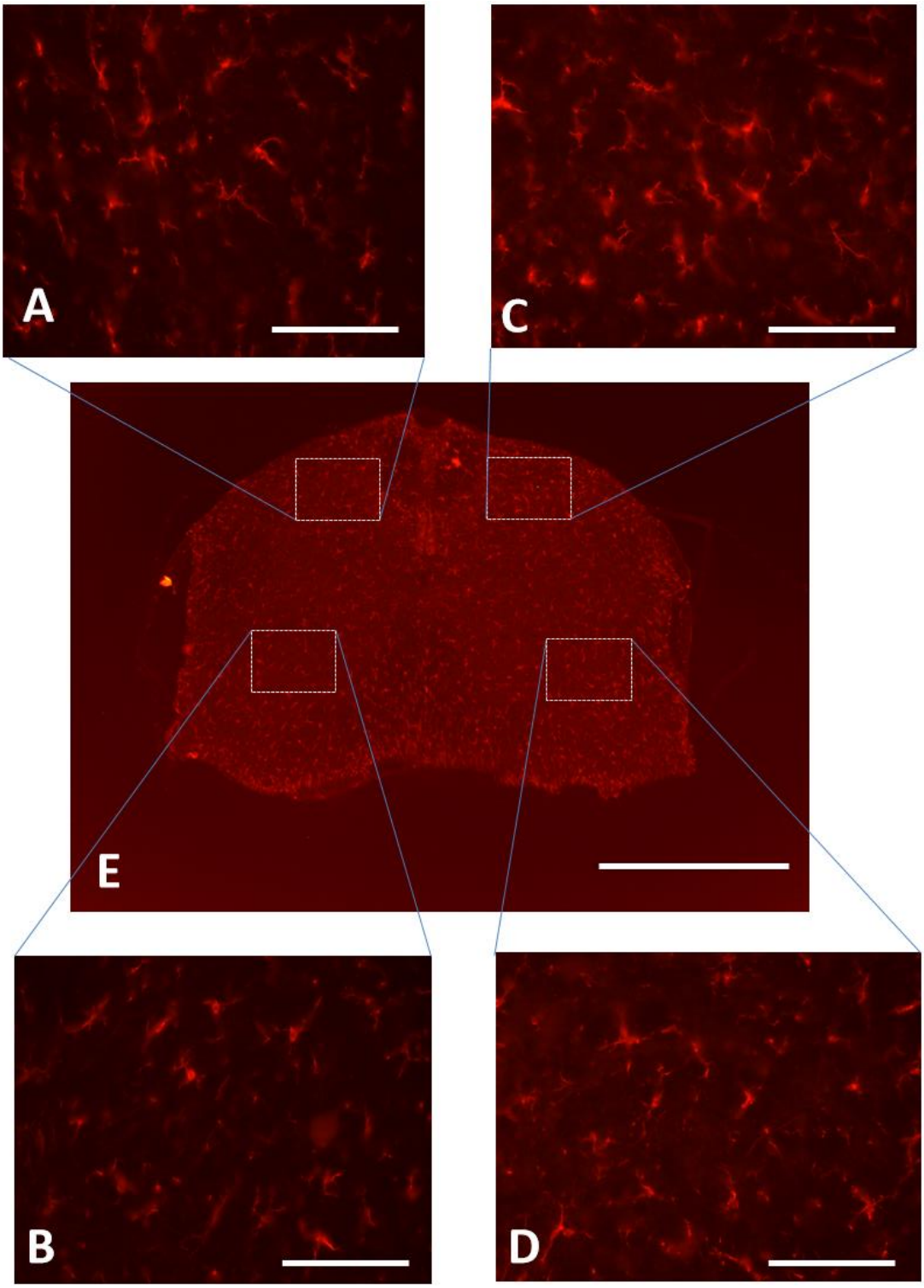

Figure 3.7: A section of spinal cord from an uninjured animal shows microglial activation (E using 5x magnification). A) Ipsilateral dorsal horn, B) Ipsilateral ventral horn. C) Contralateral dorsal horn. D) Contralateral Ventral horn (A,B,C,D using 40x magnification). Scale bar A,B,C and D = 0.1mm, E = 1.0mm.

The mean percentage area of Iba-1 labelling (indication of the degree of microglial activation) for each group is shown in Table 3.1. The same data and the statistical comparison between the groups is illustrated in Figure 3.8.

Table 3.1: Percentages of microglial activation for Nylon, G-PCL, S-PCL and intact groups.

IBA-1 (Microglia)%	Nylon	G-PCL	S-PCL	Intact
Ipsilateral Dorsal horn	18.8	9.1	10.6	8.5
Contralateral Dorsal horn	9.1	7.8	8.6	8.1
Ipsilateral Ventral horn	33.4	9.9	10.6	8.3
Contralateral Ventral horn	10.1	8.1	8.2	7.7

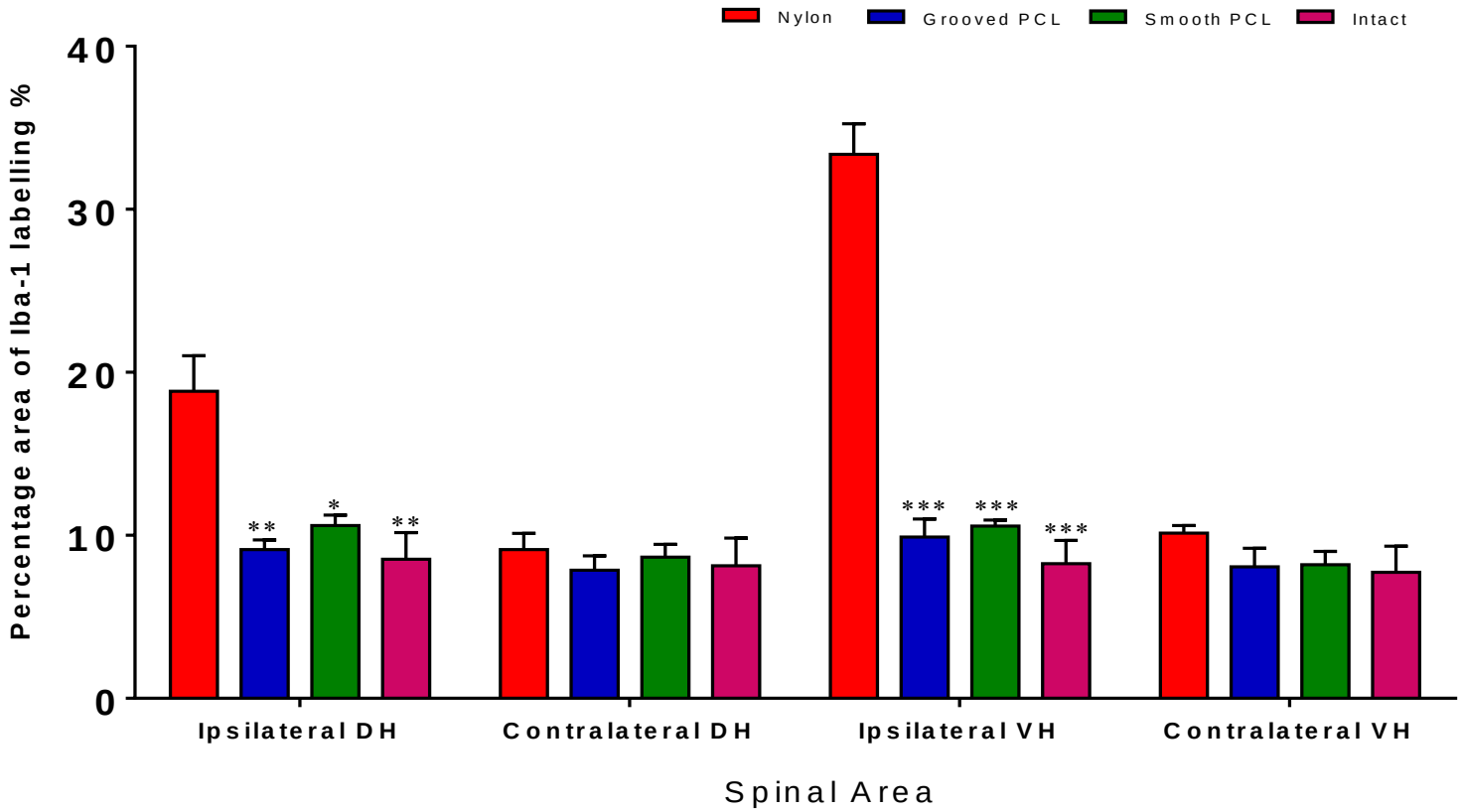

Figure 3.8: Immunohistochemical analysis of microglia for Nylon, G-PCL, S-PCL, and intact groups. *, ** and *** denote significant difference compared to Nylon group, $p<0.05$, $p<0.01$ and $p<0.001$, respectively. Error bars denote SEM. Statistical test: 1-way ANOVA with Bonferroni's multiple comparisons test. VH=Ventral Horn. DH=Dorsal Horn.

As described in section 2.2.8.1(B), some variation in the background staining was noted. Thus, percentage increase of the ipsilateral (injured) side over the contralateral (uninjured) side, ‘‘staining ratio’’ was performed. Comparisons between the groups when assessing the staining gave similar results to those described above. The increase in staining (Ipsilateral/Contralateral) ratio for Iba-1 in the Nylon NGC group was significantly higher than in other groups in dorsal (105% vs 14% [G-PCL; $p<0.001$], 21% [S-PCL; $p<0.001$] and 6% [intact; $p<0.001$]) and ventral (230% vs 28% [G-PCL; $p<0.001$], 32% [S-PCL; $p<0.001$] and 8% [intact; $p<0.001$]) horns (Figure 3.9). No significant differences were observed between G-PCL, S-PCL and intact groups in either dorsal or ventral horns ($p>0.05$) (Figure 3.9).

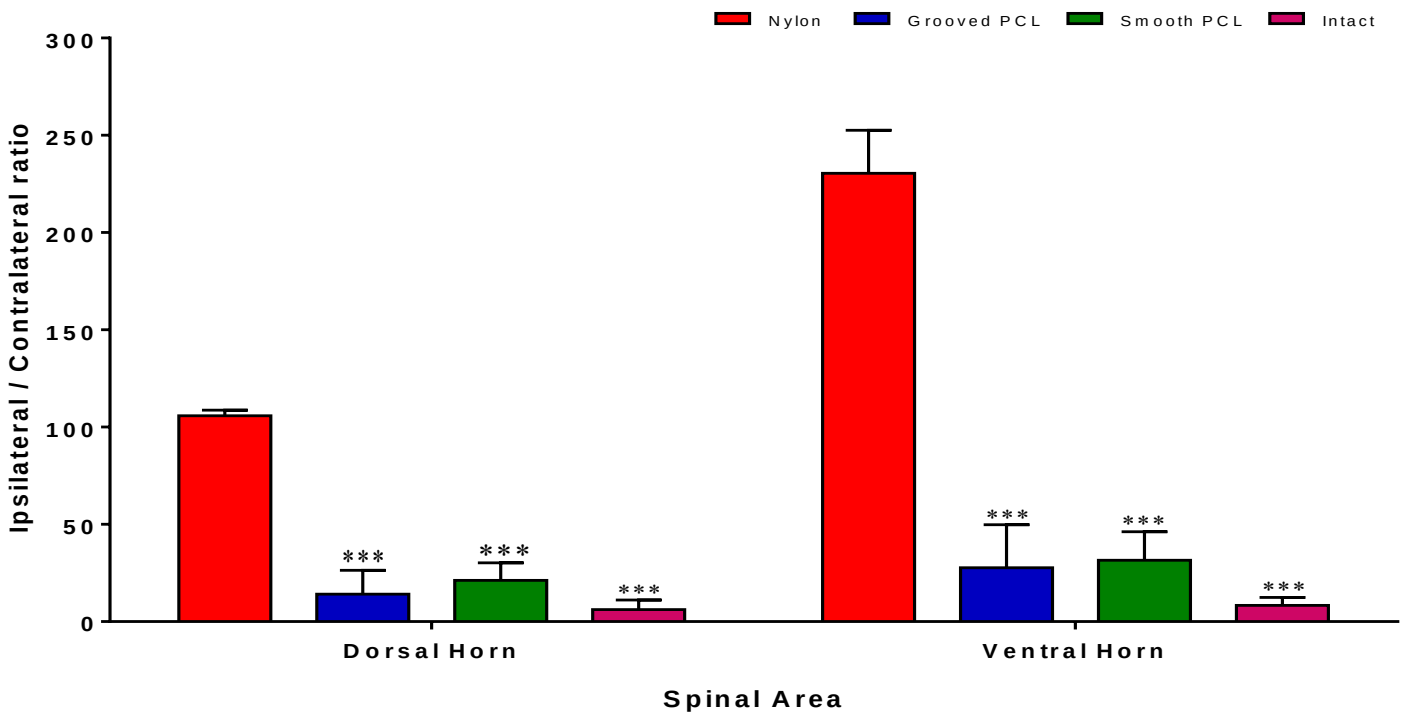

Figure 3.9: Ipsilateral/Contralateral ratio of spinal microglia shows the difference of percentage increase in the ipsilateral side over the contralateral side in ventral and dorsal horns of the spinal cord for Nylon, G-PCL, S-PCL, and intact groups. *** denote significant difference compared to Nylon group, $p<0.001$. Error bars denote SEM. Statistical test: 1-way ANOVA with Bonferroni's multiple comparisons test.

3.4.1.2.ii Quantification of GFAP Expression

Quantification of labelling for astrocyte activation within the four groups demonstrates that the nylon NGC group had significantly higher levels than other groups in both ipsilateral dorsal (19.7% vs 8.1% [G-PCL; $p<0.05$], 11.3% [S-PCL; $p<0.05$] and 8.7% [intact; $p<0.05$]) and ventral (22.1% vs 9.1% [G-PCL; $p<0.001$], 11.8% [S-PCL; $p<0.01$] and 8.2% [intact; $p<0.001$]) horns (Table 3.2 & Figure 3.14). There were no significant differences in labelling between G-PCL, S-PCL and intact groups (refer to Table 3.2 & Figure 3.14). In the corresponding contralateral side, the percentage area of GFAP labelling in the dorsal horn was slightly higher in the Nylon NGC group (7.7%) compared with the G-PCL group (6.4%), while slightly lower compared to S-PCL group (8.1%) and intact group (8.5%). In the ventral horn, the percentage area in the Nylon NGC group was slightly higher (8.6%) compared with G-PCL group (6.8%), S-PCL group (6.3%) and intact group (7.7%) (refer to Table 3.2 & Figure 3.14); these differences in contralateral side (dorsal and ventral horns) were not significant between the groups. The activation areas of GFAP in each group are shown in Figures 3.10-3.13.

Nylon Conduit

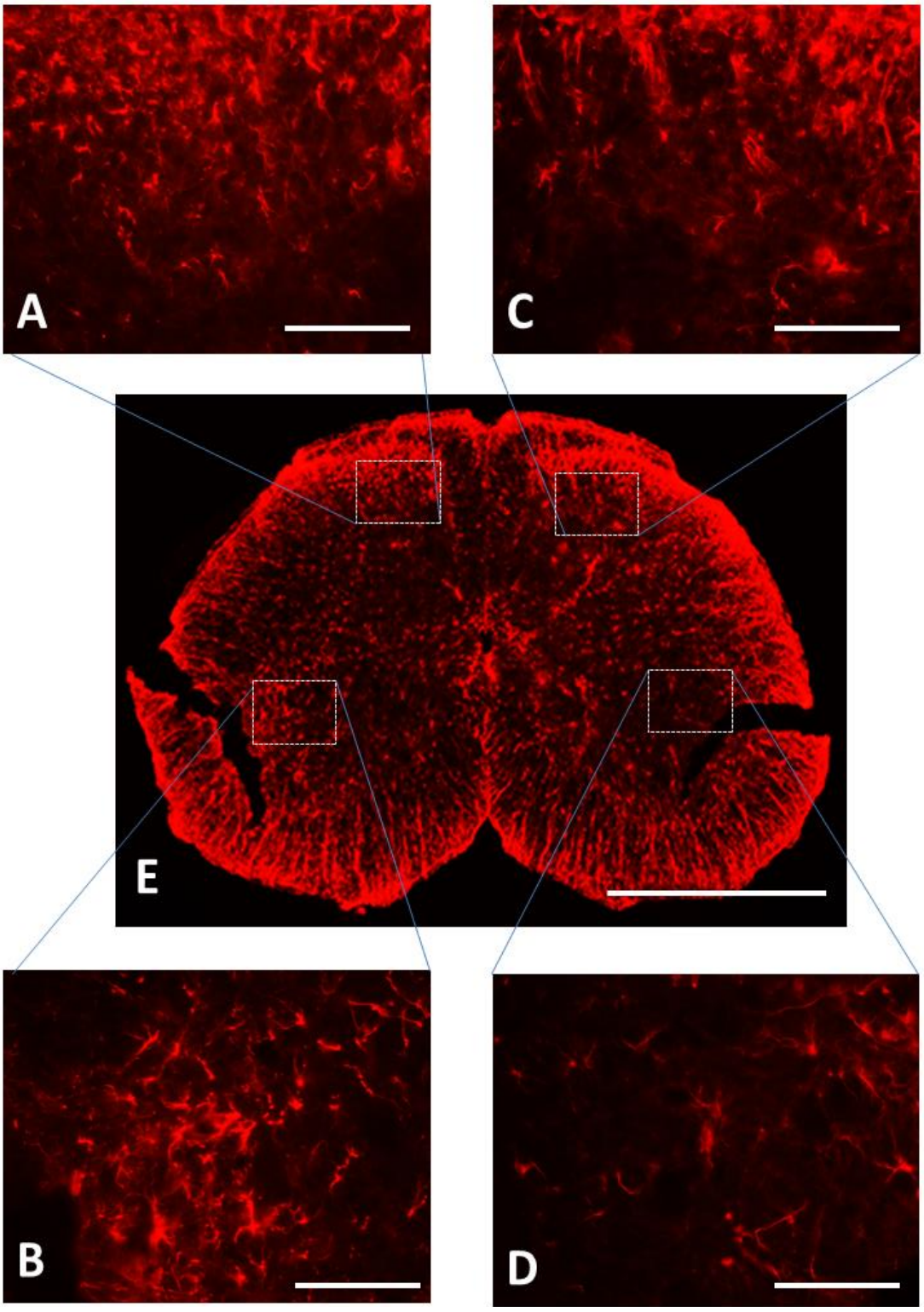

Figure 3.10: A section of spinal cord following nerve repair with a Nylon conduit shows astrocyte activation (E using 5x magnification). A) Ipsilateral dorsal horn, B) Ipsilateral ventral horn. C) Contralateral dorsal horn. D) Contralateral Ventral horn (A,B,C,D using 40x magnification). Scale bar A,B,C and D = 0.1mm, E = 1.0mm.

Grooved-PCL Conduit

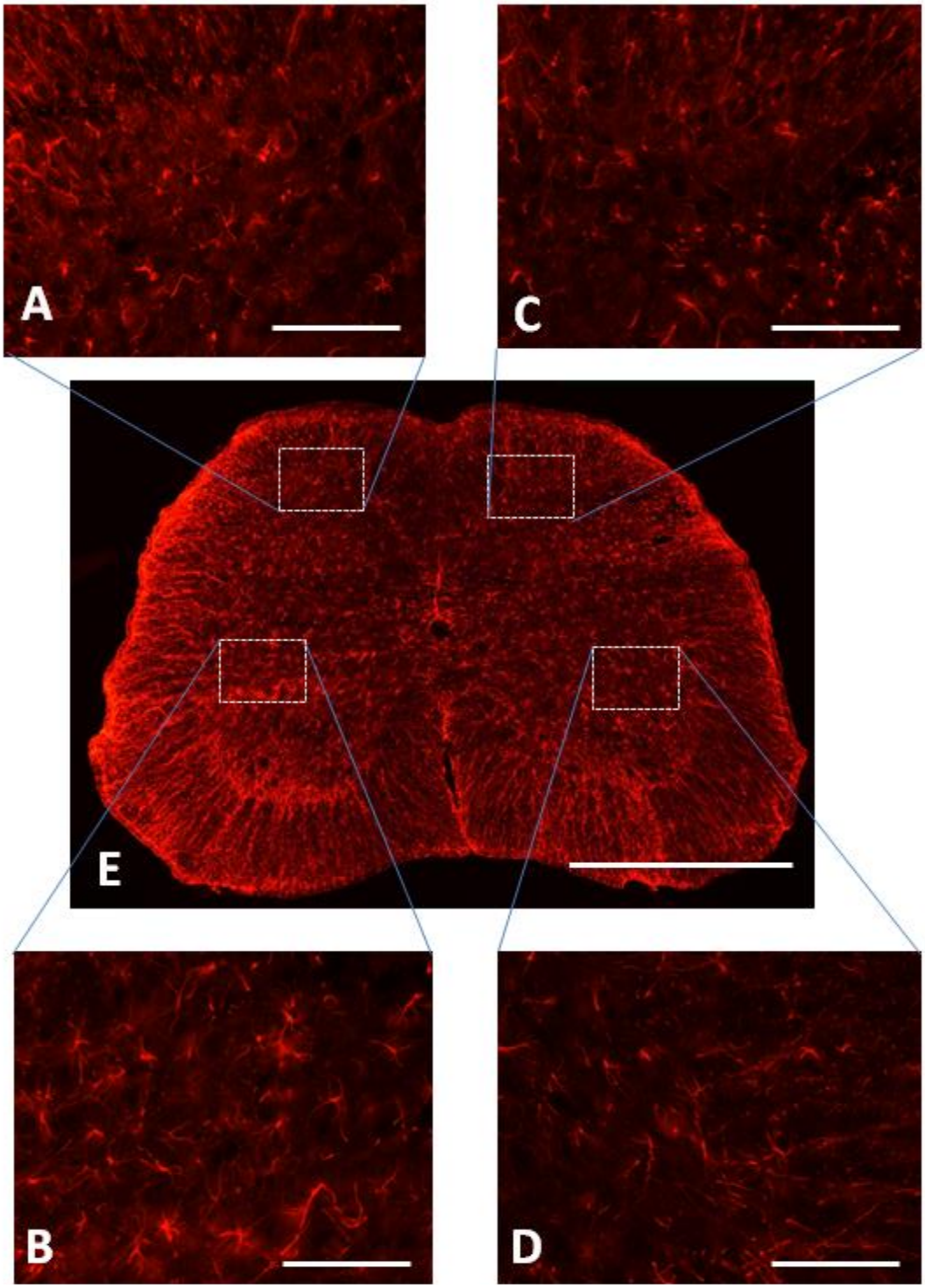

Figure 3.11: A section of spinal cord following repair with a G-PCL conduit shows the astrocyte activation (E using 5x magnification). A) Ipsilateral dorsal horn, B) Ipsilateral ventral horn. C) Contralateral dorsal horn. D) Contralateral Ventral horn (A,B,C,D using 40x magnification). Scale bar A,B,C and D = 0.1mm, E = 1.0mm.

Smooth-PCL Conduit

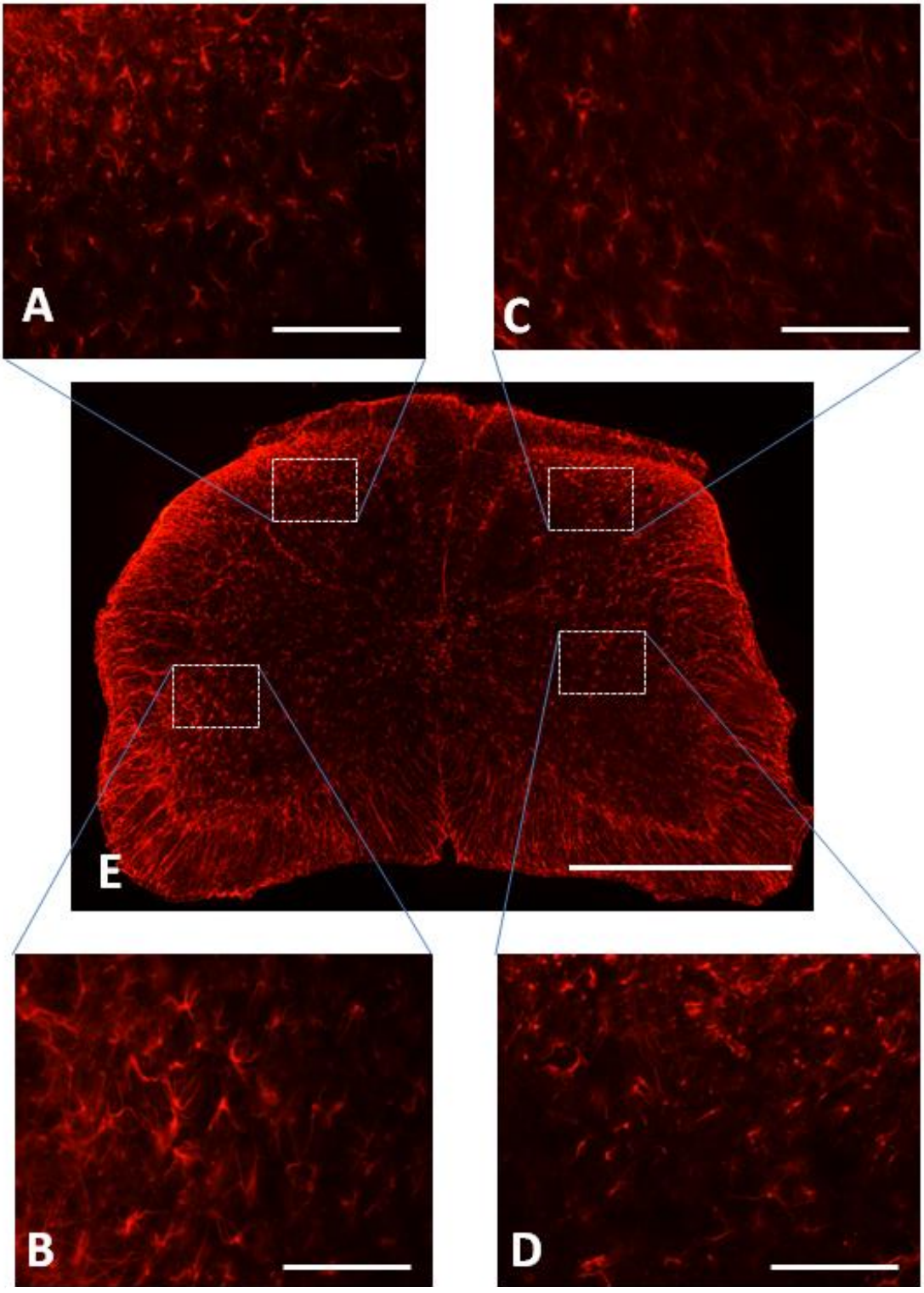

Figure 3.12: A section of spinal cord following repair with a S-PCL conduit shows astrocyte activation (E using 5x magnification). A) Ipsilateral dorsal horn, B) Ipsilateral ventral horn. C) Contralateral dorsal horn. D) Contralateral Ventral horn (A,B,C,D using 40x magnification). Scale bar A,B,C and D = 0.1mm, E = 1.0mm.

Intact Cord

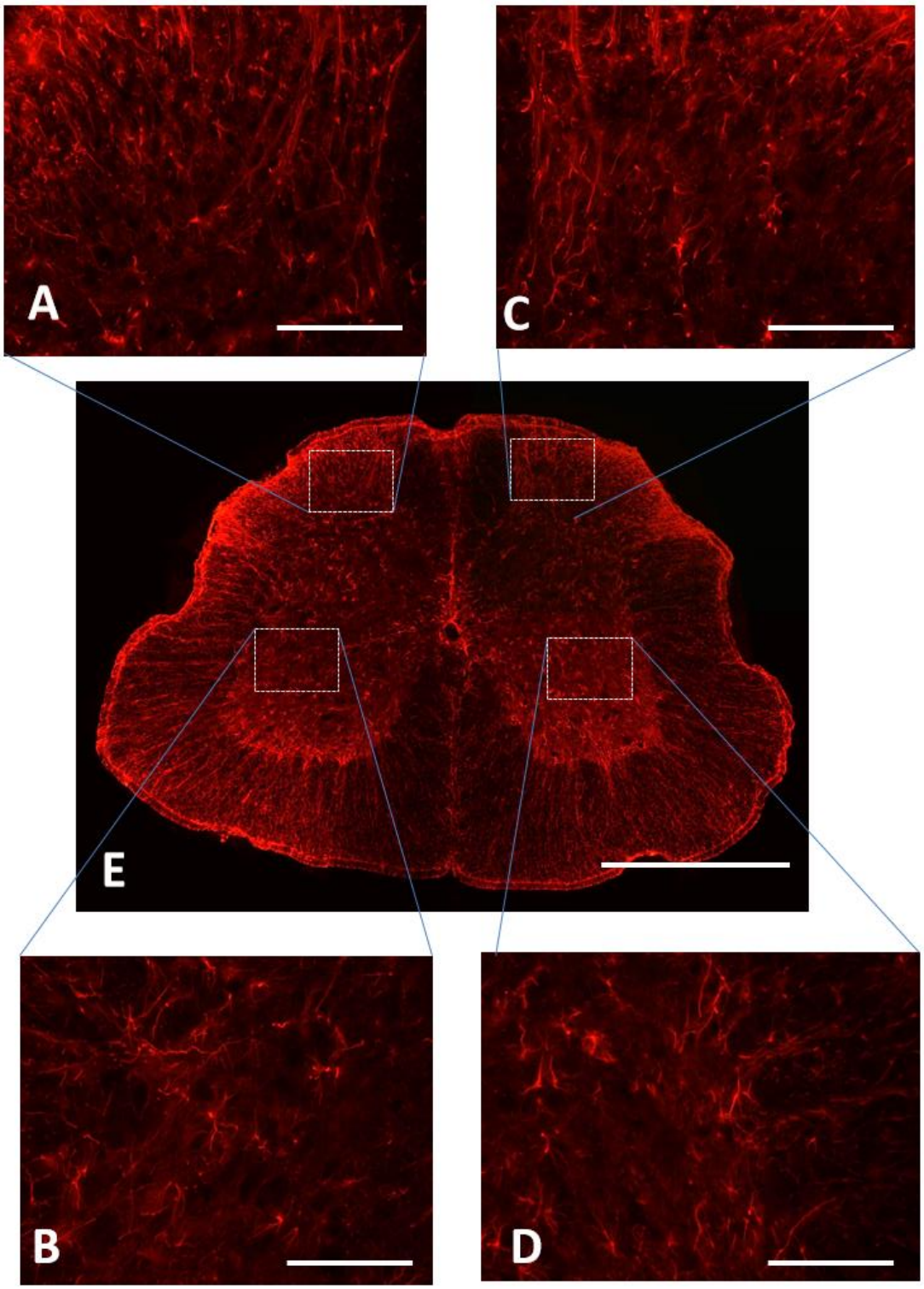

Figure 3.13: A section of spinal cord from an uninjured animal shows astrocyte activation (E using 5x magnification). A) Ipsilateral dorsal horn, B) Ipsilateral ventral horn. C) Contralateral dorsal horn. D) Contralateral Ventral horn (A,B,C,D using 40x magnification). Scale bar A,B,C and D = 0.1mm, E = 1.0mm.

The mean percentage area of GFAP labelling (indication of the degree of astrocyte activation) for each group is shown in Table 3.2. The same data and the statistical comparison between the groups is illustrated in Figure 3.14.

Table 3.2: Percentages of astrocyte activation for Nylon, G-PCL, S-PCL and intact groups.

GFAP (astrocyte)%	Nylon	G-PCL	S-PCL	Intact
Ipsilateral Dorsal horn	19.7	8.1	11.3	8.7
Contralateral Dorsal horn	7.7	6.4	8.1	8.5
Ipsilateral Ventral horn	22.1	9.1	11.8	8.2
Contralateral Ventral horn	8.6	6.8	6.3	7.7

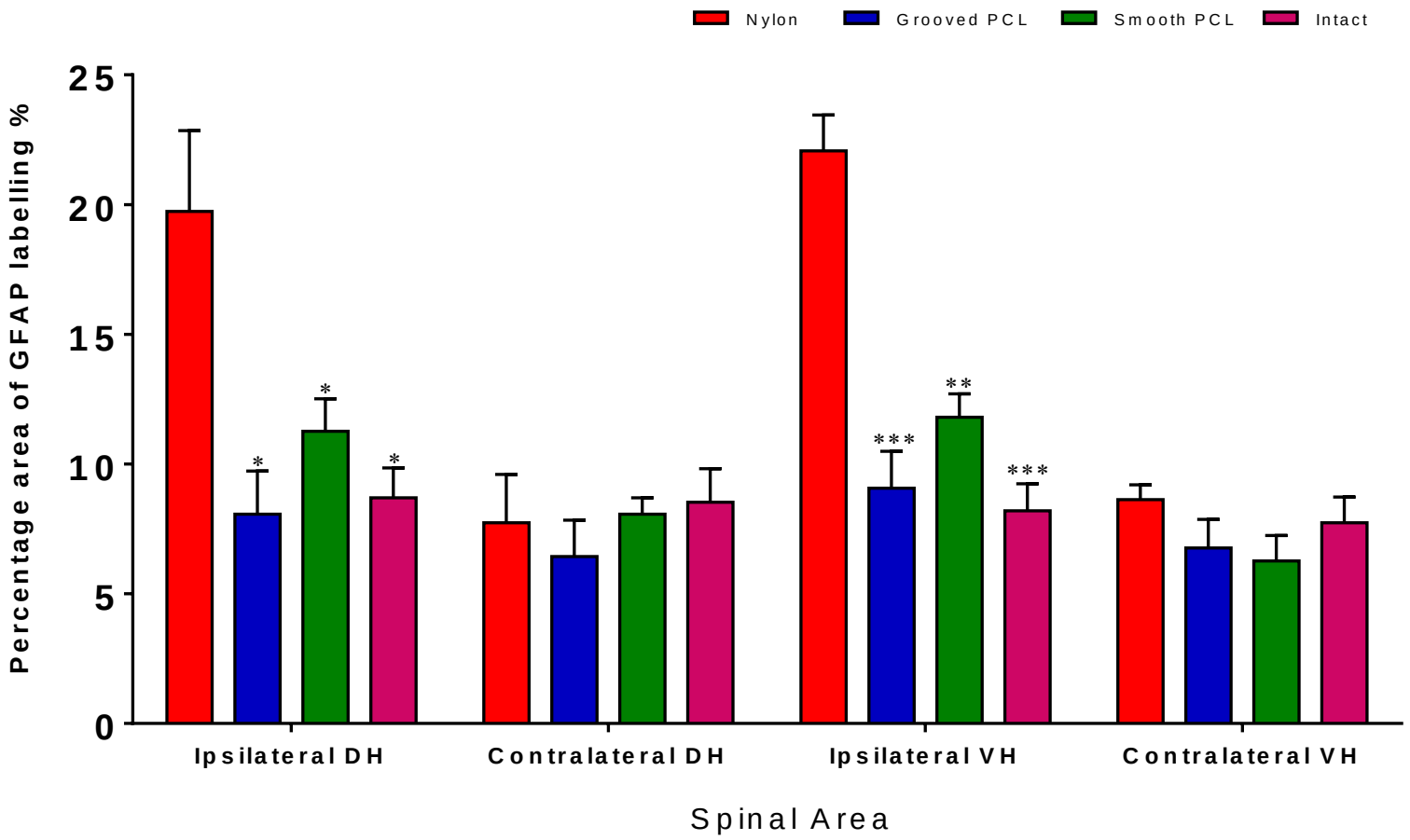

Figure 3.14: Immunohistochemical analysis of astrocyte for Nylon, G-PCL, S-PCL, and intact groups. *, ** and *** denote significant difference compared to Nylon group, $p<0.05$, $p<0.01$ and $p<0.001$, respectively. Error bars denote SEM. Statistical test: 1-way ANOVA with Bonferroni's multiple comparisons test. VH=Ventral Horn, DH=Dorsal Horn.

The increase in staining (Ipsilateral/Contralateral) ratio for GFAP in the Nylon NGC group was significantly higher than in other groups in dorsal (171% vs 29% [G-PCL; $p<0.01$], 39% [S-PCL; $p<0.01$] and 3% [intact; $p<0.001$]) and ventral (157% vs 34% [G-PCL; $p<0.001$], 42% [S-PCL; $p<0.01$] and 6% [intact; $p<0.001$]) horns (Figure 3.15). No significant differences were observed between G-PCL, S-PCL and intact groups in either dorsal or ventral horns ($p>0.05$) (Figure 3.15).

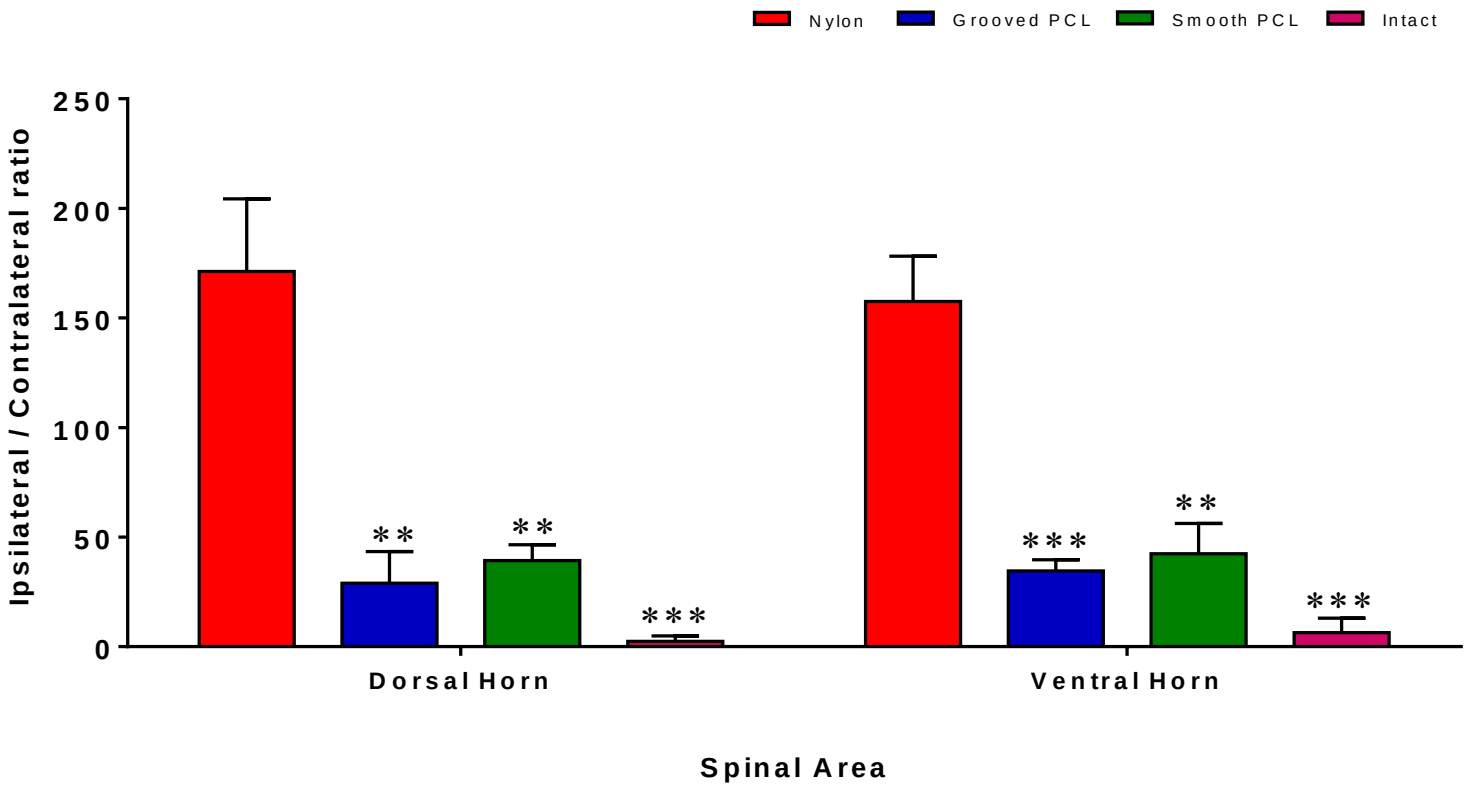

Figure 3.15: Ipsilateral/Contralateral ratio of spinal astrocyte shows the difference of percentage increase in the ipsilateral side over the contralateral side in ventral and dorsal horns of the spinal cord for Nylon, G-PCL, S-PCL, and intact groups. **and *** denote significant difference compared to Nylon group, $p<0.01$ and $p<0.001$ respectively. Error bars denote SEM. Statistical test: 1-way ANOVA with Bonferroni's multiple comparisons test.

3.5 DISCUSSION

3.5.1 Correlation Between Glial Activation and Neuropathic Pain

The results of this chapter were obtained from qualitative and quantitative analysis of glial activation. The idea of glial qualitative and quantitative analysis was reported in Erikson et al's (1993) study. In their study, spinal cord sections were stained by OX-42-IR, a microglial marker. They reported that the reactive microglial cells were higher in ipsilateral dorsal horn compared to contralateral dorsal horn following sciatic nerve injury due to a proliferative process. The curve of the time course for microglial activation gradually increased till it reached the peak at the first week, and then gradually declined. They concluded that using image analysis to quantify the labelling area provides a more accurate evaluation of the activation than just visual inspection (Erikson et al., 1993).

The current study has shown that Iba-1 and GFAP expression are present in the injured (ipsilateral), uninjured (contralateral) sides, and spinal cord of intact animals. It also shows that the highest expression is observed in a specific region of the grey matter in both dorsal horns ns (where the sensory afferent terminals are located) and ventral horns (where the cell bodies of the motor efferents are located) of the L4 segment following the injury of the common fibular and sciatic nerve (Xu et al., 2016). Following peripheral nerve injury, glial became activated as is characterised by cell proliferation and morphological changes. As described in previous studies in their resting state, glial cells have a ramified shape, while after nerve injury they became either hypertrophied or amoeboid in shape (Figure 3.3A, B, C, and D) (Coly 1998, Xu et al., 2016). Mika et al (2009) evaluated the effect of the application of three glial inhibition drugs (minocycline hydrochloride, pentoxifylline, and fluorocitrate) after chronic constriction injury (CCI) of the sciatic nerve. The drugs were injected subcutaneously before CCI and then twice daily. In summary, they reported that glial activation was significantly higher in the ipsilateral spinal cord than contralateral at 7 days post CCI. The level of microglial activation was decreased at 17 days post CCI, while astrocytes activation returned to the control level. They also mentioned that minocycline and pentoxifylline diminished the neuropathic pain, and both tactile (von Frey test) and cold (cold plate test) sensitivity (Mika et al., 2009).

The results reported in this chapter have concentrated mainly on glial activation following nerve injury repair. The immunohistochemical staining suggests that nerve repair with Nylon NGC (created by SLS) produces the highest level of glial activation (in both dorsal and ventral horns), indicating that neuropathic pain is more likely to develop in this group. This alone may indicate that Nylon NGC is not a good choice to bridge gaps in peripheral nerve injuries. There were significant differences between the Nylon group and the other groups (G-PCL and S-PCL). When comparing the results for nerves repaired with G-PCL (created by µSL) and S-PCL (created by UV curing), it was hard to find an obvious difference between them. The G-PCL group expressed slightly lower glial activation than S-PCL group, indicating that neuropathic pain maybe less likely to develop in these groups, but it is not clear that there would be any notable clinical difference. In addition, both G-PCL and S-PCL repair groups had no significant differences compared to the uninjured group.

3.5.2 Correlation Between Glial Activation and Nerve Regeneration

Several studies have been carried in our laboratory to determine a standard level of performance for hollow conduits created by µSL for the purpose of ensuring that these conduits allow nerve regeneration to occur (Harding, 2014, Pateman et al., 2015). The majority of these hollow conduits were successful in enabling the regeneration across the defect area.

The results in this chapter can be collated with a previous study, done in our laboratory, which investigated regeneration in the groups referred to within this chapter by using axon counting and tracing analysis methods on repaired CF nerve. The results of the previous study reported that axons only regenerated part-way into the Nylon NGC without reaching the distal nerve ending. Thus, the nerve regeneration was obviously poor compared to that observed when using G-PCL (Figure 3.16 and 3.17) (Harding, 2014).

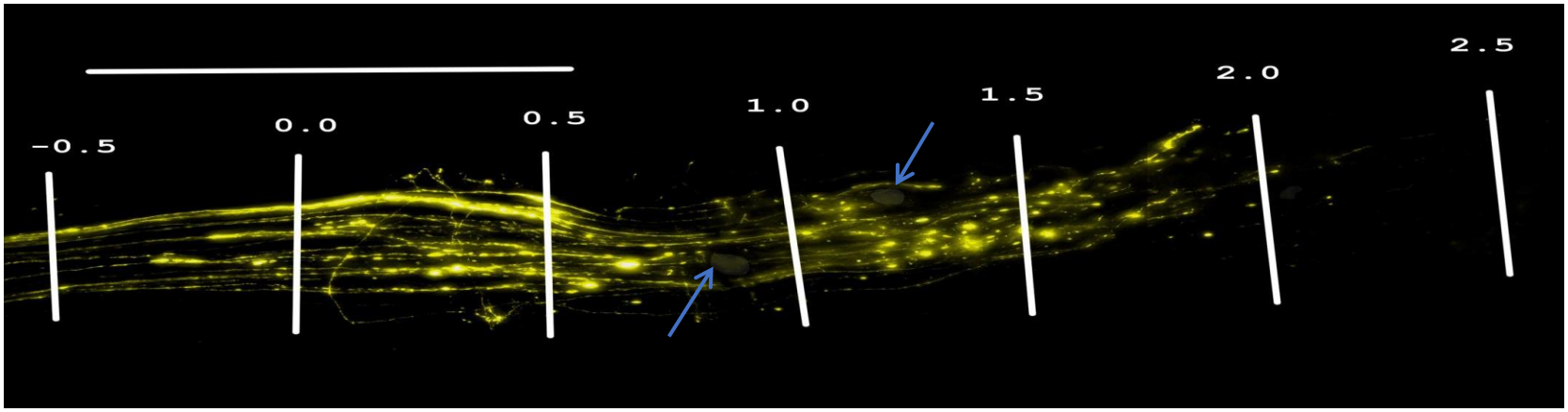

Figure 3.16: Image of a common fibular nerve repaired with Nylon conduit showing the poor regeneration of the nerve (few axons reaching interval 2.5mm). Also it shows some opaque specks (un-sintered nylon-12 powder) marked by blue arrows. Scale bar =1.0mm. (Harding, 2014).

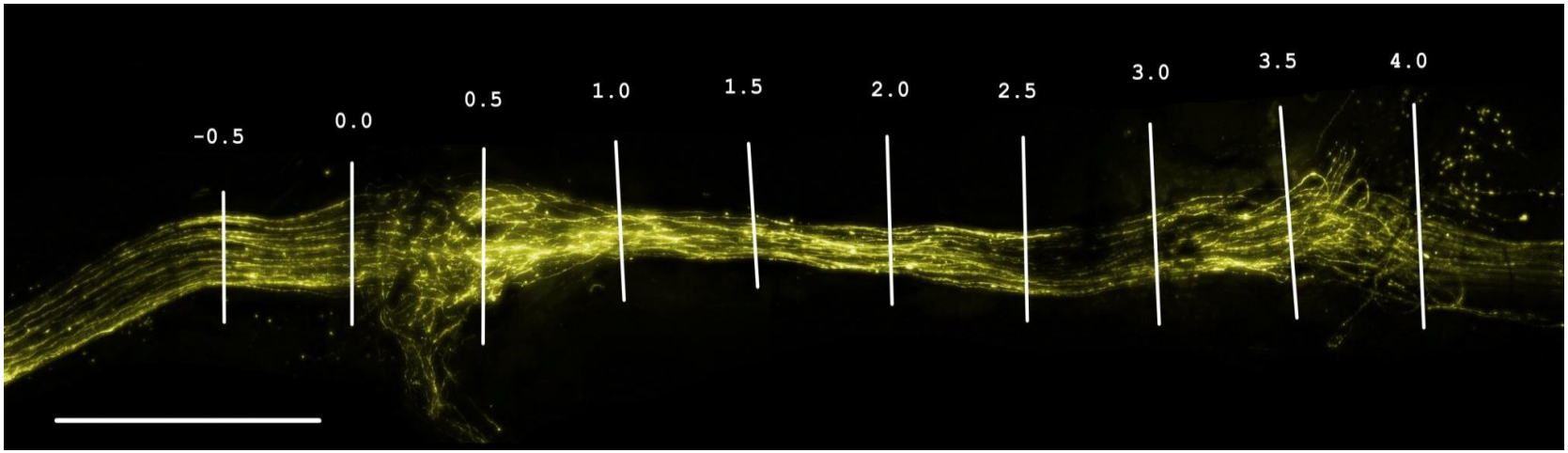

Figure 3.17: Image of a common fibular nerve repaired with G-PCL conduit showing good regeneration of the nerve (a large proportion of the axons travelled all the way through and reached the distal stump). Scale bar =1.0mm. (Harding, 2014).

Taken together the data of increased glial activation (in the current study) and poor regeneration (in the previous study) in the Nylon group, a number of factors behind this can be suggested such as conduit material and internal diameter. First, the type of the conduit material may irritate the tissue and produce a greater inflammatory response forming an unsuitable environment to regenerate. Although using nylon-12 powder is unlikely to cause such this problem as it is considered to be a biologically inert material (Williams and Blayney, 1987), the presence of un-sintered powered inside the conduit lumen may block the regenerated axons and irritate them. The images of nerves repaired with Nylon NGCs showed some opaque specks within the regenerating tissue, suggesting that these specks are un-sintered nylon-12 powder which remained from the time of creating the conduits (Figure 3.16).

Second, although many steps were applied to ensure that the conduits were free of any un-sintered nylon-12 powder (i.e pressurized air, a hypodermic needle filled with alcohol, soaking in denatured alcohol), it was noted that these steps failed to clear out all the loose and partially sintered nylon-12 powder, resulting in reducing the actual internal diameter to approximately 0.6mm. This may congest and block the regenerating axons inside the conduit, reducing their ability to successfully regenerate (Harding, 2014). The dimensions of the Nylon NGC were close to the resolution limit of the SLS machine as the internal diameter of the conduit was smaller than the actual design sizes, mainly due to the precision of the SLS machine as the laser heating is not very accurate (it is not possible to have 100% heat where it's needed and 0% where it is not required) so some extra powder either side of the desired dimensions partially melts. The combination of un-sintered powder and reduced conduit dimensions may lead to poor regeneration and that itself may influence glial activation.

Although the G-PCL and S-PCL are made from the same materials, they express different outcomes in both nerve regeneration and glial activation. The regeneration following repair with S-PCL conduits reported in the previous study was poor, but better than Nylon conduits, compared to the G-PCL. As mentioned earlier that S-PCL was produced using a simple UV curing while G-PCL was produced using µSL that forms conduits layer by layer providing a more microstructured internal surface. This implies that the physical structure, including the internal structure, of the

conduits plays an essential role to support nerve regeneration (Harding 2014). Following repair with G-PCL or S-PCL produced low levels of glial activation, suggesting that PCL material most probably does not have such a negative effect on the regenerating axons and providing a more suitable environment for them. By pooling all the data of the three conduits for both nerve regeneration and glial activation, it can be suggested that using a suitable materials and improving the internal structure of the conduit will enhance the outcome of the nerve regeneration and therefore decreasing the potential development of neuropathic pain.

3.6 CONCLUSION

Findings in this chapter are in agreement with previous reports that spinal glial cells are activated following peripheral nerve injury. Peripheral nerve injury repaired by different types of conduit, each producing differing regeneration levels, results in different levels of spinal glial activation. Nerve repair with Nylon conduits produced by SLS produces a high level of glial activation and poor regeneration, which may increase the potential development of neuropathic pain. Images of both glial activation and nerve regeneration of Nylon NGCs suggest that the SLS conduit has an inhibitory effect on nerve regeneration. This means that the use of SLS for creating nerve guide conduits is currently not suitable as it is difficult to achieve the optimal model (internal diameter and wall thickness), with improved materials and manufacturing resolution required. Although nylon-12 powder is considered to be a biologically inert material, it has some properties undesirable in artificial nerve guides. Nylon-12 is rigid, non-degradable and non-porous (Harding, 2014, Williams and Blayney, 1987).

On the other hand, G-PCL conduits produced by µSL express lower levels of glial activation and demonstrate good regeneration, which may decrease the potential development of neuropathic pain. With the use of S-PCL conduits, produced by UV curing, resulting in similar glial activation to G-PCL but comparatively poorer regeneration, it could be suggested that glial activation is greatly increased when regeneration is obstructed (i.e. Nylon NGC) but generally remains at a lower level when the regenerative environment is simply non-supportive (i.e. S-PCL).

Following the positive results from the regeneration study, and paired with the relatively low glial activation reported in this chapter, it was decided to investigate the potential of G-PCL, produced by µSL, conduits at supporting regeneration across longer gaps (see chapter 5).

CHAPTER 4

THE EFFECTS OF LOCAL ADMINISTRATION OF MANNOSE-6-PHOSPHATE ON GLIAL ACTIVATION AND NERVE REGENERATION

SUMMARY

The study reported in this chapter was designed to investigate the effect of applying Mannose-6-Phosphate (600mM) at the site of injury of graft repair using a method of application (incorporated within fibrin glue). Immunohistochemistry was performed to investigate glial activation, which acts as a potential indicator of the development of neuropathic pain, while axon tracing and counting analysis was performed to assess nerve regeneration. The overall impact of M6P in this study was limited in terms of effects observed in glial activation and nerve regeneration as no significant differences were observed when comparing to control group. This apparent therapeutic failure could be due to inappropriate dosage, timing, duration, or route of administration. Thus further investigation may be warranted in order to optimise dosage, administration route and determine any effect.

4.1 INTRODUCTION

Recovery after nerve repair is highly variable and full functional recovery is very rare (Robinson et al., 2000). The outcome depends on many factors occurring after injury such as scarring, neural cell death, and the formation of a neuroma around the site of injury. It has been reported that scar formation occurs after peripheral nerve injury in both repaired and unrepaired nerves (Mathur, 1983). Scar tissue can cause obstruction of the regenerating axons, resulting in the formation of a neuroma (Foltan et al., 2008), which can lead to the development of neuropathic pain.

The influence of scar formation on nerve regeneration following peripheral nerve repair was reported by Atkins et al. (2006b). They compared regeneration of the sciatic nerve in two transgenic mice strains with an increased propensity for scarring [IL-4L/IL-10 null mice] or decreased propensity for scarring [M6PR/IGF2 null mice] with regeneration in normal mice. This revealed an inverse correlation between the level of peripheral nerve regeneration and the level of scar formation, providing "proof of concept" that targeting scarring using therapeutic agents could enhance regeneration (Atkins et al., 2006b, Ngeow et al., 2011a). Following this, several studies have been undertaken with the aim to find a therapeutic anti-scarring agent, which could help to reduce scarring and enhance regeneration after peripheral nerve injury.

One of the approaches to improve regeneration by reducing the amount of scar formation at the site of injury is to inhibit the activation of latent TGF-β using Mannose-6-Phosphate (M6P), a potential anti-scarring agent, as it acts competitively on the same receptor as latent TGF-β (see section 1.9.1.1 for more details on TGF-β and scarring). Several recent studies (Harding et al., 2014, McCallion and Ferguson, 1996, Ngeow, 2010, Ngeow et al., 2011a, Ngeow et al., 2011b) have reported that M6P treatment results in decreased scar formation or enhanced nerve regeneration.

There are many potential ways to treat the site of nerve repair with M6P. In Ngeow et al's (2011a) study, approximately 20µl of M6P (200mM or 600mM) was injected beneath epineurium of the sciatic nerve. The nerve was then transected and immediately repaired using sutures. The remaining M6P solution (80µl) was then injected around the injury site and into the surrounding muscles. They reported that

600mM M6P had an effect to reduce scarring, whereas 200mM did not. In Harding et al's (2014) study, approximately 3.0mm of the common fibular nerve of a wild type mouse was transected and removed. The removed nerve was then immersed in a vial containing M6P (600mM) for 30 minutes before being placed in the YFP mouse and secured by fibrin glue. While these application methods resulted in M6P affecting regeneration, neither are ideally suited for clinical use as they are technically difficult and time consuming.

The use of fibrin as a natural adhesive began in the early 1900s (Gibble and Ness, 1990). Fibrin glue (Fibrin sealant) is a product that mimics the final stage of coagulation cascade via the activation of fibrinogen by the addition of thrombin, leading to the formation of fibrin clot that is completely absorbed during healing without foreign body reaction (Brennan, 1992; Radosevich et al., 1997). Replacing the suture with fibrin glue in peripheral nerve repairs has been reported in several studies. A study by Bhandari (2013) evaluated the effect of using fibrin glue in the repair of brachial plexus injury. The results of that study showed that using fibrin glue is an effective and alternative technique for peripheral nerve repair as it provides a simple application, reduced operation time by 30% compared to suturing technique, good strength sufficient to hold the two ends of the nerve together, and similar functional recovery compared to those obtained with sutures (Bhandari, 2013). In recent years, fibrin glue has been used as a gel for cell delivery and as a vehicle for drug delivery (Spicer and Mikos, 2010). Applying M6P via fibrin glue provides an easier and quicker modality of use than previous research applications.

4.2 AIM OF THIS STUDY

The present chapter describes the effect of applying M6P (600mM) at the site of injury of graft repair using a method of application (incorporated within fibrin glue) with greater clinical relevance than previous studies. In addition to testing a new application method, the study described within this chapter also investigated the effects of M6P on spinal glial activation, as although the effect of M6P has previously been shown to enhance nerve regeneration, its ability to influence the degree of glial activation and potential development of neuropathic pain following nerve injury and

repair has not been investigated. We hypothesise that using M6P (600mM) incorporated with fibrin glue will reduce glial activation and enhance regeneration.

4.3 MATERIAL AND METHODS

The protocol for this study was based on previous protocols used in our laboratory at the University of Sheffield, and have been described in Chapter 2. Some more specific information involved to the present study is described below.

4.3.1 Animal Numbers and Groups

28 mice were used in the study: 17 *thy-1-YFP-H* mice on a C57BL6 background and 14 wild type mice (to provide graft material), divided into 3 experimental groups: mice treated with fibrin glue with M6P (n=7), mice treated with fibrin glue alone (n=7), and injured (unrepaired) mice (n=3) (Figure 4.1).

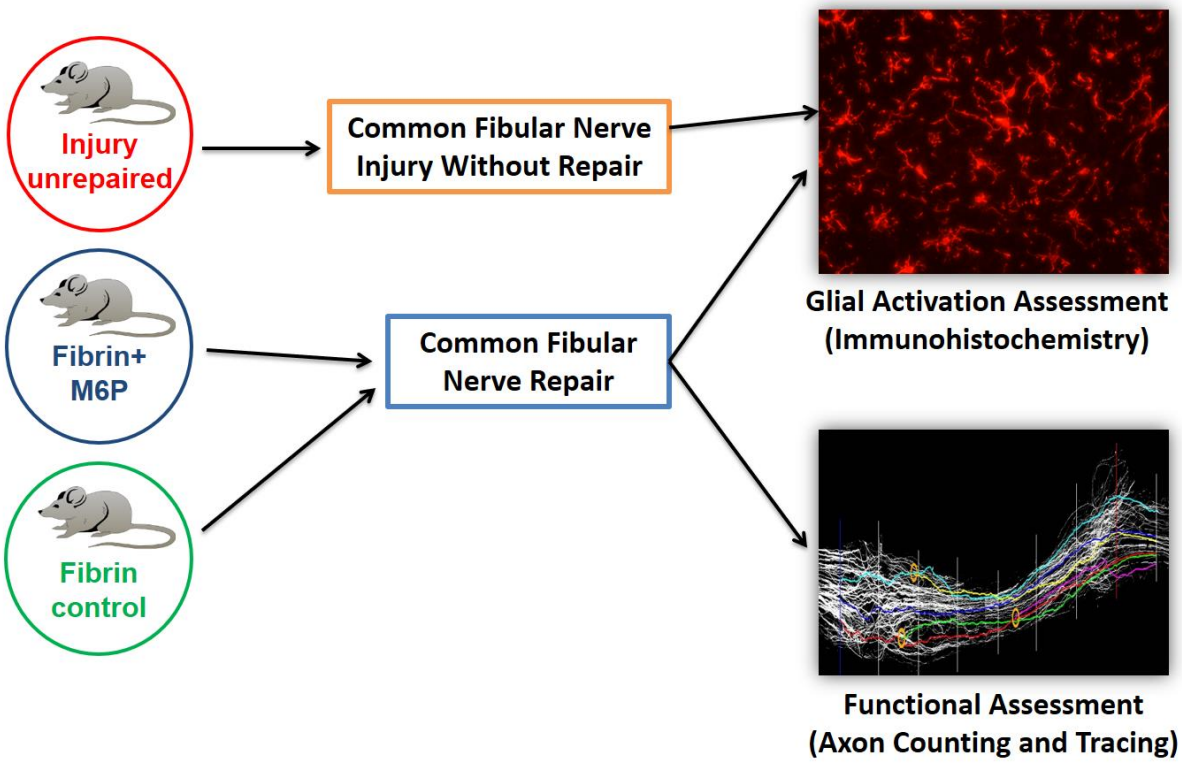

Figure 4.1 Summary of groups for the investigation of the M6P.

4.3.2 Experimental Methods

Wild type mice were anaesthetised (see section 2.2.3.2.i) and the common fibular (CF) nerve exposed, freed from the surrounding tissues, and then re-covered to keep it healthy. YFP-H mice were anaesthetised (see section 2.2.3.1.i), and placed beside the wild type. The common fibular nerve was exposed, and prepared for receiving the nerve graft. Graft tissue of 3.0mm was obtained from the wild type mouse and placed next to the CF nerve in the YFP-H mouse. The CF nerve of the YFP-H mouse was transected, and a gap of approximately 2.5mm made (see section 2.2.3.1.ii). A 5.0mm silicone trough was then placed underneath the two ends and the gap was bridged using the obtained tissue (3.0mm) from the wild type mouse (see section 2.2.3.1.iii). The nerve ends and graft were then aligned and secured with fibrin glue with/without M6P (600mM) (Figure 4.2). For the injured, unrepaired group, a part of the common fibular nerve was removed, and then the proximal and distal nerve ends were tied-off with silk suture in order to prevent axon regeneration. Animals were allowed to recover for 14-days to allow regeneration through the graft and for distal fluorescent to clear.

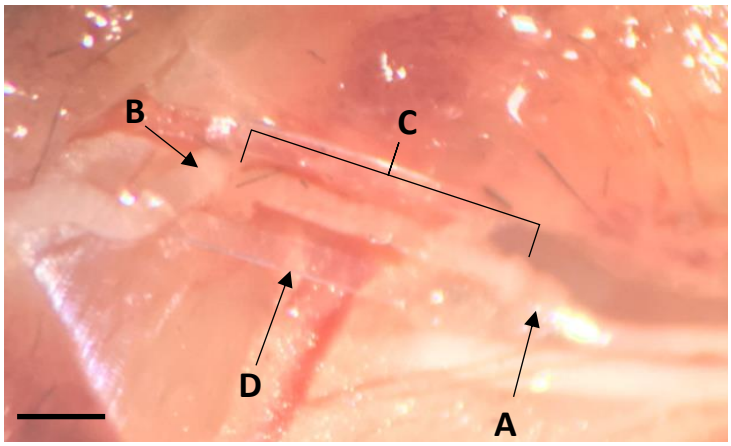

Figure 4.2: Image shows the nerve graft between the two ends of the CF nerve and secured by glue. A) The proximal stump. B) The distal stump. C) The nerve graft. D) Silicone rough. Scale bar = 1.0mm.

Following the recovery period, animals were anaesthetised (see section 2.2.3.2.i), and the CF nerve was fixed, harvested (see sections 2.2.3.2.ii) and prepared for analysis using a fluorescent microscope (see sections 2.2.7). In addition, spinal cord was also harvested, fixed and prepared for immunohistochemical labelling of microglial and astrocytes using primary antibodies raised in goat against Iba-1 (to

label microglia) and in rabbit against GFAP (to label astrocytes) (see sections 2.2.4). Immunohistochemical labelling and axon counting and tracing analysis were quantified as described in Chapter 2. In all cases, analysis was carried out blind. For the unrepaired group, only spinal cord was harvested, as the effects of this process on nerve regeneration have been established previously (Harding, 2014).

4.3.3 Sample Size Calculation

The sample size for this chapter were calculated using both PiFace software [v1.76: *homepage.stat.uiowa.edu/~rlenth/Power*] (for axon tracing) and Biomath software [Source: G.W. Snedecor & W.G. Cochran. *http://www.biomath.info/power/ttest.htm*] (for axon disruption as PiFace software does not perform t-test) with standard deviation (SD) data obtained from a previous study by Harding et al. (2014) in our laboratory. The sample size chosen for the study was n=7, which would be sufficient to detect differences between groups of 14.42% and 7.372 for axon tracing [Figure 4.3] and axon disruption [Figure 4.4], respectively.

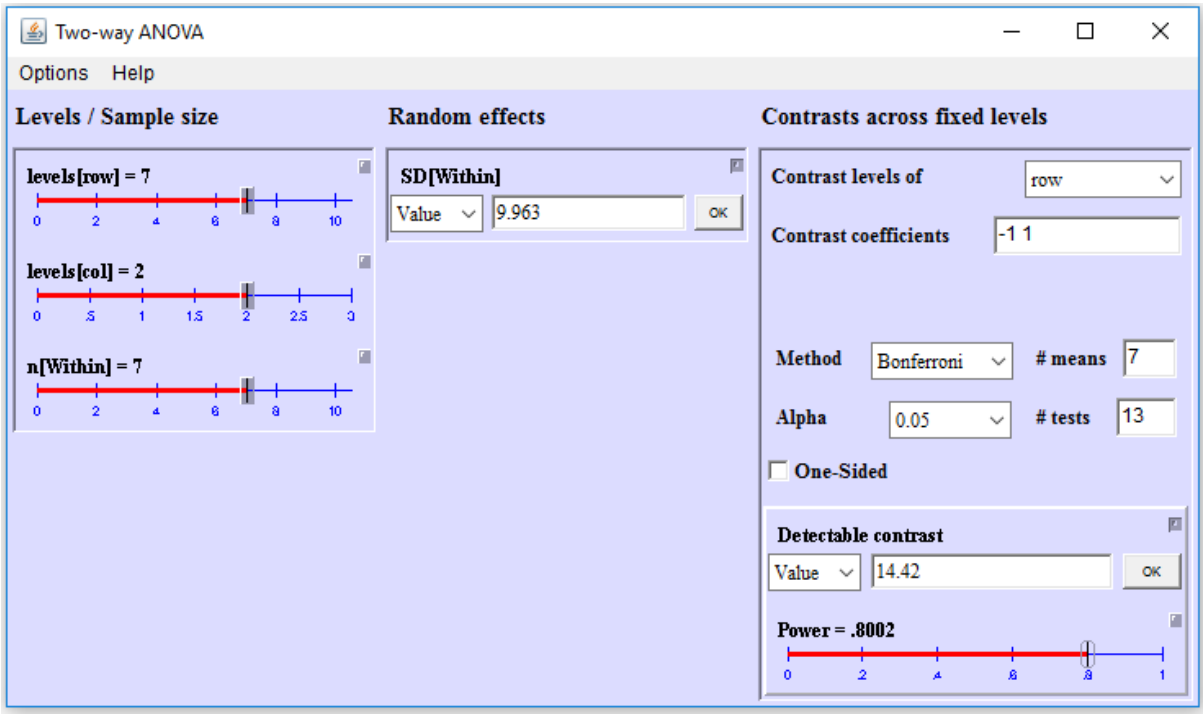

Figure 4.3: Axon tracing analysis of power calculation for a sample size of 7 animals in each group. Levels[row] = number of intervals; levels[col] = number of groups; n[Within] = sample size; SD[Within] = standard deviation value. Number of intervals [# means] multiplied by number of repair groups minus one gives the number of t-tests required for the Bonferroni's multiple comparisons test [# tests].

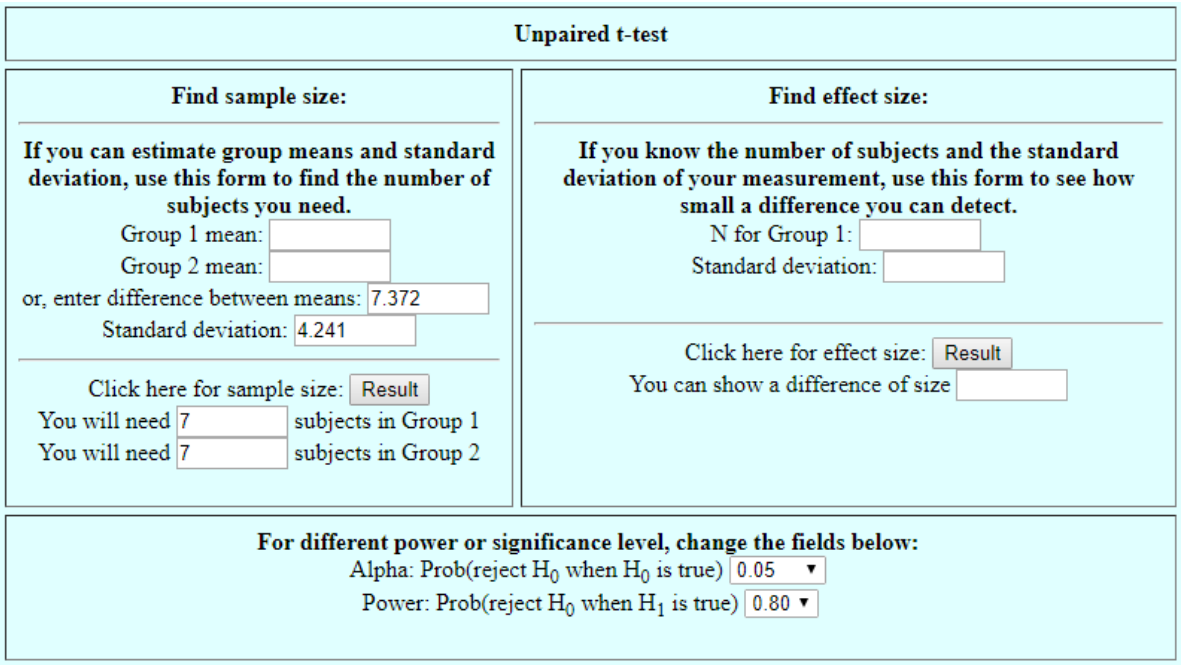

Figure 4.4: Axon disruption analysis of power calculation for a sample size of 7 animals in each

4.3.4 Statistical Analysis

Statistical comparisons between groups were carried out as stated in section 2.3.7. A short summary is provided below.

4.3.4.1 Statistical Analysis of Glial Activation in Spinal Cord

For statistical analysis of glial activation, a 1-way ANOVA with Bonferroni's multiple comparisons test was used.

4.3.4.2 Statistical Analysis of Nerve Regeneration

For sprouting index and axon tracing results, a 2-way ANOVA with Bonferroni's multiple comparisons test was used in order to detect overall and individual intervals differences between the experimental groups, while for axon disruption results an unpaired t-test (two-tailed) was used.

All statistical analysis was performed using GraphPad Prism 7 software (GraphPad Prism Inc, CA, USA). Differences were considered to be significant at a *p* value below 0.05.

4.4 RESULTS

All animals recovered well from the procedure without any sign of infection. The results in the present chapter were obtained through a combination of two methods, immunohistochemistry of the spinal cord and axon counting and tracing analysis of the regenerated nerve. The immunohistochemistry was performed to investigate glial activation, which acts as a potential indicator of the development of neuropathic pain, while axon tracing and counting analysis was performed to assess nerve regeneration.

4.4.1 Assessment of Glial Activation

4.4.1.1 Qualitative Observations of Spinal Cord

Glial activation was apparent in the injured side for all repair groups and the greatest observed immunoreactivity was present in a specific area of grey matter. This represents the region of the spinal cord to which the common fibular nerve projects. The activation was comparably high in the unrepaired group, and amoeboid glia were observed (Figure 4.5A). The level of activation was minimal in both M6P and control groups and a number of hypertrophied glia were observed. However, the cells in the M6P group appeared less inflamed compared to those in the control group (Figure 4.5B and C).

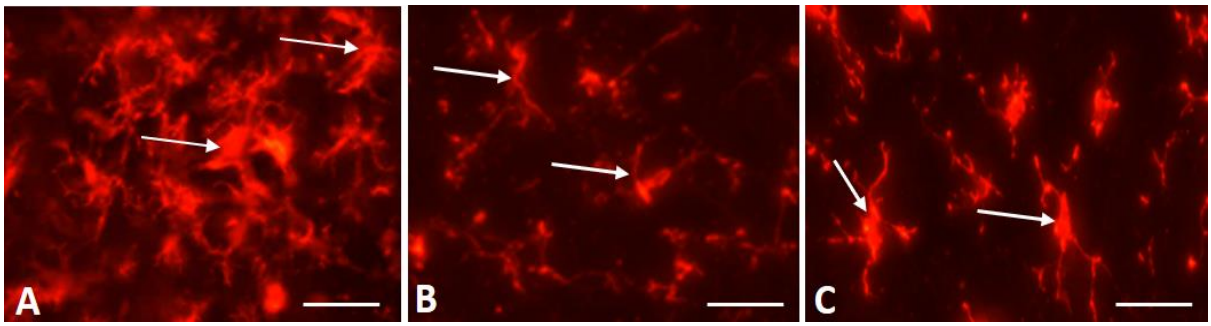

Figure 4.5: Sections of spinal cord after Immunohistochemistry staining with antibody Iba-1 showing different morphological phenotypes of microglial cells. A) Unrepaired group showing amoeboid microglia (white arrows). B) M6P and C) Control groups showing hypertrophied microglia (white arrows). Scale bar = 0.1mm.

4.4.1.2 Quantitative Analysis of Spinal Cord

As described in section 2.2.8.1(A), the percentage area of labelling for Iba-1 and GFAP was calculated in defined regions of the dorsal and ventral horns of the spinal cord both ipsilaterally and contralaterally to the nerve repair.

4.4.1.2.i Quantification of Iba-1 Expression

Quantification of labelling for microglial activation within the three groups demonstrates that the unrepaired group had significantly higher levels than other groups in both ipsilateral dorsal (7.5% vs 4.4% [M6P; $p<0.01$] and 4.2% [control; $p<0.001$]) and ventral (8.9% vs 3.1% [M6P; $p<0.001$] and 2.7% [control; $p<0.001$]) horns (Table 4.1 & Figure 4.9). M6P-treated mice had similar levels of labelling in both the ipsilateral dorsal and ventral horns compared with the control group (fibrin glue alone); there were no significant differences in labelling between these two groups (refer to Table 4.1 & Figure 4.9). In the corresponding contralateral side, the percentage area of Iba-1 labelling in the dorsal horn was slightly higher in the unrepaired group (3.8%) compared with the M6P-treated mice (3.3%) and the control group (3.2%). In the ventral horn, the percentage area in the unrepaired group was slightly higher (3.1%) compared with the M6P-treated group (2.5%) and significantly higher than in the control group (2.1%; $p<0.05$) (refer to Table 4.1 & Figure 4.9). The activation areas of Iba-1 in each group are shown in Figures 4.6-4.8.

Unrepaired group

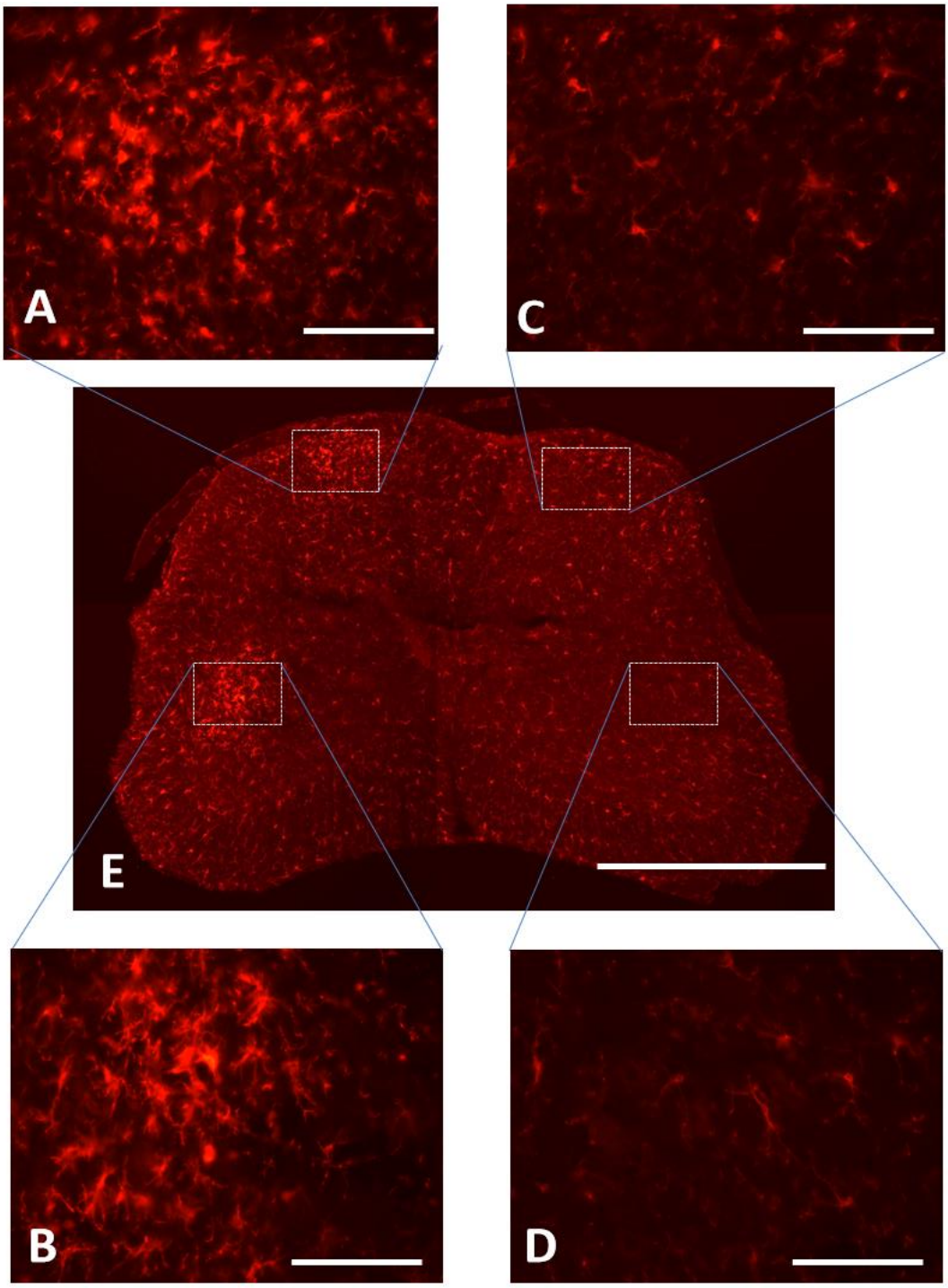

Figure 4.6: A section of spinal cord from an injured (unrepaired) animal shows microglial activation (E using 5x magnification). A) Ipsilateral dorsal horn, B) Ipsilateral ventral horn. C) Contralateral dorsal horn. D) Contralateral Ventral horn (A,B,C,D using 40x magnification). Scale bar A,B,C and D = 0.1mm, E = 1.0mm.

M6P group

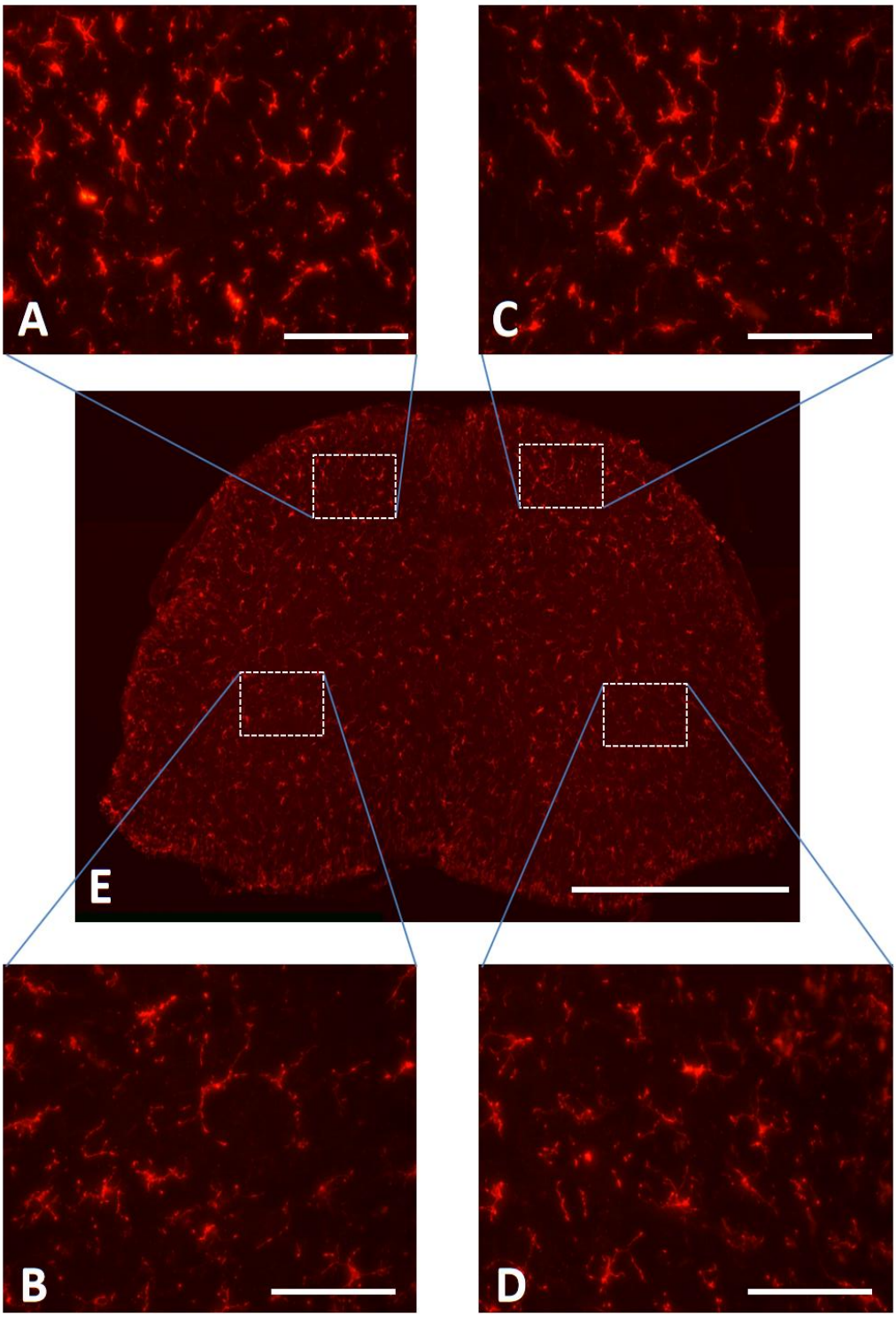

Figure 4.7: A section of spinal cord following nerve repair with fibrin glue and M6P shows microglial activation (E using 5x magnification). A) Ipsilateral dorsal horn, B) Ipsilateral ventral horn. C) Contralateral dorsal horn. D) Contralateral Ventral horn (A,B,C,D using 40x magnification). Scale bar A,B,C and D = 0.1mm, E = 1.0mm.

Control group

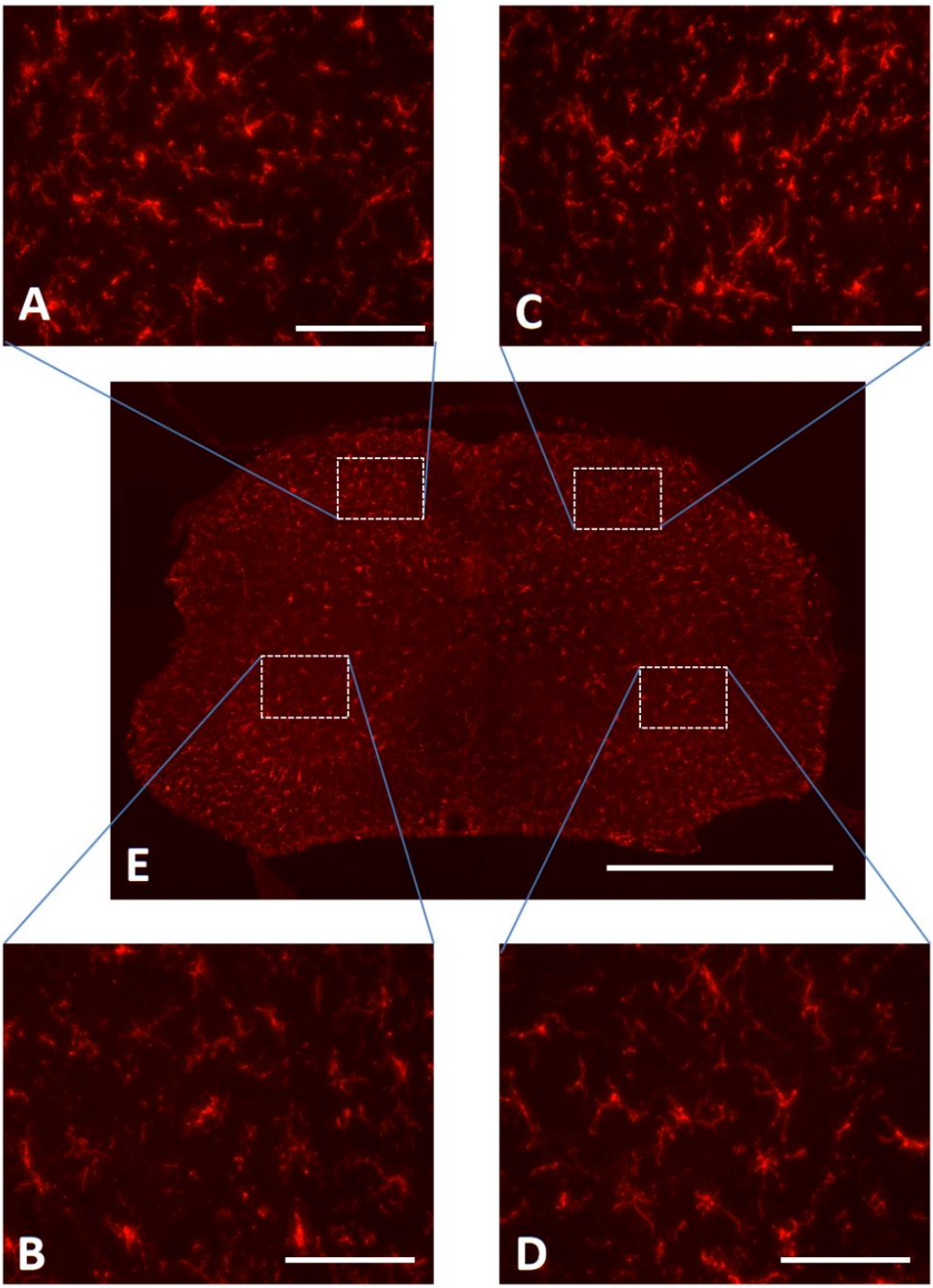

Figure 4.8: A section of spinal cord following nerve repair with fibrin glue alone (control) shows microglial activation (E using 5x magnification). A) Ipsilateral dorsal horn, B) Ipsilateral ventral horn. C) Contralateral dorsal horn. D) Contralateral Ventral horn (A,B,C,D using 40x magnification). Scale bar A,B,C and D = 0.1mm, E = 1.0mm.

The mean percentage area of Iba-1 labelling (indication of the degree of microglial activation) for each group is shown in Table 4.1. The same data and the statistical comparison between the groups is illustrated in Figure 4.9.

Table 4.1: Percentages of microglial activation for unrepaired, M6P and control groups.

IBA-1 (Microglia)%	Unrepaired	M6P	Control
Ipsilateral Dorsal horn	7.5	4.4	4.2
Contralateral Dorsal horn	3.8	3.3	3.2
Ipsilateral Ventral horn	8.9	3.1	2.7
Contralateral Ventral horn	3.1	2.5	2.1

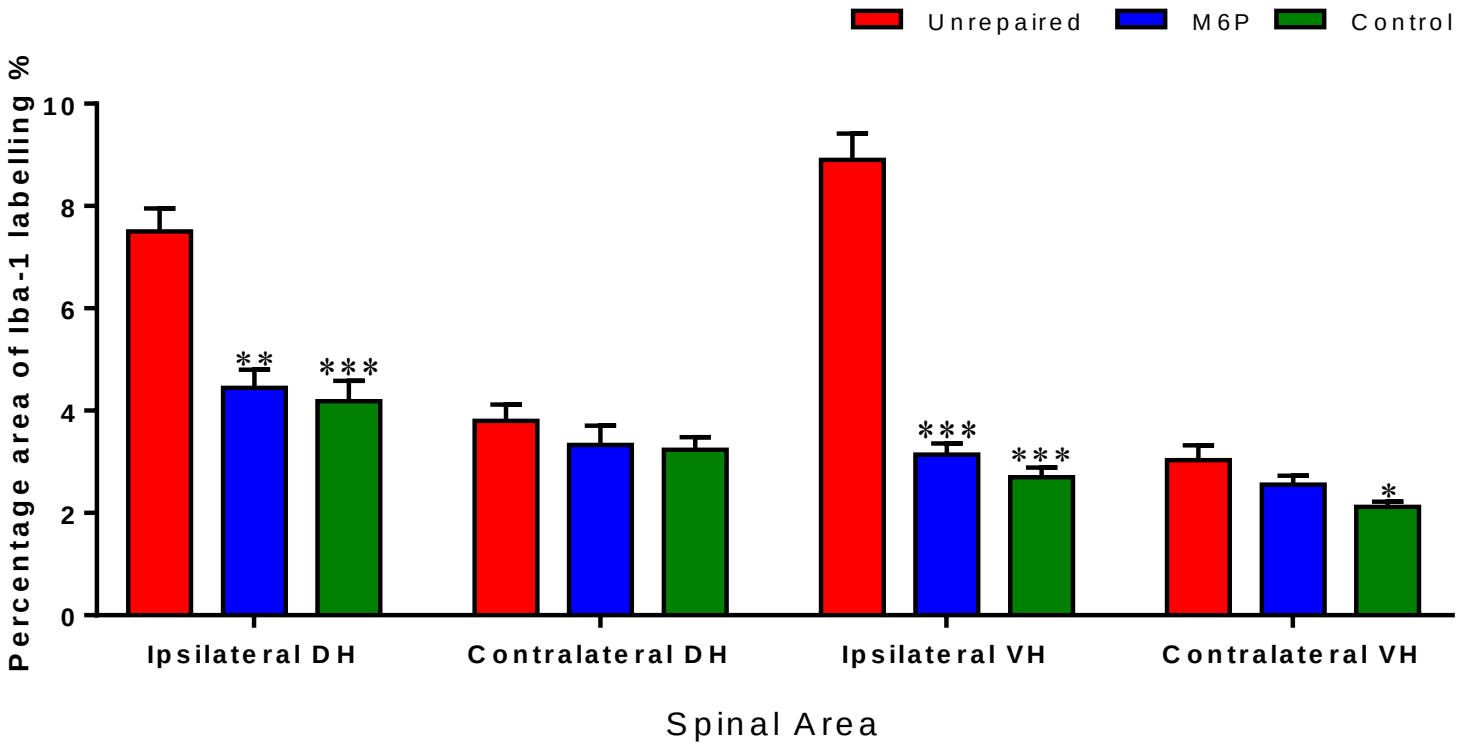

Figure 4.9: Immunohistochemical analysis of microglia for M6P, control and unrepaired groups. *, ** and *** denote significant difference compared to unrepaired group, $p<0.05$ $p<0.01$ and $p<0.001$ respectively. No significant difference between M6P and control group. Error bars denote SEM. Statistical test: 1-way ANOVA with Bonferroni's multiple comparisons test. DH: Dorsal horn. VH: Ventral horn.

As described in section 2.2.8.1(B), some variation in the background staining was noted. Thus, percentage increase of the ipsilateral (injured) side over the contralateral (uninjured) side, ‘‘staining ratio’’ was performed. Comparisons between the groups when assessing the staining gave similar results to those described above. The increase in staining (Ipsilateral/Contralateral) ratio for Iba-1 in the unrepaired group was significantly higher than in other groups in both dorsal (98.5% vs 36.8% [M6P; $p<0.001$] and 29.1% [control; $p<0.001$]) and ventral (196.2% vs 23% [M6P; $p<0.001$] and 27.2% [control; $p<0.001$]) horns (Figure 4.10). The M6P-treated group had a slightly higher percentage increase in the dorsal horn compared with the control group, whereas in the ventral horn, the M6P-treated group had a marginally lower percentage increase compared with the control group; these differences were not significant (Figure 4.10).

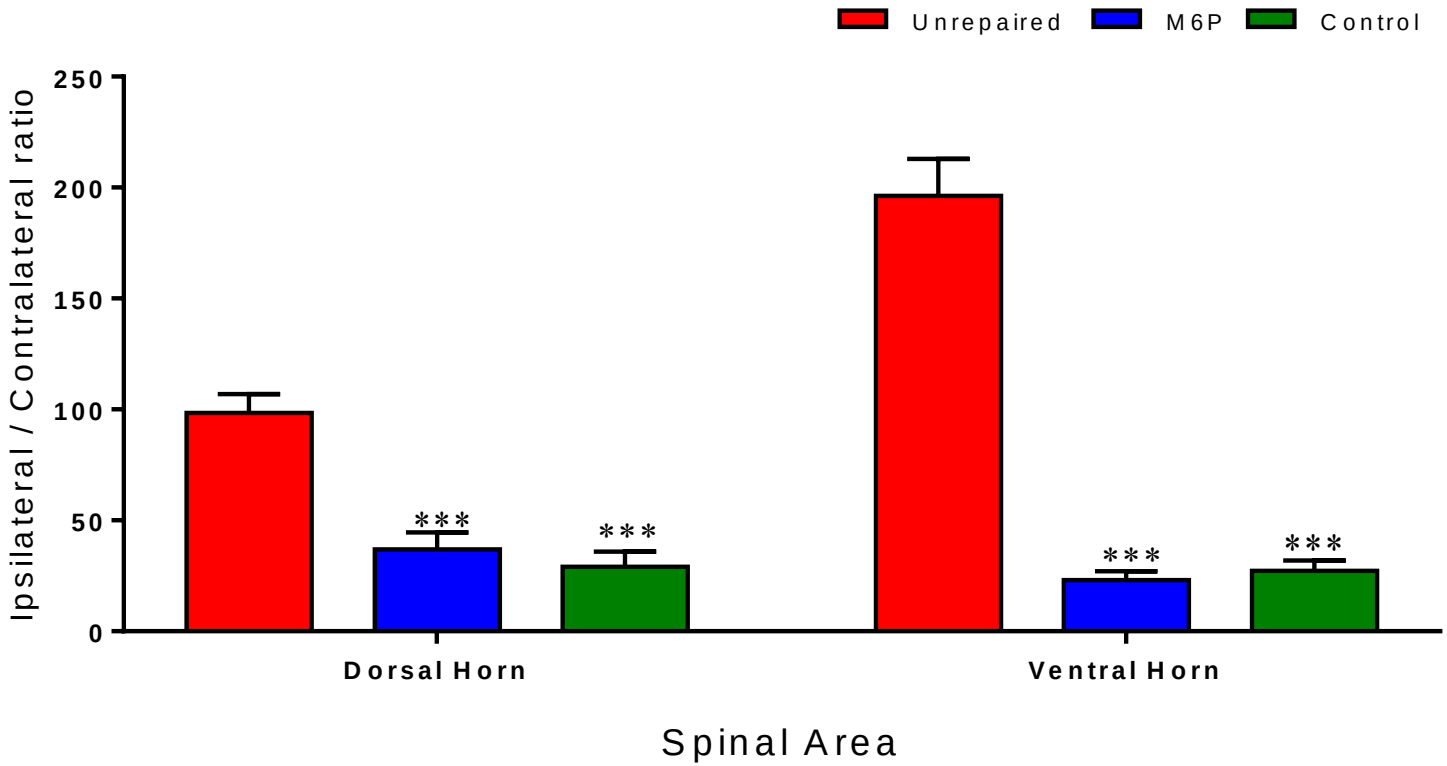

Figure 4.10: Ipsilateral/Contralateral ratio of microglia shows the difference of percentage increase in the ipsilateral side over the contralateral side in dorsal and ventral horns of the spinal cord for unrepaired, M6P and control groups. *** denote significant difference compared to unrepaired group, $p<0.001$. The M6P-treated group expresses higher activation on dorsal horn and lower on ventral horn compared to control group. No significant different were observed between the M6P and control groups. Error bars denote SEM. Statistical test: 1-way ANOVA with Bonferroni's multiple comparisons test.

4.4.1.2.ii Quantification of GFAP Expression

Quantification of labelling for astrocyte activation within the three groups demonstrates that the unrepaired group had significantly higher levels than other groups in both ipsilateral dorsal (7.1% vs 4.0% [M6P; $p<0.01$] and 4.4% [control; $p<0.05$]) and ventral (6.5% vs 3.1% [M6P; $p<0.001$] and 3.1% [control; $p<0.001$]) horns (Table 4.2, Figure 4.14). M6P-treated mice had similar levels of labelling in both the ipsilateral dorsal and ventral horns compared with the control group (fibrin glue alone); there were no significant differences in labelling between these two groups (refer to Table 4.2, Figure 4.14). In the corresponding contralateral side, the percentage area of GFAP labelling in the dorsal horn was slightly higher in the unrepaired group (3.8%) compared with the M6P-treated mice (3.2%) and the control group (3.4%). In the ventral horn, the percentage area in the unrepaired group was slightly higher (2.7%) compared with the M6P-treated group (2.4%) and the control group (2.3%) (refer to Table 4.2, Figure 4.14). The activation areas of GFAP in each group are shown in Figures 4.11-4.13.

Unrepaired group

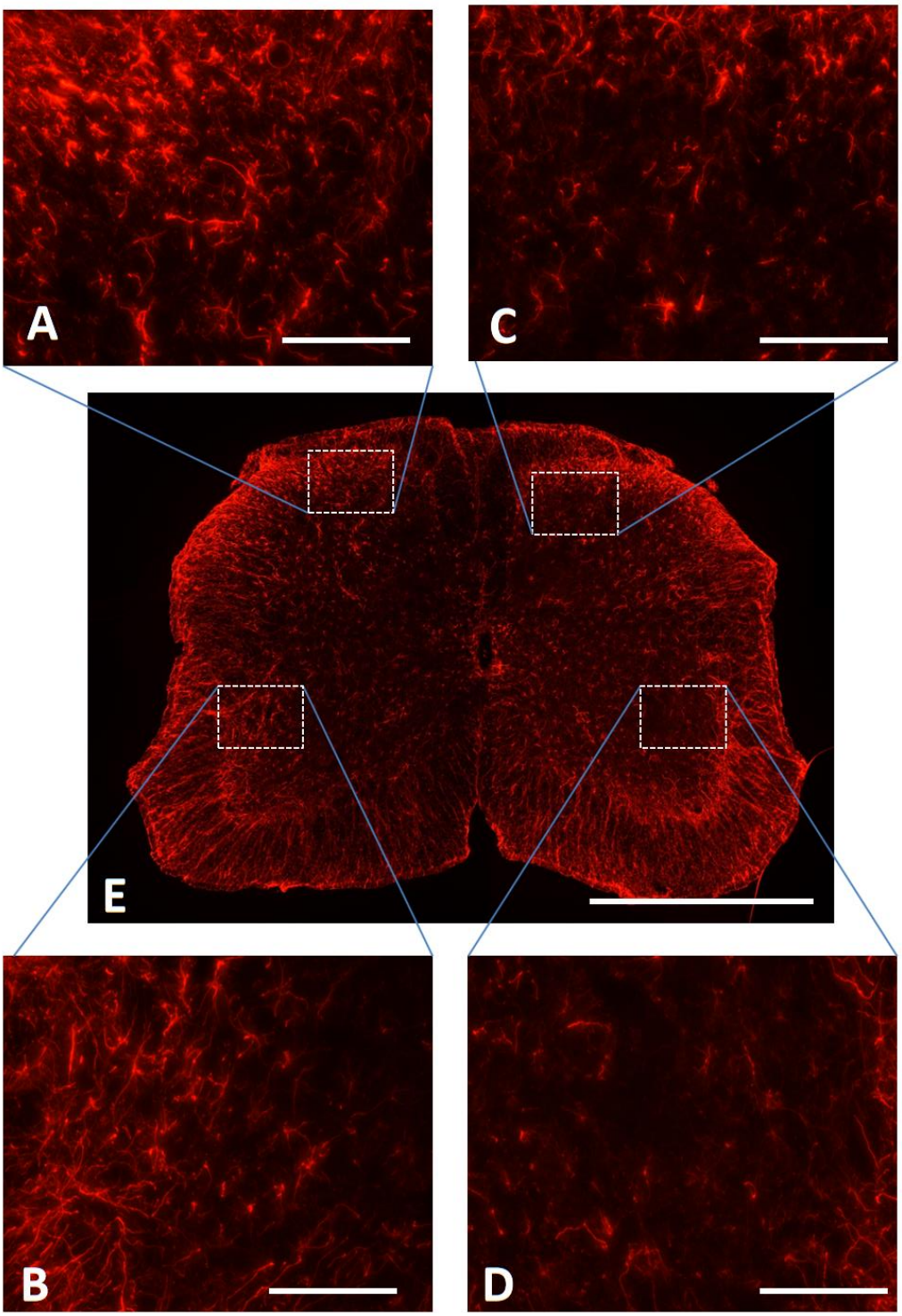

Figure 4.11: A section of spinal cord from an injured (unrepaired) animal shows astrocyte activation (E using 5x magnification). A) Ipsilateral dorsal horn, B) Ipsilateral ventral horn. C) Contralateral dorsal horn. D) Contralateral Ventral horn (A,B,C,D using 40x magnification). Scale bar A,B,C and D = 0.1mm, E = 1.0mm.

M6P group

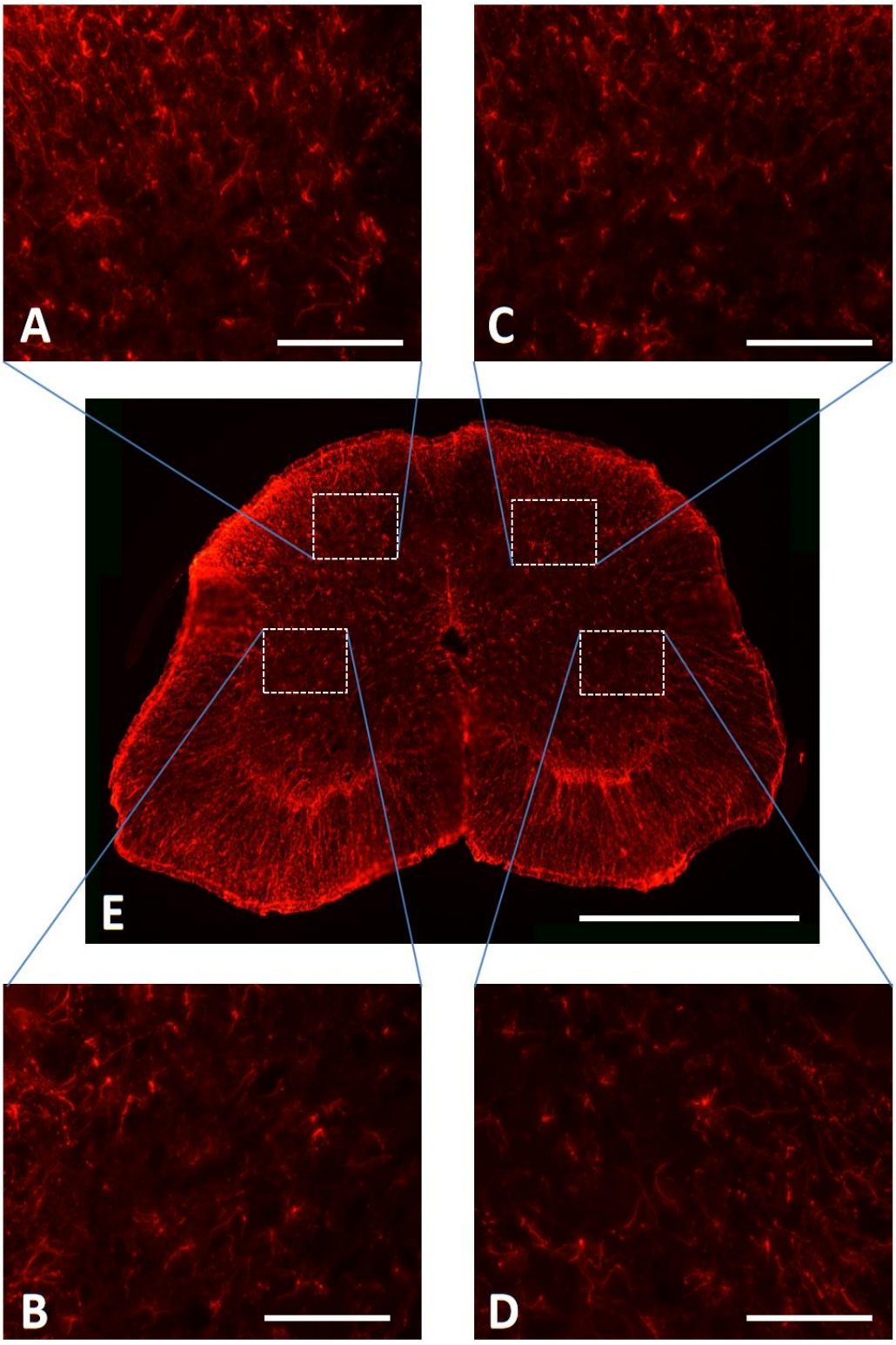

Figure 4.12: A section of spinal cord following nerve repair with fibrin glue and M6P shows astrocyte activation (E using 5x magnification). A) Ipsilateral dorsal horn, B) Ipsilateral ventral horn. C) Contralateral dorsal horn. D) Contralateral Ventral horn (A,B,C,D using 40x magnification). Scale bar A,B,C and D = 0.1mm, E = 1.0mm.

Control group

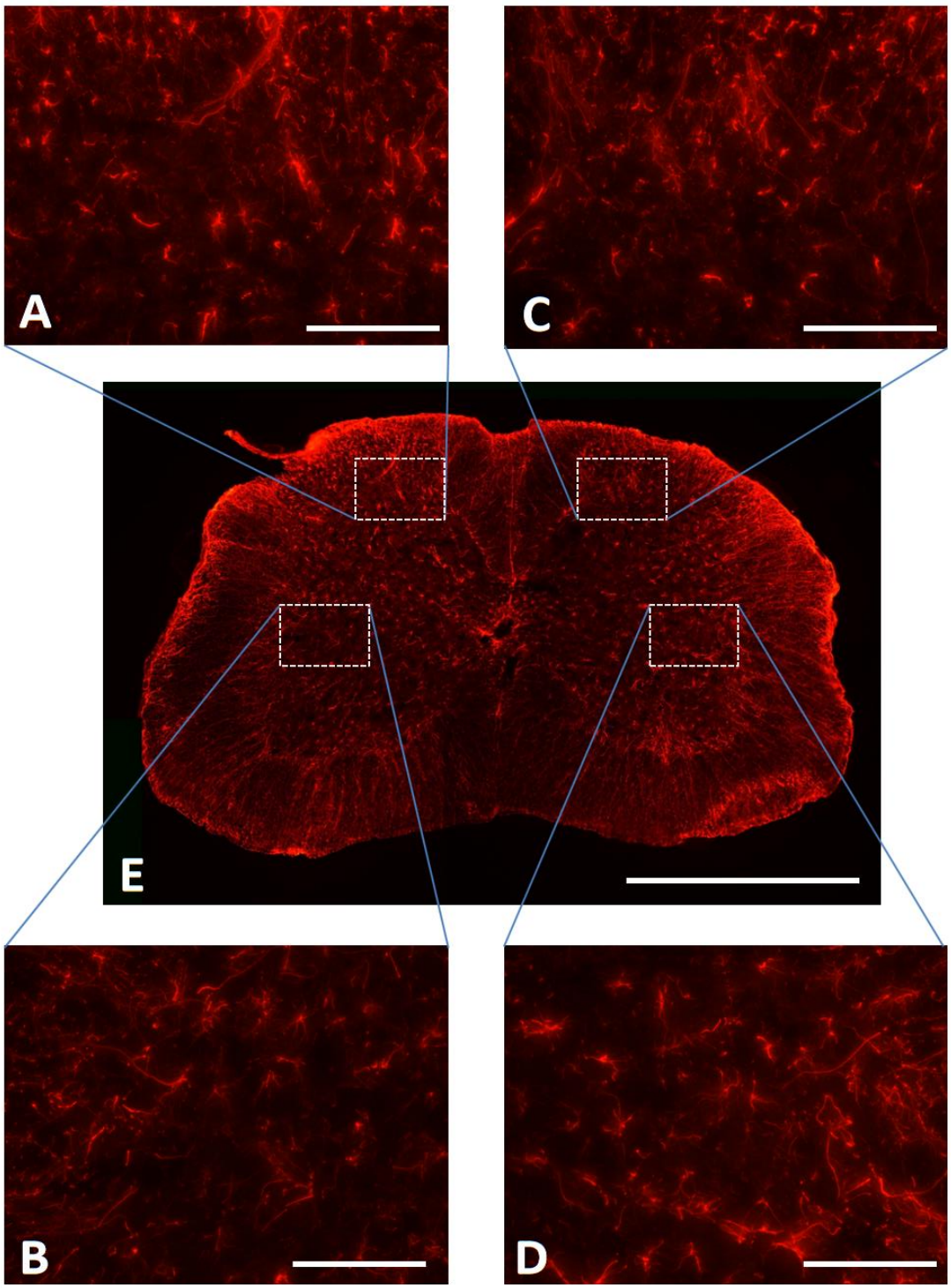

Figure 4.13: A section of spinal cord following nerve repair with fibrin glue alone (control) shows astrocyte activation (E using 5x magnification). A) Ipsilateral dorsal horn, B) Ipsilateral ventral horn. C) Contralateral dorsal horn. D) Contralateral Ventral horn (A,B,C,D using 40x magnification). Scale bar A,B,C and D = 0.1mm, E = 1.0mm.

The mean percentage area of GFAP labelling (indication of the degree of astrocyte activation) for each group is shown in Table 4.2. The same data and the statistical comparison between the groups is illustrated in Figure 4.14.

Table 4.2: Percentages of astrocyte activation for Unrepaired, M6P and control groups.

GFAP (astrocytes)%	Unrepaired	M6P	Control
Ipsilateral Dorsal horn	7.1	4.0	4.4
Contralateral Dorsal horn	3.8	3.2	3.4
Ipsilateral Ventral horn	6.5	3.1	3.1
Contralateral Ventral horn	2.7	2.4	2.3

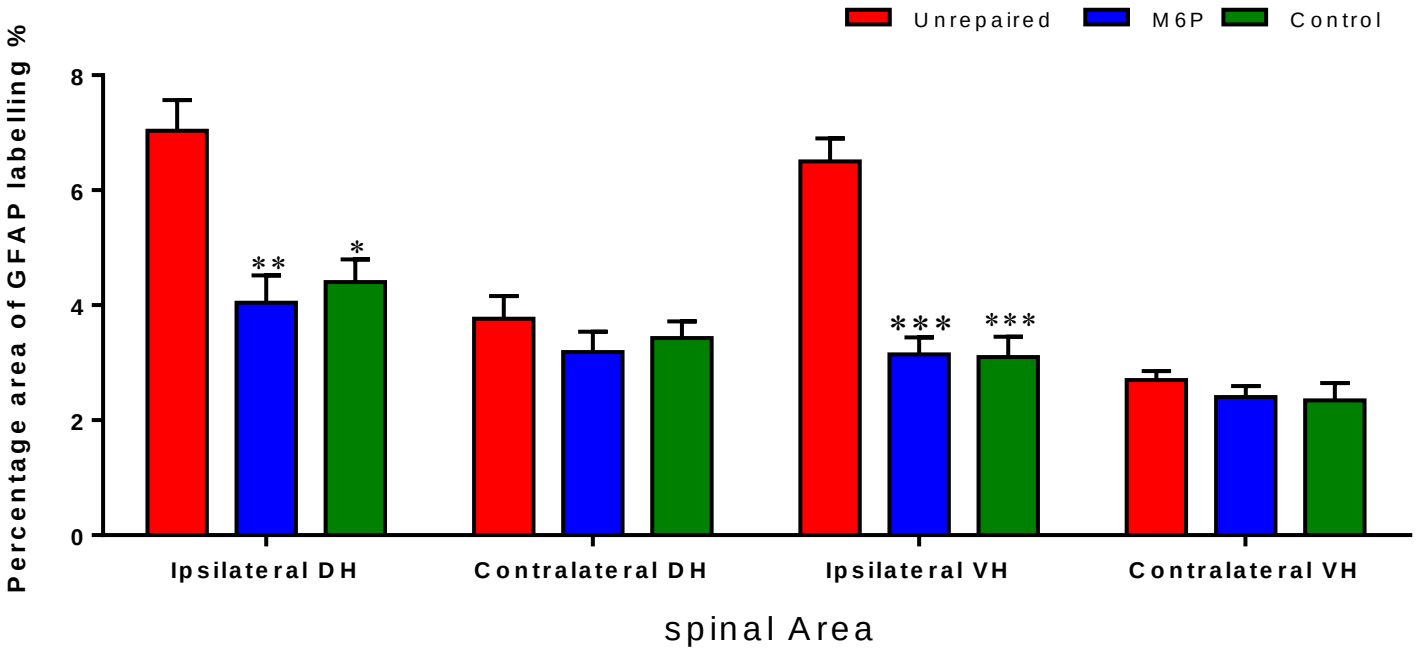

Figure 4.14: Immunohistochemical analysis of astrocyte for M6P, control and unrepaired groups. *, ** and *** denote significant difference compared to unrepaired group, $p<0.05$ $p<0.01$ and $p<0.001$ respectively. No significant difference between M6P and control group. Error bars denote SEM. Statistical test: 1-way ANOVA with Bonferroni's multiple comparisons test. IDH: Ipsilateral dorsal horn. CDH: Contralateral dorsal horn. IVH: Ipsilateral ventral horn. CVH: Contralateral ventral horn.

The increase in staining (Ipsilateral/Contralateral) ratio for GFAP in the unrepaired group was significantly higher than in other groups in both dorsal (88.3% vs 26.0% [M6P; $p<0.001$] and 28.4% [control; $p<0.001$]) and ventral (142.5% vs 28.7% [M6P; $p<0.001$] and 34.9% [control; $p<0.001$]) horns (Figure 4.15). The M6P-treated group had a slightly lower percentage increase in the dorsal and ventral horns compared with the control group; these differences were not significant (Figure 4.15).

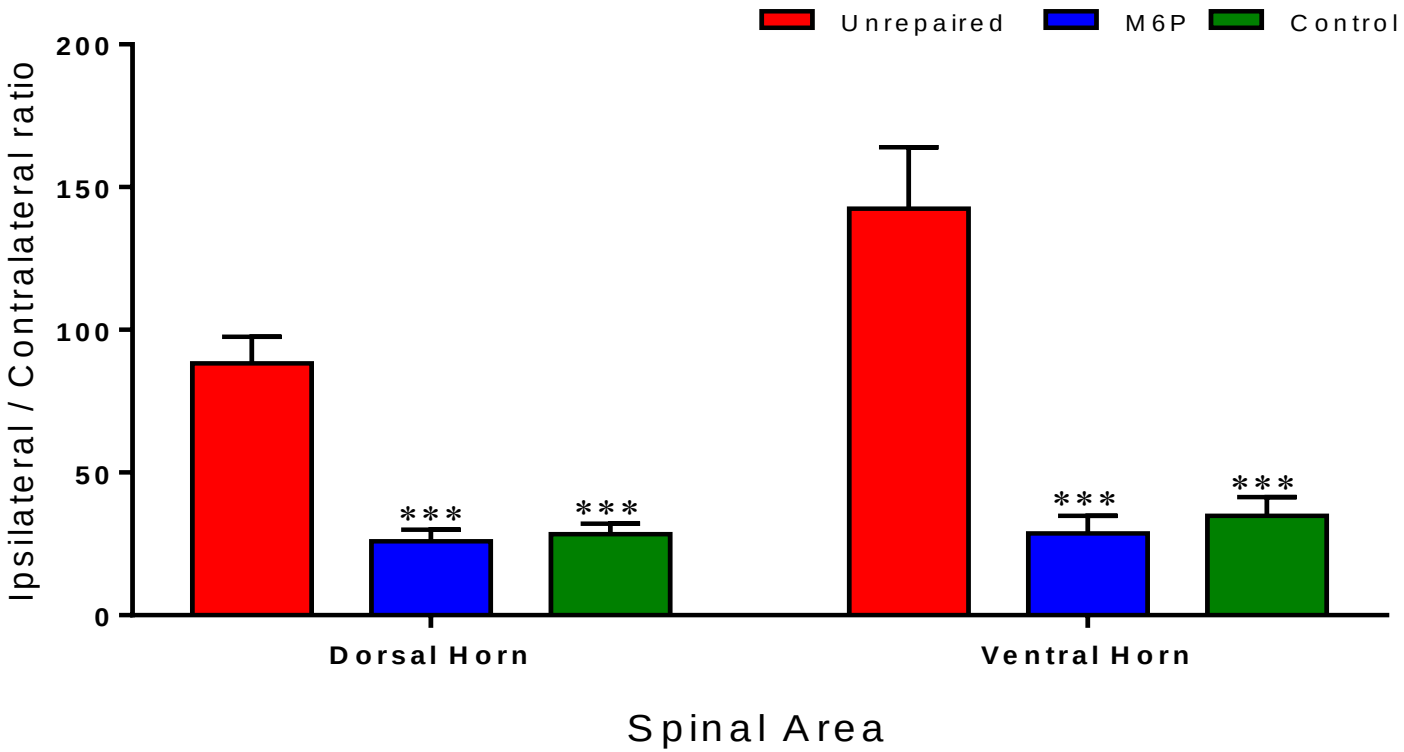

Figure 4.15. Ipsilateral/Contralateral ratio of astrocyte shows the difference of percentage increase in the ipsilateral side over the contralateral side in ventral and dorsal horns of the spinal cord for M6P, control and unrepaired groups. *** denote significant difference compared to unrepaired group, $p<0.001$. The M6P-treated group expresses slightly lower activation in both dorsal and ventral horns compared to control group, but no significant differences were observed. Error bars denote SEM. Statistical test: 1-way ANOVA with Bonferroni's multiple comparisons test.

4.4.2 Assessment of Functional Recovery Using Axon Counting and Tracing Analysis

Axon counting and tracing was carried out only on the M6P and control groups. The outcome of regeneration in the unrepaired group has been reported previously (Harding, 2014), in summary there was no axonal regeneration at the distal nerve end as the suture around proximal stump prevents axonal growth (Figure 4.16), therefore no regeneration data is presented for this group.

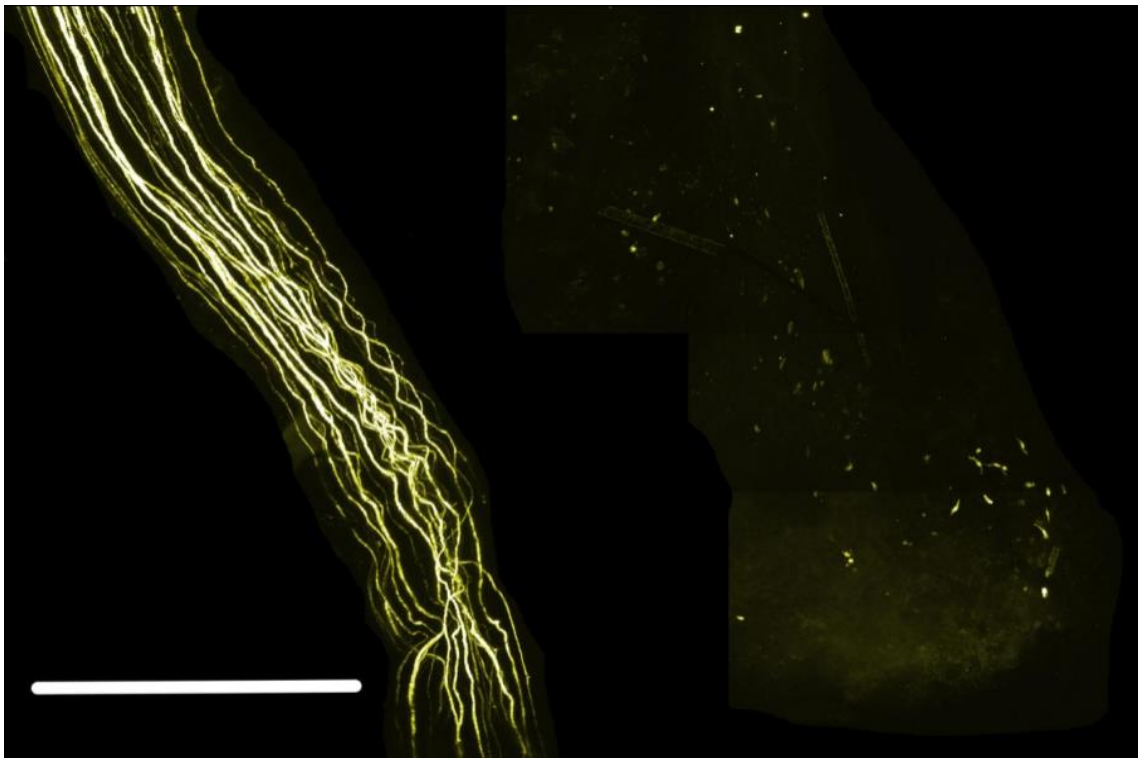

Figure 4.16: Proximal (left) and distal (right) nerve endings following two-weeks after transection with no repair. Scale bar = 1.0mm. (Harding, 2014).

4.4.2.1 Qualitative Observation of Regenerated Nerves

Axons entered the graft and extended distally toward the distal end. The use of *thy-1-YFP-H* mice enables visualisation of the regenerated nerves at the level of the individual axon. It is clear that there is a region of disrupted axons at the proximal end, where axons pass from the proximal stump of the nerve into the nerve graft, and distal end, where axons pass from the nerve graft into the distal stump of the nerve (Figure 4.17B and C). These regions are not observed in the uninjured nerves, where the axons run in a parallel course across the entire nerve length (Figure 4.17A).

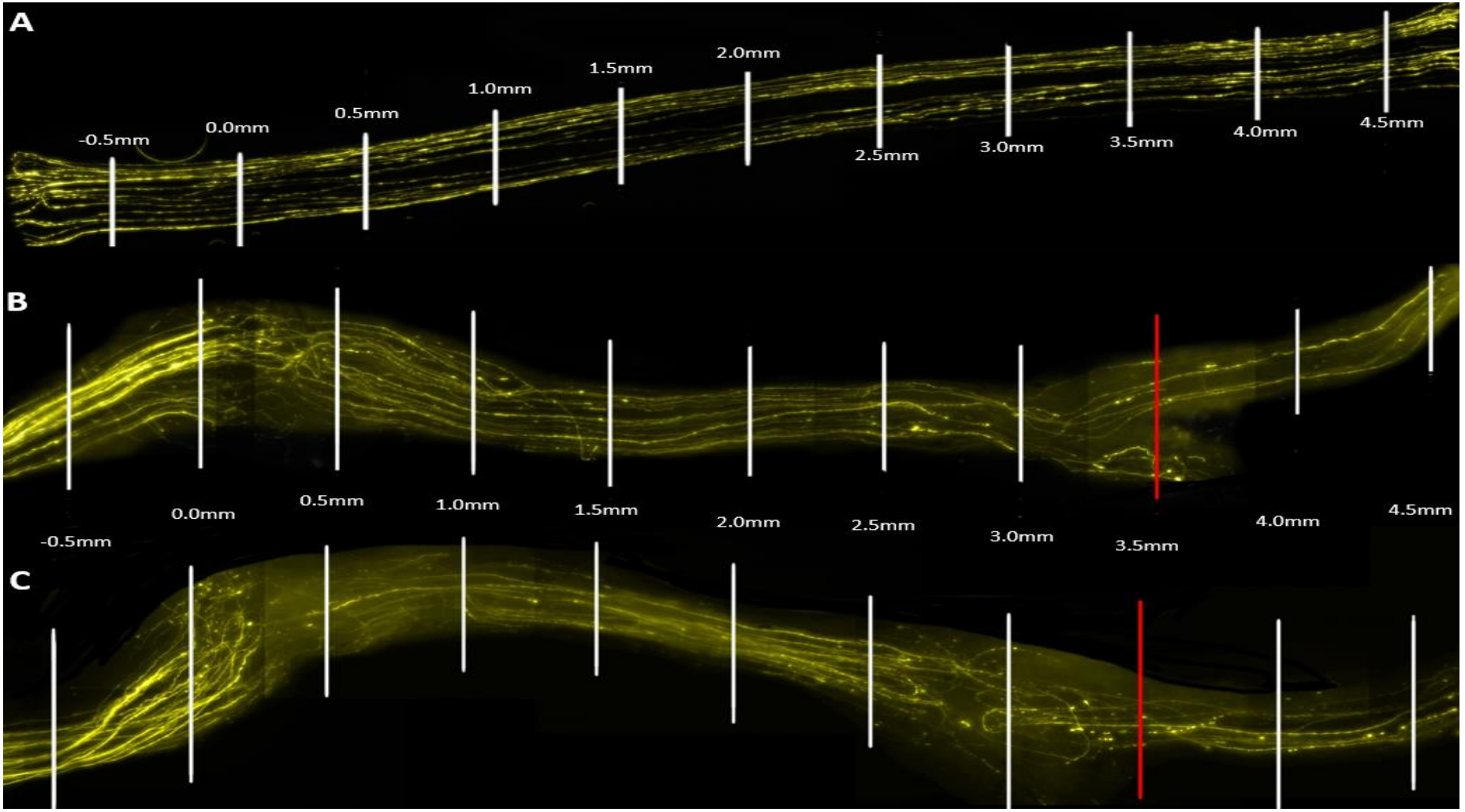

Figure 4.17: A) Typical uninjured nerve. B) Repaired nerve with M6P treatment. C) Control repaired nerve. All nerves presented with intervals marked.

4.4.2.2 Quantitative Analysis of Regenerated Nerves

4.4.2.2.i Sprouting Index

As described in section 2.2.7.3.i, the sprouting index was calculated at 0.5mm intervals through the regenerating nerve. There were no significant differences observed in sprouting index analysis between the M6P and control groups at any interval. However, the M6P group displayed slightly lower sprouting at almost all of the intervals apart from the 4.0mm Interval where it showed slightly higher sprouting compared to the control group (Table 4.3 & Figure 4.18).

Table 4.3: Sprouting index levels of M6P and control groups (%).				
Repair Position (Intervals)	**M6P**	**SEM**	**Control**	**SEM**
-0.5	100.0	0.0	100.0	0.0
0.0	119.8	5.9	123.7	5.1
0.5	87.0	9.9	96.3	10.7
1.0	81.6	7.3	85.8	10.0
1.5	59.0	9.3	60.5	6.0
2.0	50.0	8.7	53.2	11.3
2.5	50.8	8.7	54.3	9.2
3.0	45.6	7.5	48.8	11.8
3.5	39.6	8.1	40.2	13.3
4.0	27.7	4.2	18.0	8.5

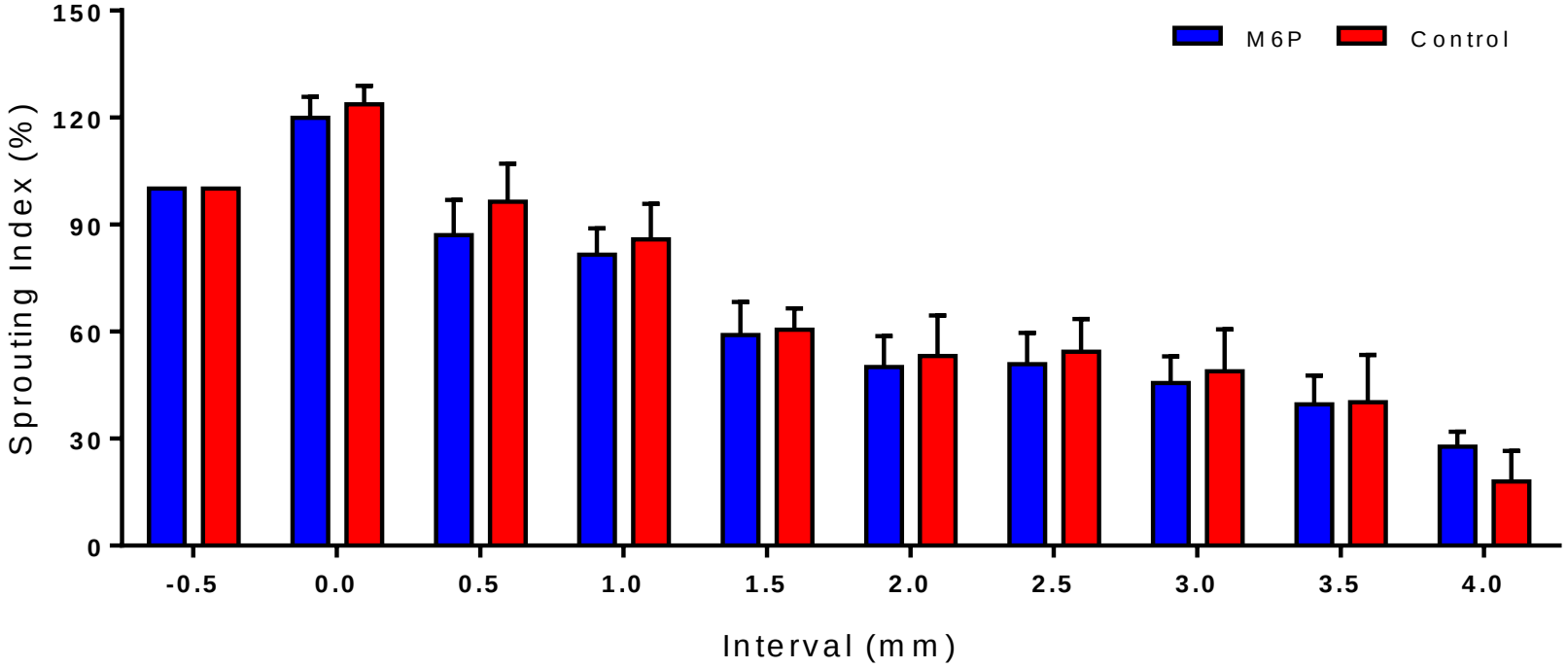

Figure 4.18: Sprouting index levels for the M6P and control groups at 0.5mm intervals along the graft. No significant different were detected between the repair groups. Error bars denote SEM. Statistical test: 2-way ANOVA with Bonferroni's multiple comparisons test.

4.4.2.2.ii Axon Tracing

Axon tracing indicates the number of unique axons that successfully regenerate from the repair start to the distal nerve ending. As described in section 2.2.7.3.ii, a minimum of 75% of axons are traced from the 3.5mm interval back toward to the 0.0mm interval (Figure 4.19). The proportion of unique axons represented at each interval was marginally higher in the M6P group than control groups, but there were no significant differences observed between the groups overall or at any individual interval. The highest decline in unique axons was found between the 0.0mm and 0.5mm intervals. The percentage of unique axons continued to drop at each subsequent interval, until it reached 17.1% (M6P) and 11.3% (control) at the 3.5mm (final interval) (Table 4.4 & Figure 4.20).

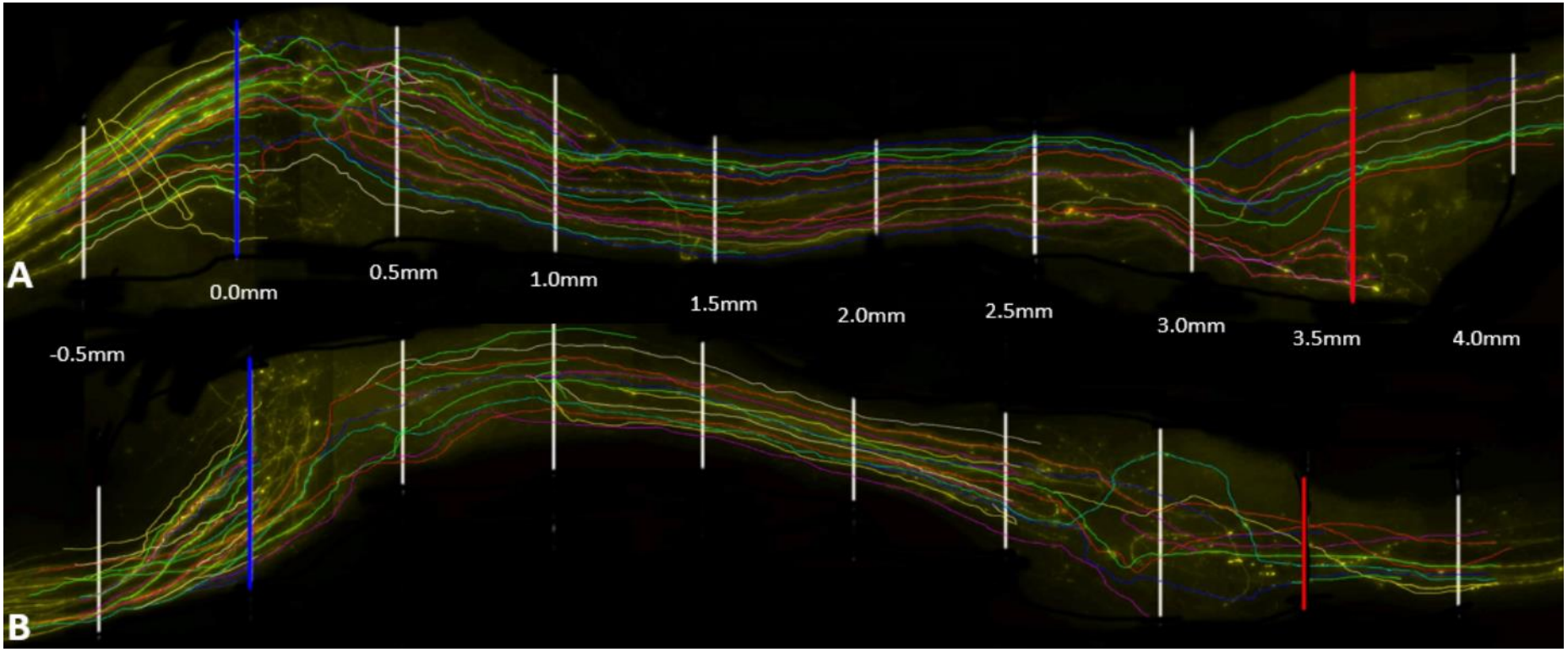

Figure 4.19: Image of traced axons from 3.5mm interval back toward to the 0.0mm in both M6P (A) and control (B).

Table 4.4: Axon tracing levels for M6P and control groups (%).				
Repair Position (Intervals)	**M6P**	**SEM**	**Control**	**SEM**
0.0	100.0	0.0	100.0	0.0
0.5	53.6	5.3	49.1	4.6
1.0	37.5	3.6	31.5	4.9
1.5	28.7	4.3	26.0	1.8
2.0	26.5	3.5	19.6	2.5
2.5	26.3	3.7	19.7	2.6
3.0	20.4	2.1	16.8	2.3
3.5	17.1	1.7	11.3	2.7

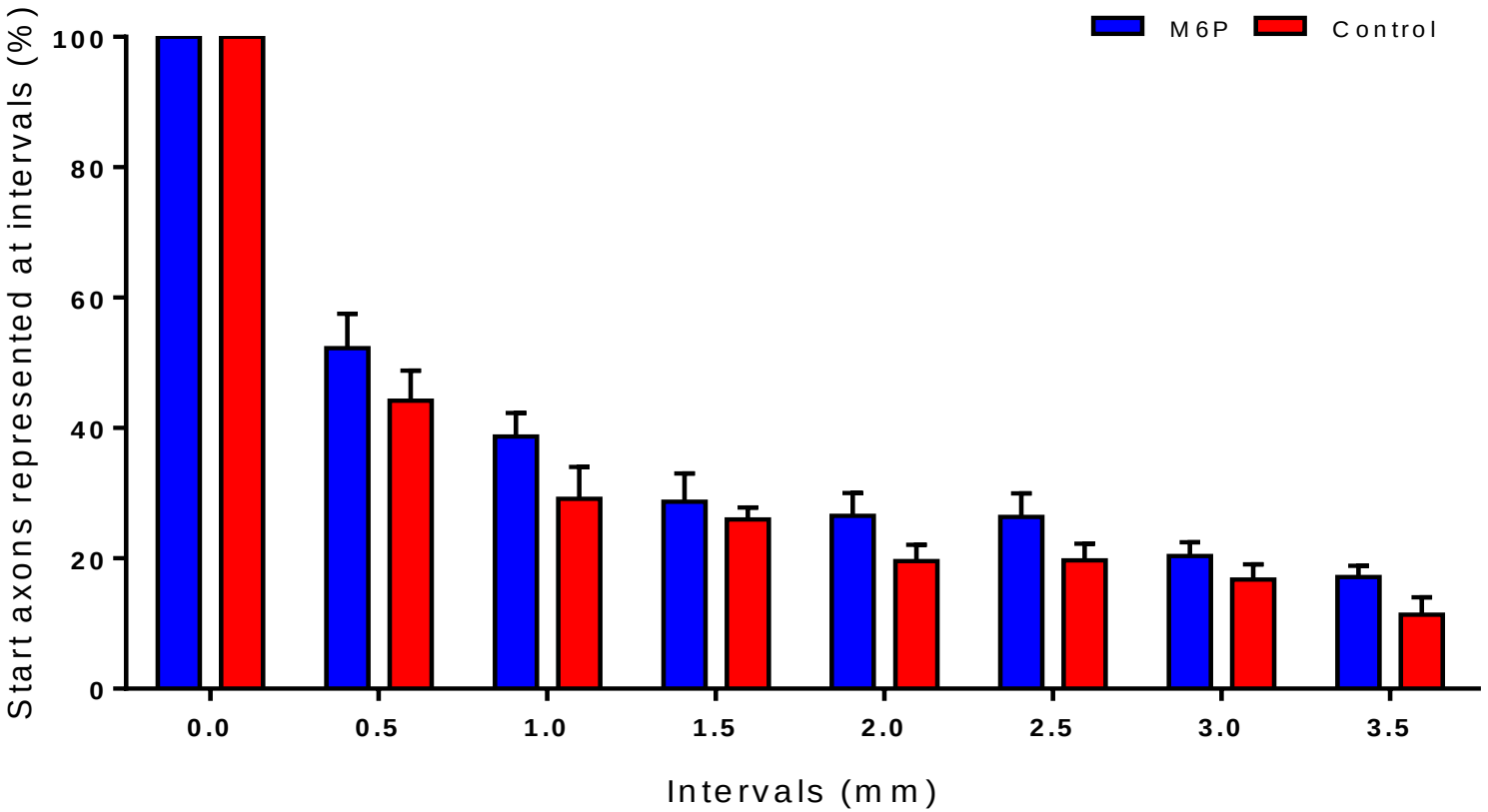

Figure 4.20: Unique axon percentages across repair for M6P and control groups. No significant different were detected between the repair groups at any interval. Error bars denote SEM. Statistical test: Two-way ANOVA with Bonferroni's multiple comparisons test.

4.4.2.2.iii Axon Disruption

As described in section 2.2.7.3.ii, axon lengths across the portion of nerve between the 0.0mm and 1.5mm intervals were measured, and the average axon length in each group was determined. The difference between the axon length and actual distance (1.5mm) was expressed as percentage increase of axon length relative to the actual distance (Figure 4.21).

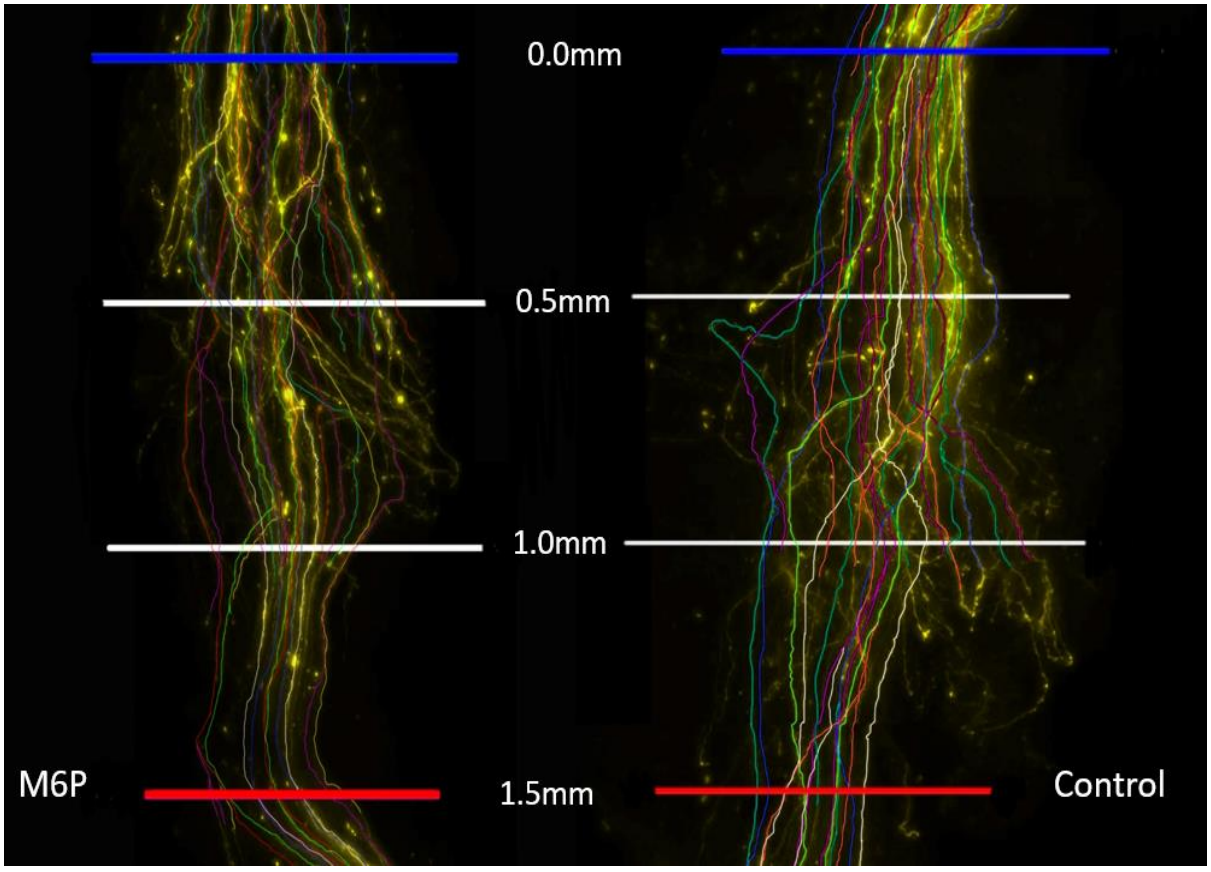

Figure 4.21: Image showing traced axon disruption between 0.0mm (blue line) and 1.5mm (red line) in both nerve repairs: M6P and control.

The average increase in axon length in M6P group was marginally lower (18.3% [±2.8SEM]) than the control group (20.5% [±2.1]), but there was no significant difference (p=0.578) (Figure 4.22).

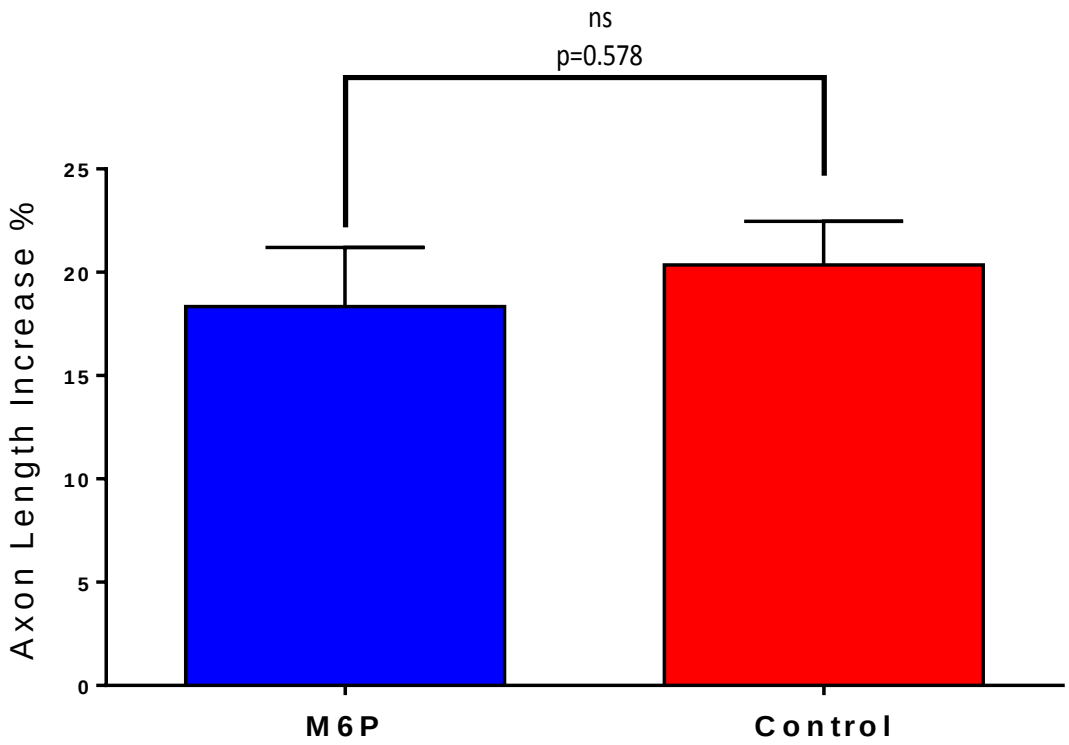

Figure 4.22: Percentage increase in axon length between 0.0mm and 1.5mm in M6P and control groups. No significant differences were observed between the repair groups. Error bars denote SEM. Statistical test: unpaired t-test (two-tailed).

4.5 DISCUSSION

4.5.1 Fibrin Glue as a Therapeutic Carrier

Using of fibrin glue as an alternative to sutures has been reported in several studies. Menovsky and Beek (2001) performed a comparison between the use of fibrin glue, suture and CO_2 laser in peripheral nerve repairs. They reported no difference in the functional, histological and morphological results between the fibrin glue, suture and CO_2 laser repairs. Because of fibrin glue's clinical use and acceptance, it has gained attention as a potential means to deliver drug therapies. Fibrin glue has a number of attractive features that lend it to the enforcement of controlled release. Spicer and Mikos (2010) reported that fibrin glue is an attractive drug delivery system because of the interactions that occur with endogenous factors. It serves as a binding reservoir for these factors. Several studies have investigated the use of fibrin glue for delivery of a number of molecules including endogenously produced factors [i.e. transforming growth factors-β1 (TNF-β1) (Catelas et al., 2009) vascular endothelial growth factor (VEGF) (Sahni and Francis, 2000) and growth factor-binding protein (Campbell et al 1999)], synthetic factors [i.e. lidocaine (Zhibo and Miaobo, 2009) and chemotherapeutic agents such as fluorouracil mitomycin C (Yoshida et al., 2000)], and gene delivery vectors [i.e. adenoviral vectors (Breen et al 2009)]. In addition, fibrin glue can be included along with suture in nerves under mild tension. Also it can be used for non-nerve tissue repairs; with appropriate anti-scarring effects internal suturing could be coupled with therapeutic fibrin glue to reduce scarring.

In the study described in this chapter, the fibrin glue was used as a drug delivery system, which might provide a simple method that could prolong length of delivery and possible be clinically useful as a route for M6P administration.

4.5.2 The Effect of M6P on Spinal Glial Activation

Although the effects of M6P have previously been shown to enhance nerve regeneration (Harding et al., 2014, Ngeow et al., 2011a, Ngeow et al., 2011b), its effects on spinal glial activation and the development of neuropathic pain following nerve injury was unknown prior to this study.

The results presented herein show no difference in glial activation and thus suggest no difference in potential for neuropathic pain development between the M6P-treated and control groups (fibrin glue alone). Ipsilateral/contralateral/ ratio was generally lower in the ventral horn for the M6P-treated group for both astrocyte and microglia activation compared to the control group. Differences in the dorsal horn were mixed, the M6P-treated group had lower astrocyte activation and higher microglial activation of contralateral/ipsilateral ratio compared to the control group. The differences observed in microglia activation (higher activation in dorsal horn, lower activation in ventral horn) may indicate that M6P may be more beneficial towards motor rather than sensory axons. However, the data in this study do not provide conclusive data in relation to potential use of M6P in the reduction of glial activation. This method of administration did not significantly influence nerve regeneration, whereas our other studies (discussed below), using different methods of administration have shown that M6P is effective in enhancing nerve regeneration. Thus further studies using other methods of administration need to be carried out in order to establish the efficacy of M6P in the reduction of glial activation.

In the unrepaired group, glial activation was high in both dorsal and ventral horns, indicating that repair reduces glial activation and may reduce the potential for the development of neuropathic pain development, compared with the case where there is no repair and little or no regeneration.

4.5.3 The effect of M6P on nerve regeneration

When the outcomes from the two repair groups in the three steps of axon counting and tracing analysis were determined, they revealed no significant correlation between the level of nerve regeneration and use of M6P mixed with fibrin glue.

4.5.3.1 Axon Sprouting Levels

It is well demonstrated that the level of injured axon sprouting increases with the severity of injury, and injured axons may sprout into multiple branches during the early phases of the regeneration (Sunderland, 1978, Xu et al., 2008). The axons mainly emerge from the last node of Ranvier, and less frequently from the terminal of the axon itself (after the last node of Ranvier) (Gordon and Borschel, 2017, Griffin and Thompson, 2008; Tam and Gordon, 2003; Tam and Gordon, 2008). The results of Xu et. al (2008) demonstrated that regenerating axons following 2mm long sciatic nerve injury had a lower level of sprouting compared to 20mm long injuries, suggesting that axon sprouting increases in longer segmental crushed injuries. The level of sprouting was measured at a similar point distally to the site of injury in both groups.

The use of the sprouting index method to investigate the nerve regeneration was previously reported in two studies by Groves et al. (2005) and Sabatier et al. (2008). The studies depended on the use of YFP mice in order to calculate the ratio of sprouting index proximal and distal to the repair site. In Harding et al's (2014) study, the equivalent outcome measure of sprouting index was performed at several separate intervals. These intervals extend from the most proximal part of the injury through the entire nerve graft to the point where the regenerating axons enter the distal stump (the same method was used in this study and the others reported in this thesis). By using multiple intervals and not just a single interval, more details about the sprouting index ratio can be obtained (Harding, 2014, Harding et al., 2014).

Following imaging of repaired nerves in both groups, it was found that the highest disruption and potential axon sprouting occurred at the proximal end (where

regenerating axons enter the nerve graft) in both M6P and saline control groups. A smaller disruption was noticed at the distal end of the graft (where axons exit the nerve graft and enter the distal stump) (Figure 4.16B and C).

The use of M6P in peripheral nerve regeneration was investigated in a recent study by Harding et al. (2014). In Harding's study quantification of sprouting index showed that the group treated with M6P had a slightly lower sprouting index compared to the control group at all intervals. The highest sprouting index was observed at 0.5mm and 1.0mm intervals, while the lowest sprouting index was reported at 3.5mm interval. They reported that these findings were not statistically significant. The results of the current study showed that M6P-treated group had a slightly lower sprouting index in all intervals except 4.00mm interval where it had a slightly higher sprouting index compared to the control group. The highest sprouting index was observed at 0.5mm interval in both groups, and the lowest sprouting index was observed at 4.00mm interval where the axons start to extend into the distal nerve.

4.5.3.2 Axon Tracing

A higher number of axons passing the injury site and entering the nerve graft is an indication of better regeneration. This indicates the number of unique axons crossing the injury site, rather than just the number of sprouts (which may reflect multiple sprouts from a small number of axons). This provides unique data, which cannot be revealed by standard axon counting results. For example, a study by Atkins et al. (2007) investigated the use of the anti-inflammatory cytokine interleukin-10 (IL-10), as an anti-scarring agent after peripheral nerve injury. They reported that IL-10 significantly reduced intraneural scarring and increased the degree of axonal regeneration using electrophysiological methods. However, both IL-10 and control (saline) groups had similar axon count results. This suggested that high level of intraneural scarring/disruption stimulated the axons to sprout more, but this did not equate to the degree of regeneration (Atkins et al., 2007). Thus in the assessment of peripheral nerve regeneration, the morphological analysis can often be disproportionate to functional

recovery. A study by Taha et al. (2004) investigated the effect of retinoic acid on rat tibial nerve. The results demonstrated that rats treated with retinoic acid had a significantly better morphological regeneration (improved axon density) compared to control group, while no improvement in motor activity (walking track analysis) was observed between the two groups (Taha et al., 2004). The same outcome was reported by Pagnussat et al. (2012), when comparing the effect of various training therapies on both nerve regeneration and functional recovery in rats. The outcomes of the comparison demonstrated that rats treated with skilled and unskilled training scored higher level of functional recovery compared to other groups (no training/control). In contrast, no significant differences were observed between the groups in the basis of morphological analysis (Pagnussat et al., 2012). The method of axon tracing which is possible with the YFP mice enables the tracing of unique axons across the injury site, providing a much clearer assessment of likely functional recovery than other methods using morphological analysis.

Due to the short recovery period 2-weeks (to investigate early stage regeneration) and the use of common fibular nerve module (small numbers of muscles affected), carrying out a behavioural assessment (e.g. CatWalk) was not viable. The potential recovery function in the current study was evaluated by inverted axon tracing of each interval to calculate the percentage of axons from the reference line (0.0mm interval) that were represented at each subsequent interval. A better potential for future recovery function was indicated by a higher percentage of unique axons reaching the 3.5mm interval (final interval).

Harding et al. (2014) reported that no significant differences were observed on the basis of axon tracing between M6P-treated and vehicle-treated groups. The outcomes showed that only 25% of axons present at the 0.0mm interval reached the 3.5mm interval in both repair groups. More than 50% of axons from the 0.0mm interval were lost by the 1.5mm interval. They also reported that in the M6P-treated group, the percentage of start axons represented at 3.5mm interval was slightly higher compared to vehicle-treated group (Harding et al., 2014). In contrast to Harding's and the current

studies, Ngeow et al. (2011a) reported that M6P improved regeneration (see section 4.5.3.3).

In the Kohta et al. (2009) study, the drug Taxol was used in traumatic spinal cord injury of rats to inhibit TGF-β1 signalling. The results of the study demonstrated that Taxol-treated rats had decreased scarring, increased regeneration, and enhanced locomotor recovery (Bastien and Lacroix, 2014; Hellal et al., 2011). However, these studies were done in the central nervous system.

The results of the current study showed that no significant differences between M6P-treated and control groups. Only 17% of axons present at 0.0mm interval reached the 3.5mm interval in M6P-treated compared to 11% in control group. Approximately 50% of axons from 0.0mm interval were lost by the 0.5mm interval; this is where the axons cross the injury site and enter the nerve graft. The percentage of start axons represented at 3.5mm interval was slightly higher in the M6P-treated group compared to control group in all intervals.

4.5.3.3 Axon Disruption

As mentioned earlier in section 4.3.2, it was clearly observed that there is a region of disrupted axons at each side of the nerve graft. The larger region is located where the axons pass from the initial proximal end of the nerve to the nerve graft (0.0mm-0.5mm interval). It was observed that the highest sprouting index occurred and approximately 50% of axons were lost at this region in both groups. It is believed that when the axons took a shorter path to cross the injury site this indicates better regeneration, while when axons are meeting with resistance to regeneration (eg physical barriers such as scar tissue) they may take a longer path resulting in greater axon disruption.

In Harding et al's (2014) study, the M6P-treated group had a significantly shorter average length of axons compared to vehicle-treated group on a 2-week post-repair. They concluded that M6P appears to have an excellent effect in reducing the amount of disruption of axons. So, axons were able to follow a shorter, more direct, path across

the site of injury. Their finding supported results previously reported by Ngeow et al. (2011a, 2011b), in which the electrophysiology results showed significant improvement of compound action potential and faster conduction velocities in the M6P-treated group compared to the PBS-treated group at 6-weeks (early regeneration) but not 12-weeks (late regeneration) post repair. It is difficult to make a direct comparison between the three previous studies (Harding et al., 2014, Ngeow et al., 2011a, Ngeow et al., 2011b) and the current study due to different experimental factors such as different nerves, recovery periods, methods of repair and evaluation used in each study. Ngeow et al. (2011a, 2011b) used direct suturing of the sciatic nerve (with injection of M6P under the epineurium) and evaluated recovery using electrophysiology and walking gait analysis at 6 and 12 weeks post repair, while Harding et al. (2014) used nerve grafting of a common fibular nerve (soaked in M6P) and evaluated recovery using axonal tracing at 2 weeks. This study used direct transplant of nerve graft secured using fibrin glue (+/- M6P), and evaluated recovery using axonal tracing at 2 weeks post repair. However it is apparent that the method of applying M6P used is this study did not influence axonal regeneration, unlike the methods used in Harding's and Ngeow's studies.

Evidence has suggested that the rate of regeneration could be improved. For example, the introduction of a 'conditioning lesion' in sciatic nerve injury models (Forman et al., 1980), application of immunosuppressive agents (Kuffler, 2009), and matrix metalloproteinase inhibition (Liu et al., 2010). The impact of M6P on the rate of axonal regeneration was not examined directly in this study; however, their path across the injury site was examined. Axons taking a shorter route to cross the injury site are most likely to reach their end target faster than those that take a longer route to cross the injury site, and may therefore limit atrophy of the affected muscles. So, faster crossing of the site of injury could result in better recovery function. In the present study, there were no significant differences in axon disruption between M6P-treated and control group. Although axons in the M6P-treated group had slightly shorter axon lengths, the difference was not significant.

Finally, no sign of autotomy was observed in any of the experimental animals including the unrepaired group. It has been reported that autotomy is one of the signs that suggest the development of neuropathic pain (Coderre et al., 1986, Wall et al., 1979) because of ectopic discharges sent from the damaged axons. In general, autotomy appears to be more common in rats than mice (Rigaud et al., 2008).

Several possible reasons can be suggested for the overall results that no difference were observed in the current study. First, the age and strain of used mice play an essential role in the outcomes (Jackson et al., 2017). The current study used the same strain of mice, *thy-1-YFP-H*, as used in Harding et al's (2014) study. However, the ages of mice in this study was 12-18 weeks old compared to 9-12 weeks old in Harding et al's (2014). This may have an effect on the overall results. It is difficult to compare the results of this study with Ngeow et al's (2011b) results as mice strain, age, nerve, recovery period and analysis method were different. Secondly, the analysis methods were different. Although Harding et al's (2014) used the same analysis method, axon counting and tracing, identification of the graft start point is objective with regard to the placement of the 0.0mm interval. Third, the method or repair was different. As mentioned previously, in Harding et al's (2014) study, the CF nerve graft was soaked in a solution of M6P for 30 minutes before implantation while Ngeow et al. (2011b) injected the sciatic nerve directly with M6P before transecting and suturing. However, in the current study M6P was loaded into the fibrinogen and applies at the time of repair with the addition of thrombin to form fibrin glue. This may cause decrease in release of M6P from the fibrin glue. Finally, due to hyperosmotic effect of the M6P. The osmolality of 600 mM M6P was measured by Wong et al. (2014) and was considerably hypertonic at 1500 mOsm. High number of stress-shielded cells was observed after the application of 600 mM M6P in their study. They suggested that application of M6P (high osmolar) might have biological effects through osmotic shock (Wong et al., 2014). Further investigation is needed to evaluate the amount of released M6P from the fibrin glue. In addition, Ngeow et al. (2011b) injected another dose of M6P in the muscles surrounding the repair area, while this was not performed in the current study.

4.5.4 Suggestions from Previous Studies

A number of suggestions were put forward in the Harding et al. (2014) and Ngeow et al. (2011a, 2011b) studies to account for improvements in regeneration in M6P-treated animals. Collectively these studies showed that M6P reduced disruption of axons across the injury site, and improved regeneration at 6 weeks post repair (early) compared to control group, but this effect was lost by 12 weeks post-injury (late) where both groups showed equal levels of regeneration. The authors suggested that these changes may be due to a number of factors including:

- Initial collagen formation may be reduced by the inhibition of TGF-β activation by the application of M6P
- Collagen remodelling happens sooner in M6P repairs
- There is a faster rate of axonal regeneration in M6P repairs (as axons are able to cross the injury site more quickly due to decreased axonal disruption).

4.6 CONCLUSION

A ‘‘proof of concept’’ by Atkins et al. (2006b) revealed a relationship between the level of intraneural scar formation and the level of peripheral nerve regeneration. Following this, several studies indicated the success impact of applying of M6P, a possible anti-scarring agent, at the site of injury (Harding et al., 2014, Ngeow et al., 2011a, Ngeow et al., 2011b). The route of M6P administration described in these previous studies was not suited to clinical use, and applying M6P incorporated with fibrin glue provides an attractive method which is simple and well suited to clinical use. However, with this method of application no significant differences observed between M6P and control groups. The overall impact of M6P in this study was limited in terms of effects observed in glial activation and nerve regeneration as no significant differences were observed when comparing to control group.

This apparent therapeutic failure could be due to inappropriate dosage, timing, duration, or route of administration. Thus further investigation may be warranted in order to optimise dosage, administration route and determine any effect.

CHAPTER 5

THE EFFECT OF LOCAL ADMINISTRATION OF ETANERCEPT ON NERVE REGENERATION AFTER (POLY-CAPROLACTONE) NERVE GUIDE CONDUIT REPAIR

SUMMARY

The study reported in this chapter was designed to investigate the effect of the etanercept on glial activation and peripheral nerve regeneration following nerve repair with a PCL conduit. There is evidence to indicate that TNF-α antagonism may reduce the inflammation around the injury site, which may result in the reduction of glial activation and improve nerve regeneration. Immunohistochemistry was performed to investigate spinal glial activation, which acts as a potential indication of the development of neuropathic pain, while electrophysiology and axon counting and tracing analyses were performed to assess the functional recovery of nerve regeneration. CatWalk gait analysis is thought to provide an assessment of both functional recovery of the injured nerve and neuropathic pain. A model of sciatic nerve repair was used. The results demonstrated that local administration of etanercept appears to reduce glial (microglial and astrocyte) activation - indicating reduced potential for neuropathic pain development - and enhance functional recovery of the nerve when compared to controls. Moreover, PCL conduits support axonal regeneration across 4.0mm defect. Fibrin glue had some limitations for the usage on sciatic nerve repairs. Further studies are underway to compare regeneration of sciatic nerve following graft and PCL conduit repairs.

5.1 INTRODUCTION

As described in sections 1.7.1 and 1.7.3, artificial nerve guide conduits have been established as a promising alternative to nerve graft repair. The Addition of supportive cells or drugs into conduits is a more recent approach, beginning within the last 20 years (Ao et al., 2011).

The process of healing starts with the early inflammatory phase and finishes with scar maturation. Because of this, the use of anti-inflammatory agents is established for use as scar reducing agents. Many studies have been carried out previously in our laboratory to investigate potential nerve injury treatments with therapies to reduce scar formation at the site of injury, especially in relation to decreasing the level of inflammation and scar formation (Atkins et al., 2007, Ngeow et al., 2011b). TNF-α is a pro-inflammatory cytokine that mediates several immune functions and is well known to be involved in the regulation of inflammatory, infectious and autoimmune phenomena (Pasparak et al., 1996). TNF-α has also been shown to have a negative impact on neurite outgrowth and inhibits proliferation of Schwann cells that play a principle role in successful nerve regeneration following peripheral nerve injury (Chandross et al., 1996). Neutralisation of TNF-α activity during the acute phase of inflammation has been widely investigated in many autoimmune inflammatory diseases and in spinal cord injuries (Bastien and Lacroix, 2014, Khan et al., 2005). Inhibition of TNF-α following a sciatic nerve crush injury has been reported to enhance regeneration in rats (Kato et al., 2010). Etanercept is a genetically engineered fusion protein of type II TNF receptor that acts to diminish the effectiveness of TNF-α (Weinblatt et al., 1999). It has been shown that removing of TNF-α by etanercept decreases oligodendroglial and neuronal apoptosis, reduces tissue damage and demyelination, and promotes better recovery of locomotor function (Chen et al., 2011).

As described in Chapter 3, PCL conduits produced by µSL technique had the best outcomes (in terms of both nerve regeneration and glial activation) compared to the other evaluated conduits. Poly-caprolactone is a FDA approved material that has shown

excellent results in peripheral nerve regeneration (Cho et al., 2015, Reid et al., 2013, Sun et al., 2010). The outcomes of the *in vitro* and *ex vivo* studies (previously done by Christopher Pateman in the laboratory of Prof. John Haycock [unpublished data]) demonstrated that neurites align along the topographical grooves of the PCL produced by μSL, potentially directing regeneration from the proximal toward the distal stump when using *in vivo* (Harding, 2014). The study described in this chapter uses PCL to create conduits using μSL with dimensions appropriate for repair of the sciatic nerve to bridge a longer gap (4.0mm) than that used for previous studies. Sciatic nerve was chosen for this study in lieu of CF nerve because it is bigger, supplying more muscles (better to assess the recovery function) and longer (facilitating assessment of longer gap injuries). Although the repaired gap in the study is slightly longer that study described in Chapter 3, this is the first study in our laboratory to assess the use of conduits in sciatic nerve repair and thus a similar gap to that used in our previous studies is useful for establishing the model. In this study we have also expanded the methodology used to assess regeneration to include electrophysiological assessment and functional assessment using gait analysis.

5.2 AIM OF THIS STUDY

The aim of the study in this chapter was to evaluate the effect of the etanercept on glial activation and peripheral nerve regeneration following nerve repair with a PCL conduit. We hypothesised that inhibition of TNF-α using etanercept could inhibit the inflammation around the nerve injury site, resulting in the reduction of glial activation and improved regeneration. The study also evaluates the use of PCL conduit in a model of sciatic nerve repair. This model will facilitate the evaluation of outcomes longer gap repairs, as the CF model is restricted to a nerve gap of 3.0mm.

5.3 MATERIAL AND METHODS

The protocol for this study was based on previous protocols performed in our laboratory at the University of Sheffield, and have been described in Chapter 2. Additional, specific information involved in the present study is described below. All PCL conduits used in the current study were provided by Jonathan Field from the lab of Dr. Frederik Claeyssens and Prof. John Haycock, Kroto Research Institute, University of Sheffield. All PCL conduits were created by µSL technique (see section 2.2.2.1). Two designs were evaluated in the study. The first design (0.9mm internal diameter, 0.34mm wall thickness, 6.00mm length) was used for the pilot study. The second design (0.9mm internal diameter, 0.34mm wall thickness, 5.00mm length) was used for the actual study (Figure 5.1).

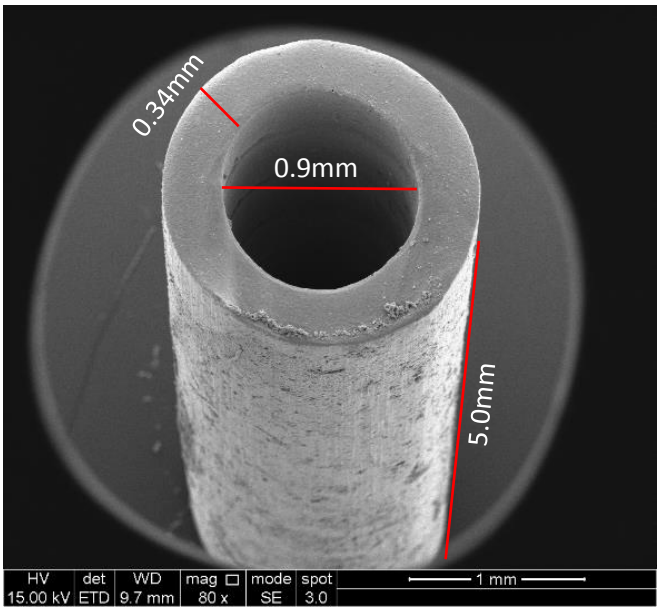

Figure 5.1: SEM image of the PCL conduit showing the diameters (Provided by Jonathan Field).

5.3.1 Animal Numbers and Groups

20 *thy-1-YFP-H* mice on a C57BL6 background aged between 8 and 13 weeks were used in the study and were divided into 2 experimental groups: 10 mice treated with PCL conduit plus etanercept and 10 mice treated with PCL conduit plus normal saline (Figure 5.2).

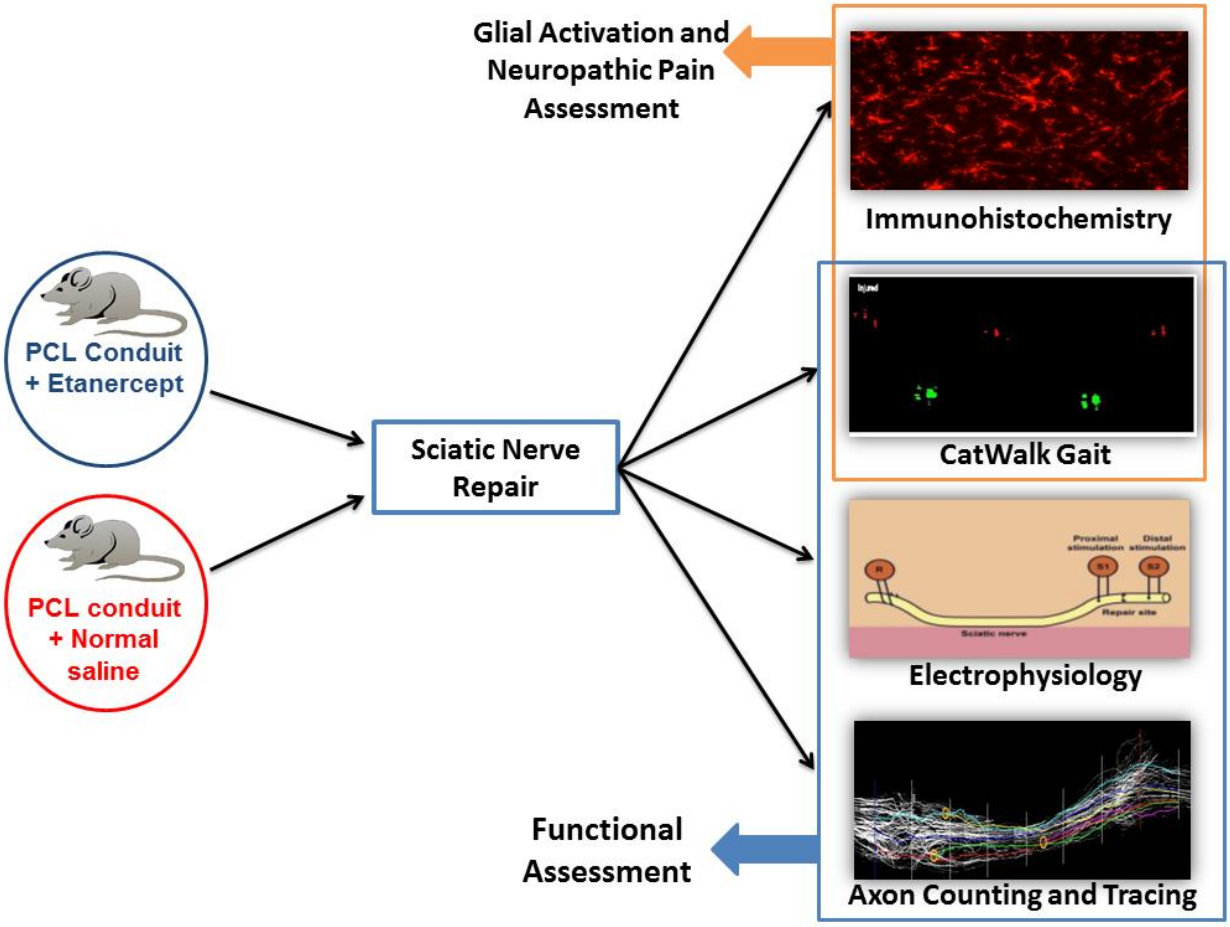

Figure 5.2: Summary of materials and methods for the investigation of the conduits/Etanercept.

5.3.2 Experimental Methods

5.3.2.1 Implantation of Nerve Guide Conduit

YFP-H mice were anaesthetised (see section 2.2.3.1.i) and the sciatic nerve exposed, transected, and a 4.0mm gap was made (see section 2.2.3.1.ii) and repaired using PCL conduit plus either etanercept (Enbrel® 25mg, Pfizer Limited, Sandwich, UK/Reino Unido) or normal saline. Both of the proximal and distal nerve ends were secured by fibrin glue to a depth of 0.5mm into the conduit, leaving a 4.0mm gap between them (see sections 2.2.3.1.iv) (Figure 5.3).

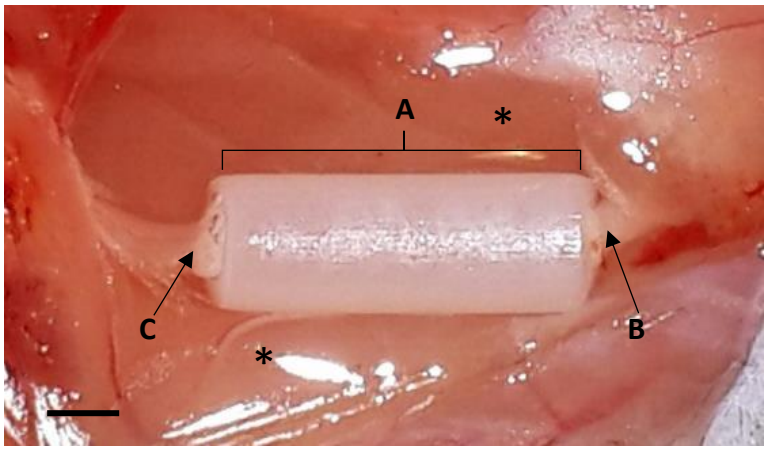

Figure 5.3: Sciatic nerve repair using 5mm PCL conduit (A) showing the proximal (B) and distal (C) nerve ends secured inside the conduit by fibrin glue. (*) area of muscle injection. Scale bar = 1.0mm.

5.3.2.2 Administration of Etanercept

Administration of 100µl of either etanercept (0.15mg) or normal saline was made in three steps: 2x15µl were injected beneath the epineurium prior to sectioning, 30µl were injected within the conduit, and 2x20µl were injected beneath muscles surrounding the nerve after application of the conduit (see section 2.2.3.1.v) (Figure 5.4). This administration was performed by Hisham Shembesh.

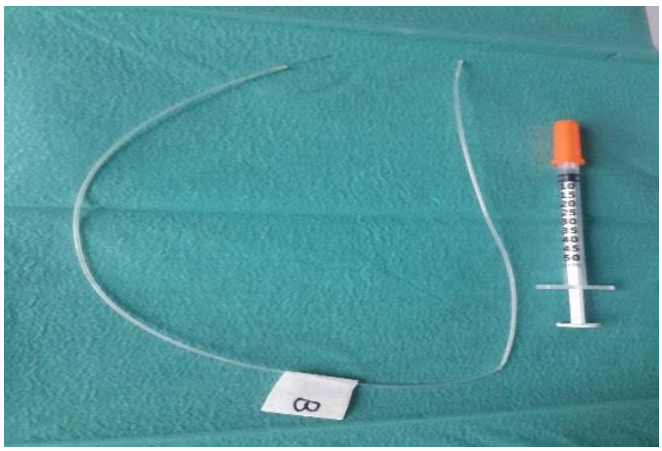

Figure 5.4: A fine microdialysis needle connected to a cannula that used to inject the etanercept or normal saline beneath the epineurium on the sciatic nerve, inside the conduit and in the surrounded muscles.

Animals were allowed to recover for 5 weeks to allow the regenerating nerve to regenerate sufficiently to allow it to be harvested intact. Following the recovery period, animals were anaesthetised (see section 2.2.3.2.i) and electrophysiological recordings of compound action potentials made (see section 2.2.6) the electrophysiology was carried out by Hisham Shembesh. Following electrophysiology, the sciatic nerve and spinal cords were harvested (see sections 2.2.3.2.ii) and prepared for analysis using confocal microscopy (sciatic nerves) and immunohistochemistry (spinal cords) (see section 2.2.4). Immunohistochemical labelling and axon counting and tracing analysis were quantified as described in Chapter 2. In all cases, analysis was carried out blind.

5.3.3 Sample Size Calculation

The sample size for this chapter were calculated using Biomath software [Source: G.W. Snedecor & W.G. Cochran. *http://www.biomath.info/power/ttest.htm*] with standard deviation (SD) data obtained from a previous study by Ngeow et al. (2011a) in our laboratory. The sample size chosen for the study was n=8, which would be sufficient to detect differences between groups of 0.21 for electrophysiology [Figure 5.5]. Two additional mice were added in each group to make sure that we got at least 8 animals for analysis. This sample size should also be sufficient to detect differences in axon tracing and axon disruption as previously calculated (see section 4.3.3).

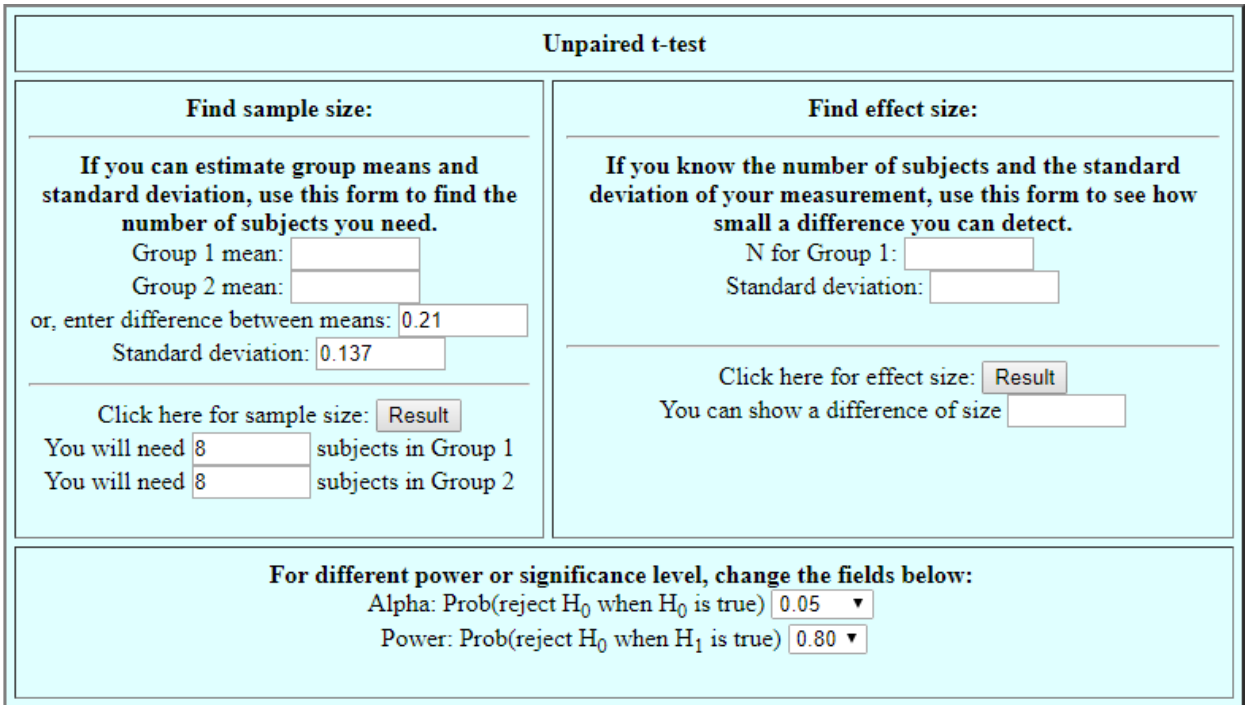

Figure 5.5: Electrophysiological analysis of power calculation for a sample size of 8 animals in each group.

5.3.4 Statistical Analysis

Statistical comparisons between groups were carried out as stated in section 2.3.7.1. For statistical analysis of glial activation, electrophysiology and axon disruption, unpaired t-test (two-tailed) was used. While for CatWalk, sprouting index and axon tracing, 2-way ANOVA with Bonferroni's multiple comparisons test was used.

All statistical analysis was performed using GraphPad Prism 7 software (GraphPad Prism Inc, CA, USA). Differences were considered to be significant at a *p* value below 0.05.

5.4. RESULTS

After harvesting the nerves, it was only possible to carry out analysis on a total of eight mice (four in each group). In the remaining mice, the proximal and distal nerve endings were found to be disconnected from the conduit, thus there was no regeneration and analysis could not be carried out.

The results of the immunohistochemistry of the spinal cord were provided by myself microglial activation) and Hisham Shembesh (astrocyte activation). The functional recovery results were obtained from a combination of CatWalk gait analysis, electrophysiology and axon counting and tracing techniques. The CatWalk analysis was performed by myself and Hisham Shembesh. Electrophysiology was performed by Hisham Shembesh, while axon counting and tracing was performed by myself.

Immunohistochemistry was performed to investigate spinal glial activation which acts as a potential indication of the development of neuropathic pain, while electrophysiology and axon counting and tracing analyses were performed to assess the functional recovery of nerve regeneration. CatWalk gait analysis is thought to provide an assessment of both functional recovery of the injured nerve and neuropathic pain.

Prior to the study reported in this chapter, two pilot experiments were performed using PCL conduits of 6.00mm in length. After a 4-week recovery period, the axons had regenerated well through the conduit; however, there was not enough space to perform the electrophysiology as the conduit occupied the majority of the sciatic nerve. For that reason, it was decided to use PCL conduits with a 5.00mm length.

5.4.1 Assessment of Glial Activation

5.4.1.1 Qualitative Observations of Spinal Cord

Glial activation was apparent in the injured side for all repair groups, particularly in PCL+Normal saline group, and the greatest observed immunoreactivity was present in a specific area of grey matter. This represents the region of the spinal cord to which the sciatic nerve projects. A number of hypertrophied glia were observed in both repair groups; However, the cells in the PCL+etanerceptgroup showed less hypertrophy compared to those in the PCL+Normal saline group (Figure 5.6A and B).

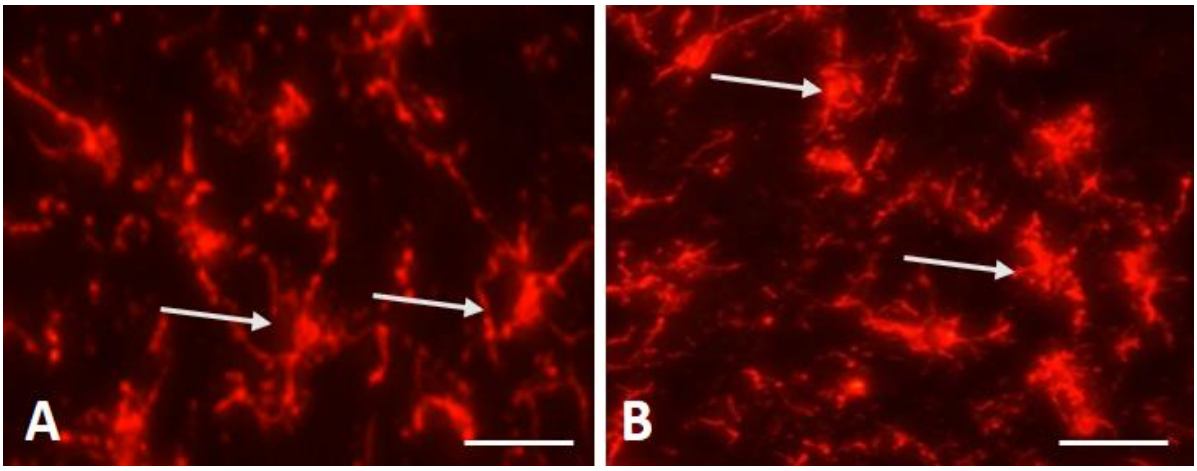

Figure 5.6: Sections of spinal cord after Immunohistochemistry staining with antibody Iba-1 showing hypertrophied microglia (white arrows) in both repair groups. A) PCL+Etanercept group. B) PCL+Normal saline group. Scale bar = 0.1mm.

5.4.1.2 Quantitative Analysis of Spinal Cord

As described in section 2.2.8.1(A), the percentage area of labelling for Iba-1 and GFAP was calculated in defined regions of the dorsal and ventral horns of the spinal cord both ipsilaterally and contralaterally to the nerve repair.

5.4.1.2.i Quantification of Iba-1 Expression

Quantification of labelling for microglial activation within the two groups demonstrates that the PCL+etanercept group had significantly lower levels than PCL+Normal saline group in ipsilateral dorsal horn (10.5% vs 12.6% [PCL+Normal saline; $p<0.05$]) and slightly lower in ipsilateral ventral horn (7.5% vs 8.3% [PCL+Normal saline; $p>0.05$]) (Table 5.1 & Figure 5.9). In the corresponding contralateral side, the percentages area of Iba-1 labelling in the dorsal and ventral horns were similar in both repair groups (refer to Table 5.1). The activation areas of Iba-1 in each group are shown in Figures 5.7 and 5.8.

PCL+Etanercept

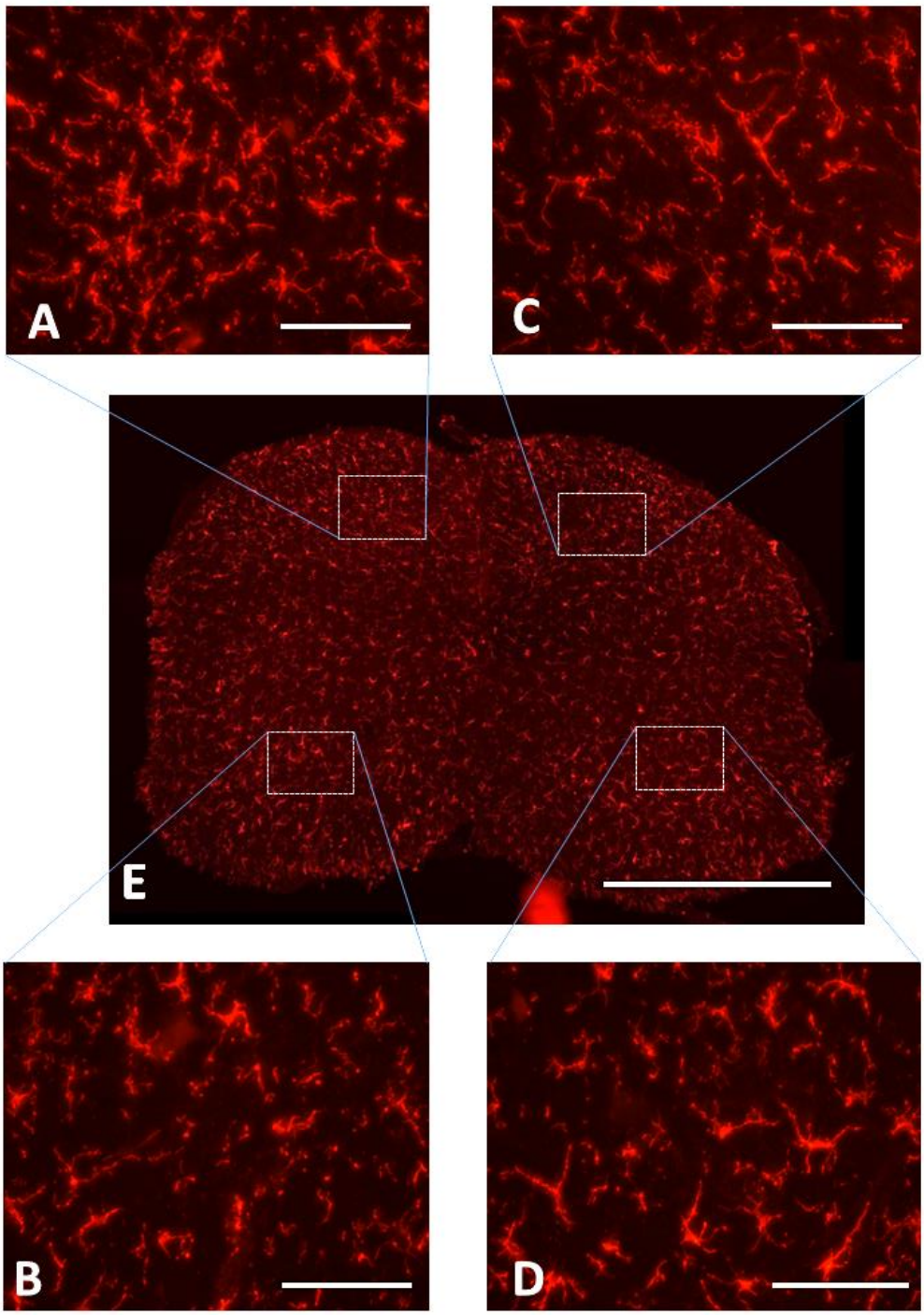

Figure 5.7: A section of spinal cord following repair with PCL+Etanercept shows microglial activation (E using 5x magnification). A) Ipsilateral dorsal horn, B) Ipsilateral ventral horn. C) Contralateral dorsal horn. D) Contralateral Ventral horn (A,B,C,D using 40x magnification). Scale bar A,B,C and D = 0.1mm, E = 1.0mm.

PCL+Normal saline

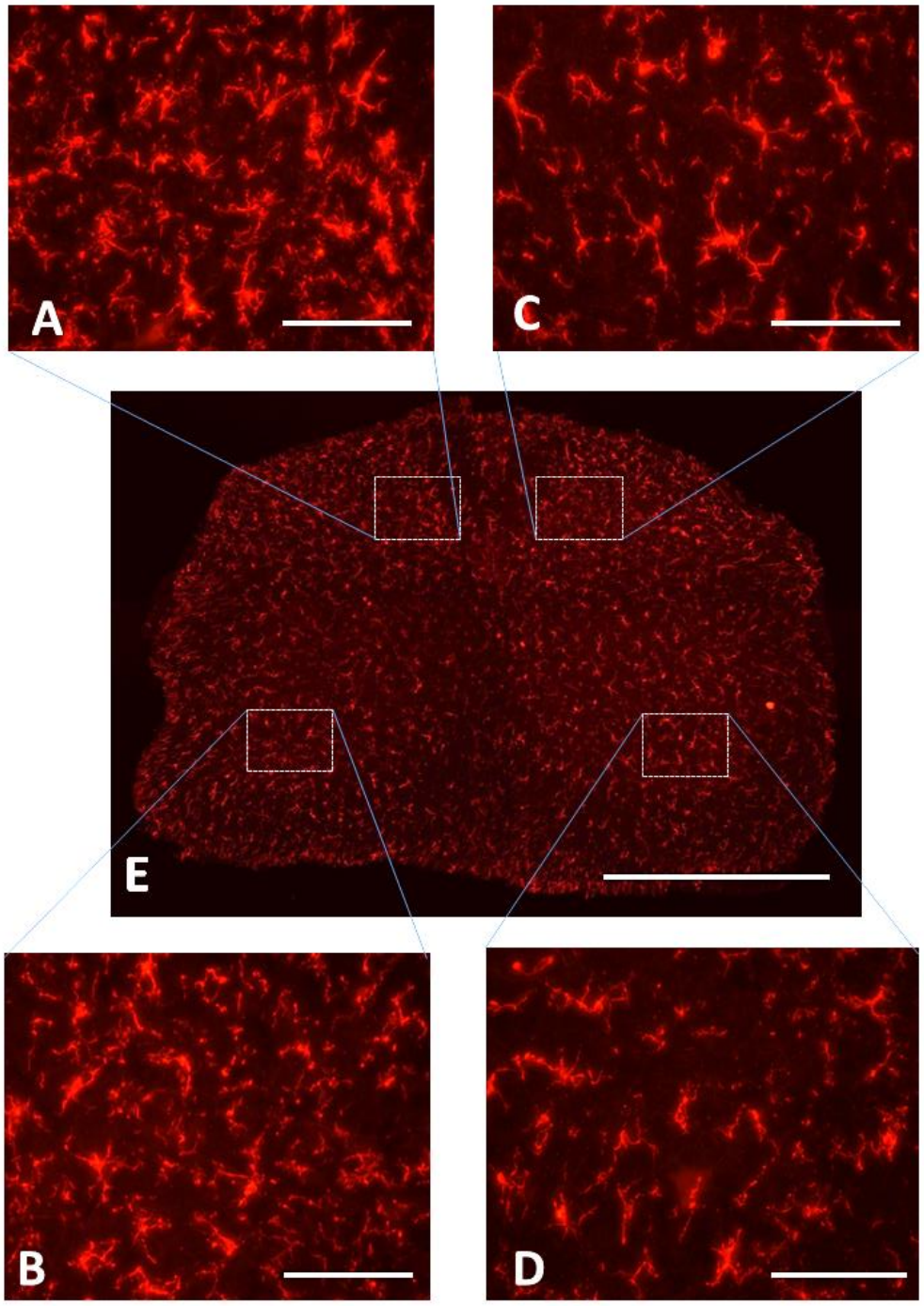

Figure 5.8: A section of spinal cord following repair with PCL+Normal saline shows microglial activation (E using 5x magnification). A) Ipsilateral dorsal horn, B) Ipsilateral ventral horn. C) Contralateral dorsal horn. D) Contralateral Ventral horn (A,B,C,D using 40x magnification). Scale bar A,B,C and D = 0.1mm, E = 1.0mm.

The mean percentage area of Iba-1 labelling (indication of the degree of microglial activation) for each group is shown in Table 5.1. The same data and the statistical comparison between the groups is illustrated in Figure 5.9.

Table 5.1: Percentages of microglial activation for PCL+Etanercept and PCL+Normal saline groups.

Iba-1 (Microglia)%	PCL+Etanercept	PCL+Normal saline
Ipsilateral Dorsal horn	10.5	12.6
Contralateral Dorsal horn	8.2	8.4
Ipsilateral Ventral horn	7.5	8.3
Contralateral Ventral horn	6.0	5.9

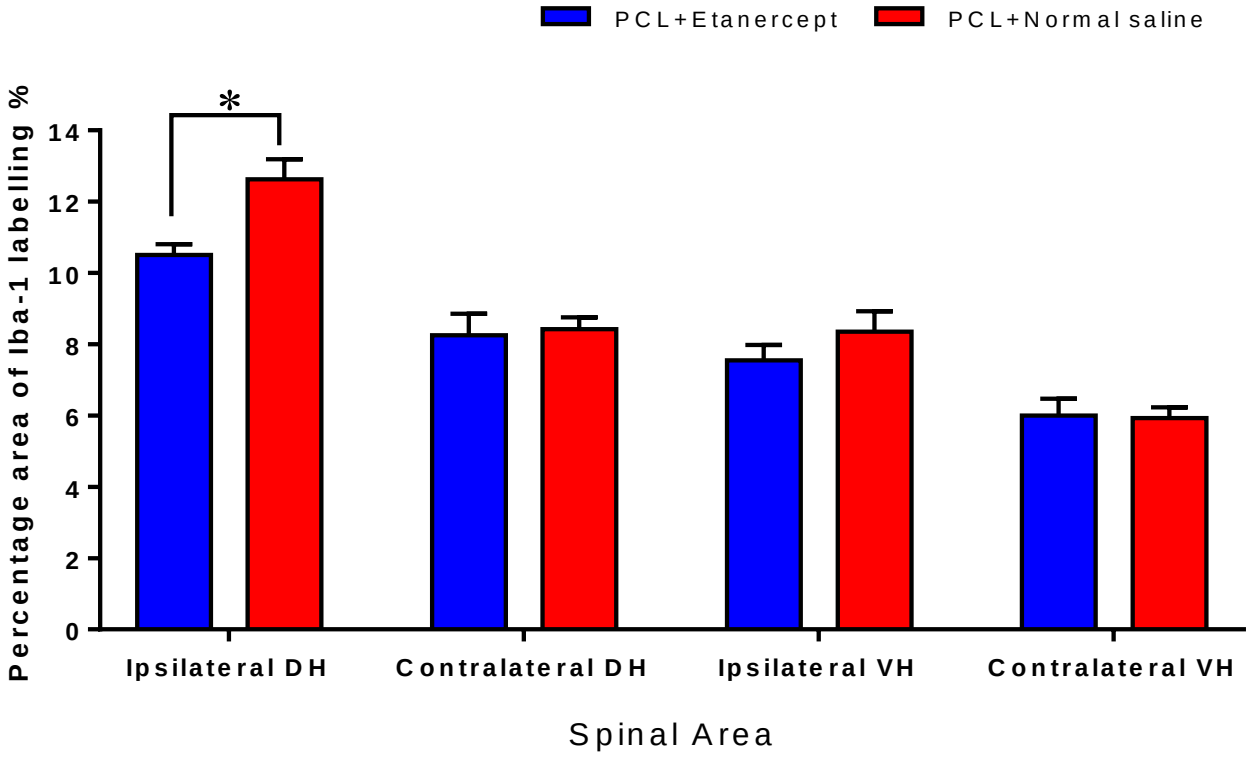

Figure 5.9: Immunohistochemical analysis of microglia for PCL+Etanercept and PCL-Normal saline groups. * denote significant difference compared PCL+NS, $p<0.05$. Error bars denote SEM. Statistical test: unpaired t-test (two-tailed). DH= Dorsal horn, VH= Ventral horn.

As described in section 2.2.8.1(B), some variation in the background staining was noted. Thus, percentage increase of the ipsilateral (injured) side over the contralateral (uninjured) side, ‘‘staining ratio’’ was performed. Comparisons between the groups when assessing the staining gave similar results to those described above. The increase in staining (Ipsilateral/Contralateral) ratio for Iba-1 in the PCL+Etanercept group was significantly lower than in PCL+Normal saline group in dorsal horn (29.3% vs 49.8% [PCL+Normal saline; $p<0.05$]) and slightly lower in ventral horn (26.4% vs 40.1% [PCL+Normal saline; $p>0.05$]) (Figure 5.10).

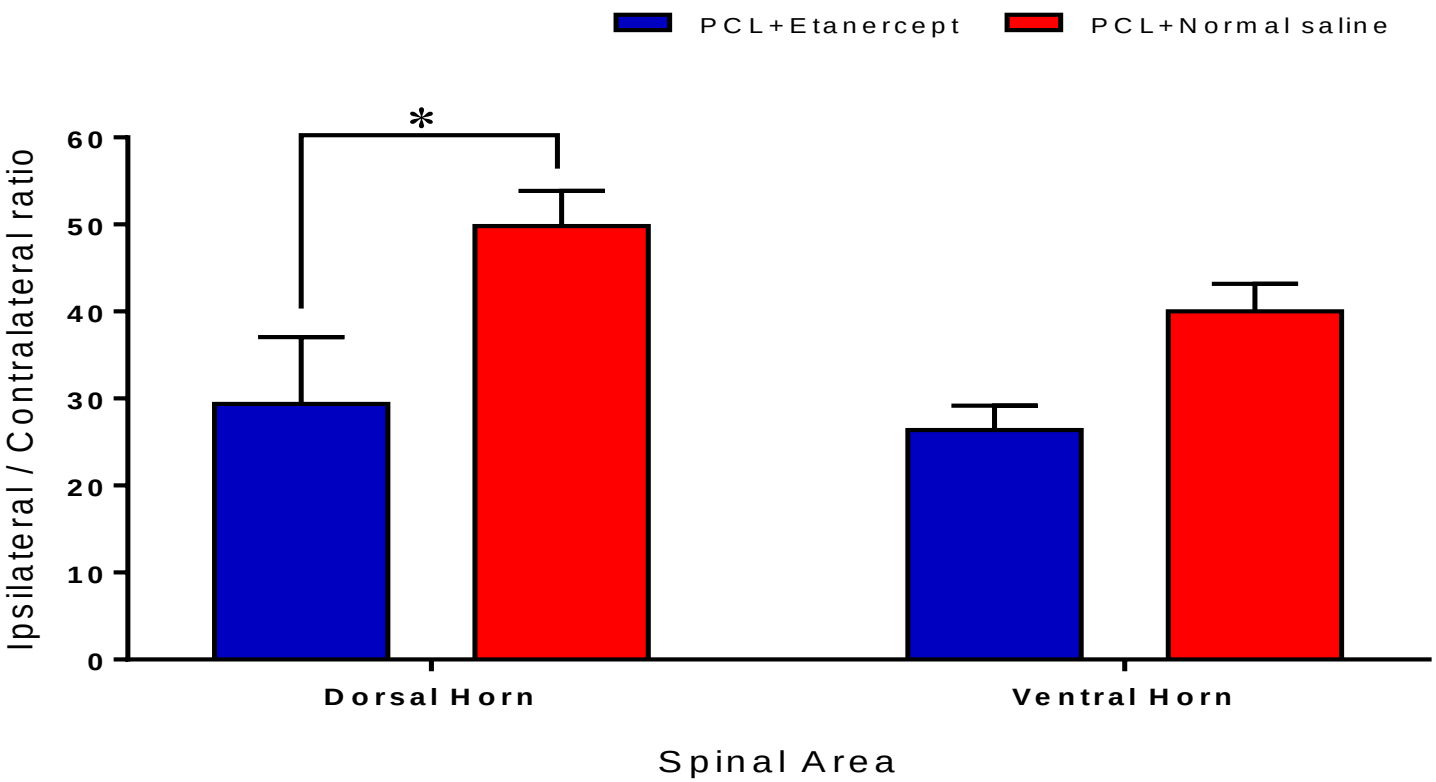

Figure 5.10: Ipsilateral/Contralateral ratio of microglia shows the difference of percentage increase in the ipsilateral side over the contralateral side in dorsal and ventral horns of the spinal cord for PCL+Etanercept and PCL+Normal saline groups. * denote significant difference compared to PCL+NS group, $p<0.05$. Error bars denote SEM. Statistical test: unpaired t-test (two-tailed).

5.4.1.2.ii Quantification of GFAP Expression

Quantification of labelling for astrocyte activation within the two groups demonstrates that the PCL+Etanercept group had slightly lower levels than PCL+Normal saline group in ipsilateral dorsal (8.7% vs 10.3% [PCL+Normal saline; $p>0.05$]) and ventral horn (6.7% vs 7.4% [PCL+Normal saline; $p>0.05$]) horns (Table 5.2 & Figure 5.13). In the corresponding contralateral side, the percentages area of GFAP labelling in the dorsal and ventral horns were similar in both repair groups (refer to Table 5.2 & Figure 5.13). The activation areas of Iba-1 in each group are shown in Figures 5.11 and 5.12.

PCL+Etanercept

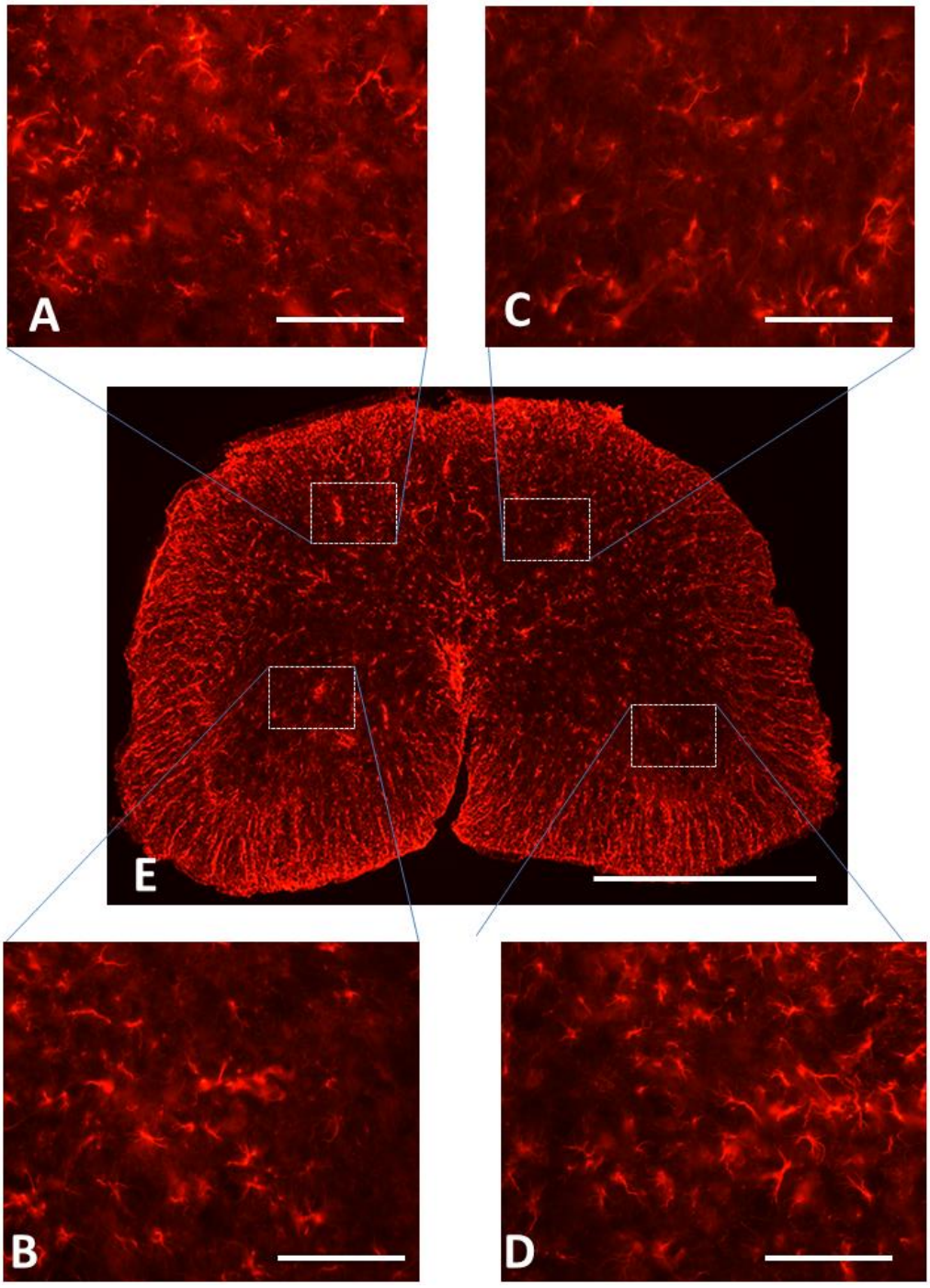

Figure 5.11: A section of spinal cord following repair with PCL+Etanercept shows astrocyte activation (E using 5x magnification). A) Ipsilateral dorsal horn, B) Ipsilateral ventral horn. C) Contralateral dorsal horn. D) Contralateral Ventral horn (A,B,C,D using 40x magnification). Scale bar A,B,C and D = 0.1mm, E = 1.0mm.

PCL+Normal saline

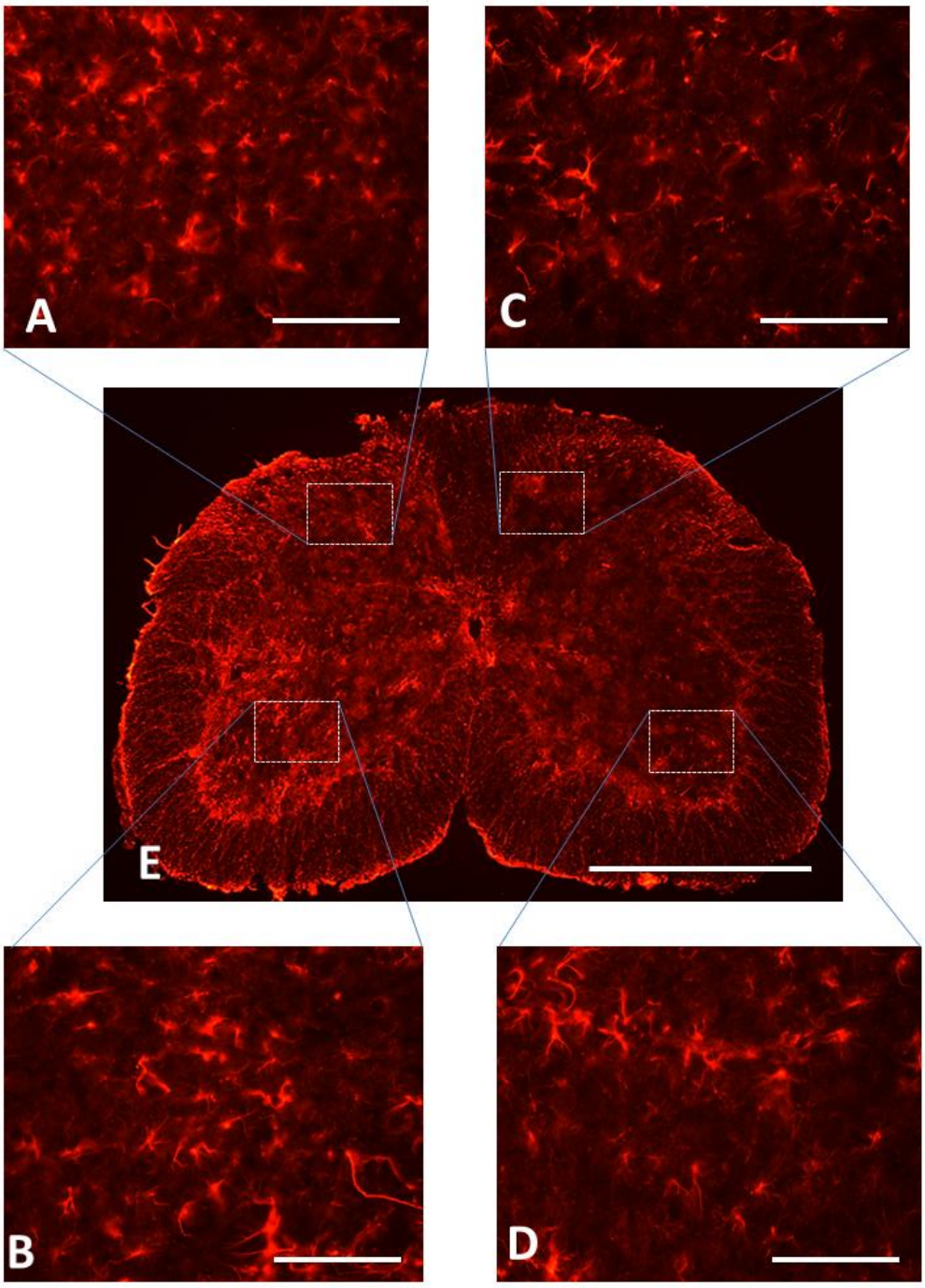

Figure 5.12: A section of spinal cord following repair with PCL+Normal saline shows astrocyte activation (E using 5x magnification). A) Ipsilateral dorsal horn, B) Ipsilateral ventral horn. C) Contralateral dorsal horn. D) Contralateral Ventral horn (A,B,C,D using 40x magnification). Scale bar A,B,C and D = 0.1mm, E = 1.0mm.

The mean percentage area of GFAP labelling (indication of the degree of astrocyte activation) for each group is shown in Table 5.2. The same data and the statistical comparison between the groups is illustrated in Figure 5.13.

Table 5.2: Percentages of astrocyte activation for PCL+Etanercept and PCL+Normal saline groups.

GFAP (Astrocyte)%	PCL+Etanercept	PCL+Normal saline
Ipsilateral Dorsal horn	8.7	10.3
Contralateral Dorsal horn	7.2	7.3
Ipsilateral Ventral horn	6.7	7.4
Contralateral Ventral horn	5.8	6.1

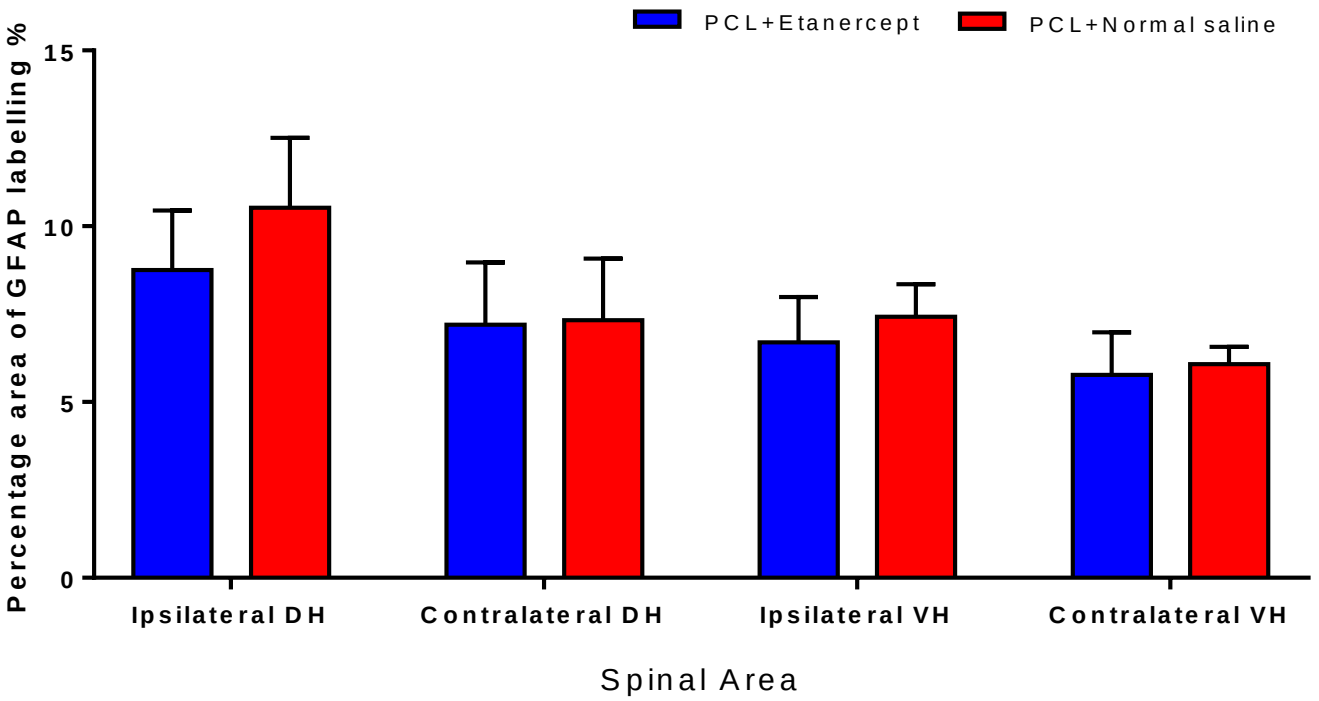

Figure 5.13: Immunohistochemical analysis of astrocytes for PCL+Etanercept and PCL+Normal saline groups. Statistical test: unpaired t-test (two-tailed). DH= Dorsal horn, VH= Ventral horn.

The increase in staining (Ipsilateral/Contralateral) ratio for GFAP in the PCL+Etanercept group was significantly lower than in PCL+Normal saline group in dorsal horn (22.6% vs 46.5% [PCL+Normal saline; $p<0.05$]) and slightly lower in ventral horn (16.5% vs 23.2% [PCL+Normal saline; $p>0.05$]) (Figure 5.14).

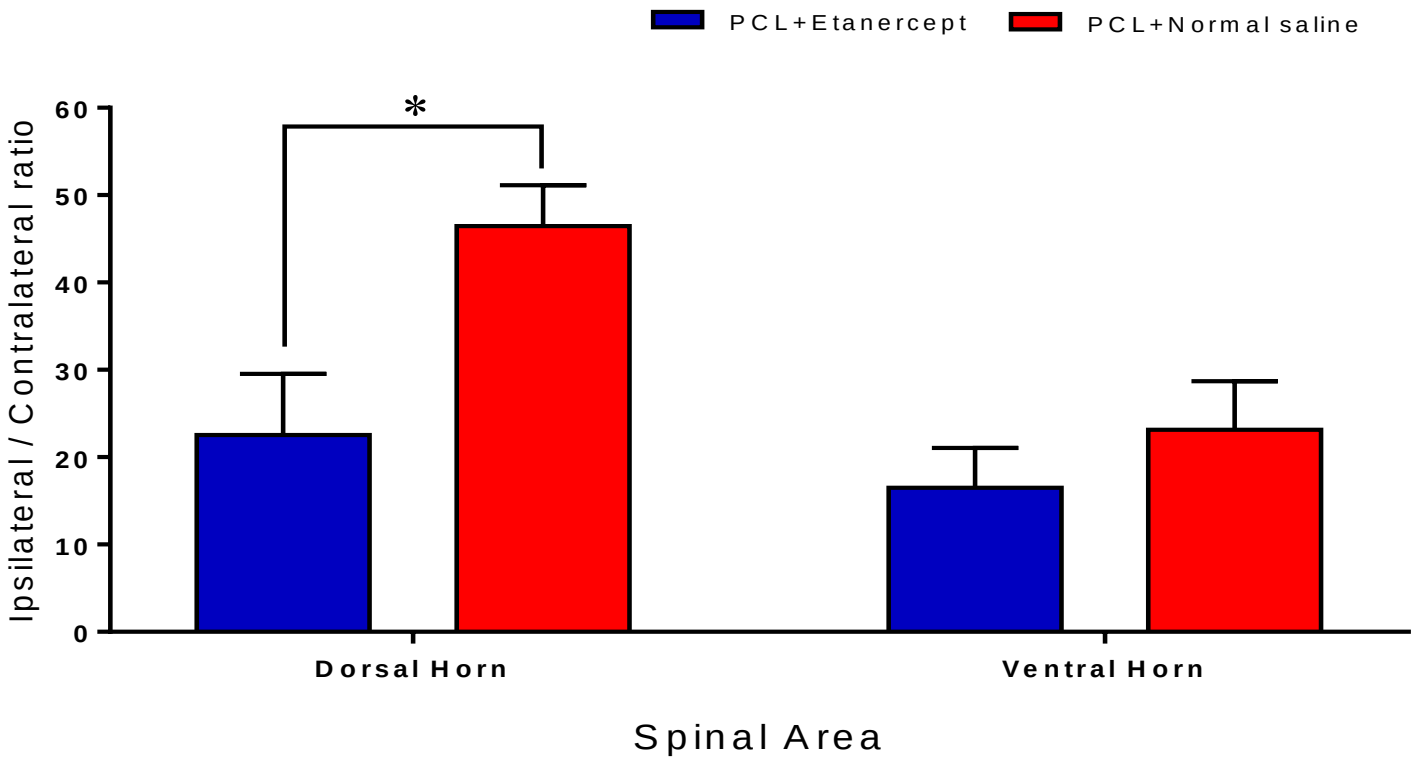

Figure 5.14: Ipsilateral/Contralateral ratio of astrocyte shows the difference of percentage increase in the ipsilateral side over the contralateral side in ventral and dorsal horns of the spinal cord for PCL+Etanercept and PCL-Normal saline groups. * denote significant difference compared to PCL+NS group, $p<0.05$. Error bars denote SEM. Statistical test: unpaired t-test (two-tailed).

5.4.2 Assessment of Neuropathic Pain and Functional Recovery

5.4.2.1 CatWalk Gait System

Data were obtained a day before surgery and weekly after surgery. The last data were obtained on the day of harvesting (week 5). No loss of weight was observed in any mice, suggesting that all mice were in good health. All mice had gained weight (1-4g) by week 5, and this was observed in both groups meaning the body weights were similar between the two groups pre and postoperation. Despite the injury, the mice could still make un-interrupted runs. An example of the recording is presented in Figure 5.15.

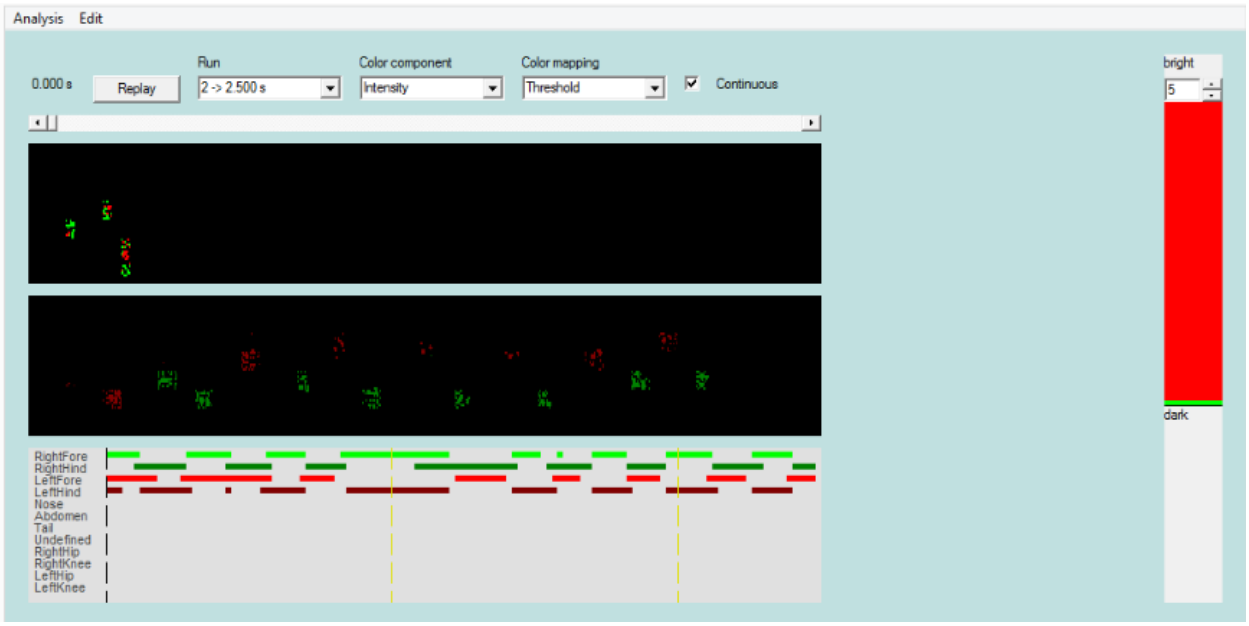

Figure 5.15: An example of CatWalk software showing the analysis of the mouse's runs.

5.4.2.1.i Intensity of the Paw Print

Data from CatWalk analysis demonstrated that PCL+Etanercept repairs had higher percentages of left hind paw intensity in all weeks than PCL+Normal saline repairs. These differences were significantly higher at weeks 2 and 3 for PCL+Etanercept (73.3% and 74.8%, respectively) compared to PCL+NS (50.8% and 52.6%, respectively) (Table 5.3). Following week 1, the percentage in the PCL+Etanercept increased up to week 3 where it dropped notably at week 4 and then slightly decreased at week 5. Whereas, in PCL+Normal saline the percentage remained at the same level (approximately ±3-9%) from week 1 onwards (Figure 5.16A).

The percentages of intensity in the right paw were similar in both groups at all weeks (Figure 5.16B). After the recovery period (week 5), the difference in intensity percentages on both left and right paws was approximately 5% in PCL+Etanercept and 11% in PCL+Normal saline (Table 5.3).

Table 5.3: Percentages of Intensity of paw print for PCL+Etanercept and PCL-Normal saline groups

Intensity %	**PCL+Etanercept**		**PCL-Normal saline**	
Recovery period	**Left Paw**	**Right Paw**	**Left Paw**	**Right Paw**
Baseline	100.0	100.0	100.0	100.0
Week 1	67.3	74.3	56.5	67.0
Week 2	73.3	71.6	50.8	74.5
Week 3	74.8	75.9	52.6	76.3
Week 4	61.0	65.6	50.1	74.0
Week 5	64.5	69.9	52.3	63.7

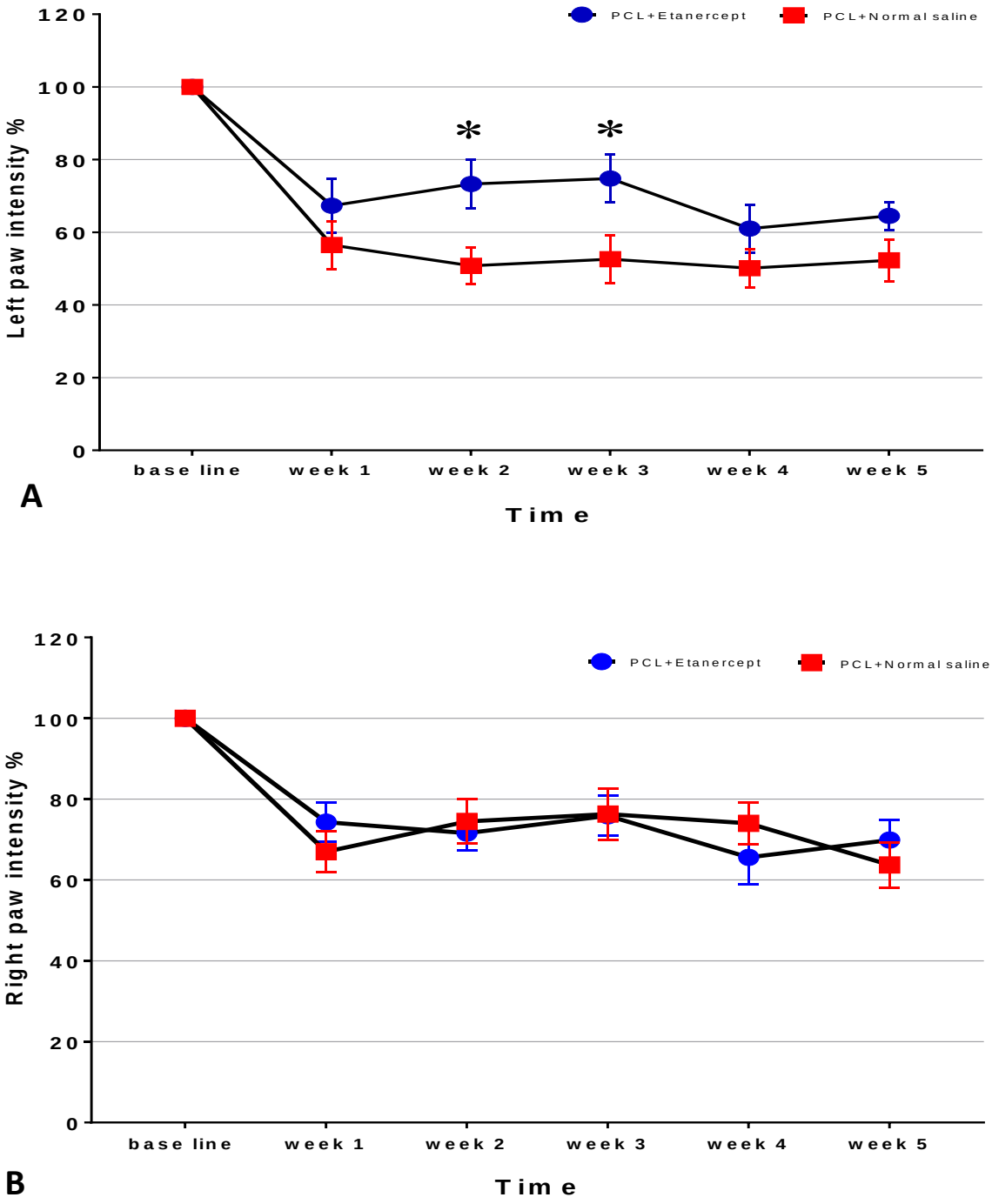

Figure 5.16: CatWalk analysis showing the percentages of the intensity in both groups. A) Intensity percentage in left paw. B) Intensity percentages in right paw. * denotes significant difference compared PCL+Normal saline, $p<0.05$. Error bars denote SEM. Statistical test: 2-way ANOVA with Bonferroni's multiple comparisons test.

5.4.2.1.ii Print area

Data from CatWalk analysis showed that PCL+Etanercept repairs had higher percentages of left hind paw print area overall in all weeks compared to PCL+Normal saline repairs. These differences were significantly higher only at week 3 in PCL+Etanercept (54.7%) compared to PCL-Normal saline (29.8%) (Table 5.4). The highest drop of print area for PCL+Etanercept was observed at week 4, while in PCL+Normal saline this was observed at week 3 (Figure 5.17A). The percentage steeply rose after week 4 in both repair groups.

The percentages of print area in the right paw were similar in both groups at all weeks (Figure 5.17B). After the recovery period (week 5), the difference in print area percentages on both left and right paws was approximately 4% in PCL+Etanercept and 12% in PCL+Normal saline (Table 5.4).

Table 5.4: Percentages of print area for PCL+Etanercept and PCL+Normal saline groups.

Print area%	**PCL+Etanercept**		**PCL+Normal saline**	
Recovery period	**Left Paw**	**Right Paw**	**Left Paw**	**Right Paw**
Baseline	100.0	100.0	100.0	100.0
Week 1	58.7	52.4	39.1	64.2
Week 2	61.1	67.7	42.1	53.3
Week 3	54.7	52.5	29.8	45.8
Week 4	40.2	48.5	21.1	42.3
Week 5	54.2	49.7	39.3	51.2

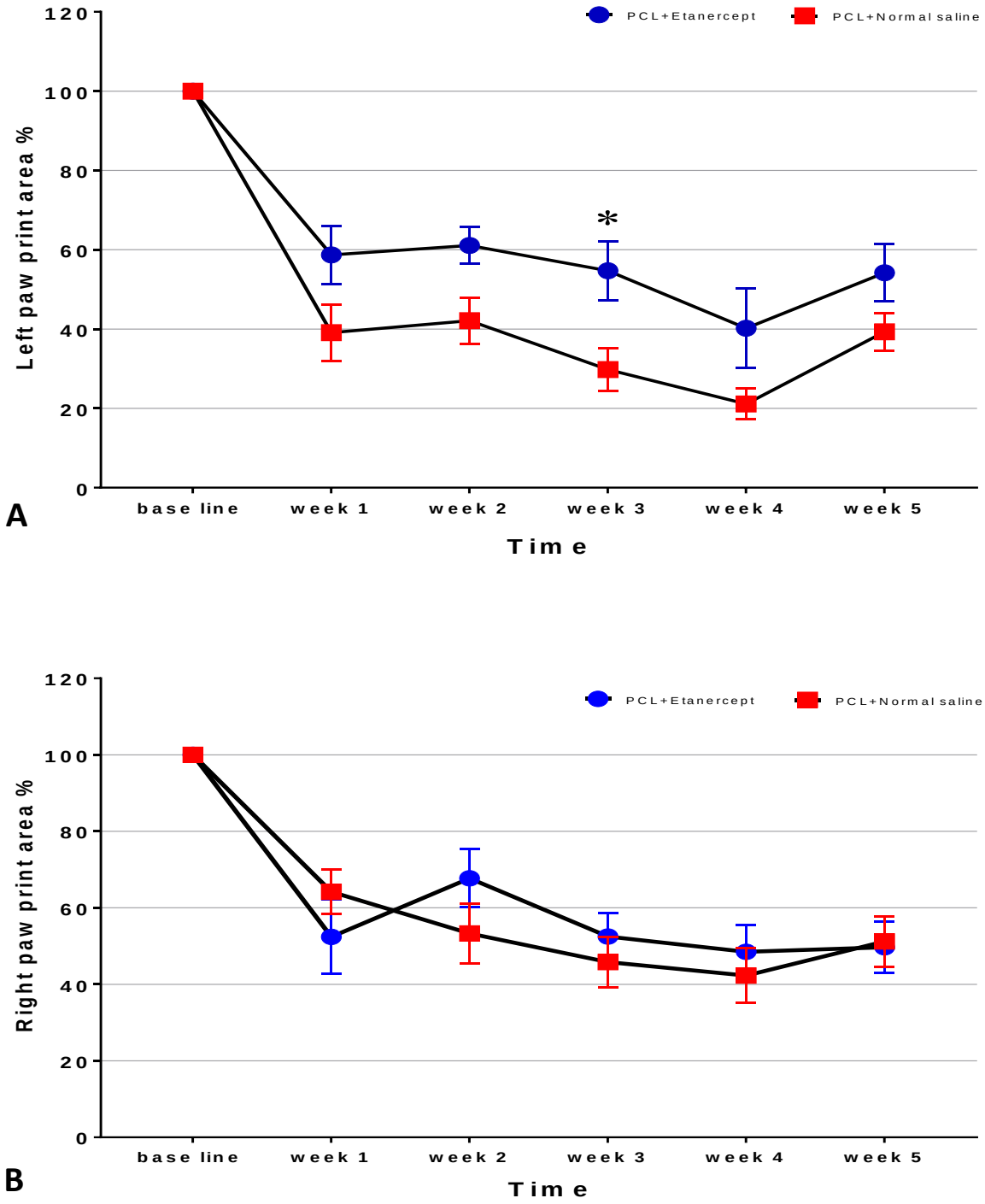

Figure 5.17: CatWalk analysis showing the percentages of the print area in both groups. A). Print area percentage in left paw. B). Print area percentages in right paw. * denote significant difference compared PCL+Normal saline, $p<0.05$. Error bars denote SEM. Statistical test: 2-way ANOVA with Bonferroni's multiple comparisons test.

5.4.3 Assessment of Functional Recovery

5.4.3.1 Electrophysiology Recordings

5.4.3.1.i Compound Action Potential Modulus Ratio

No significant difference was observed between the two groups. However, PCL+Etanercept had a slightly higher compound action potential (CAP) modulus ratio than PCL+Normal saline. The CAP modulus ratios in each group are shown in Figure 5.18, and the recorded CAP ratios are shown in Figure 5.19.

The average CAP modulus ratio in PCL+Etanercept repairs was 0.253 [±0.063 SME], indicating that very small CAPs were evoked by stimulation distal to the repair. In PCL+Normal saline repairs, the average CAP modulus ratio was 0.203 [±0.034], which is smaller than PCL+Etanercept but not significant.

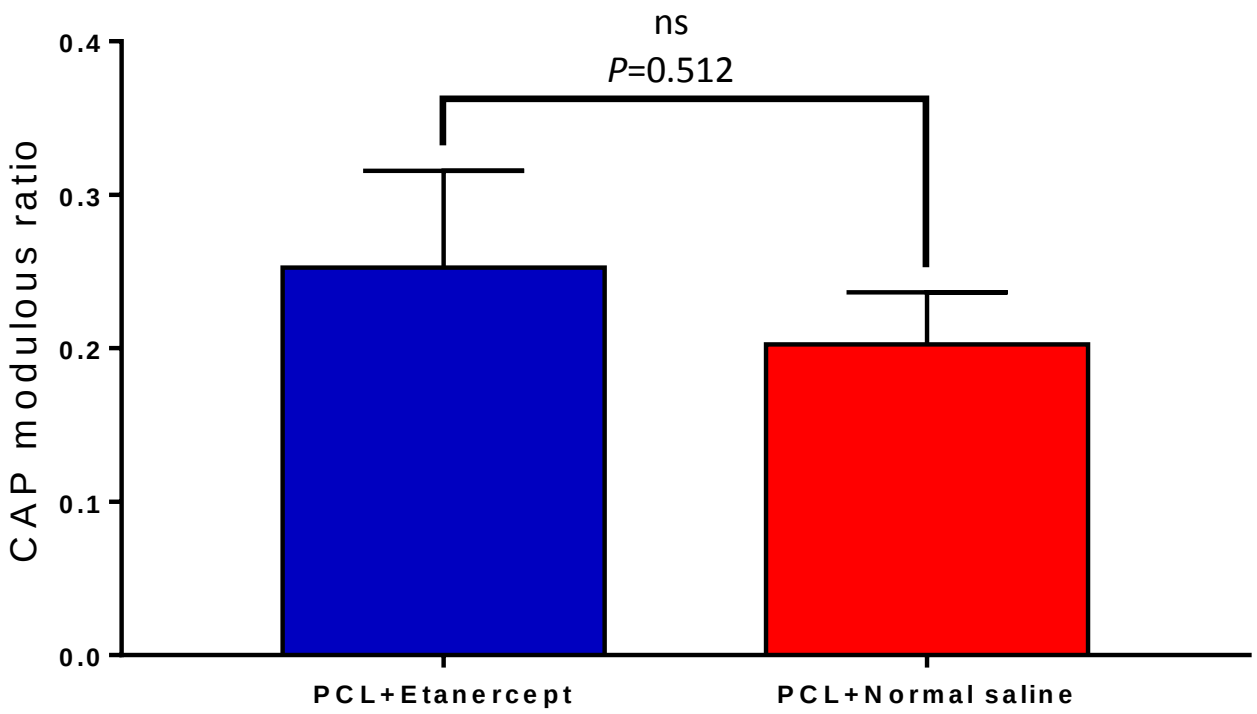

Figure 5.18: Electrophysiology analysis shows the average of CAP modulus ratios on PCL+Etanercept and PCL+Normal saline groups. There were no statistically significant differences between repair groups. Error bars denote SEM. Statistical test: Unpaired t test with Bonferroni post-tests.

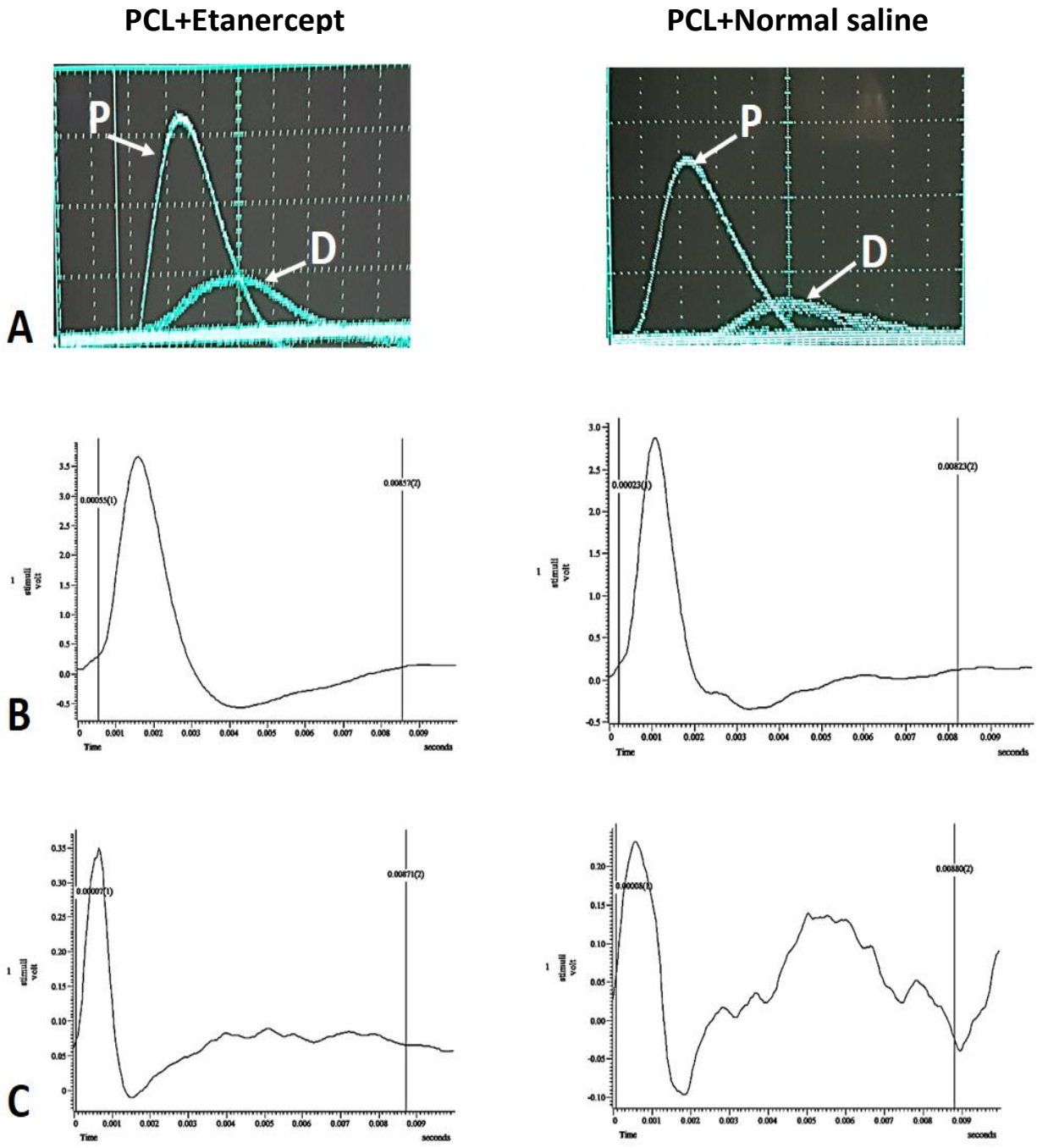

Figure 5.19: A) Calculation of compound action potential (CAP) modulus ratio as seen on the oscilloscope in PCL+Etanercept and PCL+Normal saline groups. Large and small response (10 superimposed sweeps) was evoked by stimulation proximal modulus (P) and distal modulus (D) to the repair site, respectively. B) Showing the proximal stimulation. C) Showing the distal stimulation.

5.4.3.1.ii Conduction Velocity

No significant difference was observed between the two groups. The conduction velocities (CV) in each group are shown in Figure 5.20. The results shown here demonstrate the average conduction velocity of the fastest components in CAP and are dependent on the response evoked by distal stimulating electrodes. The average conduction velocity of the fastest axons was faster in PCL+Etanercept repairs 0.31ms^{-1} [±0.052SEM] compared to PCL+Normal saline 0.28ms^{-1} [±0.047], but this difference was not significant.

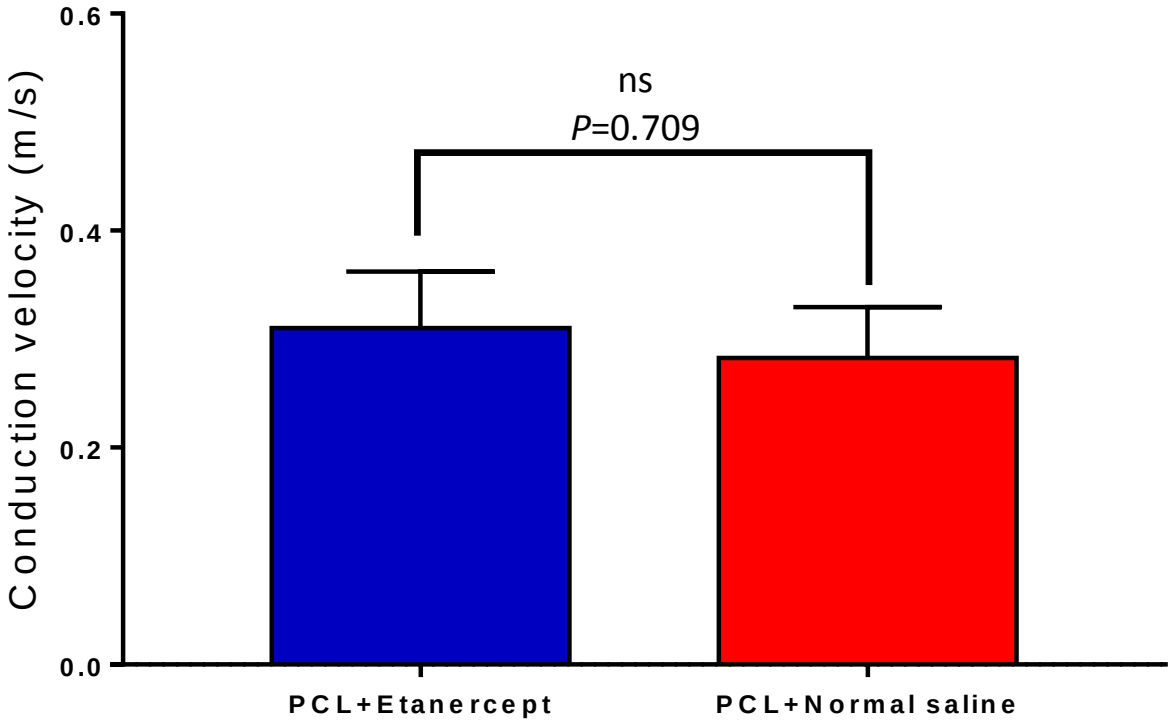

Figure 5.20: Electrophysiology analysis shows the average of conduction velocity on PCL+Etanercept and PCL+Normal saline groups. There were no statistically significant differences between repair groups. Error bars denote SEM. Statistical test: unpaired t test (two-tailed).

5.4.3.2 Axon Counting and Tracing

5.4.3.2.i Qualitative Observation of Regenerated Nerves

Axons have entered the conduits and have extended distally toward the distal end (Figure 5.21). Axons were able to reach the distal nerve ending, extending beyond the branching of the sciatic nerve within the recovery period (5-weeks).

5.4.3.2.ii Quantitative Analysis of Regenerated Nerves

A. Sprouting Index

Sprouting index analysis showed a significant drop in the number of axons in both repair groups at the 0.5mm interval. There were higher percentages in PCL+NS compared to PCL+Etanercept overall**.** The percentages of the repair groups at the 0.0mm 'start' interval were 115.8% in PCL-Normal saline and 93% in the PCL+Etanercept**.** At the 0.5mm interval, the sprouting index was significantly higher in PCL+Normal saline (69%) compared to the PCL+Etanercept (41.33%). Following that, the percentages in the PCL+Normal saline repairs decrease until reaching its lowest level (44.74%) at the 2.5mm interval, increasing gradually at all subsequent intervals. For PCL+Etanercept repairs, sprouting index values fluctuated across the repair up to the 3.5mm interval, following which the sprouting index increased at all subsequent intervals (Figure 5.21). All sprouting index values were illustrated in Table 5.5 and Figure 5.22. It is believed that a high level of sprouting index is not an indication of better regeneration.

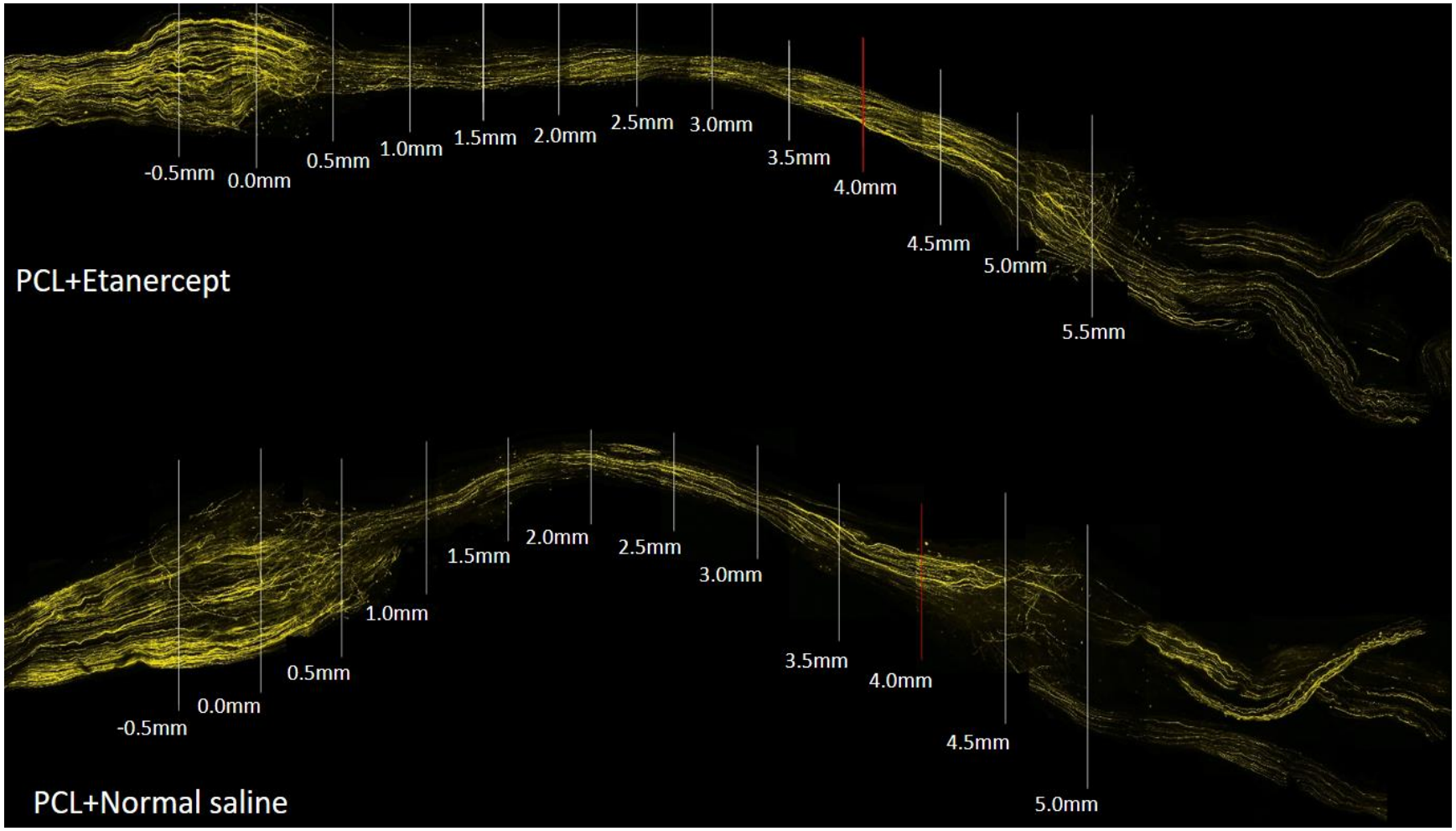

Figure 5.21: Repaired nerve with PCL+Etanercept and PCL+Normal saline groups. All nerves presented with intervals marked, showing the start interval and the final interval (red).

Table 5.5: Sprouting index levels of PCL+Etanercept and PCL+Normal saline groups (%).				
Repair Position (Intervals)	**PCL+Etanercept**	**SEM**	**PCL+Normal Saline**	**SEM**
-0.5	100.0	0.0	100.0	0.0
0.0	93.0	12.5	115.8	4.1
0.5	41.3	6.8	69.0	10.2
1.0	35.3	1.2	52.0	4.1
1.5	37.3	3.8	49.0	2.9
2.0	39.3	4.6	45.7	2.2
2.5	40.0	6.4	44.7	2.2
3.0	38.0	5.8	47.5	4.9
3.5	34.6	5.3	48.7	3.5
4.0	37.6	8.8	53.0	3.2
4.5	40.3	8.2	56.5	2.6
5.0	46.0	11.6	56.7	2.1

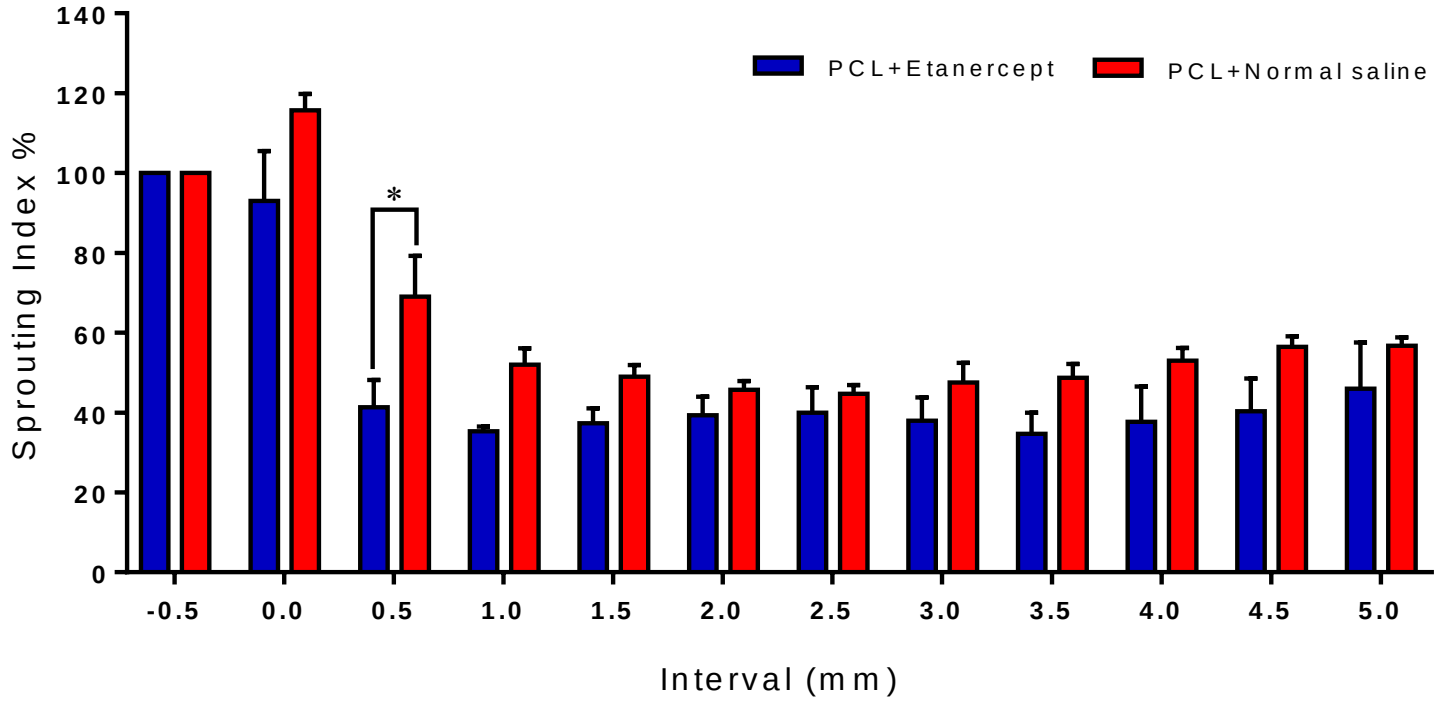

Figure 5.22: Sprouting index levels on PCL+Etanercept and PCL+Normal saline at 0.5mm intervals along the nerve. * denote significant difference compared to PCL+Normal saline, $p<0.05$. Error bars denote SEM. Statistical test: 2-Way ANOVA with Bonferroni's multiple comparisons test.

B. Axon Tracing

A minimum of 75% of axons are traced from the final interval (5.0mm) back toward to the 0.0mm interval (Figure 5.23). The proportion of unique axons represented at each interval indicated that both repairs groups had similar percentages at all intervals except at the 0.5mm interval where the PCL+Etanercept had a significantly higher proportion (50.76%) than PCL+Normal saline repairs (38.87%) (Table 5.6 and Figure 5.24). The largest decline of unique axons was observed between the 0.0mm and 0.5mm intervals. Following that, the percentages of unique axons of both PCL+Etanercept and PCL+Normal saline remained steady with an approximate decline of 3-9% and 6-11% respectively at each interval from the 1.0mm interval, (where unique axons represented 35.13% and 34.1% respectively).

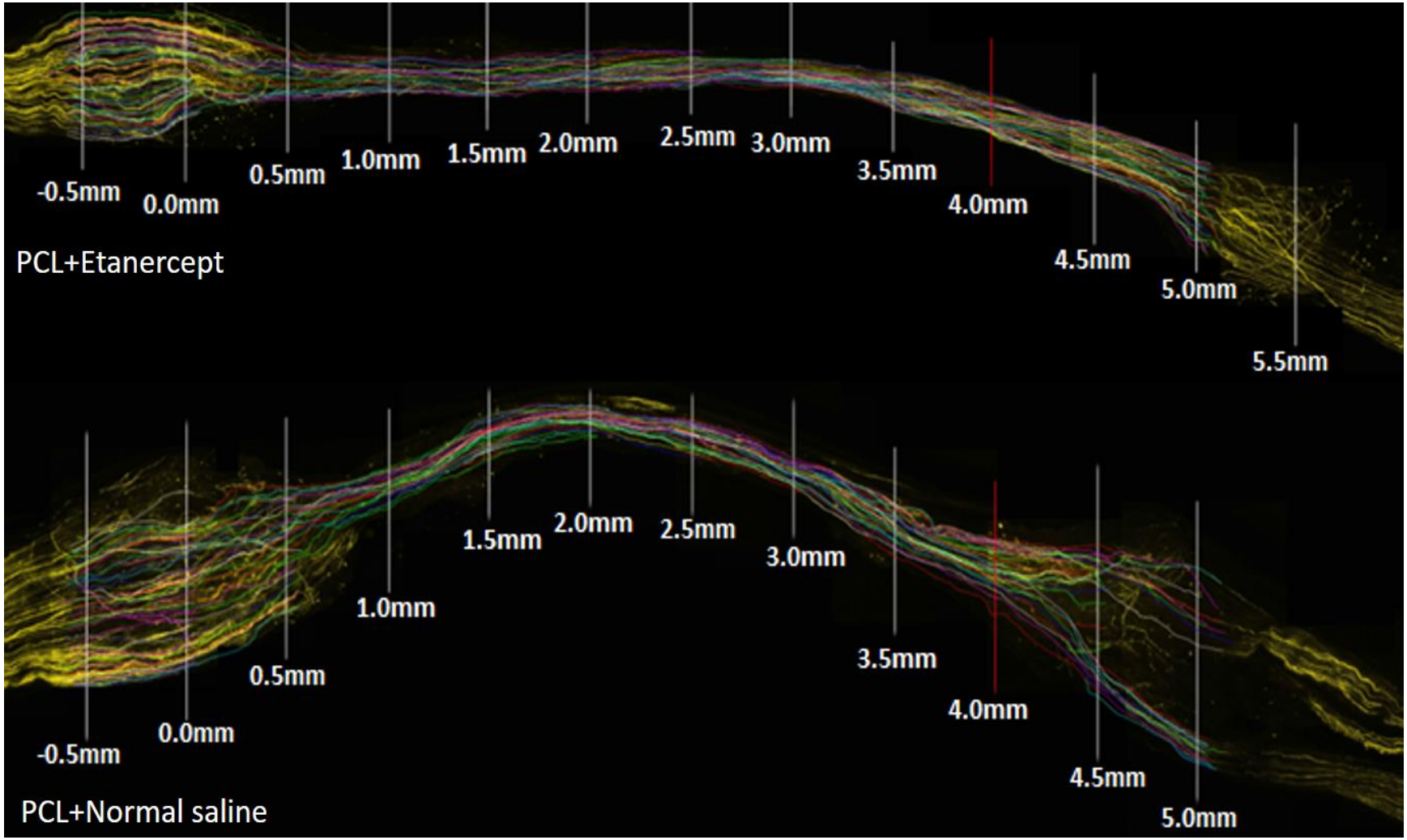

Figure 5.23: Image of traced axons from 5.0mm interval back toward to the 0.0mm in both PCL+Etanercept and PCL+Normal saline.

Table 5.6: Axon tracing for PCL+Etanercept and PCL+Normal saline groups (%).				
Repair Position (Intervals)	**PCL+Etanercept**	**SEM**	**PCL+Normal Saline**	**SEM**
0.0	100.0	0.0	100.0	0.0
0.5	50.8	3.1	38.9	6
1.0	35.1	3.9	34.1	3.6
1.5	31.3	1.9	28.8	1.7
2.0	29.2	1.6	27.5	0.6
2.5	28.4	2.3	26.2	0.9
3.0	26.9	2.1	26.5	1.5
3.5	27.1	1.9	23.6	0.9
4.0	26.8	2.0	24.1	1.7
4.5	27.5	2.0	24.8	1.4
5.0	27.1	1.9	24.3	1.5

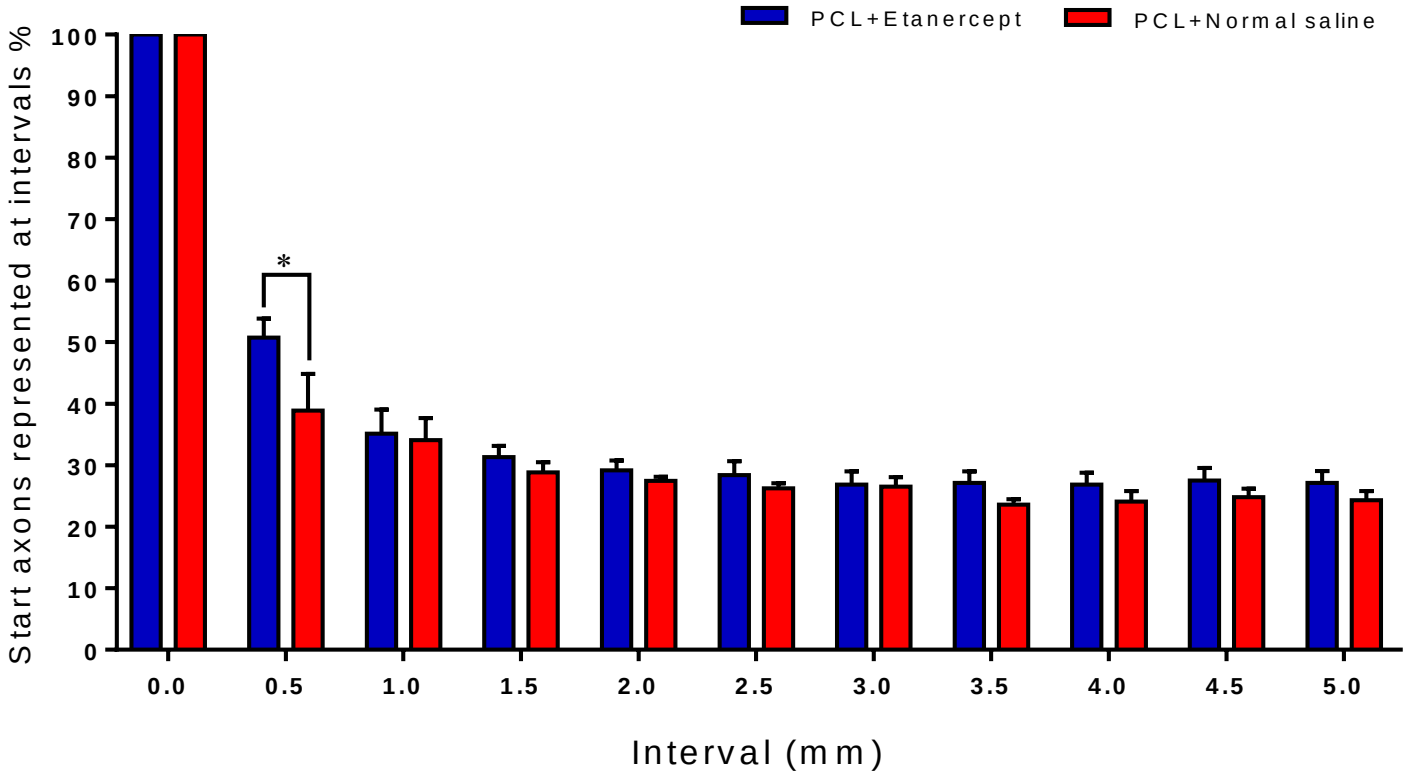

Figure 5.24: Unique axon percentages across repair in both groups. *denote significant difference compared to PCL+Etanercept, $p<0.05$. Error bars denote SEM. Statistical test: 2-way ANOVA with Bonferroni's multiple comparison test.

C. Axon Disruption

Axon lengths across the portion of nerve between the 0.0mm and 1.5mm intervals were measured, and the average axon length in each group was determined (Figure 5.25). The difference between the axon length and actual distance (1.5mm) was expressed as percentage increase of axon length relative to the actual distance.

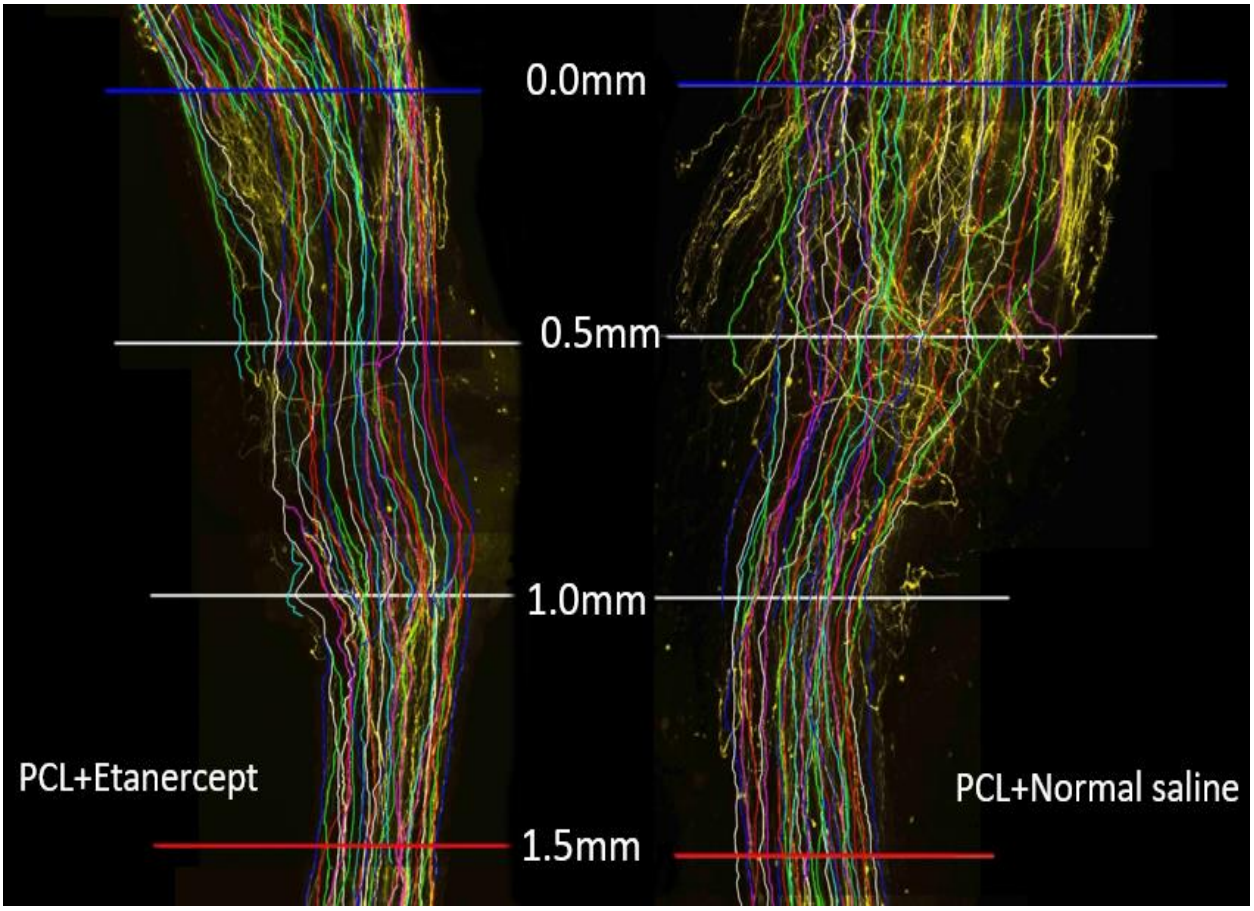

Figure 5.25: Image showing traced axon disruption between 0.0mm (blue line) and 1.5mm (red line) in both nerve repairs: PCL+Etanercept (on the left) and PCL+Normal saline (on the right).

The average increase in axon length in the PCL+Normal saline group was significantly higher (12.36% [1.98]) compared to PCL+Etanercept group (7.29% [0.66SEM]) p=0.0392) (Figure 5.26).

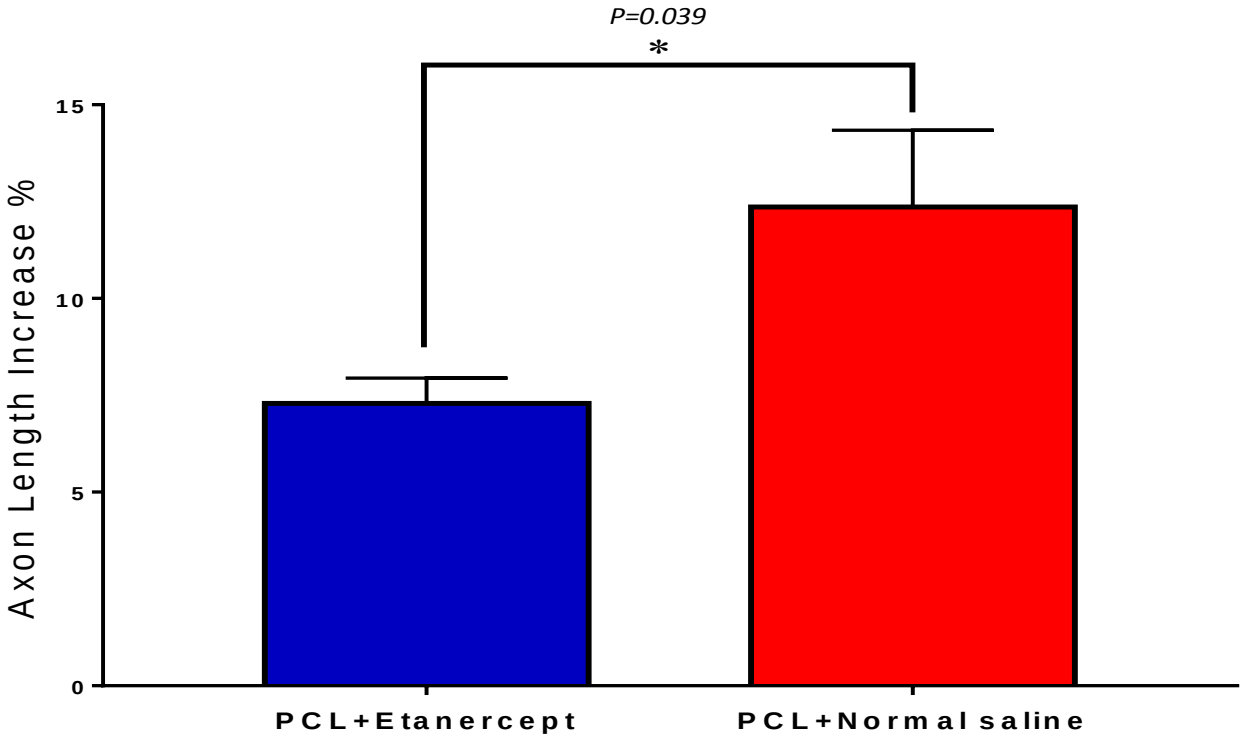

Figure 5.26: Percentage increase in axon length between 0.0mm and 1.5mm in both groups. *denote significant difference compared to PCL+Etanercept, $p<0.05$. Error bars denote SEM. Statistical test: unpaired t test (two-tailed).

5.5 DISCUSSION

Based on our previous studies and those of others, which reported that PCL conduits are successful nerve guides (Choi et al 2015, Harding 2014, Reid et al 2013, Sun et al 2010), and reported that the use of etanercept may reduce the level of inflammation and enhance nerve regeneration (Alsalihi et al., 2017, Kato et al., 2010, Weinblatt et al., 1999), it was hypothesised that a PCL conduit combined with etanercept treatment would improve nerve regeneration as well as decrease the potential for development of neuropathic pain. A combination of four analyses (immunohistochemistry, CatWalk gait, electrophysiology and axon counting and tracing analysis) were performed in this chapter to assess the potential development of neuropathic pain and the functional recovery of the nerve. In general, conduit plus etanercept gave better outcome than conduit plus vehicle.

5.5.1 The Effect of PCL and Etanercept on Spinal Glial Activation

As mentioned in Chapter 3, PCL conduit repairs had low percentages of glial activation. The results obtained in this chapter demonstrated that PCL+Etanercept repairs had significantly lower glial activation in dorsal horn in both microglia and astrocytes compared to PCL+Normal saline repairs. Despite the injury being made in the larger, sciatic nerve in this study, both repairs expressed relatively low levels of glial activation. This may suggest that neuropathic pain is unlikely to have developed in either repair group; this is especially true in, PCL+Etanercept repairs, as they express significantly lower activation percentages in dorsal horn than PCL+Normal saline repairs. However, the longer recovery time in this study (compared to chapter 3) will have influenced glial activation as it has been reported that microglial activation increases following nerve injury reaching a peak in the first week, and then gradually declining (Erikson et al., 1993).

The role of TNF-α in glial activation in the brain was previously evaluated by Bruce et al. (1996). In their study, wild-type mice were compared to genetically modified TNFR-KO mice (lacking both TNF receptors). They reported that after brain injury the level of microglial activation was high in the wild-type mice while it was low in the TNFR-KO mice. This suggests that TNF is one of several factors increased following

brain injury, and that it plays an important role in the activation of microglia. For astrocyte activation, both wild-type and TNFR-KO mice expressed similar levels of activation, indicating that TNF-α has a limited role in astrocyte activation (Bruce et al,1996). In contrast, a previous study by Selmaj et al. (1990) reported that TNF-α can induce astrocytes proliferation. A study by Genovese et al. (2008) found that deletion of TNFR1 gene or blocking of TNF in mice with spinal cord injury leads to reduced inflammation and enhanced functional recovery. Lindenlaub et al. (2000) investigated the role of neutralizing antibodies to TNF in CCI of sciatic nerve of mice and reported that antibodies to TNF can reduce mechanical allodynia and thermal hyperalgesia.

Etanercept was investigated by Alsalihi et al. (2017) in olfactory nerve transection in mice. Their study reported that the application of etanercept in the acute phase after injury can suppress local inflammatory cells and glial scar formation, facilitating morphological and functional recovery (Alsalihi et al., 2017). These results correlate with their previous studies that reported administration of anti-IL-6 antibody and steroid (dexamethasone) reduced the local inflammation and glial scar formation in olfactory nerve regeneration in mice (Kobayashi and Costanzo, 2009, Kobayashi et al., 2013). They concluded that local inflammation and gliosis can reduce the level of nerve regeneration and recovery, and use of ant-inflammatory agents such as TNF-α antagonist, anti-IL-6 antibody and steroids can be useful for regeneration and recovery after injury (Alsalihi et al., 2017). They also reported that etanercept reduced the proliferation and reaction of both astrocytes and microglia that are strongly associated with glial scar formation (Alsalihi et al., 2017, Johansson et al 1999). TNF-α that is secreted after injury can alert astrocytes chemically and physically (Abd-El-Basset 2013), thus the results of this chapter provide further evidence that supports Alsalihi et al's (2017) findings. The impact of systemic administration of etanercept in crushed sciatic nerve of rats on axonal regeneration was evaluated using GAP-43, an axonal regeneration marker (Seijffers et al 2007). Elevated GAP-43 expression was observed in both ipsilateral dorsal (site of sensory neuronal) and ventral (site of motor neuronal) spinal cord in etanercept group (Kato et al., 2010).

Although behavioural tests such as tactile (Von Frey test) or cold (cold plate test) sensitivity was not performed, this study focused on glial activation as a marker to detect potential development of neuropathic pain. Glial activation in PCL+Etanercept repairs was lower than PCL+Normal Saline repairs, with a significant difference in the dorsal horn, this may indicate that etanercept may be more beneficial towards sensory axons than motor. Interestingly M6P, reported in Chapter 4, may have the opposite effect (more beneficial towards motor axons than sensory).

5.5.2 The Effect of PCL and Etanercept on Nerve Regeneration

Most experimental studies have frequently used three methods for assessing nerve recovery, i.e. gait analysis, electrophysiological, and morphological analysis. Generally, obtaining results from more than one method provides a more accurate conclusion. For the present study, a combination of CatWalk gait, electrophysiology and axon counting and tracing analysis were performed.

5.5.2.1 CatWalk Gait System

The value of functional assessment is the ability to evaluate the impairment and recovery of functions following an intervention to repair a nerve injury. CatWalk gait analysis is one of the most popular gait analysis tools used in the assessment of functional recovery after nerve injury (Chen et al., 2017).

Deumens et al. (2007) demonstrated a variety of gait parameters that can be affected following nerve injury such as intensity, print area, stance duration and regularity index. Later they focused their work to examine these parameters and identify which of them is of particular interest to assess functional recovery following severed axon regeneration. In 2008, they concluded that intensity of paw print is of particular interest when evaluating the functional axon regeneration, because this parameter obtains full recovery 4 weeks following nerve crush injury - where the nerve is expected to fully recover to its previous level (Bozkurt et al., 2008).

5.5.2.1.i Intensity of the Paw Print

The intensity of the paw reflects the mean pressure applied by an individual paw during the contact with the glass surface of the CatWalk system, across the length of the walkway (Vrinten and Hamers, 2003). The more pressure that is applied, the larger area of paw-floor contact, leading to brighter pixel display. Measuring this parameter gives an indication of the ability of the animal to apply pressure using the affected limb. More pressure suggests less pain affected the paw and vice versa. As mentioned in section 6.4.3.1.i, PCL+Etanercept repairs had higher left hind paw print intensity parameter at all weeks compared to PCL+Normal Saline. These differences were significant at both week 2 and 3. At the end of the recovery period (week 5) both groups had similar percentages (58.4% and 52.3%) for (PCL+Etanercept and PCL+Normal saline, respectively). An interesting finding observed at week 4 in which the percentage of both groups declined and then started to increase, this may reflect the time point when re-innervation of the paw begins and thus there may be some degree of mechanical allodynia developing at this time point. Further studies would be required to assess this further (e.g. by testing mechanical sensitivity using Von Frey filaments).

5.5.2.1.ii Paw Print Area

The print area reflects the total surface area that was contacted during the stance phase by the paw (Vrinten and Hamers, 2003). Deumens et al. (2007), Bozkurt et al (2008) and Blackburn et al (2008) found that print area is a useful parameter that detects changes in recovery functions following transection of the sciatic nerve in rats. As mentioned in section 6.4.3.1.ii, PCL+Etanercept repairs had higher left hind paw print area parameter at all weeks compared to PCL+Normal Saline. These differences were significant at week 3.

When comparing the results of this study with a study by Ngeow et al (2011), it can be noted that the recovery of intensity parameter in the current study achieved around (60-65%) of normal values by week 5 and that is similar to that reported by Ngeow et al. (2011) (55-65%). However, the recovery of print area parameter in the

current study was higher (50-55%) compared with (20-25%) in their study. In addition, Ngeow et al. (2011) reported that the print area reached the lowest percentage at week 3 and then started to increase. While in the current study, print area reached the lowest percentage at week 4 and then started to increase. This may suggest that axons in the current study took a longer time to reach their end point than those in Ngeow et al's (2011). The differences seen in outcomes between Ngeow's and the current study may be due to the different methods used to repair the nerves.

Although CatWalk gait analysis was used in the current study to assess the functional recovery, it can also be used to assess neuropathic pain (Vrinten and Hamers, 2003). Mice with hyperalgesia will try to apply less pressure on the affected limb during runs. In the current study, PCL+Etanercept treated mice tended to increase the intensity, returning to 74% of normal by week 3. Then dropped to 60% by week 5. These percentage levels agree with those reported by Deumens et al. (2007), as they reported that the intensity was within the 50-60% range. This suggested that the mice in the current study probably did not suffer from hyperalgesia. In addition, no sign of autotomy was observed. A close-up investigation in weeks 4 and 5 in the current study may indicate that this declined may result from either delayed contraction of muscles supplied by the affected nerve or that the animal was trying to avoid using the affected limb due to the development of hyperalgesia (mechanical allodynia) (Ngeow et al., 2011, Vrinten and Hamers, 2003).

Vrinten and Hamers (2003) compared CatWalk gait as a novel method to assess mechanical allodynia with Von Frey testing. Von Frey is one of the most used methods to measure mechanical allodynia, a behavioural sign of neuropathic pain. Although Von Frey filaments have been shown to be reproducible and objective (Bell-Krotoski and Tomancik, 1987), there are some reported disadvantages. First, there are several possible ways to estimate and define mechanical withdrawal thresholds. Second, filaments wear off after several extensive uses. Third, the process takes a long time (Andrews, 1993, Moller et al., 1998). In contrast, use of CatWalk has many advantages such as it allows investigation of many parameters at the same time during a single run, the process takes short time and it may detect

small differences in mechanical behiviours that cannot be detected by Von Frey. The results of their study showed a strong correlation between CatWalk parameters (intensity) and Von Frey mechanical withdrawal thresholds. They concluded that CatWalk method might be an alternative to Von Frey in assessing the mechanical allodynia as it can be used for a variety of animals (Vrinten and Hamers, 2003).

Gait parameters can be affected by the speed of gait (Koopmans et al., 2005, Walker et al., 1994). In some previous studies on rats, reliable gait speed was achieved by training the rats for the purpose to make uninterrupted runs for two weeks (Bozkurt et al 2008, Deumens et al., 2007, Hamers et al., 2001). In contrast, other previous studies were successfully performed without training the mice (Neumann et al., 2009). These reports suggested that the speed of gait is unlikely to affect the overall obtained results. This supports the reliability of the results in this chapter, as the study was carried out without training the mice. Another factor that can affect the gait parameters is the animal's weight, which may increase or decrease over the recovery period, creating more or less pressure. The weights of the animals in both groups were fairly similar all over the current study (see section 5.4.2.1), negating any effect that could have occurred.

5.5.2.2 Electrophysiology

Electrophysiology analysis gives important indications about the functional recovery of regenerating axons. Two parameters were calculated in this chapter; CAPs and CVs.

5.5.2.2.i Compound Action Potential Modulus Ratio

A higher CAP modulus ratio is an indication of better regeneration, suggesting that a higher percentage of axons have crossed the repaired gap successfully and reached the distal stimulating electrodes. The results reported in the current chapter demonstrated that electrophysiological recordings were similar in both groups. In PCL+Etanercept group, the average CAP modulus ratio was 25.3%, indicating that a smaller CAP was evoked by stimulation distally to the injury site than the proximal site. Whereas, in PCL+Normal saline group, the average CAP modulus ratio was

20.3%, indicating lower CAP was evoked than those seen in PCL+Etanercept group. The low CAP ratios seen in both groups indicate that the neural functional recovery was not complete distally to the repair site, thus resulting in a fewer number of axons presented at the distal stimulation site. Ngeow et al. (2011b) compared the CAPs of uninjured controls and nerve repair groups, and reported that CAPs were always lower after repair. They concluded that this may result from a decrease in the size and/or number of regenerated axons that are presented at the distal nerve part, and these are well reported as a consequence of nerve injury and repair (Fisher et al., 1985, Sunderland, 1978).

It is of interest to note that Ngeow et al. (2011b) reported that the highest CAP ratio was 63% and the lowest was 13%, while in the current study the highest CAP was 37% and the lowest was 12% (in the successful repairs). The percentage of the highest CAP in the current study is within the middle of the range reported by Ngeow et al. (2011b), this indicates that repair with a PCL conduit produces regeneration approaching that seen using end-to-end anatomsis (as used in Ngeow's study). However, a specific study to compare conduit repair with end-to-end anastomosis is required in order to further validate this.

5.5.2.2.ii Conduction Velocity

Faster conduction velocities are achieved by better regeneration and larger axonal diameters. The results between the two groups were correlate to those reported in CAP, as the average conduction velocity of the fastest axons was higher in PCL+Etanercept repairs 0.31ms^{-1} compared to PCL+Normal saline 0.28ms^{-1}. These results are based on the response evoked by distal stimulating electrodes. The conduction velocity contains a combination of a large component (proximal to the site of repair) and a small regenerated component (distal to the site of repair). Moreover, it contains a mixture of sensory and motor fibres. Two drugs (etanercept and infliximab) have been widely used in animal and human studies. Norimoto et al. (2008) compared the intraperitoneal injection of these two drugs in sciatic nerve injury of rats, and reported that etanercept treated animals had faster conduction velocities in regenerated axons compared to infliximab treated animals.

In Al Salihi et al's (2017) study, mice treated with etanercept obtained better functional recovery in electrophysiological examination compared to control mice. Their findings were parallel to those reported by Bayrakli et al. (2012) that rabbits treated with etanercept had significant better electrophysiological recordings of somatosensory evoked potential compared to control group. However, the findings in the current study disagree with the previous studies as mice treated with etanercept showed no significant differences in both CAP ratios and conduction velocities compared to the control group.

In another study by Kato et al. (2010), etanercept was administrated intraperitoneally and local (epineurial space) at 0.3, 3.0 or 6.0mg/kg as a single dose immediately or at 0.3 and 3.0mg/kg as two dosages; 1 hour and 3 days postoperative. The assessment of functional recovery was evaluated using pinch test, and reported that administration of etanercept improved the rates of functional regeneration (Kato et al., 2010). The differences between the current study and Kato's study may relate to differences in the methods of injury and repair and route of administration of etanercept used.

To sum up, these findings suggested that etanercept has a minimum potential beneficial impact on nerve regeneration as assessed by electrophysiological methods.

5.5.2.3 Axon Counting and Tracing Analysis

Although no overall difference was observed between the two groups in terms of the visual appearance, PCL+Etanercept repair images appeared, in general, marginally better than PCL+Normal saline with axons more organised throughout the repair gap, especially at the proximal meeting (Figure 5.21).

5.5.2.3.i Sprouting Index Level

The first evidence that immediate application of etanercept improves the rate of regeneration following nerve injury was reported by Kato et al. (2010).

The results shown herein reported that sprouting index levels in PCL+Etanercept were lower than those of PCL+Normal saline for the entire nerve. An interesting finding was observed at 0.0mm interval in which the level of sprouting index of PCL-Normal saline was higher than the -0.5mm interval, indicating that axons in this group sprouted many branches during their regeneration. However, PCL+Etanercept group had a slightly higher CAP than PCL-Normal saline. Thus, when comparing sprouting index result with CAP results obtained using electrophysiology, it can be concluded that level of axon branching does not correlate with the level of axon regeneration. PCL+Etanercept repairs had lower sprouting index while higher CAP compared to PCL+Normal saline. This was previously reported by Atkins et al 2007 (see section 4.5.3.2), and is because electrophysiology only counts unique axons rather than the total number of axons (see section 5.5.2.3.ii).

Reid et al. (2013) compared a PCL conduit with nerve grafts in bridging a 10mm gap in the sciatic nerve of rats for an 18-week recovery period. Proximal and distal nerve sections were cut, and stained with Toluidine Blue in order to make the axons visible. A number of regenerated axons were then counted. They reported no significant differences in the number of axons between PCL and nerve graft in the distal section. Also, they counted the axons over the repair area and reported that both groups had a similar number (Reid et al., 2013). The same team also reported that axons could cross a 10mm gap in rats using PCL conduit within a 2-week recovery period. This indicates that PCL is a promising material for conduits in peripheral nerve regeneration (Sun et al., 2010).

5.5.2.3.ii Axon Tracing

It has been reported that etanercept can increase the percentage that axons could regenerate into the repair, and encourage them to find suitable pathways along the repair quicker than those in the control group. This was expected to cause an increase in the proportion of unique axons at the 5.0mm (final) interval in PCL+Etanercept repairs compared to PCL+normal saline repairs, as more unique axons will manage to navigate into the distal nerve ending within the recovery period.

The percentages of unique axons from the start interval represented at each 0.5mm internal were higher (though not significant) at all intervals in PCL+Etanercept repairs compared to PCL+Normal saline repairs, except at 0.5mm interval where the percentage was significantly higher in PCL+Etanercept repairs (Figure 5.24). Only 27.1% of axons presented at the 0.0mm interval reached the 5.0mm interval in PCL+ Etanercept group compared to 24.33% in PCL+Normal saline group. As with the previous chapter (see sections 4.3.2.2.ii), the majority of axon loss happened within the initial 1.5mm of the repair, with the largest amount observed between the 0.0mm and the 0.5mm intervals. The large drop in sprouting index level for PCL+Etanercept and PCL+Normal saline (approximately 52% and 47%, respectively) was observed between 0.0mm and 0.5 intervals, and the large drop in unique axons in both groups was observed at 0.5mm interval. The relationship between sprouting index level and number of unique axon is expected, as reduction in the general number of axons at an interval could affect both unique and duplicate regenerate axons equally. This relationship matches the relationship reported in two previous studies (Harding et al., 2014, Pateman et al., 2015). However, they found that the large drop in sprouting index level was observed at 1.5mm interval and in unique axon at 1.0mm interval, this may be because the interval marking is subjective regarding the placement of the 0.0mm interval.

Several factors may have an impact on these proportions, e.g. the pruning of excess axon sprouts would raise overall axon loss without influencing unique axon loss. Although potential for preferential regeneration of some axon subsets may increase or decrease unique axon loss, this depends on whether those axon subsets demonstrate increased or decreased levels of sprouting. These possibilities were beyond the scope of the current study.

It is of interest to note that when comparing the percentages of unique axons at 5.0mm interval with the CAP, both methods of assessment of regeneration gave similar results (axon tracing 27.1% and CAP 25.3%). Providing evidence that there is a good correlation between the two methods of assessment.

5.5.2.3.iii Axon Disruption

It had been anticipated that etanercept would have a positive impact on axon disruption through its role in local scar tissue reduction at the two nerve ends. This hypothesis was based on the evidence that etanercept can decrease the level of local inflammation (Chan et al., 2000, Khan et al., 2005) – as reduction of local inflammation is strongly linked to reduced intraneural scarring (Atkins et al., 2007). In addition, reduction of inflammation helps to decrease dermal tissue scarring through reduction of fibroblast proliferation and production of collagen (Daly and Weston, 1986, Ogawa et al., 1998).

The level of axon disruption was significantly reduced in PCL+Etanercept, approximately 5% lower in PCL+Etanercept than PCL+Normal saline repairs (Figure 5.26). As appeared from Figure 5.23, the region of disrupted axons at the proximal to the repair was smaller in PCL+Etanercept compared to PCL+Normal saline repairs.

5.5.3 Technical Failures

As mentioned previously, some repairs were excluded from the study as the proximal and distal nerve endings were found to be disconnected from the conduit. This may suggest some reasons behind these failures. First, the performance of the fibrin glue was not optimum. In addition, the solution of etanercept/vehicle may decrease and weak the consistency of the fibrin glue. Second, the sciatic is a large nerve and it seems to be difficult to be secured by fibrin glue alone. Thus, using fibrin glue reinforced with sutures may work better. Cruz et al. (1986) reported that following transected sciatic nerve repairs in rats using fibrin glue alone, dehiscence happened in 80% of nerves. While when using fibrin glue reinforced with two-suture, gave better outcomes but increased the inflammatory reaction. It is believed that the inflammatory reaction probably occurred due to the commercial thrombin that used to form the fibrin glue Cruz et al. (1986). Third, the two nerve ends were secured inside the conduit into 0.5mm depth. Moreover, it was observed that the two ends of the sciatic nerve were retracted even when they were secured by fibrin glue by approximately 1.0mm, creating a larger gap (5.00mm). This may indicate that the two nerve sends were easily dislocated from the conduit, suggesting that it is better to use conduits with 6.0mm length (to achieve a 4.0mm gap) and therefore secure each nerve end into1.0mm depth inside the conduit.

5.6 CONCLUSION

This study investigated the ability of PCL conduits with the addition of etanercept to enhance the peripheral nerve regeneration. It demonstrated that local administration of etanercept appears to reduce glial (microglial and astrocyte) activation - indicating reduced potential for neuropathic pain development - and enhance functional recovery of the nerve when compared to controls. In the cases where the junction between the nerve ends and the PCL conduit remained intact, the conduits supported axonal regeneration across a 4.0mm defect, and provides evidence that PCL conduits produced via the µSL manufacturing technique used in this study have potential to be used as an alternative to autograft in a larger nerve defects.

The number of failed repairs was unexpected as fibrin glue showed acceptable results in our previous studies of conduit repair to the common fibular nerve. This may suggest that in large nerves (e.g. sciatic nerve) fibrin glue alone is not enough to secure the two ends on the nerve inside conduits. Electrophysiology and CatWalk gait system analysis were used in this study in order to investigate the functional recovery of sciatic nerve as more muscles are affected than those of CF nerve. Further studies are underway to compare regeneration of sciatic nerve following graft and PCL conduit repairs.

CHAPTER 6

A NOVEL 3D-PRINTED POLY-GLYCEROL SEBACATE METHACRYLATE *IN VIVO* STUDY

SUMMARY

The study in this chapter was performed to evaluate the ability of an alternative and suturable Poly-Glycerol Sebacate (PGS) NGC to support *in vivo* nerve regeneration and compare it to nerve graft repair. The performance of the PGS NGCs was expected to be similar to that seen for graft repairs in that they would facilitate nerve regeneration. A novel formation, containing methacrylate moieties (PGSm), was used to enable to create 3D structures. The immunohistochemistry was performed to investigate glial activation, while axon tracing and counting analysis was performed to assess nerve regeneration. PGS materials showed excellent outcomes in both *in vitro* and *ex vitro* studies. The results of the *in vivo* analysis showed that PGS conduits supported regeneration and directed axonal growth. They also showed a low level of glial activation, suggesting a low potential for the development of neuropathic pain. However, sprouting index and axon tracing data demonstrate that nerve graft was better than the PGS conduit. More optimal conduit designs should be explored to determine the true potential of NP-PGS conduits.

6.1 INTRODUCTION

As mentioned in chapter 1 (section 1.8), the artificial nerve guide conduit is a potential alternative to nerve graft repair. In case that conduits can produce equivalent outcomes compared to the nerve grafts over any distance in any nerve, they would likely become the "gold standard" repair for bridging nerve gap defects as they do not include the problems caused by using nerve graft (see section 3.1). A number of different materials have been investigated in nerve guide studies with different levels of accomplishment. The material for the conduits used in this study was Poly-Glycerol Sebacate (PGS), a synthetic bioresorbable polymer that is currently attracting a great deal of attention in this area (Rai et al., 2013). This material was chosen because it has similar mechanical properties to those of nerve tissue and has potential for novel devices for nerve repair. In addition, the material seems to be more suitable for longer gap nerve repairs as it is suturable. Thus, the two nerve ends can be secured inside the conduit using sutures with/without fibrin glue, avoiding the failures reported in chapter 5 when using fibrin glue alone. PGS has been explored through several biomedical applications, ranging in form from stiff to soft. It was initially synthesized as a ratio of 2:3 (glycerol, sebacic acid) in a polycondensation reaction, forming a rigid form of PGS (Nagata et al., 1999). Following that, a ratio of 1:1 was used with thermal curing, forming a more flexible form of PGS (Wang et al 2002). Later, a second step of thermal curing was performed to form a 3D shaped form, and modified the PGS prepolymer by acrylate moieties, forming PGSa (Nijst et al., 2006).

Legnani et al. (2006) reported that sebacic acid copolymer was FDA approved for use as controlled drug delivery matrices. A wide range of uses for this material were explored for neural repair (Sundback et al., 2005), tympanic perforation (Sundback et al., 2012), retinal transplantation (Pritchard et al., 2010), and cardiac patches (Rai et al., 2013). The results of an *in vitro* study by Sundback et al. (2005) reported that PGS had no negative impact on Schwann cell metabolic activity, proliferation, or attachment, and did not induce apoptosis. These outcomes were superior to that of polylactide-co-glycolide (PLGA), a polymer commonly used for nerve guide conduits. Regarding the *in vivo* results of the same study, PGS provoked a minimal tissue response and no toxicity was reported. Although a flat sheet scaffold was used in the

in vivo test rather than a 3D structure, they suggested that PGS is an excellent potential material to create nerve guide conduits (Sundback et al., 2005).

In the current study a novel formulation, containing methacrylate moieties, of PGS was used. This formation allows a photocurable form of PGS (PGSm) to be formed. The use of this method enables the material to be 3D printed creating NGCs using microstereolithography (μSL). Two types of PGS NGCs were used in the study; non-porous PGS and porous PGS. The non-porous PGS (NP-PGS) conduits were formed as a hollow tube, while the porous PGS (P-PGS) conduits include multiple longitudinal channels (foam) (Figure 6.1A and B). The porous surface has some gaps within it allowing liquid to soak into it, whereas non-porous surface does not absorb liquid. Gerecht et al (2007) investigated the use of P-PGS materials and they suggested that it is useful to support the neural growth due to its porosity, mass loss, swelling, toxicity and mechanical properties. The same study also reported that NP-PGS can be used for neural growth as it has similar biocompatibility profiles as P-PGS (Gerecht et al., 2007).

Some studies have investigated the general abilities of PGS materials; however, their likely impact on nerve regeneration and neuropathic pain as a nerve guide conduit has not been investigated.

6.2 AIM OF THIS STUDY

The aim of the study performed in this chapter was to investigate the ability of an alternative and suturable PGS NGC to support *in vivo* nerve regeneration. In addition to investigate its effect on the glial activation, and compare them to nerve graft repair. The performance of the PGS NGCs was expected to be similar to that seen for graft repairs in that they would facilitate nerve regeneration.

6.3 MATERIAL AND METHODS

The protocol for this study was based on previous work performed in our laboratory at the University of Sheffield, and has been described in Chapter 2. Additional specific information involved in the present study is described below.

All conduits used in the current study were provided by Dharaminder Singh from the laboratories of Dr. Frederik Claeyssens and Prof. John Haycock, Kroto Research Institute, University of Sheffield. All PGS conduits were created using the µSL technique, but with different shapes and surface designs (Figure 6.1A and B).

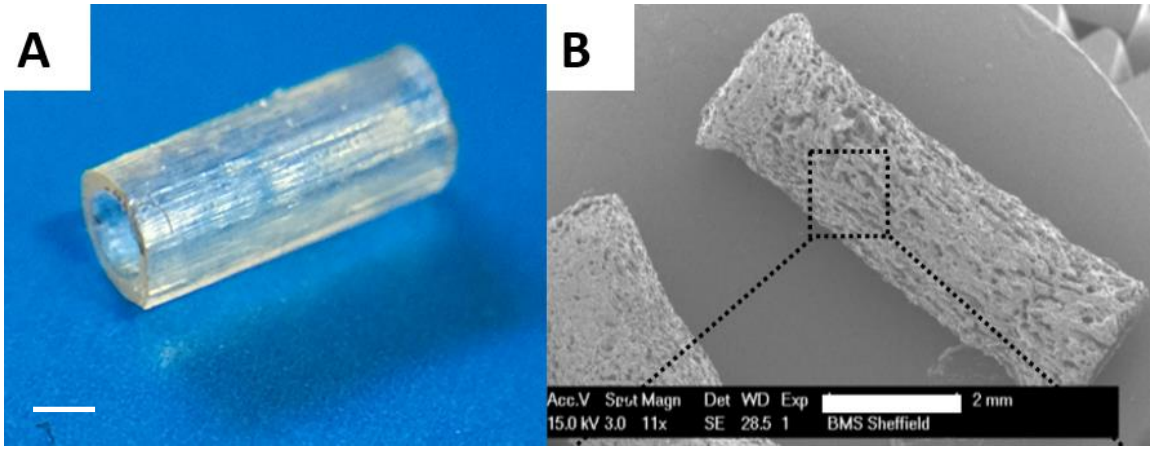

Figure 6.1: A) Non-porous PGS conduit (hollow tube). B) Porous PGS conduit (foam) (Provided by Dharaminder Singh). Scale bar = 1.0mm

6.3.1 Animal Numbers and Groups

24 mice aged between 12 and 18 weeks were used in the study: 18 *thy-1-YFP-H* mice on a C57BL6 background and 6 wild type mice and were divided into 3 experimental groups: mice treated with P-PGS conduit (n=6), mice treated with NP-PGS conduit (n=6), and mice treated nerve graft (n=6) obtained from the wild type mice (n=6) (Figure 6.2).

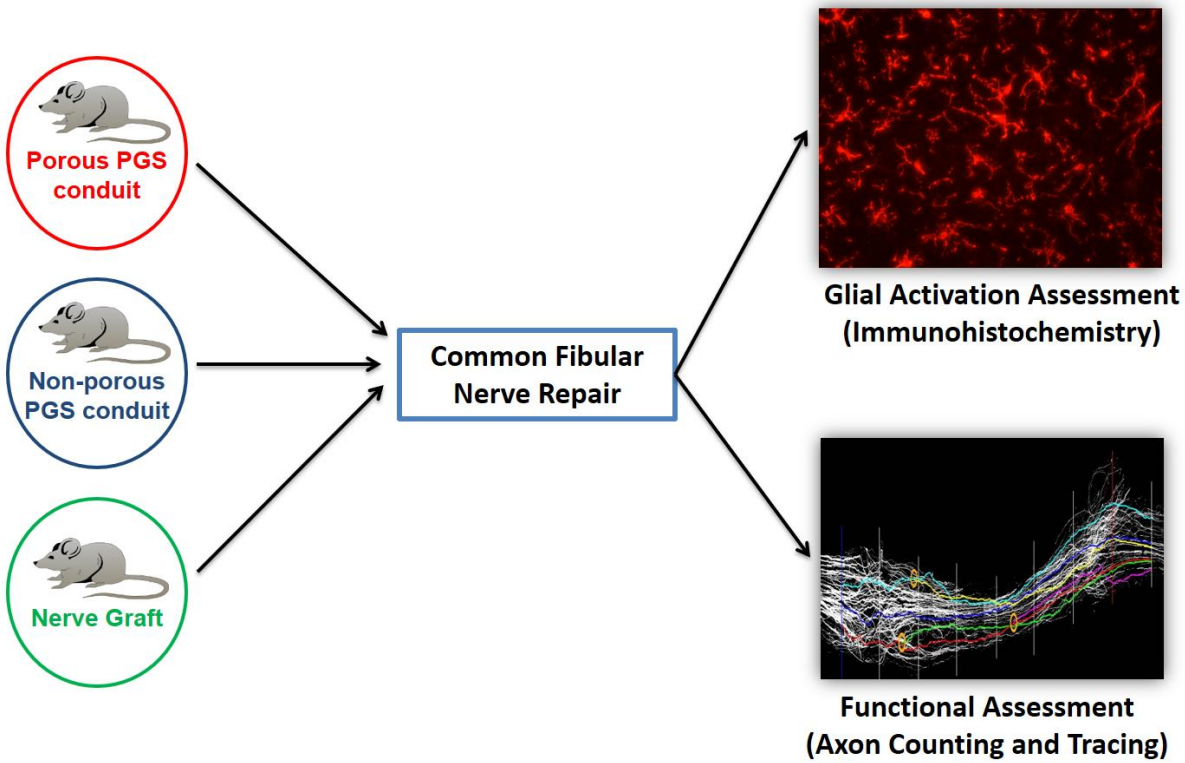

Figure 6.2: Summery of materials and methods for the investigation of the conduits/grafts.

6.3.2 Experimental Methods

6.3.2.1 Implantation of Nerve Guide Conduits

YFP-H mice were anaesthetised (see section 2.2.3.1.i) and the common fibula nerve exposed, transected, and a 3.0mm gap was made (see section 2.2.3.1.ii) and repaired using either NP-PGS or P-PGS conduits. In PGS non-porous repairs, both the proximal and distal nerve ends were secured by fibrin glue to a depth of 1.0mm into the conduit, leaving a 3.0mm gap between them (see section 2.2.3.1.iv) (Figure 6.3A). In PGS porous repair, both the proximal and distal nerve ends were secured by fibrin glue to the two side of the conduit (Figure 6.3B).

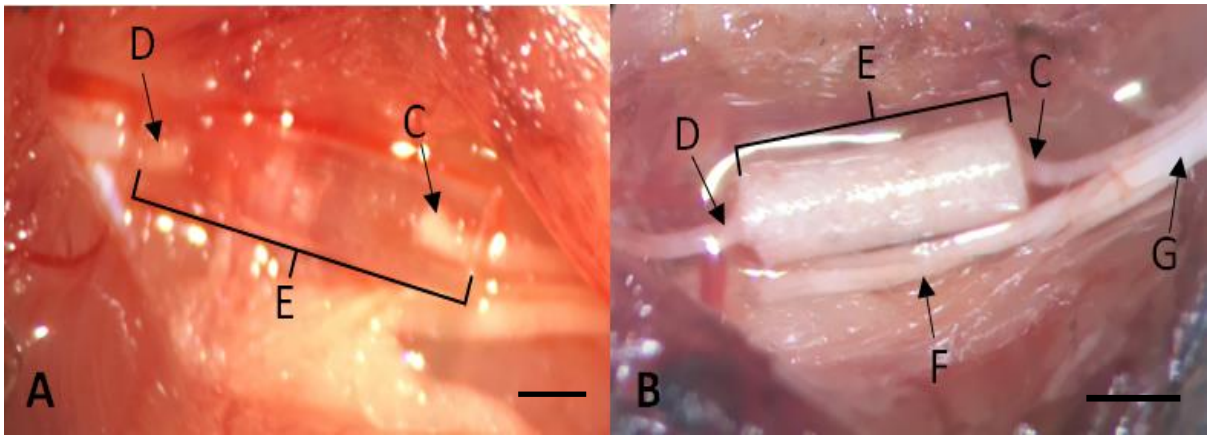

Figure 6.3: Common fibular nerve after two conduit repairs. A) Repair using 5mm PGS non-porous conduit showing the two nerve ends. B) Repair using 3.0mm PGS porous conduit showing the two nerve ends. C) The proximal stump. D) The distal stump. E) The conduit. F) The tibial nerve. G) The sciatic nerve. Scale bar= 1.0mm.

6.3.2.2 Implantation of Nerve Graft

Wild type mice were anaesthetised (see section 2.2.3.2.i) and the common fibular nerve exposed, freed from the surrounding tissues, and then re-covered to keep it healthy. YFP-H mice were anaesthetised (see section 2.2.3.1.i), and placed beside the wild type. The common fibular nerve was exposed, and prepared for receiving the nerve graft. A nerve graft of 3.0 mm was obtained from the wild type mouse and placed next to the CF nerve on the YFP-H mouse. The CF nerve of the YFP-H mouse was transected, and a gap of approximately 3.0 mm made (see section 2.2.3.1.ii). A 5.0mm silicon trough was then places underneath the two ends and the gap was then bridged by the graft obtained nerve from the wild type (see section 2.2.3.1.iii). The nerve ends and graft were then aligned and secured by fibrin glue as in chapter 4 (Figure 4.2).

Animals were allowed to recover for 21 days to allow regenerating nerve to regenerate sufficiently to remain intact during harvesting. Following the recovery period, animals were anaesthetised (see section 2.2.3.2.i), the CF nerves and spinal cords were harvested (see sections 2.2.3.2.ii) and prepared for analysis using fluorescence microscopy (CF nerve) and immunohistochemistry (spinal cords) (see sections 2.2.4). Immunohistochemical labelling and axon counting and tracing analysis were quantified as described in Chapter 2. In all cases, analysis was carried out blind.

6.3.3 Image Acquisition of PGS Non-Porous Conduit

The image acquisition of the NP-PGS conduit (a hollow tube) was described in chapter 2. The method was different for the P-PGS, as because the conduit is multichannel rather than a hollow tube it is not possible to extract the nerve intact for imaging. The OCT embedded nerve tissues within P-PGS conduits were mounted in a cryostat (Microm HM 560, Zeiss, UK), transverse and vertical sections (15µm thick) were collected for the entire tissue including the conduit. The collected sectioned were placed on glass slides (3-4 sections per slide). Because the nerves were extracted from YFP mice, no further staining was needed. All slides were coverslipped with Vectashield® (Vector Lab, Burlingame, CA, US), and examined using fluorescent microscopy to detect any axons presented at proximal and distal nerve ends as well as through the conduit.

6.3.4 Sample Size Calculation

The sample size for this chapter were calculated using both PiFace software [v1.76: *homepage.stat.uiowa.edu/~rlenth/Power*] (for axon tracing) and Biomath software [Source: G.W. Snedecor & W.G. Cochran. *http://www.biomath.info/power/ttest.htm*] (for axon disruption) with standard deviation (SD) data obtained from a previous study by Harding et al. (2014) in our laboratory. The sample size chosen for the study was n=7, which would be sufficient to detect differences between groups of 15.65% and 7.89 for axon tracing [Figure 6.4] and axon disruption [Figure 6.5], respectively**.**

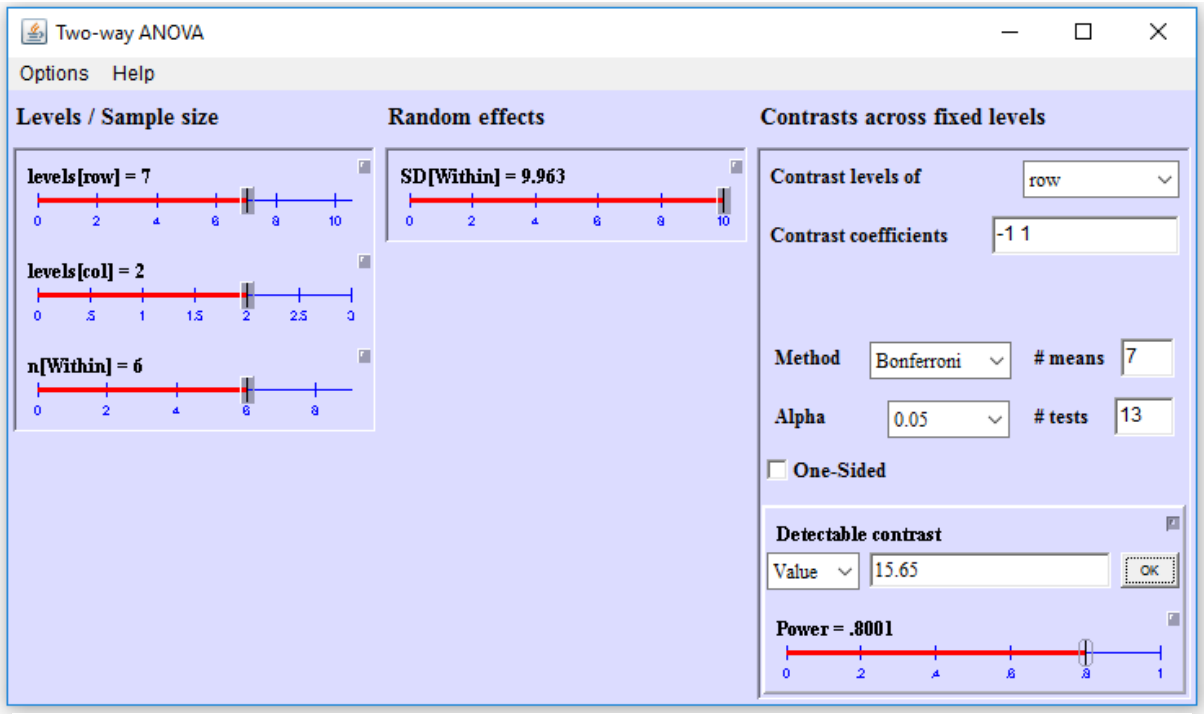

Figure 6.4: Axon tracing analysis of power calculation for a sample size of 6 animals in each group. Levels[row] = number of intervals; levels[col] = number of groups; n[Within] = sample size; SD[Within] = standard deviation value. Number of intervals [# means] multiplied by number of repair groups minus one gives the number of t-tests required for the Bonferroni's multiple comparisons test [# tests].

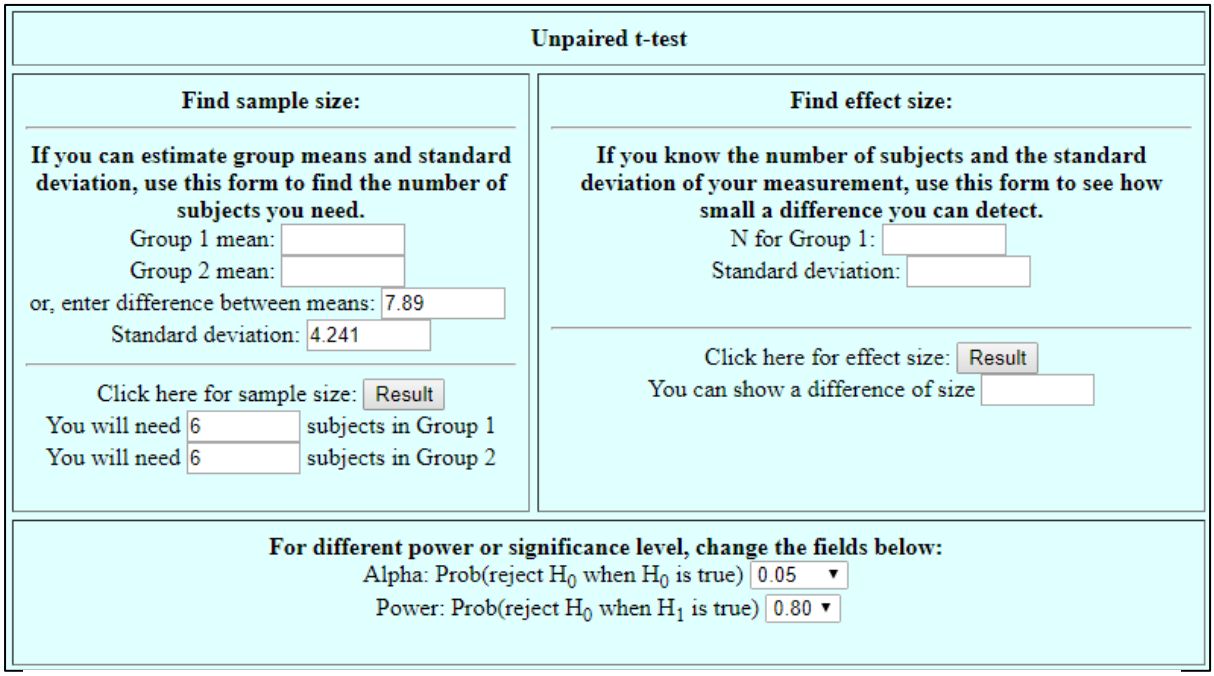

Figure 6.5: Axon disruption analysis of power calculation for a sample size of 6 animals in each group.

6.3.5 Statistical Analysis

6.3.5.1 Statistical Analysis of Glial Activation at Spinal Cord

Statistical comparisons between groups were carried out as stated in section 2.3.7.1. All glial activation results used a 1-way ANOVA with Bonferroni's multiple comparisons test. Differences were considered to be significant when $p<0.05$.

6.3.5.2 Statistical Analysis of the Nerves

For sprouting index and axon tracing results a 2-way ANOVA with Bonferroni's multiple comparisons test was used, while for axon disruption results an unpaired t-test (two-tailed) was used, in order to detect overall and individual intervals differences between the experimental groups.

All statistical analysis was performed using GraphPad Prism 7 software (GraphPad Prism Inc, CA, USA). Differences were considered to be significant at a *p* value below 0.05.

6.4 RESULTS

The results in the present chapter were obtained from *in vitro, ex vivo and in vivo* studies. *In vitro* and *ex vivo* analysis were carried out by Dharaminder Singh, while *in vivo* analysis was performed by myself. So, all results related to *in vitro* and *ex vitro* were provided by Dharaminder Singh. Two methods were used for *in vivo* analysis: immunohistochemistry of the spinal cord and axon counting and tracing analysis of the nerve. The immunohistochemistry was performed to investigate the spinal glial activation which acts as a potential indication of the development of neuropathic pain, while axon counting and tracing analysis was performed to assess nerve regeneration.

6.4.1 *In vitro* Neuronal and Schwann Cell Result

In vitro analysis was performed on a flat disk of PGS (with variable degrees of methacrylation) and a glass control. Live/dead neuronal results demonstrated a high percentage of live cells in all samples (Figure 6.8A). PGS samples had a significantly

higher percentages of live cells on day 4 (93% vs 78% [glass control; $p<0.001$]) and day 6 (90% vs 72% [glass control; $p<0.001$]), suggesting that cells were able to proliferate on the PGS polymer surface.

Neurite outgrowth length was compared between PGS materials and glass controls (Figure 6.8B). PGS samples had slightly lower neurite length than glass control on day 4 (55% vs 59% [glass control; $p>0.05$]), and was slightly higher on day 6 (74% vs 61% [glass control; $p<0.05$]), suggesting that the neurites were able to growth and extend with time. This concludes that PGS materials are permissive for neuronal differentiation.

The results of Schwann cell live/dead assays indicated a very high percentage of live cells on both PGS and glass scaffolds on days 4 (91% vs 94% [glass control; $p>0.05$]) and day 6 (92% vs 90% [glass control; $p>0.05$]) (Figure 6.8C and D). This suggested no increase in Schwann cell toxicity when comparing the PGS disk with the glass control.

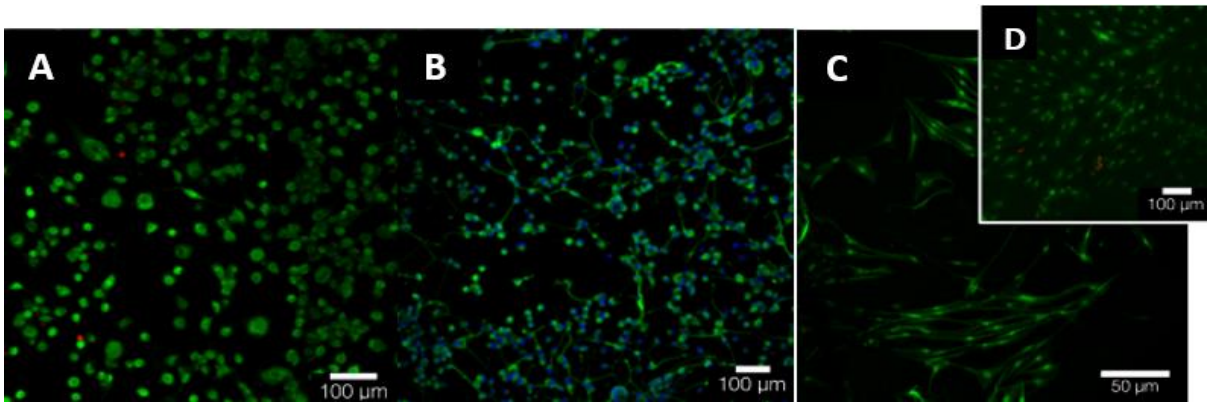

Figure 6.8: A) Neuronal live/dead staining showing the living cells (green) and dead cells (red). B) Neurite length staining showing neurite length (green) and nucleus (blue). C&D) Schwann cell live/dead staining showing the living cells (green) and dead cells (red) (Provided by Dharaminder Singh).

6.4.2 *Ex vivo* Result

PGS in a hemi-tube shape was used to seed dorsal root ganglions (DRGs) which were maintained in culture for 3 weeks. Anti S100β polyclonal antibody, Anti β-III-tubulin antibody and DAPI were used to immunohistochemically label the hemi-tube. Images of DRGs were acquired with z-stack sections through the hemi-tube, and then merged together into single images, showing a complete image of DRG within the hemi-tube. Along the topographical conduit cues, neurite outgrowth and alignment were analysed. Three zones were mapped on the neurites; zone one was the adjacent zone to the DRG body, zone two was the farthest zone from the DRG body, and zone three presented the wall of the conduit. Zone three was the only zone that did not have topographical grooves, so the neurite alignment was poorest on this zone (Figure 6.9). High number Neurite alignment was high in zone two although it was farthest from the DRG.

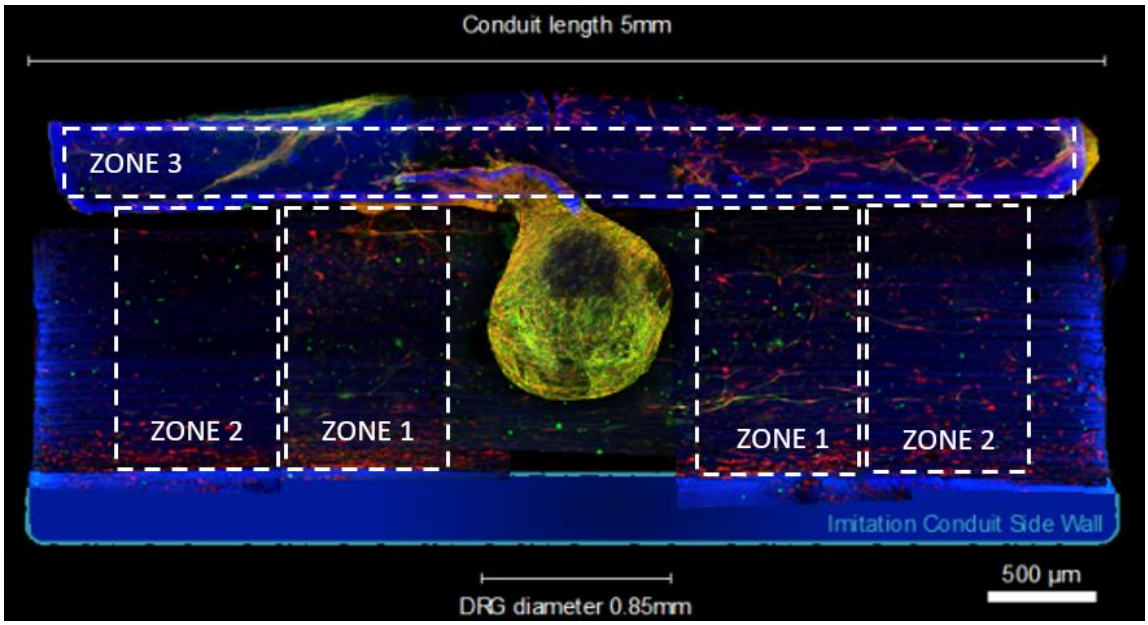

Figure 6.9: The body of DRG attached to the hemi-tube NGC with the neurite outgrowth and migration of the Schwann cell in the three zones (Provided by Dharaminder Singh).

6.4.3 *In vivo* Result

All animals recovered well from the recovery procedure without any sign of infection or autotomy. After harvesting, two mice treated with NP-PGS repairs were excluded from the final analysis, as the proximal and distal nerve endings were found to be disconnected from each other.

6.4.3.1 Assessment of Glial Activation

6.4.3.1.i Qualitative Observations of Spinal Cord

Glial activation was apparent in the injured side for all repair groups. The activation was high in the P-PGS group, where amoeboid glia were observed (Figure 6.10A). The level of activation was minimal in both NP-PGS and graft groups, but a number of hypertrophied glia were observed in these groups (Figure 6.10B and C).

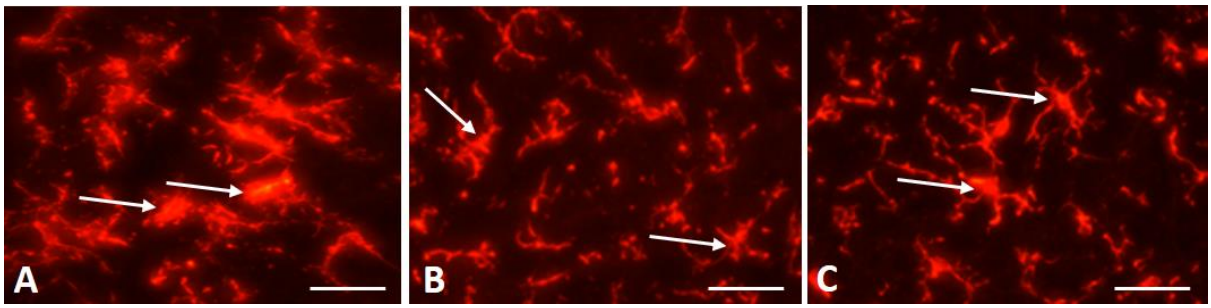

Figure 6.10: Sections of spinal cord after Immunohistochemistry staining with antibody Iba-1 showing different morphological phenotypes of microglial cells. A) PGS porous group showing amoeboid microglia. B) PGS non-porous and C) graft groups showing hypertrophied microglia. Scale bar = 0.1mm.

6.4.3.1.ii Quantitative Analysis of Spinal Cord

As described in section 2.2.8.1(A), the percentage area of labelling for Iba-1 and GFAP was calculated in defined regions of the dorsal and ventral horns of the spinal cord both ipsilaterally and contralaterally to the nerve repair.

A. Quantification of Iba-1 Expression

Quantification of labelling for microglial activation within the three groups demonstrates that the P-PGS group had significantly higher levels than nerve graft group in both ipsilateral dorsal (9.8% vs 7.7% [$p<0.01$]) and ventral (7.5% vs 5.3% [$p<0.05$]), while slightly higher compared to NP-PGS in both dorsal (8.6%) and ventral (5.4%) horns (Table 6.1 & Figure 6.14). NP-PGS group had similar levels of labelling in both the ipsilateral dorsal and ventral horns compared with the nerve graft group; there were no significant differences in labelling between these two groups (refer to Table 6.1 & Figure 6.14). In the corresponding contralateral side, the percentage area of Iba-1 labelling in the dorsal and ventral horns were similar in all groups (refer to Table 6.1 & Figure 6.14). The activation areas of Iba-1 in each group are shown in Figures 6.11-6.13.

Porous PGS Conduit

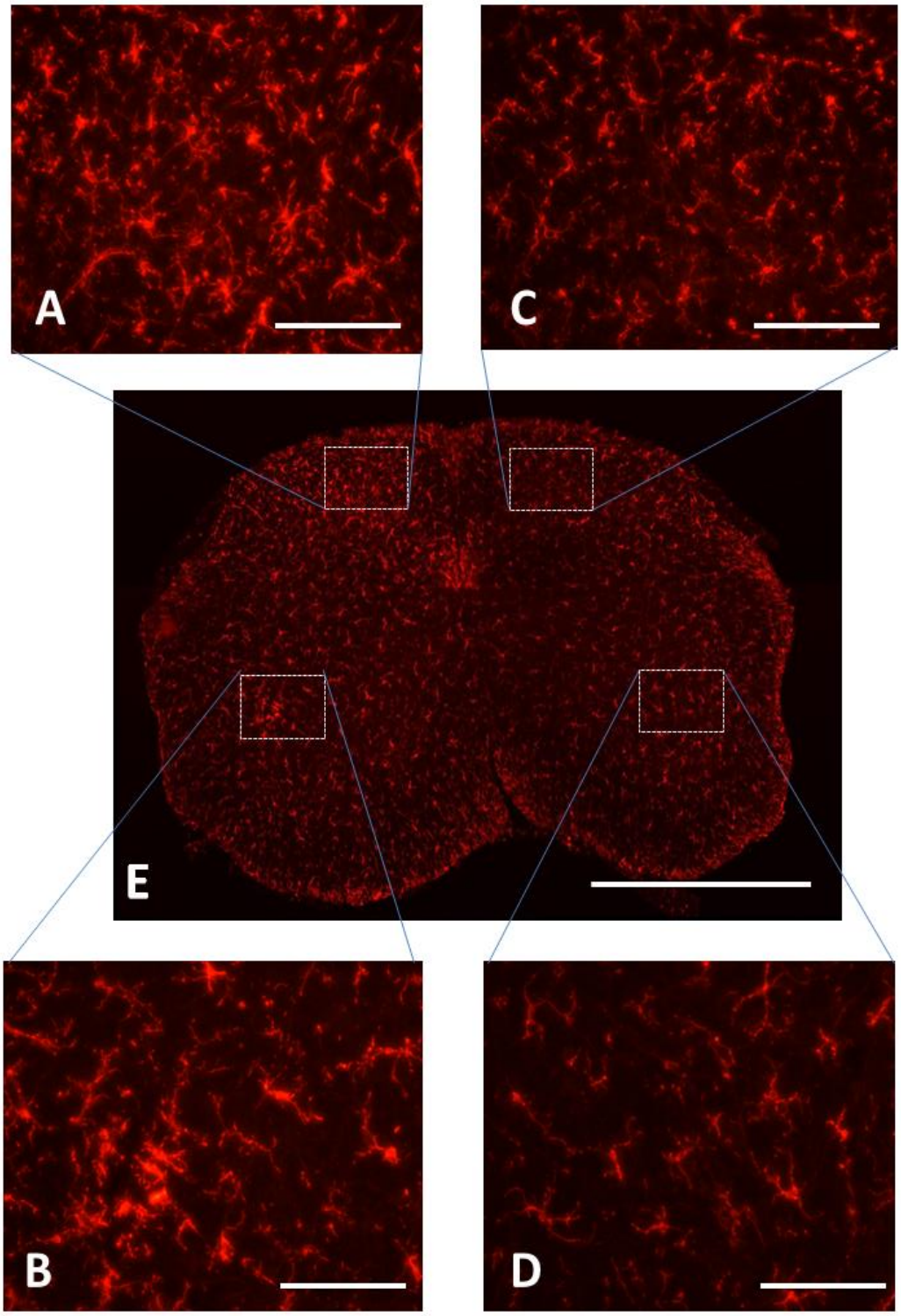

Figure 6.11: A section of spinal cord following repair with a porous PGS conduit shows microglial activation (E using 5x magnification). A) Ipsilateral dorsal horn, B) Ipsilateral ventral horn. C) Contralateral dorsal horn. D) Contralateral Ventral horn (A,B,C,D using 40x magnification). Scale bar A,B,C and D = 0.1mm, E = 1.0mm.

Non-porous PGS Conduit

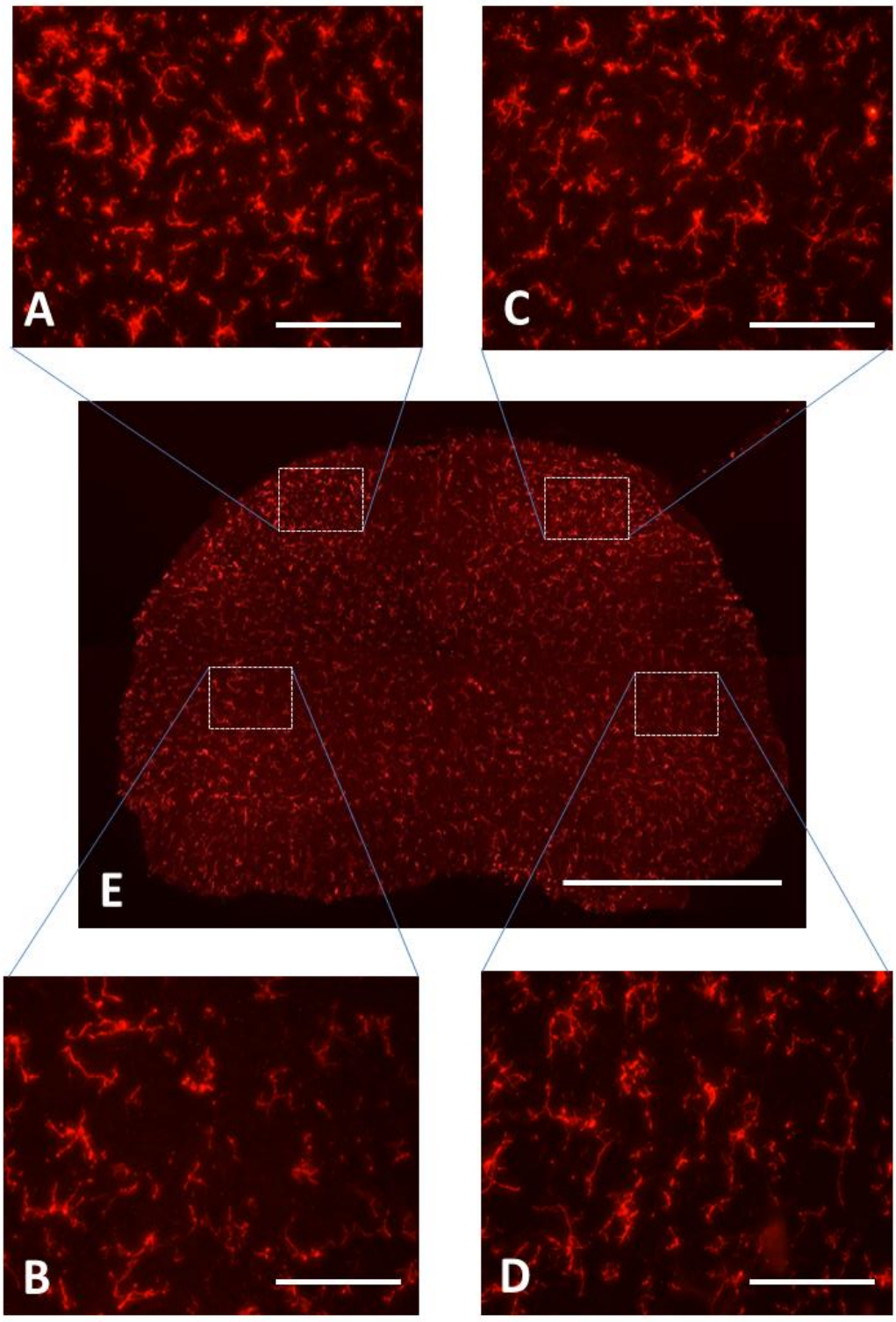

Figure 6.12: A section of spinal cord following repair with a non-porous PGS conduit shows microglial activation (E using 5x magnification). A) Ipsilateral dorsal horn, B) Ipsilateral ventral horn. C) Contralateral dorsal horn. D) Contralateral Ventral horn (A,B,C,D using 40x magnification). Scale bar A,B,C and D = 0.1mm, E = 1.0mm.

Nerve Graft

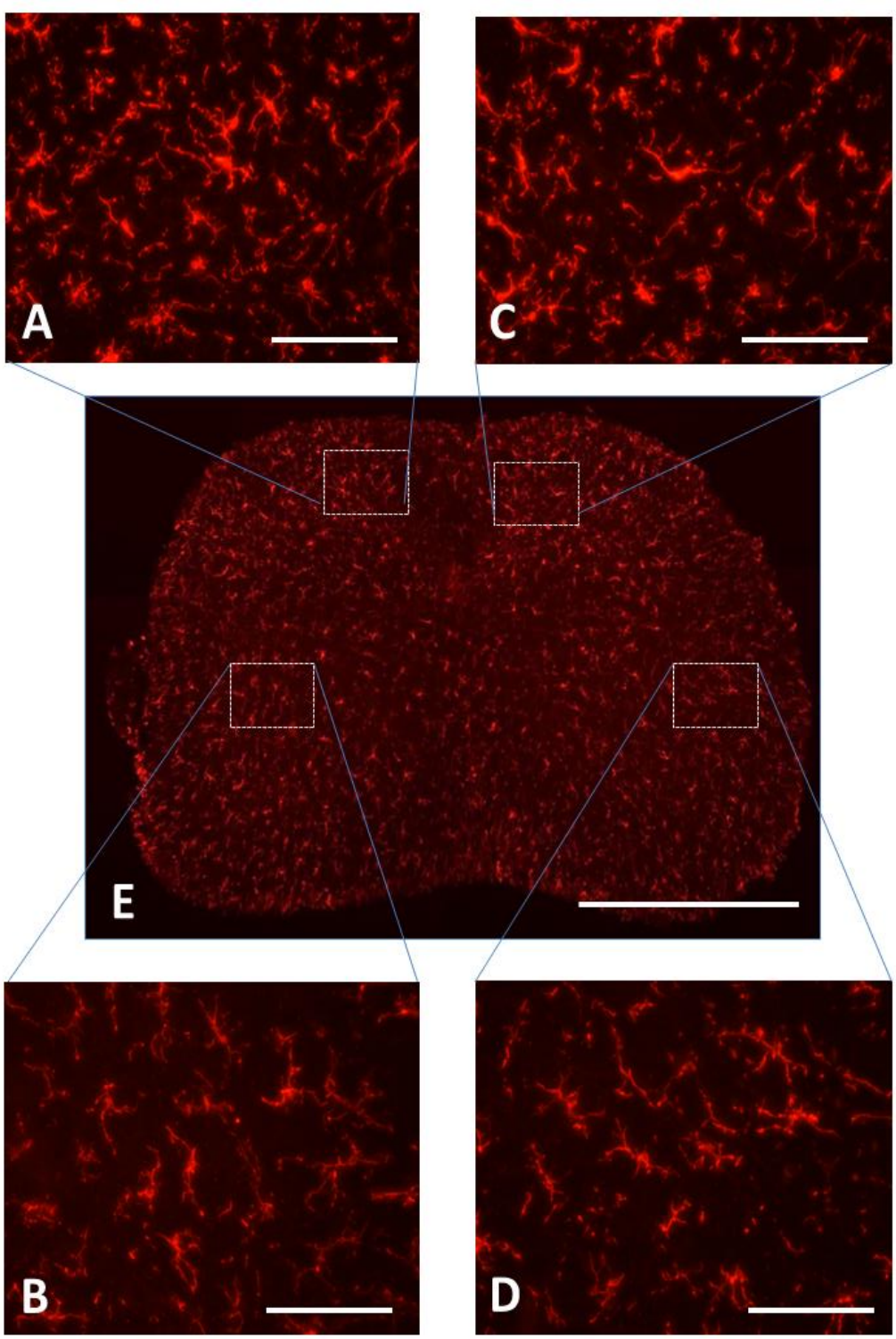

Figure 6.13: A section of spinal cord following repair with nerve graft shows microglial activation (E using 5x magnification). A. Ipsilateral dorsal horn, B. Ipsilateral ventral horn. C. Contralateral dorsal horn. D. Contralateral Ventral horn (A,B,C,D using 40x magnification). Scale bar A,B,C and D = 0.1mm, E = 1.0mm.

The mean percentage area of Iba-1 labelling (indication of the degree of microglial activation) for each group is shown in Table 6.1. The same data and the statistical comparison between the groups is illustrated in Figure 6.14.

Table 6.1: Percentages of microglial activation in P-PGS, NP-PGS and nerve graft groups activation in all groups.

IBA-1 (Microglia)%	P-PGS	NP-PGS	Nerve Graft
Ipsilateral Ventral horn	9.8	8.6	7.7
Contralateral Ventral horn	6.4	6.6	6.0
Ipsilateral Dorsal horn	7.5	5.4	5.3
Contralateral Dorsal horn	4.7	4.1	4.1

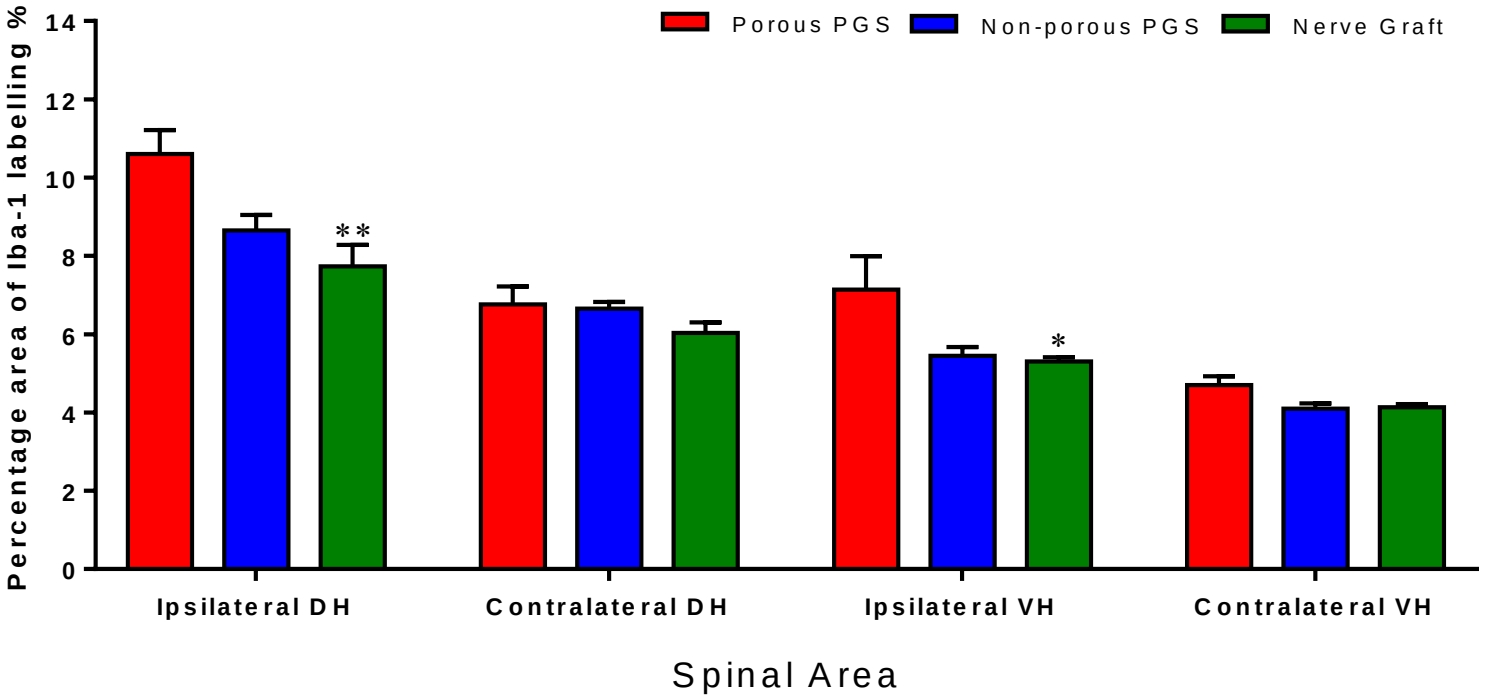

Figure 6.14: Immunohistochemical analysis of microglia for porous PGS conduit, non-porous PGS conduit and nerve graft groups. * and ** denote significant difference compared to PGS porous conduit, $p<0.05$ and $p<0.01$ respectively. Error bars denote SEM. Statistical test: 1-way ANOVA with Bonferroni's multiple comparisons test. DH= Dorsal horn VH= Ventral horn.

As described in section 2.2.8.1(B), some variation in the background staining was noted. Thus, percentage increase of the ipsilateral (injured) side over the contralateral (uninjured) side, ‘‘staining ratio’’ was performed. Comparisons between the groups when assessing the staining gave similar results to those described above. The increase in staining (Ipsilateral/Contralateral) ratio for Iba-1 in the P-PGS group was significantly higher than in other groups in dorsal horn (58.2% vs 30.0% [NP-PGS; $p<0.05$] and 27.7% [nerve graft; $p<0.01$]). In the ventral horn, P-PGS group had a lightly higher percentage increased than in other groups (49.9% vs 32.9% [NP-PGS; $p>0.05$] and 28.3% [nerve graft; $p>0.05$]) horns. There were no significant differences in labelling between NP-PGS and nerve graft groups (Figure 6.15).

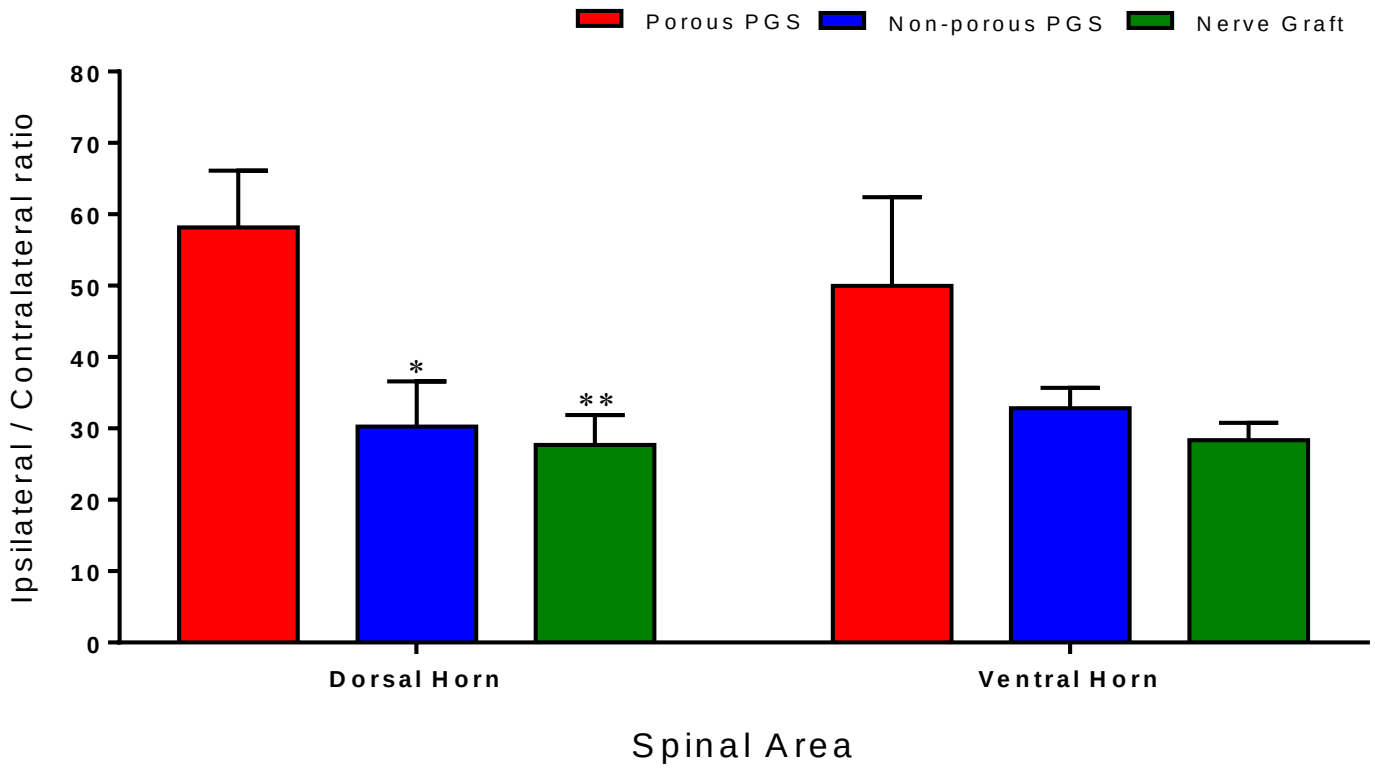

Figure 6.15: Ipsilateral/Contralateral ratio of microglia shows the difference of percentage increase in the ipsilateral side over the contralateral side in dorsal and ventral horns of the spinal cord for porous PGS conduit, non-porous PGS conduits and nerve graft groups. * and ** denote significant difference compared to PGS porous conduit, $p<0.05$ and $p<0.01$ respectively. Error bars denote SEM. Statistical test: 1-way ANOVA with Bonferroni's multiple comparisons test.

B. Quantification of GFAP Expression

Quantification of labelling for astrocyte activation within the three groups demonstrates that the P-PGS group had slightly higher levels than other groups in both ipsilateral dorsal (11.7% vs 10.8% [NP-PGS; $p>0.05$] and 9.9% [nerve graft; $p>0.05$) and ventral (6.9% vs 5.4% [$p>0.05$] and 5.4% [$p>0.05$]) (Table 6.1 & Figure 6.14). There were no significant differences in labelling between these two groups (refer to Table 6.2 & Figure 6.19). In the corresponding contralateral side, the percentage area of GFAP labelling in the dorsal and ventral horns were similar in all groups (refer to Table 6.2 & Figure 6.19). The activation areas of Iba-1 in each group are shown in Figures 6.16-6.18.

Porous PGS

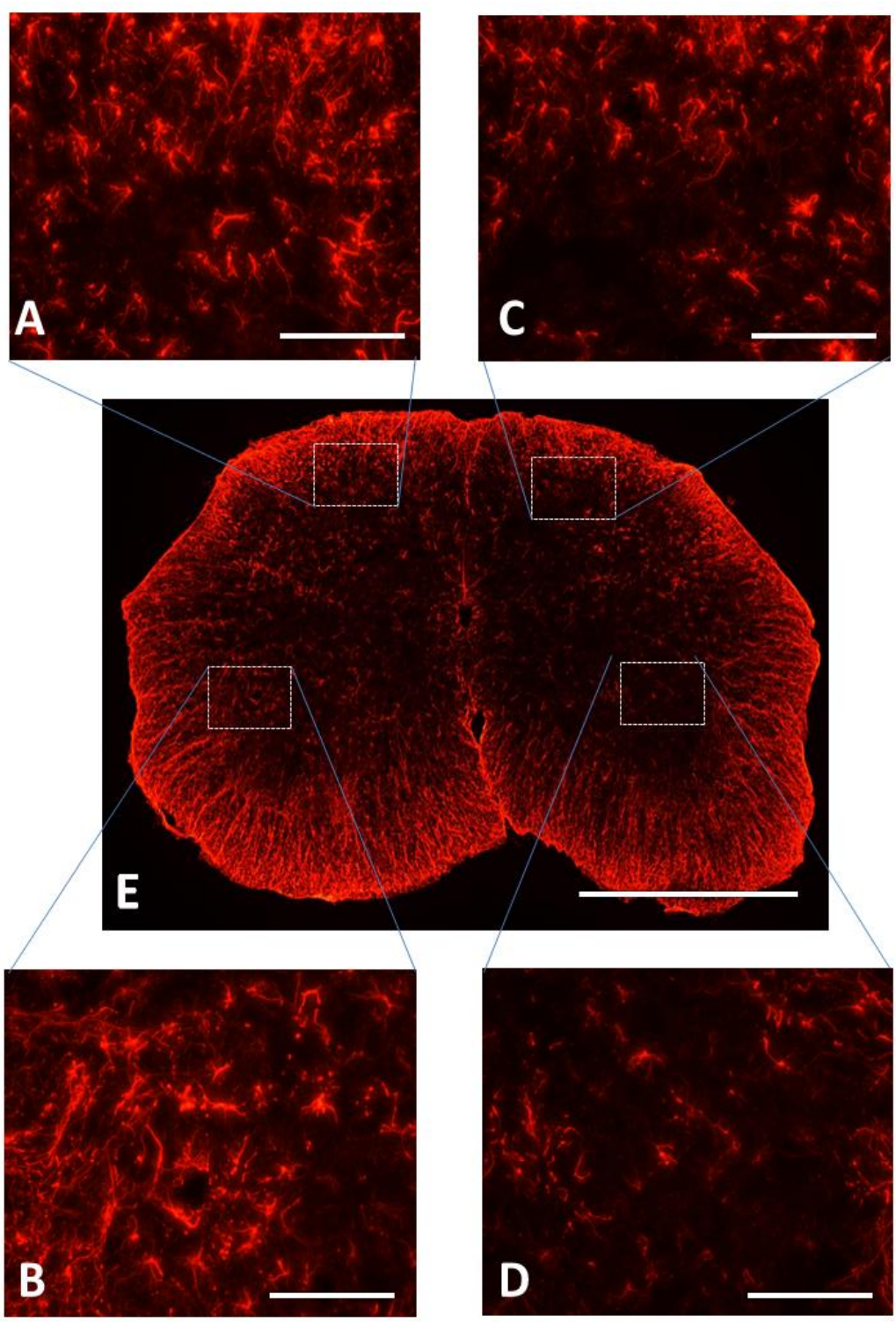

Figure 6.16: A section of spinal cord following repair with a porous PGS conduit shows astrocyte activation (E using 5x magnification). A) Ipsilateral dorsal horn, B) Ipsilateral ventral horn. C) Contralateral dorsal horn. D) Contralateral Ventral horn (A,B,C,D using 40x magnification). Scale bar A,B,C and D = 0.1mm, E = 1.0mm.

Non-porous PGS conduit

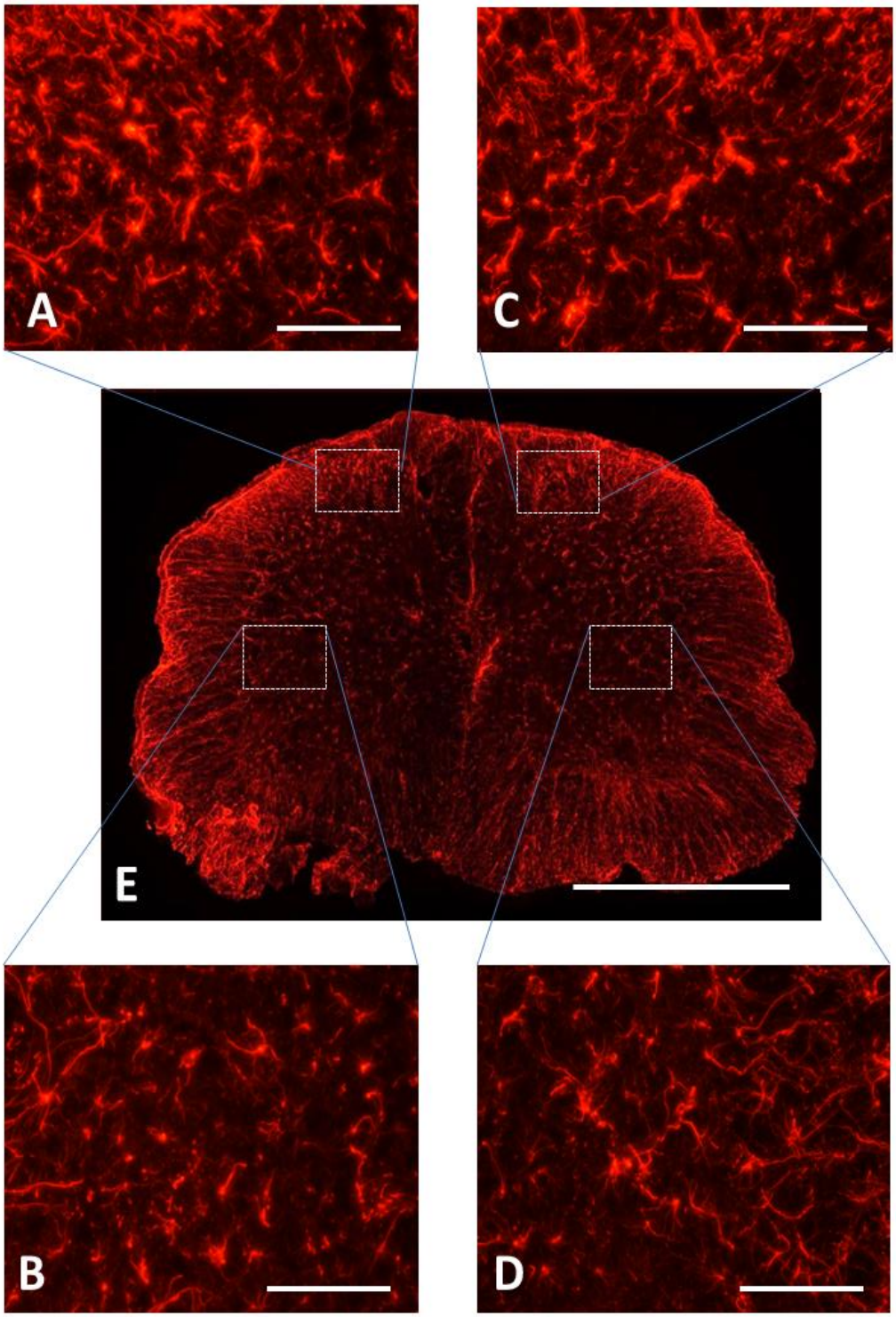

Figure 6.17: A section of spinal cord following repair with a non-porous PGS conduit shows astrocyte activation (E using 5x magnification). A) Ipsilateral dorsal horn, B) Ipsilateral ventral horn. C) Contralateral dorsal horn. D) Contralateral Ventral horn (A,B,C,D using 40x magnification). Scale bar A,B,C and D = 0.1mm, E = 1.0mm.

Nerve Graft

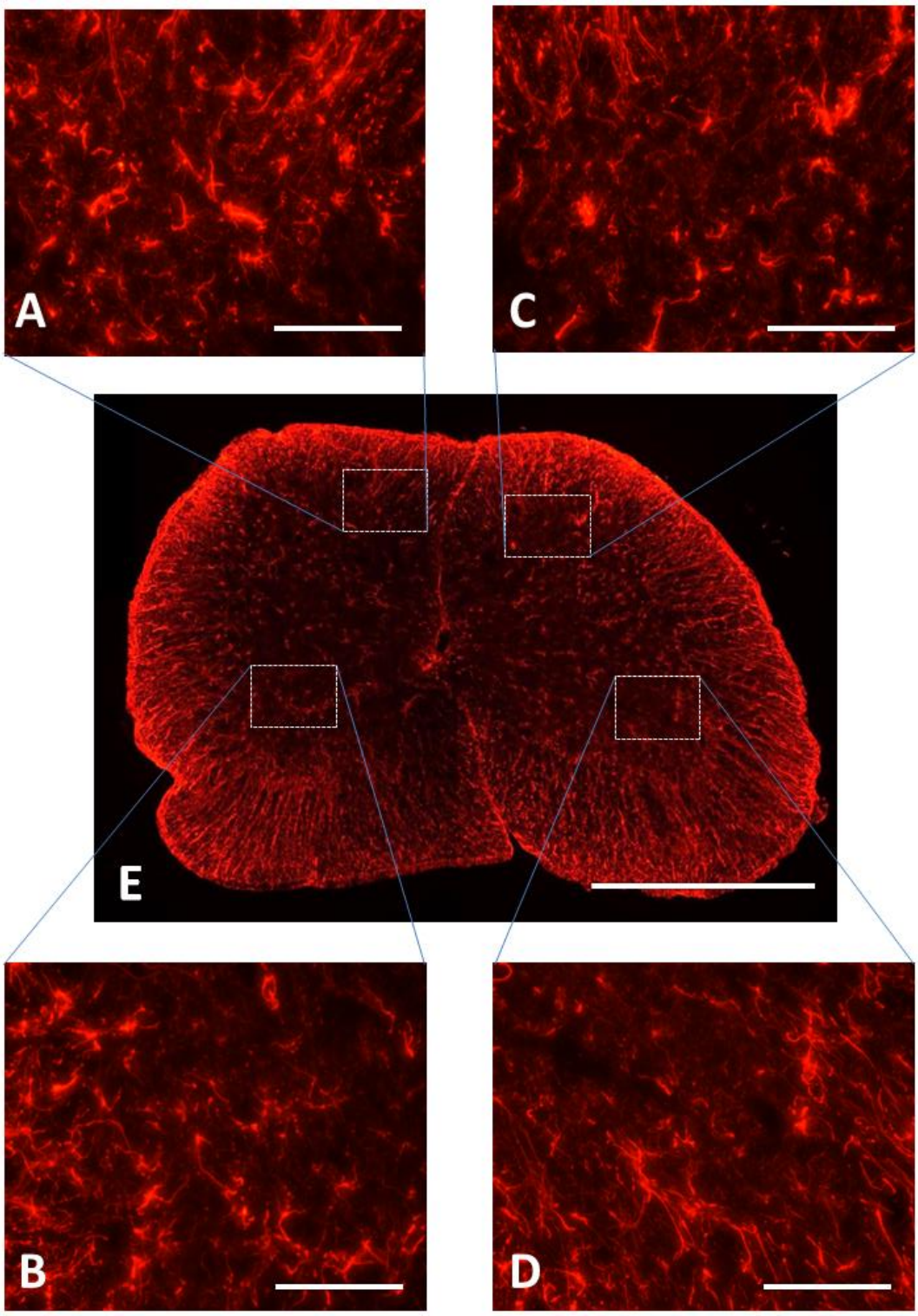

Figure 6.18: A section of spinal cord following repair with nerve graft shows astrocyte activation (E using 5x magnification). A) Ipsilateral dorsal horn, B) Ipsilateral ventral horn. C) Contralateral dorsal horn. D) Contralateral Ventral horn (A,B,C,D using 40x magnification). Scale bar A,B,C and D = 0.1mm, E = 1.0mm.

The mean percentage area of GFAP labelling (indication of the degree of astrocyte activation) for each group is shown in Table 6.2. The same data and the statistical comparison between the groups is illustrated in Figure 6.19.

Table 6.2: Percentages of astrocyte activation in P-PGS, NP-PGS and nerve graft groups activation in all groups.

GFAP (Astrocytes)%	P-PGS	NP-PGS	Nerve Graft
Ipsilateral Dorsal horn	11.7	10.8	9.9
Contralateral Dorsal horn	7.7	8.3	7.9
Ipsilateral Ventral horn	6.9	5.5	5.4
Contralateral Ventral horn	4.4	4.2	4.2

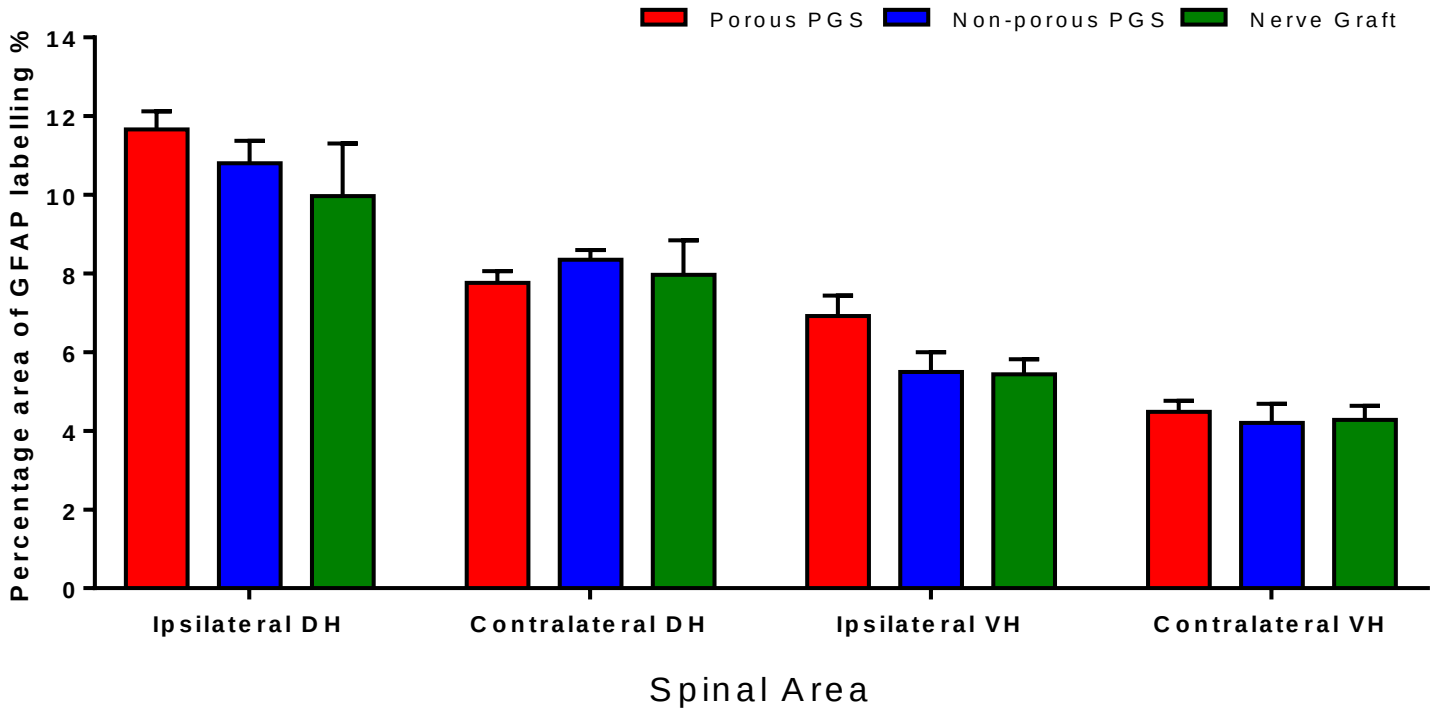

Figure 6.19: Immunohistochemical analysis of astrocyte for porous PGS conduit, non-porous PGS conduits and nerve graft groups. Statistical test: 1-way ANOVA with Bonferroni's multiple comparisons test. DH= Dorsal horn VH= Ventral horn.

The increase in staining (Ipsilateral/Contralateral) ratio for GFAP in the P-PGS group was significantly higher than in other groups in both dorsal (49.7% vs 29.3% [NP-PGS; $p<0.05$] and 24.8% [nerve graft; $p<0.05$]). In the ventral horn, P-PGS group had a lightly higher percentage increased than in other groups (36.6% vs 32.2% [NP-PGS; $p>0.05$] and 27.9% [nerve graft; $p>0.05$]) horns. There were no significant differences in labelling between NP-PGS and nerve graft groups (Figure 6.20).

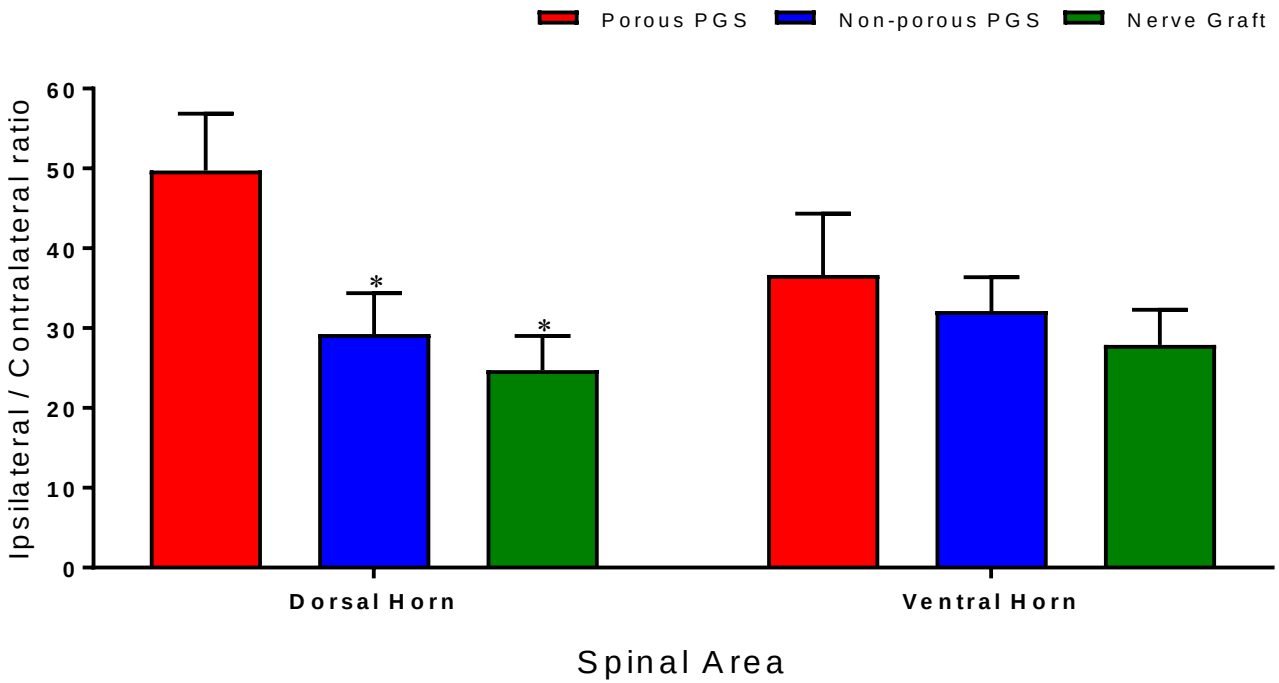

Figure 6.20: Ipsilateral/Contralateral ratio of astrocyte shows the difference of percentage increase in the ipsilateral side over the contralateral side in ventral and dorsal horns of the spinal cord for porous PGS conduit, non-porous PGS conduits and nerve graft groups. * denote significant difference compared to PGS porous conduit, $p<0.05$. Error bars denote SEM. Statistical test: 1-way ANOVA with Bonferroni's multiple comparisons test.

6.4.3.2 Assessment of Functional Recovery Using Axon Counting and Tracing Analysis

6.4.3.2.i The Initial Non-porous PGS Conduits

When implanted the first version of the PGS conduit with inner diameter 1.1mm, wall thickness 350 µm and length 5.0mm, the results demonstrated that axons could regenerate through it, but in much reduced numbers compared to previous conduit studies carried out within our laboratory. The next step was to decrease both the internal diameter (0.9mm) and wall thickness (250µm). At the time of harvesting these conduits, it was noticed that the conduit had collapsed, preventing the axons from regenerating through it (Figure 6.21). The final step was to create a more optimal design with inner diameter 0.7mm and wall thickness 350µm, which were the conduits that were used for the study reported in this chapter.

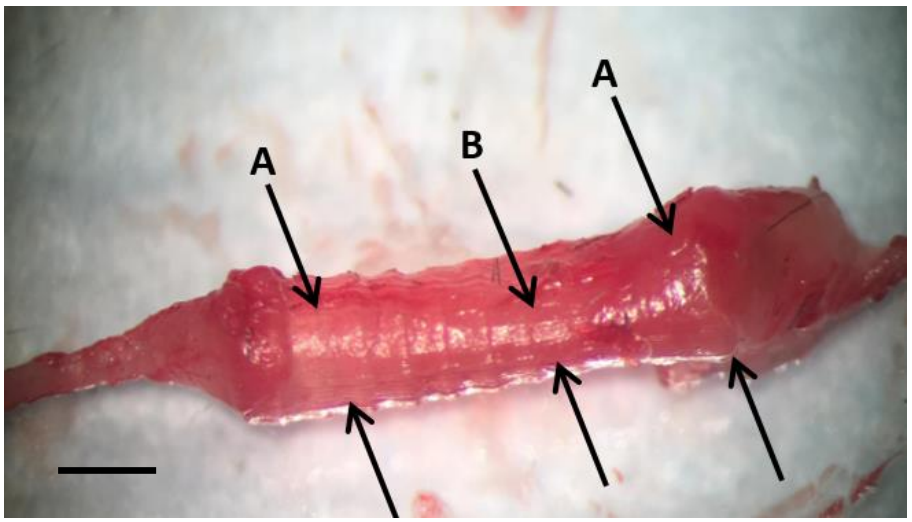

Figure 6.21: Repaired nerve with the second PGS design (decreased both internal dimeter and wall thickness. A) The arrows show the original conduit shape. B) The arrows show the shape of the conduit after the collapse. Scale bar= 1.0mm.

6.4.3.2.ii Qualitative Observation of Regenerated Nerves

For nerve analysis, comparisons were made between NP-PGS conduit and nerve grafts, as P-PGS conduits are non-hollow tubes, requiring a different analysis method. Graft repairs showed a similar gross morphology to that seen in chapter 4 with areas of disruption between both initial proximal and distal nerve ending joins when meeting the graft end. In NP-PGS conduits, the regenerated nerves appeared thinner than those in the graft repairs (Figure 6.22).

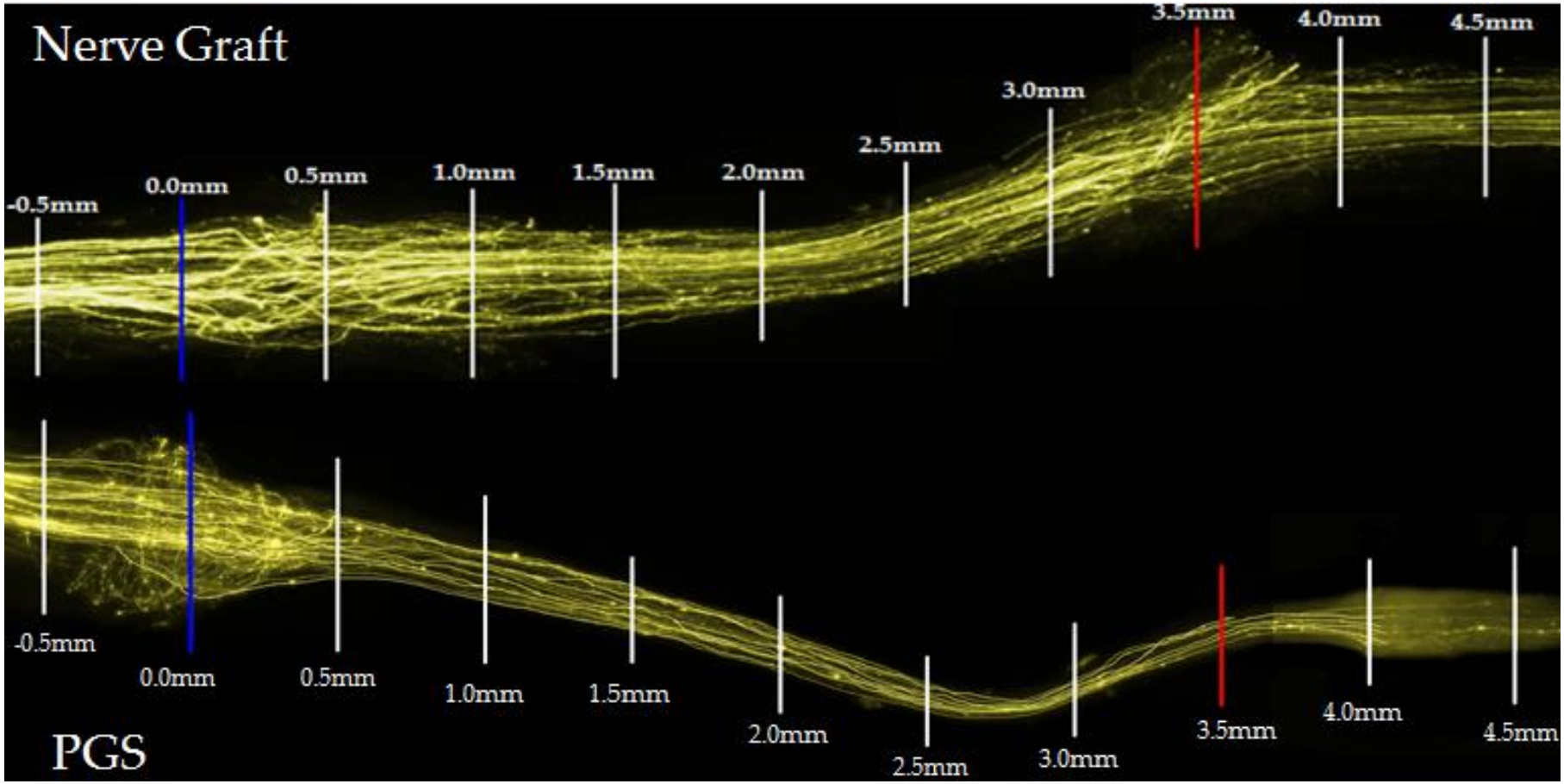

Figure 6.22: Repaired nerve with nerve graft (top) and non-porous PGS conduit (down). All nerves presented with intervals marked, showing the start interval (blue) and the final interval (red).

6.4.3.2.iii Quantitative Analysis of Regenerated Nerves

A. Sprouting Index

As described in section 2.2.7.3.i, the sprouting index was calculated at 0.5mm intervals through the regenerating nerve. Sprouting index analysis showed a significant difference between the two repair groups. There is a significant drop of overall axons in NP-PGS repairs at all intervals except at the 0.0mm 'start' interval. Both NP-PGS (126.75%) and graft (135.67%) groups had a similar level of increase in sprouting at the 0.0mm interval. Following that, both groups presented a decline in sprouting index at subsequent intervals. There was a severe decline in sprouting index of NP-PGS repair (75.0%) at the 0.5mm interval compared to graft repair (124.83%), and then a smaller decline across subsequent intervals. The lowest sprouting index for NP-PGS repair (25.0%) was observed at the 3.0mm interval where it remained around this level until the 4.00mm interval (initial distal nerve end). For graft repair, the sprouting index gradually declined until the 2.0mm interval where the lowest sprouting index (79.67%) was observed. Following that, the sprouting index increased until the 4.0mm interval where it declined (86.33%). All sprouting index values are illustrated in Table 6.3 and Figure 6.23.

.

Table 6.3: Sprouting index levels for PGS non-porous conduit and nerve graft repairs (%).				
Repair Position (Intervals)	**Non-porous PGS**	**SEM**	**Nerve graft**	**SEM**
-0.5	100.0	0.0	100.0	0.0
0.0	126.8	8.8	139.7	5.1
0.5	75.0	14.5	124.8	13.6
1.0	49.5	9.6	119.2	11.7
1.5	45.0	8.7	88.5	5.5
2.0	33.0	7.0	79.7	7.4
2.5	29.0	5.5	82.7	5.9
3.0	25.0	4.3	96.5	9.5
3.5	25.0	3.9	104.5	8.3
4.0	27.3	4.3	86.3	7.5

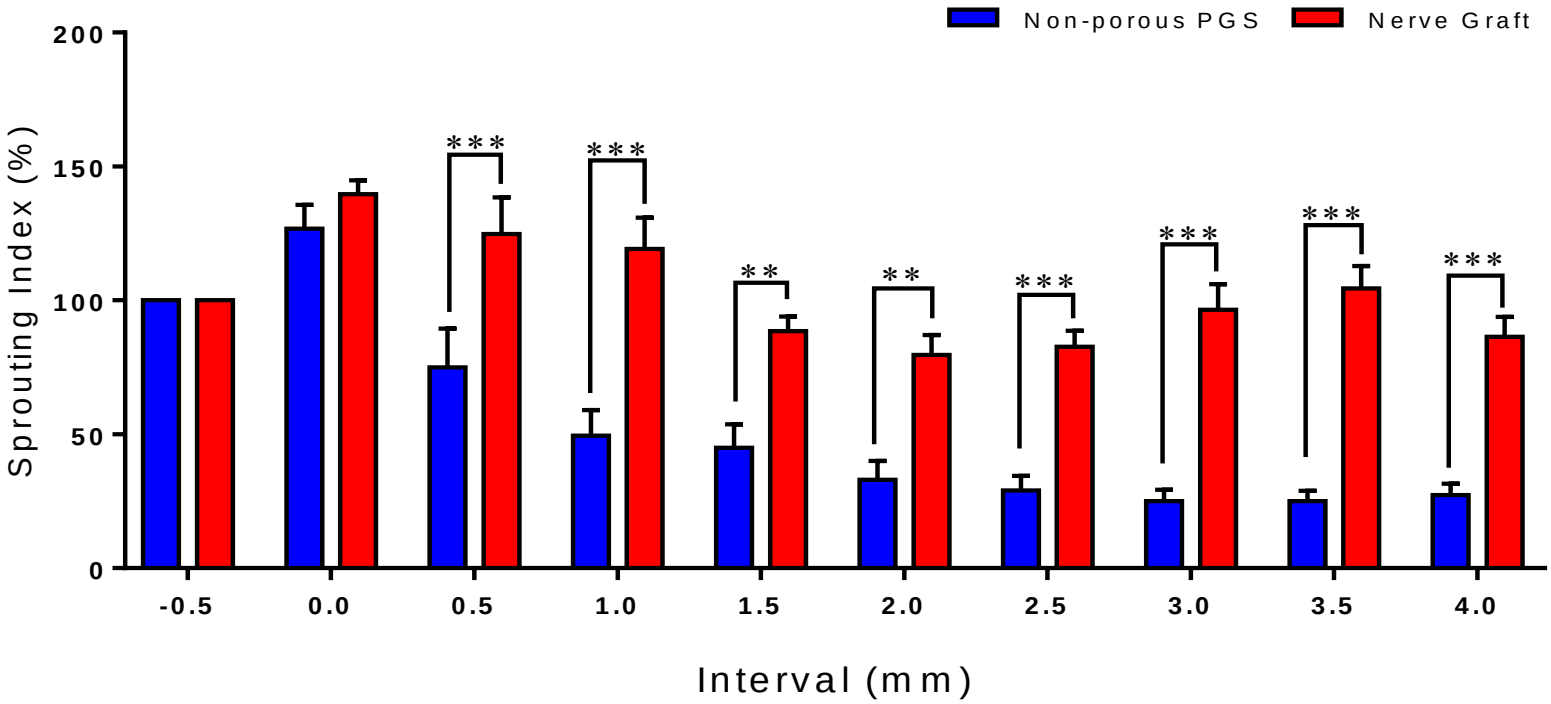

Figure 6.23: Sprouting index levels on non-porous PGS and nerve repairs at 0.5mm intervals along the nerve. ** and *** denote significant difference compared to nerve graft, $p<0.01$ and $p<0.001$ respectively. Error bars denote SEM. Statistical test: 2-Way ANOVA with Bonferroni's multiple comparisons test.

B. Axon Tracing

Axon tracing indicates the number of unique axons that successfully regenerate from the repair start to the distal nerve ending. As described in section 2.2.7.3.ii, a minimum of 75% of axons are traced from the final interval (3.5mm) back toward to the 0.0mm interval (Figure 6.24)**.** The proportion of unique axons represented at each interval was higher in the graft group than NP-PGS group at all intervals, but the difference was significant only at the 1.0mm interval (23.7% PGS-NP, 42.0% Graft; $p<0.01$). The highest decline of unique axons in both groups was found between the 0.0mm and the 0.5mm interval. The percentage of unique axons continued to decline at each subsequent interval, until it reached 13.1% (NP-PGS repairs) and 22.2% (graft repairs) at the 3.5mm interval ($p>0.05$) (Table 6.4 & Figure 6.25).

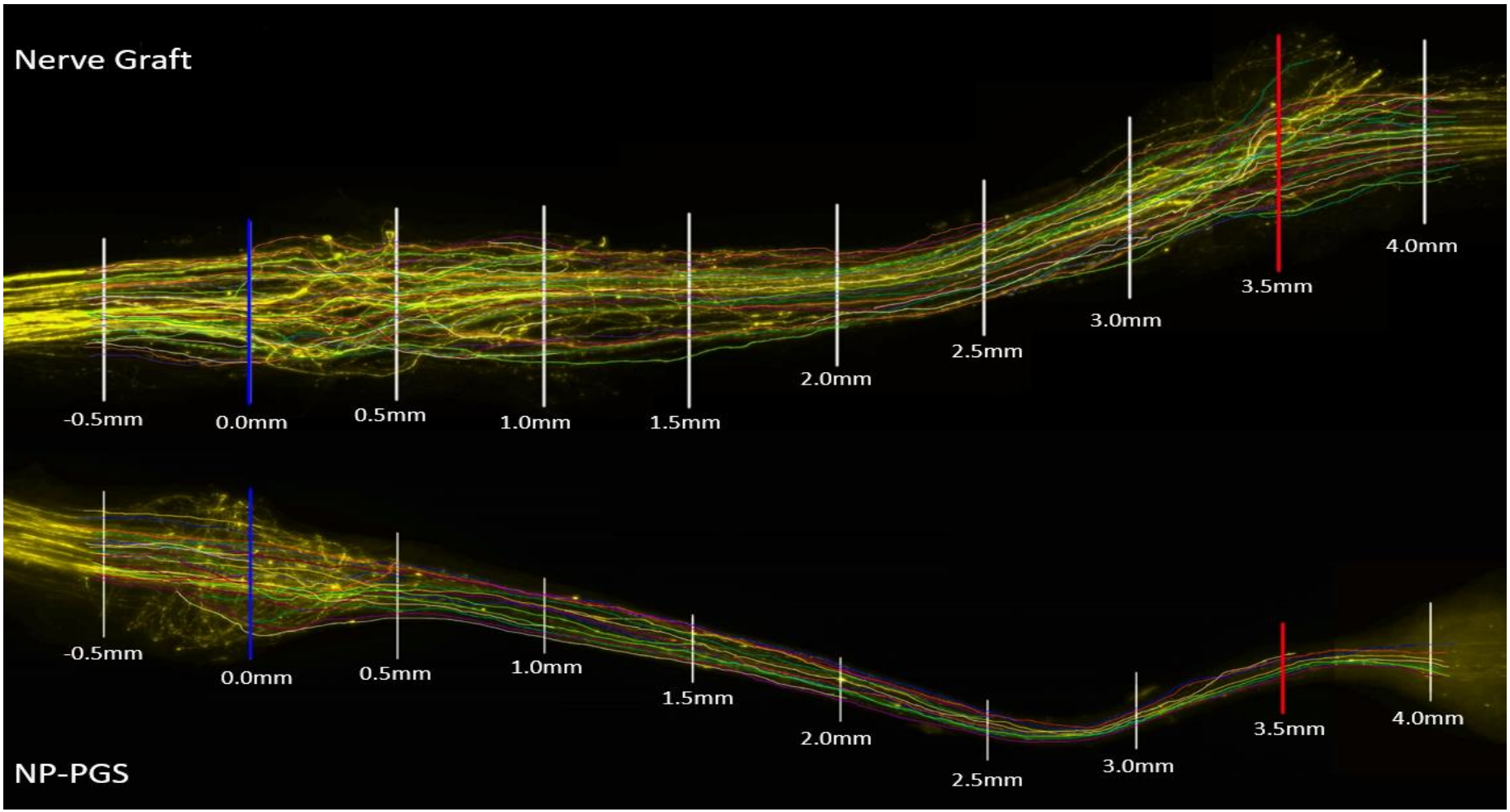

Figure 6.24: Image of traced axons from 3.5mm interval back toward to the 0.0mm in both nerve graft and NP-PGS.

Table 6.4: Axon tracing for PGS non-porous conduit and nerve graft repairs (%).

Repair Position (Intervals)	Non-porous PGS	SEM	Nerve graft	SEM
0.0	100.0	0.0	100.0	0.0
0.5	41.8	7.1	56.0	3.7
1.0	23.7	3.4	42.0	4.5
1.5	20.2	3.1	34.9	5.1
2.0	15.4	2.7	29.4	3.9
2.5	13.0	2.1	27.8	3.6
3.0	12.6	2.5	24.2	3.0
3.5	13.1	2.5	22.2	3.1

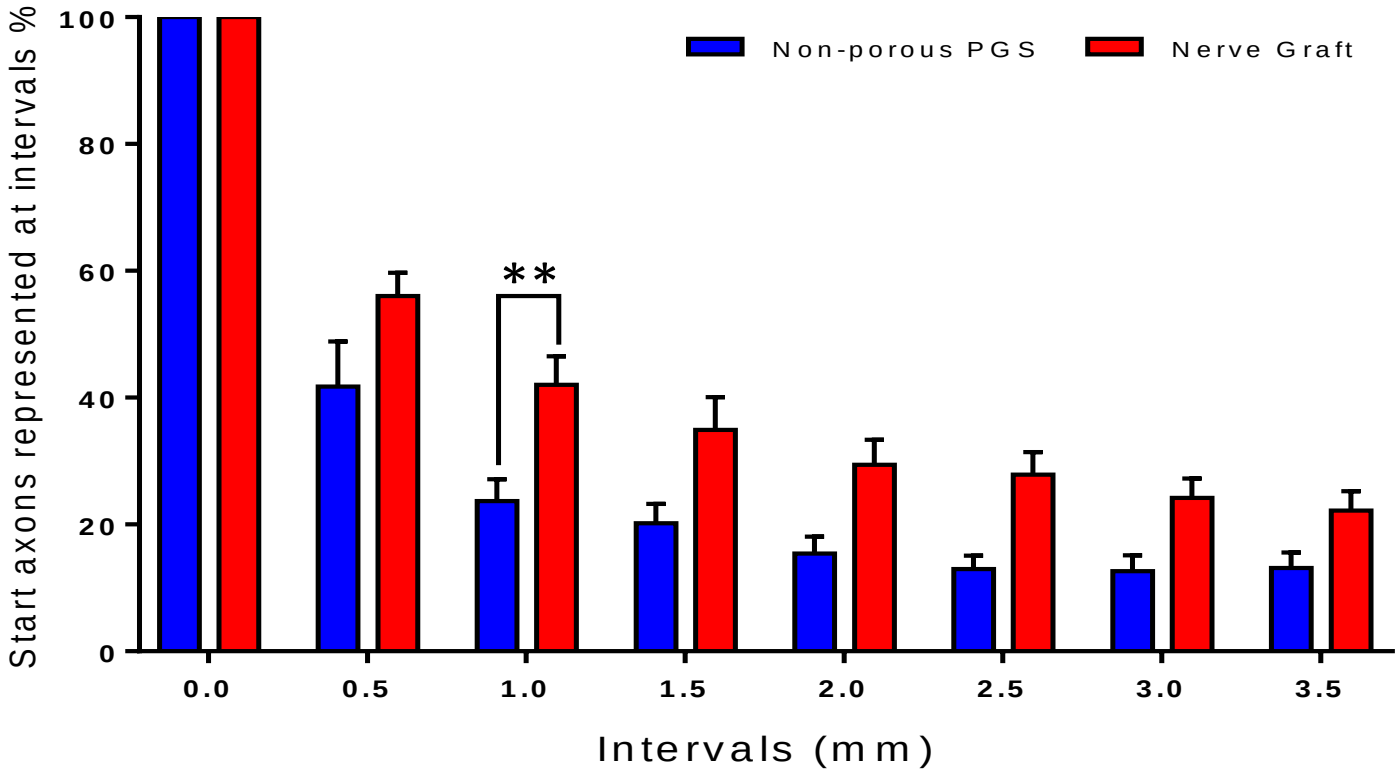

Figure 6.25: Unique axon percentages across repair in both groups. ** denote significant difference compared to nerve graft, $p<0.01$. Error bars denote SEM. Statistical test: 2-way ANOVA with Bonferroni's multiple comparison test.

C. Axon Disruption

Axon lengths across the portion of nerve between the 0.0mm and 1.5mm intervals were measured, and the average axon length in each group was determined. The difference between the axon length and actual distance (1.5mm) was expressed as percentage increase of axon length relative to the actual distance (Figure 6.26).

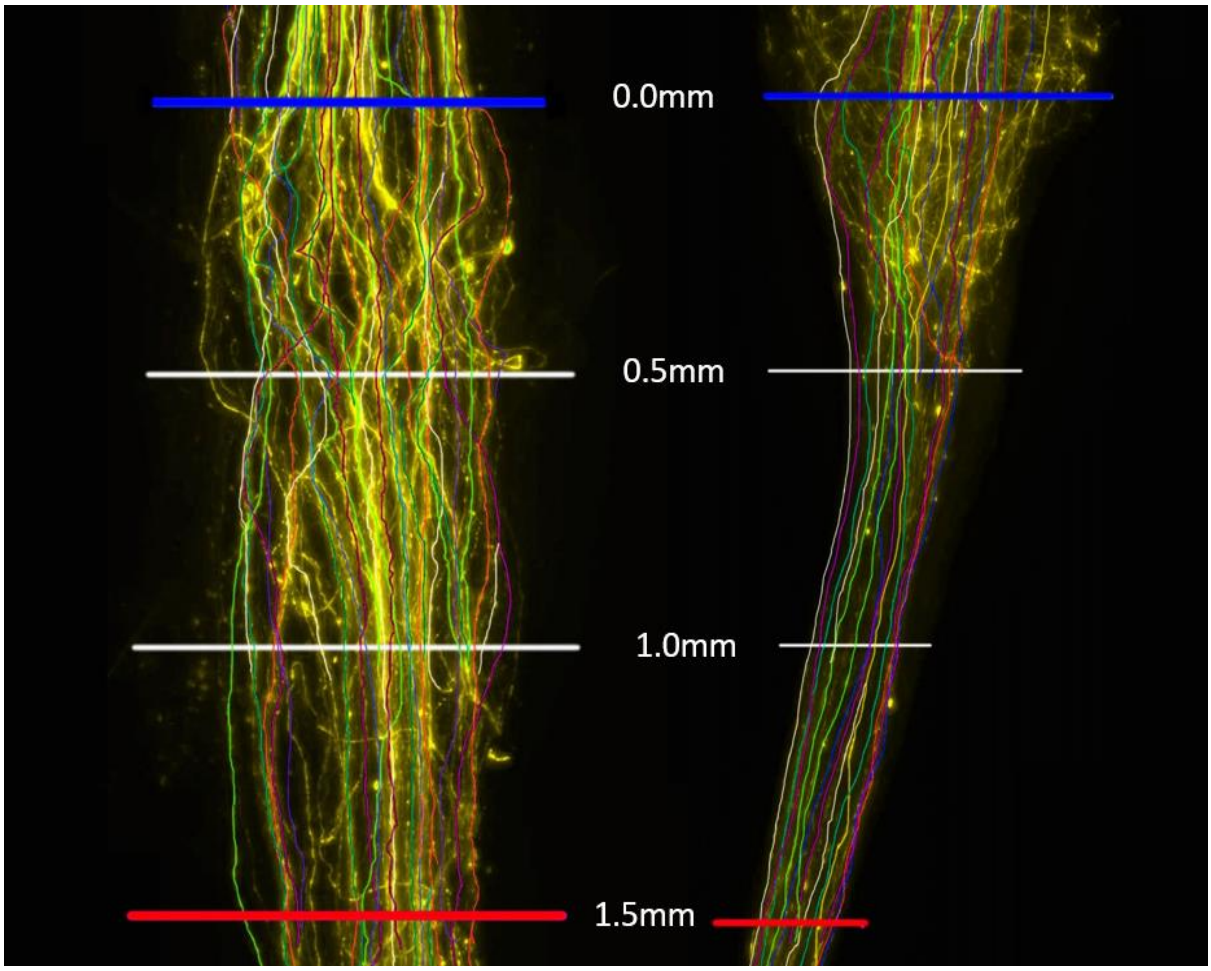

Figure 6.26: Image showing traced axon disruption between 0.0mm (blue line) and 1.5mm (red line) in both graft repair (on the left) and non-porous PGS (on the right).

The average increase in axon length in NP-PGS group was marginally lower (9.2% [±1.8SEM]) than the graft group (12.1% [±2.8]), but there was no significant difference (p=0.46) (Figure 6.27).

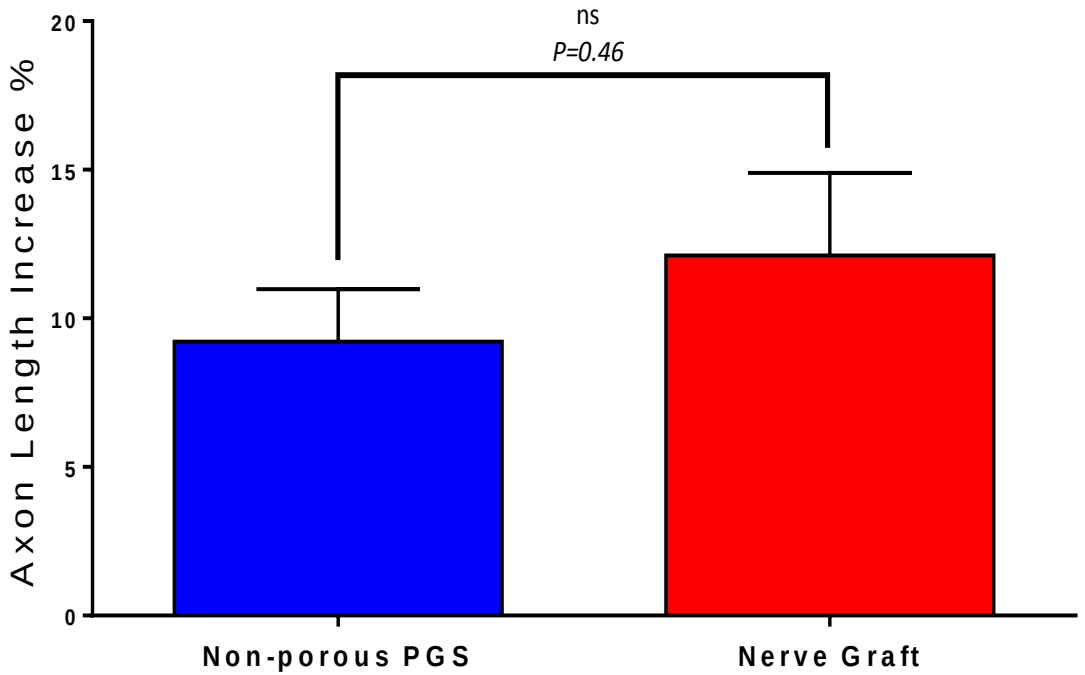

Figure 6.27: Percentage increase in axon length between 0.0mm and 1.5mm in both graft and non-porous PGS groups. No significant different were observed between the repair groups. Error bars denote SEM. Statistical test: unpaired t test (two-tailed).

6.4.3.2.iv Porous PGS Conduit Result

Longitudinal images of nerves from P-PGS conduit showed high numbers of axons present only at the proximal nerve end. Whereas it was clearly observed that no axons passed through the conduit or at the distal nerve end (Figure 6.28A). In the Transverse images, only 2-4 axons can be seen inside the conduit (Figure 6.28B).

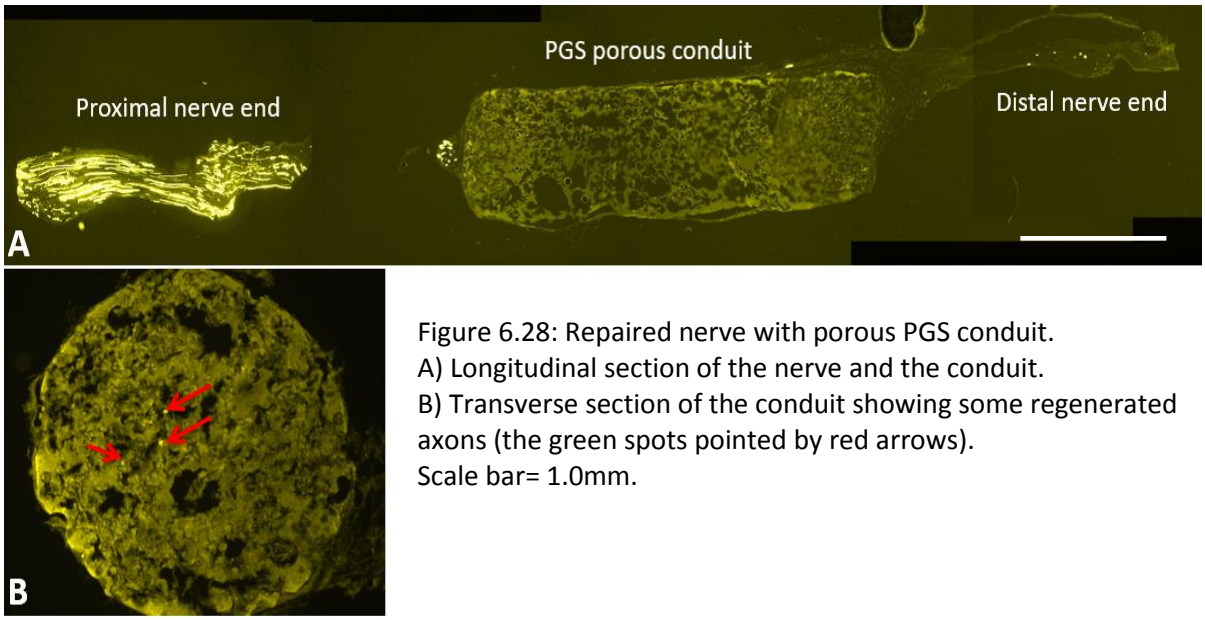

Figure 6.28: Repaired nerve with porous PGS conduit.
A) Longitudinal section of the nerve and the conduit.
B) Transverse section of the conduit showing some regenerated axons (the green spots pointed by red arrows).
Scale bar= 1.0mm.

6.5 DISCUSSION

A few experimental studies have investigated PGS as a potential material for peripheral nerve injury repair. However, forming 3D printed PGS conduits and implanting them in peripheral nerve injury (*in vivo*) has not been explored prior to this study. A novel formulation of methacrylate moieties was added to synthesized PGS prepolymer, forming PGSm. This formulation allows photocurable PGSm to be formed into 3D printed structures using µSL to prepare it for use as a NGC in peripheral nerve injury repair.

One of the principal properties that is required to be present in a useful NGC is to be able to direct axonal growth across the nerve gap. This was investigated in *ex vivo* analysis when the DRGs were seeded onto a PGS hemi-tube. DRGs adhered to the surface, and Schwann cells and neurites were able to extend out along the entire PGS conduit. These outcomes demonstrated that neurites align along the topographical grooves of the PGS, helping to direct the regeneration from the proximal toward the distal stump.

Based on the previous literature, which suggested that PGS is a valuable material in soft tissue engineering applications (Rai et al., 2012, Sundback et al., 2005), it had been expected that PGS in a form of a NGC would have promoted axons regeneration and improved overall nerve regeneration.

6.5.1 The Effect of PGSs and Graft on Spinal Glial Activation

The results in this chapter obtained from immunohistochemical analysis demonstrated that no significant differences were present between NP-PGS and graft repairs in term of microglial or astrocytes activation. Both repairs expressed low levels of glial activation, this may suggest that the neuropathic pain is unlikely to have developed.

The levels of microglial and astrocyte activation in P-PGS repairs were significantly higher compared to NP-PGS and graft repairs, suggesting higher potential for developing neuropathic pain. The high level of activation may be due to axons being unable to regenerate through the conduit.

6.5.2 The Effect of Non-porous PGS and Nerve Graft on Nerve Regeneration

The difference between the NP-PGS and graft was clear from visual observation alone. In NP-PGS, the nerves look thin with relatively few axons passing from proximal to distal stumps. While in grafts, the nerves look thicker with a higher number of axons (Figure 6.22).

6.5.2.1 Axon Sprouting Levels

At the 0.0mm interval, both repairs had higher percentages than the -0.5mm interval (proximal nerve end), demonstrating that axons are sprouting many branches during their regeneration. Following that, NP-PGS had significantly lower sprouting index levels at all subsequent intervals compared to graft repairs. At the 3.0mm interval, sprouting index level was slightly increased in both groups, suggesting that axons branch more at each meeting (central and distal).

Pateman et al. (2014) evaluated the use of poly-ethylene glycol (PEG) as a nerve guide conduit nerve regeneration using the same surgery protocols and axon counting and tracing analysis described in this chapter. They reported that the highest sprouting index value for the PEG conduits was observed at the 0.5mm interval (145.4%), and the lowest were observed at the 4.0mm interval (65.3%). In the current study, the sprouting index on PGS at the 0.5mm interval was (75%) and at the 4.0mm interval was (27.25%). However, this is the first time ever for the PGS to be evaluated as a NGC. Moreover, as mentioned in chapter 4, deciding the start point for the intervals is objective.

The internal diameter and thickness of the wall of conduits play a vital role in, and may affect, the degree of regeneration. As described in the results section, three versions of the NP-PGS conduit were evaluated. In the first version, the internal diameter and the thickness of the wall (1.1mm and 350µm, respectively) were considered to be the most likely reason for the poor regeneration. There is some debate regarding the optimal size of the internal diameter of conduits. Some studies suggested a dimeter equal to 2.5-3.0 times the nerve's size (Ducker and Hayes, 1968), while most recent studies suggested a lower size of 1.3 times (Lundborg et

al., 2004). The diameter of the common fibular nerve is approximately 0.35mm, and the diameter of the nerve (at the join between nerve and graft) upon graft repairs increases to approximately 0.6-0.7mm (Harding, 2014). In this instance the diameter was more than 3 times the diameter of the CF nerve. The results of Ducker and Hayes' (1968) study reported that the axonal growth was achieved in tubes with internal diameter twice that of the nerve, and no sign of neuroma or connective tissue building was detected. Whereas, in tubes with internal diameter greater than three times of that of the nerve, the axonal growth failed and connective tissue build-up was observed at the site of the repair. Thus, it seems that the dimensions of the first version were unsuitable to the regenerated nerve as the conduits has too large internal diameter.

The wall thickness of the conduit plays another important role in the final outcome of axonal regeneration. For the second version of NP-PGS, we tried to decrease both the internal diameter (250µm) and thickness of the wall (0.9mm) to give an overall external diameter of (1.4mm). This version of the conduit could not survive against the effect of pressure from the surrounding tissues, and it collapsed at the mid-point preventing the axons from regeneration during the recovery period (21 days); likely as a result of reducing the thickness of the conduit wall. In Ducker and Hayes's (1968) study, a range of wall thickness was evaluated. They reported that neuroma build up was observed at proximal and distal sides of the thicker-walled tubes, while neuroma was not detected in thinner-walled tubes. Another study concluded that when using conduits with too small an internal diameter and too thick of a wall, a swelling that occludes the conduit and hampers regeneration will form. On the other hand, when using conduits with too thin of a wall, the conduit will collapse (Den Dunnen et al., 1998).

Although the total number of axons was lower in NP-PGS conduit repairs compared to graft repairs, it has previously been reported that the average diameter of fibres after polymer conduits repairs was significantly greater than that after autograft repairs. This suggested that the regeneration environment in the tissue engineered conduits may favour regeneration of myelinated motor fibers (Hadlock et al., 2000). Hadlock et al. (2000) reported that the mean diameter of regenerated axons in conduit repairs is significantly higher (3.7µm) compared to autograft repairs (2.3µm).

6.5.2.2 Axon Tracing

The percentages of unique axons from the start interval represented at each the 0.5mm internal were lower (but not significantly) in NP-PGS repairs compared to graft repairs, except at the 1.0mm interval where the percentage was significantly lower in NP-PGS repairs (Figure 6.24). Only 13.1% of axons present at the 0.0mm interval reached the 3.5mm interval in NP-PGS group compared to 22.2% in graft group. Pateman et al (2014) reported that only 24% of axons present at the 0.0mm interval reached the 3.5mm interval in PEG conduits. Approximately 60% of axons in NP-PGS repairs and 45% in graft repairs from the 0.0mm interval were lost by the 0.5mm interval, this is where the axons passed the injury site and entered the conduit/graft. The same was reported by Pateman et al (2014), as approximately 50% of axons in PEG conduits were lost by the 0.5mm interval.

From the results of the *in vitro* and *ex vivo* studies, it had been anticipated that PGS material would enhance the regeneration, thus allowing the regenerated axons to be promoted well inside the conduit. The results illustrated that the percentage of axon tracing in graft repairs dropped continuously and gradually over the subsequent intervals, while in NP-PGS repairs the percentage significantly dropped only at the 1.0mm interval and when axons entered the conduit the drops were relatively small.

6.5.2.3 Axon Disruption

The level of axon disruption in NP-PGS and nerve graft was similar (9.2% and 12.1%, respectively), with only approximately 3% less in NP-PGS than graft repairs (Figure 6.27). A similar average increase in axon length was reported for PEG conduits (11.4%) (Pateman et al 2014). The regions of disrupted axons at each side of the repair were smaller in PGS compared to graft repairs. The NP-PGS conduits were not expected to increase axon disruption as they are flexible and their surface does not possess its own inflammatory cells, as graft tissues do. In addition, axons are able to regenerate through any region of the conduit, whereas in the case of graft repairs an axon can only regenerate into the graft once it has entered a endoneurial tube, which may result in increased axon disruption.

6.5.3 Porous PGS Conduits

Based on previously published studies, conduits including channels have been reported to have a better level of peripheral nerve regeneration than hollow conduits (Calder et al., 1995, Evans et al., 1994, Glasby et al., 1994, Hadlock et al., 2000, Yao et al., 2010). Comparing the recovery function of multichannel and single channel conduits was mentioned in a study by Yao et al. (2010). Their study investigated the role of applying multichannel (1, 2, 4, 7 channels) within a collagen conduit for the purpose of enhancing the physical structure of the conduits and improving regeneration outcomes. The results from compound muscle action potential (CMAP) and nerve morphology were superior in conduits with 1 and 4 channels compared to the other conduits in axonal regeneration. The results of simultaneous tracing showed a significantly lower percentage of motor neurons in conduits with 2 and 4 channels compared to other conduits. They conclude that a conduit with 4 channels is a suitable design for peripheral nerve regeneration (Yao et al., 2010). Another study by Hadlock et al. (2000) also reported that using PLGA porous conduits with longitudinal multichannel showed promise for directed regenerated axons over a 7.0mm gap size.

The results of the P-PGS repairs that were reported in this chapter contrasted with the established view, as few or no axons regenerated through the conduits, suggesting that P-PGS conduits with multi-channels are not an appropriate structure to bridge a gap in peripheral nerve injuries. It is difficult to perform a direct comparison between the current study and the above studies (Hadlock et al., 2000 and Yao et al., 2010) because each study used a different conduit material, designs and way of production. Also, the species and nerve were different as mice and CF nerve were used in the current study, while rats and sciatic nerve were used in the other two studies. Moreover, the gap size also was different (3.0mm, 7.0mm and 5.0mm) between the current, Hadlock et al. (2000) and Yao et al's (2010) studies, respectively. Although the gap size in the current study was the smallest, the conduit failed to promote the regeneration. The method of production of P-PGS conduits may have had an effect of the repair, suggesting that production methods may not optimised.

Studies by Ruiter et al. (2008 and 2009) evaluated the effect of applying single or multichannel conduits fabricated from PLGA. No significant differences were reported in their study. However, swelling in multichannel conduits closing the conduit cavities was detected, blocking the axonal growth during longer recovery period (12 weeks). the P-PGS conduits did seem to swell internally, suggesting that the main reason behind the failure is the conduit design/P-PGS manufacture.

6.5.4 Properties of PGS Conduits

PGS conduits have some properties make them preferable among the other conduits involved in this thesis. They have a translucent colour, which allowing visualization of the two nerve ends during the implantation and ensure that these two ends are inside the conduit and secured (Figure 6.3A). It was possible to make holes at each side of the PGS conduits, which can be used to pass sutures through them in the case of bridging a larger nerve gap or a nerve liable to undergo extended movement (Figure 6.29A). Also PGS conduits are flexible and soft, making them able to survive against the pressure of the surrounding tissues (Figure 6.29B).

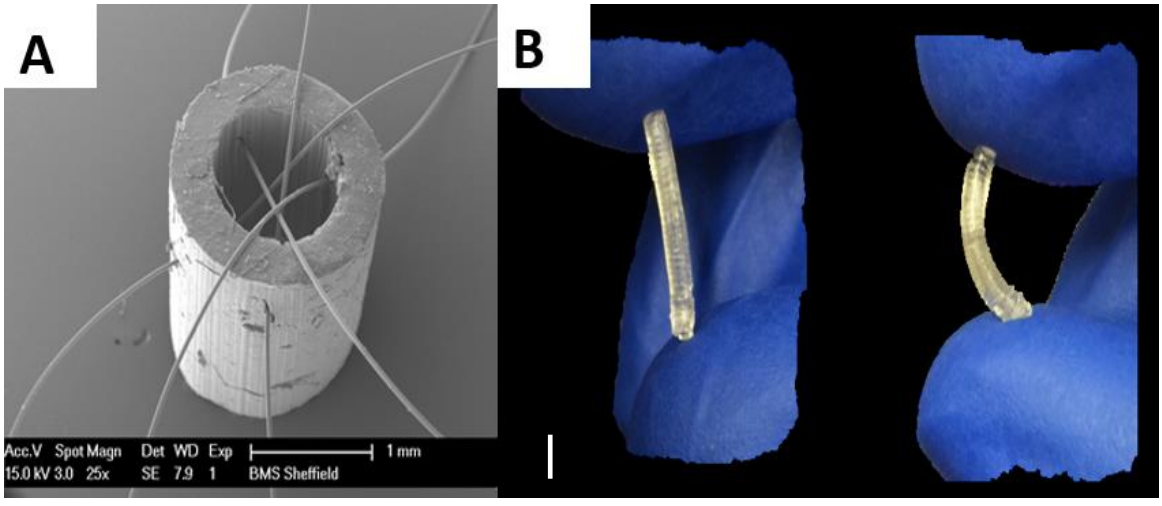

Figure 6.29: Properties of PGS conduits. A) Showing some sutures passed through the conduit. B) Showing the flexibility of the conduit against external resistance (Provided by Dharaminder Singh). Scale bar= 1.0mm.

6.5.5 Technical Failure for the Two Excluded Non-Porous Repairs

As mentioned earlier, two mice from NP-PGS repairs were excluded from the study because of technical failure. Two reasons were deemed responsible for these technical failures. The first reason was the pathway through the conduit becoming obstructed by a fibrin glue clot, preventing the regeneration. A piece of sold translucent material was observed on one repair, blocking the way between the two ends and it's believed to be a piece of the fibrin glue (Figure 6.30A). The second case of failure was associated with the proximal end of the nerve becoming dislodged from the conduit during the recovery period (Figure 6.30B). When comparing the two images of NP-PGS and graft repairs, it is notable that the two ends of the nerve in NP-PGS repair were slightly retracted even when they were secured by fibrin glue, creating a larger gap (3.5mm) compared to the graft repairs. However, fibrin glue is a reliable material and use of it glue in peripheral nerve injury repairs was investigated in previous studies, proving an excellent alternative method to the suturing method (Menovesky and Beek, 2001). Taken together the failures in the current study and the failures reported in chapter 5, suggests that this specific fibrin glue may not have been optimal in its performance.

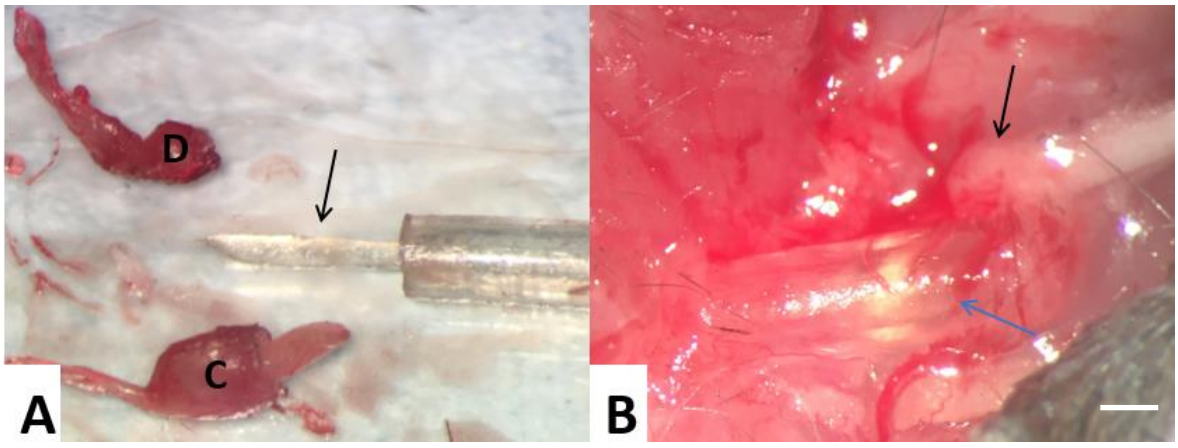

Figure 6.30: Technical failures: A) Showing the glue became solid inside the conduit (black arrow). B) Showing the proximal end (black arrow) was separated from the conduit (blue arrow). C) Proximal nerve end. D) Distal nerve end. Scale bar= 1.0mm.

6.6 CONCLUSION

This chapter investigated the ability of a novel PGS conduit to support peripheral nerve regeneration. A novel formation, methacrylate moieties (PGSm), was used to enable to create 3D structures. The material showed excellent outcomes in both *in vitro* and *ex vivo* studies. The results of the *in vivo* analysis showed that NP-PGS supported regeneration and directed axonal growth. They also showed a low level of glial activation, suggesting a low potential for the development of neuropathic pain. However, sprouting index and axon tracing reported that nerve graft was better than the NP-PGS conduit (despite similar studies with different conduit materials showing equivalent performance compared to graft), additional, more optimal conduit designs should be explored to determine the true potential of NP-PGS conduits. A nerve guide conduit with the optimal tube dimensions and design guarantee excellent outcomes quality for nerve regeneration.

In general, PGS is a promising material for create NGCs, because it is flexible, transparent and capable to be sutured. However, further optimisation studies are required in order to provide conduits capable of better regenerative support.

CHAPTER 7

GENERAL DISCUSSION

The main aim of this chapter is to summarise the results described in each of the previous chapters. It will also provide comparisons between conduits utilized in this thesis. Finally, it will indicate potential regions for future study.

7.1 GENERAL DISCUSSION

7.1.1 Peripheral nerve injury

Poor prognosis, incomplete recovery of function and neuropathic pain after peripheral nerve injury can have a major impact and significantly decrease the quality of the patients' life. Peripheral nerve injury and repair is a highly active process. The response of the peripheral nervous system to injury is unique as their axons can regenerate, whereas neurons of the central nervous system do not show this ability or regenerate. Following peripheral nerve injury two stages of process occur; one at the distal stump called Wallerian degeneration and the other one at the proximal stump called axon regeneration. These two processes play a vital role in nerve regeneration. Although the autograft is the gold standard method of repair, it has some disadvantages (see section 1.6.1.2) and the use of nerve guidance provides a potential route forward to reduce the number of autogenous nerve transplantations and their complications in the future. The goal of the current study is to restore the physiology of the injured nerve as close as possible to the normal status, through improving the performance of nerve guide conduits.

7.1.2 Nerve Guide conduit designs in peripheral nerve regeneration

Several conduit materials and designs were evaluated in this thesis. Both common fibular nerve and sciatic nerve injury models were use. PCL conduits structured by µSL performed well, nylon NGC and PGSm porous conduits did not support nerve regeneration, and PGSm non-porous showed promise outcomes. It is difficult to directly compare some of the results described in this thesis due to the effect of some factors such as different nerves, recovery periods and methods of repair in each study (Table 7.1). However, roughly comparisons can be drawn between the repair groups.

Table 7.1: Age, Nerve Injury and Recovery Period in the Repair Groups.			
Type of Treatment	**Age**	**Nerve Injury**	**Recovery Period**
Nylon Conduit	12-18 week-old	Common Fibular nerve	3 weeks
Grooved-PCL Conduit	12-18 week-old	Common Fibular nerve	3 weeks
Smooth-PCL Conduit	12-18 week-old	Common Fibular nerve	3 weeks
Nerve Graft with M6P	12-18 week-old	Common Fibular nerve	2 weeks
PGSm Conduit	12-18 week-old	Common Fibular nerve	3 weeks
PCL Conduit + Etanercept	8-13 week-old	Sciatic nerve	5 weeks

7.1.3 Intra-neural Scarring and Inflammation in Peripheral Nerve Regeneration

Scarring is important for natural wound healing process; however, the presence of scar tissue formation at the site of injury can impede the regeneration process (Graham et al., 1973, Lane et al., 1978, Sunderland, 1978). A ‘‘proof of concept’’ by Atkins et al. (2006b) revealed a relationship between the level of intraneural scar formation and the level of peripheral nerve regeneration.

Transforming growth factor-β (TGF-β) is a cytokine strongly linked to the repair of damaged tissue. Previous investigations have suggested that manipulation of TGF-β may result in a reduction of scarring (Ferguson and O’Kane, 2004, Shah et al., 1992, Shah et al., 1995). M6P inhibits the activation of latent TGFβ by competiviely inhibiting the enzyme (CI-M6PR) activating latent TGFβ which is believed to improve regenration. Following the study by Atkins et al. (2006b), several studies reported positive results after applying of M6P at the site of injury (Harding et al., 2014, Ngeow et al., 2011a, Ngeow et al., 2011b).

The study mentioned in chapter 4 was not designed to replicate these previous studies, but it assessed the effect of M6P using a different route of administration.

M6P was loaded into fibrin glue and applied at the site of injury repair in YFP mice. It was expected to decrease intraneural scar formation and therefore enhance nerve regeneration by interfering with the TGF-β pathway and inhibition its negative impacts on nerve regeneration. No improvements were observed in mice treated with fibrin glue+M6P in either glial activation or nerve regeneration (overall sprouting index, axon tracing and axon disruption).

The process of wound healing starts with the early inflammatory phase and finishes with scar maturation. Because of this, the use of anti-inflammatory agents as scar reducing agents has been established. Tumour necrosis factor alpha (TNF-α) is a pro-inflammatory cytokine that mediates several immune functions. Etanercept is a genetically engineered fusion protein of type II TNF receptor that acts to diminish the effectiveness of TNF-α (Weinblatt et al., 1999). We hypothesised that inhibition of TNF-α using etanercept could reduce the inflammation around the nerve injury site, resulting in reduced scarring and therefore improved nerve regeneration. The study showed that local administration of 0.15mg/100µl of etanercept resulted in decrease the glial activation and reduce axon disruption following peripheral nerve injury. From the results in this thesis, there is some indication that etanercept may be more beneficial towards sensory axons than motor, while M6P may be more beneficial towards motor axons than sensory.

7.1.4 Surgical Approaches to Reduce Scarring Using Fibrin Glue

Suturing helps to enhance the alignment of two nerve ends after injury. In some situations, using sutures can lead increase the possibility of scar tissue formation, irritation, foreign body reaction, and inflammation. Also, it has been reported that suturing can hinder axon sprouting and obstruct the blood supply that can affect the regeneration process (Edshage, 1964, Pabari et al., 2014, Smahel et al., 1987). For these reasons, some experimental studies have used alternative approaches (fibrin glue or laser welding) in nerves that will not be placed under tension/strain during joint movement, instead of suture to avoid these disadvantages (Ornelas et al., 2006). One study reported that using fibrin glue reduced the level of inflammation (Suri et al., 2002), and improved nerve regeneration following sciatic nerve injury (Martins et al., 2005). Reducing the time of the operation is another advantage of

using fibrin glue against suturing. In general, the findings of the current study support the view that using fibrin glue is a good alternative to suturing. However, some complications were reported in some repairs (see section 6.5.5).

7.1.5 Methodology Considerations

7.1.5.1 Analysis of Spinal Glial Activation

Although the mechanisms underlying the maintenance and persistence of neuropathic pain are still unclear, many recent studies (Mika et al., 2013) have implicated spinal glial activation as a key regulator of neuropathic pain. In the resting condition, glial cells are quiescent. In contrast, following peripheral nerve injury, glial cells become activated and release numerous pro-inflammatory factors (Liu and Yuna, 2014, Mika et al., 2013). Glial cells expression can be observed in the spinal cord in both dorsal horns (where the sensory afferent terminals are located) and ventral horns (where the cell bodies of the motor efferents are located) of the L4 segment following the injury of the common fibular and sciatic nerve (Xu et al., 2016). The results related to neuropathic pain mentioned in his thesis have mainly concentrated on the glial activation following nerve injury repair as it is believed that there is a strong link between them. High levels of glial activation are considered to be an indication of a greater potential to develop neuropathic pain, and vice versa. In this thesis glial activation showed significant findings.

Table 7.2 illustrates the differences in glial activation between the repairs groups. It shows that overall Nylon and PGSm porous had higher levels of glial activation than the other groups. Whereas PCL and PGSm non-porous generally produced low levels of glial activation. The information in Table 7.2 was obtained from comparing the groups with their control groups in each chapter.

Table 7.2: Summary of the impacts of various nerve repairs on glial activation compared to their controls.

Immunohistochemistry of spinal cord		**Microglia (Iba-1)**		**Astrocytes (GFAP)**	
Type of Repair	**Control Group**	**Dorsal Horn**	**Ventral Horn**	**Dorsal Horn**	**Ventral Horn**
Nylon Conduit	Intact	↑↑↑	↑↑↑	↑↑↑	↑↑↑
Grooved-PCL Conduit		↔I	↔I	↔I	↔I
Smooth-PCL Conduit		↔I	↔I	↔I	↔I
Nerve Graft with M6P 600mM	Nerve graft without M6P	↔I	↔D	↔D	↔D
Non-porous PGSm Conduit	Nerve graft	↔I	↔I	↔I	↔I
Porous PGSm conduit		↑	↑↑	↑↑	↑↑
PCL Conduit + Etanercept	PCL Conduit + Normal saline	↓	↔D	↓	↔D

↑↑↑ Increase ($p<0.001$) ↑↑ Increase ($p<0.01$) ↑ Increase ($p<0.05$) ↓↓↓ Decrease ($p<0.001$) ↓↓ Decrease ($p<0.01$) ↓↓ Decrease ($p<0.05$)
↔I Increase (not significant) ↔D Decrease (not significant)

7.1.5.2 Analysis of CatWalk System

The CatWalk system for gait analysis is one of the most popular gait analysis tools used in the assessment of functional recovery after nerve injury (Chen et al., 2017). The intensity of paw print and print area parameters are of particular interest when evaluating the functional axon regeneration. CatWalk gait can be also used as a behavioural test to assess the development of neuropathic pian. It was reported that CatWalk is superior to the Von Frey testing, a method has been widely used to measure mechanical allodynia Vrinten and Hamers (2003). In this thesis CatWalk gait showed significant findings.

7.1.5.3 Analysis of Electrophysiology

Several studies have used electrophysiology to evaluate the recovery function. Higher CAP modulus ratio is an indication of better regeneration, suggesting that a higher percentage of axons had crossed the repaired gap successfully and reached the distal stimulating electrodes, and vice versa**.** Better regeneration and larger axonal diameters are achieved by faster conduction velocities. In the thesis electrophysiology did not show significant findings.

Electrophysiology and CatWalk were performed only in the sciatic nerve model (Chapter 5), as the sciatic nerve innervates a larger region than the common fibular nerve and has a greater impact on gait.

7.1.5.4 Analysis of Axon Counting and Tracing

Axon Counting and Tracing analysis of nerve is a useful method that was established recently. It has the ability to allow direct observation of each individual axon as they can be seen using a fluorescent or confocal microscope. Previously, Groves et al. (2005) and Sabatier et al. (2008) used axon counting and tracing analysis on YFP mice in order to calculate the sprouting index ratio for a single point distal to the repair site. In the current study the equivalent outcome measure of sprouting index was performed at several separate intervals, extending from the proximal to the distal ends. By using multiple intervals and not just a single interval, provides more detailed information about the sprouting index ratio. The number of

labelled axons in common fibular nerve in the current study is approximately 28 axons, which is close to 36 axons that reported by Groves et al. (2005). On the other hand, the number of labelled axons in the sciatic nerve in the current study is approximately 74 axons, which is much higher than 28 axons that reported by Beirowski et al. (2004). It is unclear why much lower labelled axons were observed by Beirowski et al. (2004) compared to both the current study and Groves et al. (2005), as common fibular nerve is a terminal branch of the sciatic nerve.

7.2 SUGGESTIONS FOR FUTURE OUTLOOK

The potential negative consequences of graft repair and the promising results shown by some nerve guide conduits, provide a rationale for further work that made lead to the development of nerve conduits that can be used instead of grafts.

7.2.1 Improvement of the Effectivity of Nerve Guidance Conduits

There are a number of approaches that can be taken to improve the ability of conduits to enhance nerve regeneration.

7.2.1.1 Physical Structure

The physical structure of a conduit (e.g. material, coating, and internal structure) plays a crucial role in nerve regeneration. Flexibility and strength properties should be present in the conduit to avoid blocking the axons from regeneration and to prevent the conduit from being easy to collapse. Conductive polymer is a new approach used to enhance nerve regeneration by accelerating axonal elongation. Moreover, electrical stimulation has been reported to help to guide regenerated axons (de Ruiter et al., 2009). Xu et al. (2014) compared conductive poly (D, L-lactic acid) (PDLLA), and polypyrrole (PPY)/PDLLA, to autograft repairs after sciatic nerve injury in rats. Walking track analysis was used to calculate the sciatic function index (SFI). They reported that at 3 and 6 months postoperative, PPY/PDLLA group had a significantly higher percentage compared to PDLLA and autograft groups. Footprints analysis of the same study showed that PPY/PDLLA group had a greater enhancing

in toe spreading, which was similar to those seen in autogarft group (Xu et al., 2014). In contrast, previous studied reported that there is no effect of conductive polymers on neurite outgrowth (Lee et al., 2009, Schmidt et al., 1997). This coated method was evaluated in PCL conduits and reported by Choi et al. (2015). In their study, PCL conduit was coated with conductive materials (single-walled carbon nanotubes (SWNT) and poly (3,4-ethylenedioxythiophene): polystyrene sulfonate (PEDOT:PSS)) for facilitating regenerating axons after injury of the recurrent laryngeal nerve (RLN) of rabbit model. They compared these two coated PCL materials with non-coated PCL. The results reported that coated PCL enhanced vocal cord mobility and decreased atrophy of the thyroarytenoid muscle compare to that of the non-coated PCL group (Choi et al., 2015).

7.2.1.2 Addition of Supportive Cells

Implantation of supportive cells (e.g. Schwann and stem cells) in the conduits is another approach can help to improve the outcomes. Sasaki et al. 2011 investigated the use of a new host-derived source of cells (dental pulp (DPCs)) inside conduits because they comprise of Schwann cells, stem cells, and endothelial cells. In 2008, they reported that silicon tubes filled with DPCs promoted nerve regeneration (Sasaki et al., 2008). In 2011, they used poly-DL-lactide-co-glycolide (PLGA) (50% PLLA and 50% PGA) conduits instead of silicon because it is a biodegradable material. They transplanted these cells into a collagen gel and then filled the conduits with the gel. The results of the study suggested that these cells help to promote axon regeneration, and using of this type of conduit acts as bioactive nerve guide till the two ends reconnected then they dissolved (Sasaki et al., 2008, Sasaki et al., 2011). Another study by Evans et al., (2002) compared three types of repair; Poly (L-lactic acid) (PLLA) conduits implanted with Schwann cells, isografts, and empty silicon tubes. The study reported that there is no significant difference in the functional outcomes of PLLA conduits filled with Schwann cells and isograft repairs (Evans et al., 2002). Thus, the addition of supportive cells or drugs in conduit repairs could enhance the efficacy of the treatment.

7.2.2 Enhancing the Poly-glycerol Sebacate (PGS) Conduits

PGS showed excellent outcomes in both *in-vitro* by supporting neural cell growth and *ex-vivo* by the DRGs analysis. Also the results of the *in-vivo* showed that it had a low level of glial activation. However, PGS was inferior in some areas of nerve regeneration analysis comparing to nerve graft, suggesting that further conduit designs should be explored for the purpose of maximize the potential of the polymer.

7.2.3 Administration of Mannose-6-Phosphate

The therapeutic failure of using 600Mm M6P (chapter 4) could be due to inappropriate dosage, timing, duration, or route of administration. So, another dose of M6P injected into the surrounding tissue might help to enhance the efficacy of the used route. It is unclear how much M6P is released from the fibrin glue. Thus, further investigation may be warranted in order to optimise the dosage, administration route and determine any effect.

7.2.4 Sciatic Nerve Injury Model in YFP Mice

A further study should be carried out to investigate the regeneration of the sciatic nerve after nerve graft repair using axon counting and tracing analysis. Then compare the results with the results mentioned in Chapter 5. To date, no data has been published using a sciatic nerve injury model with axon counting and tracing analysis (in YFP mice), thus the study in this thesis is the first to use this method to assess sciatic nerve regeneration. However, tracing the larger number of axons in the sciatic nerve (compared to the common fibular nerve) is challenging.

When comparing the results related to the axons tracing for nerve graft repairs of the common fibular nerve (where 22.2% of axons reached the distal end of the graft) mentioned in Chapter 6 to those for PCL conduit repairs of the sciatic nerve (where 24.3% of the axons reached the distal end of the conduit repair) mentioned in Chapter 5, it seems that PCL conduit repair of the sciatic may produce a similar percentage of unique axons represented at the final interval (compared to nerve graft repair of the common fibular nerve) (Figure 7.1). This gives some indication that the conduit repair in the sciatic may be similar to graft repair, but clearly further studies are required to directly compare graft and conduit repair of the sciatic nerve.

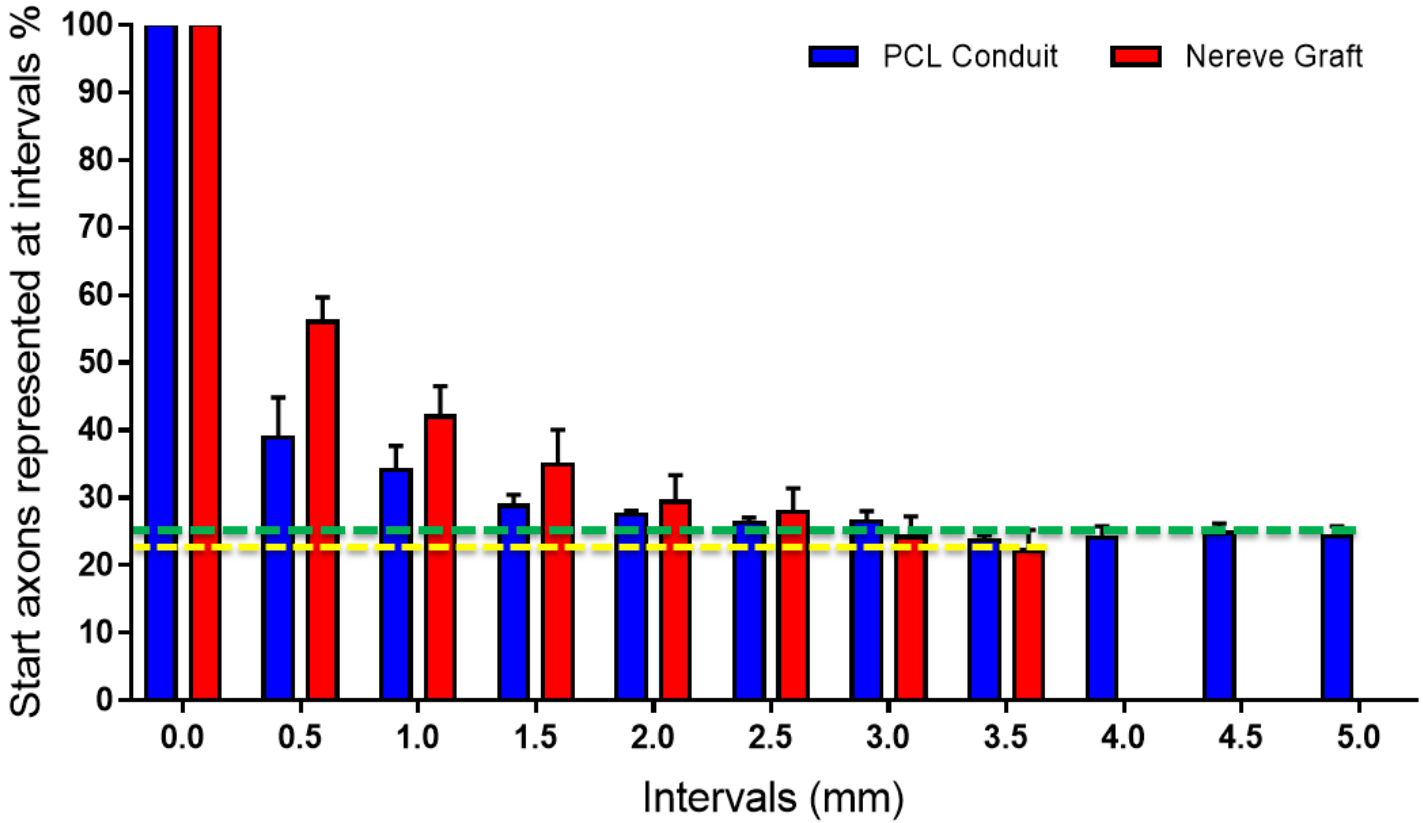

Figure 7.1: Analysis of nerve regeneration following PCL conduit and graft repairs. PCL conduit repair of sciatic nerve (blue bars) had a similar percentage (24.3%) of axons represented at the distal end of the repair compared to nerve graft repairs of common fibular nerve (red bars, 22.2%).

7.2.5 Different Angle of Forming Nerve Guidance Conduits

The 3D printing methodology allows creating a conduit with different shapes. For example, if the affected area includes bifurcated nerves such as when the sciatic bifurcate to tibial and common fibular nerves, it is possible to bridge it with an appropriately designed conduit (Figure 7.2) (Johnson et al., 2015). Whereas, this would be difficult to achieve when using nerve graft.

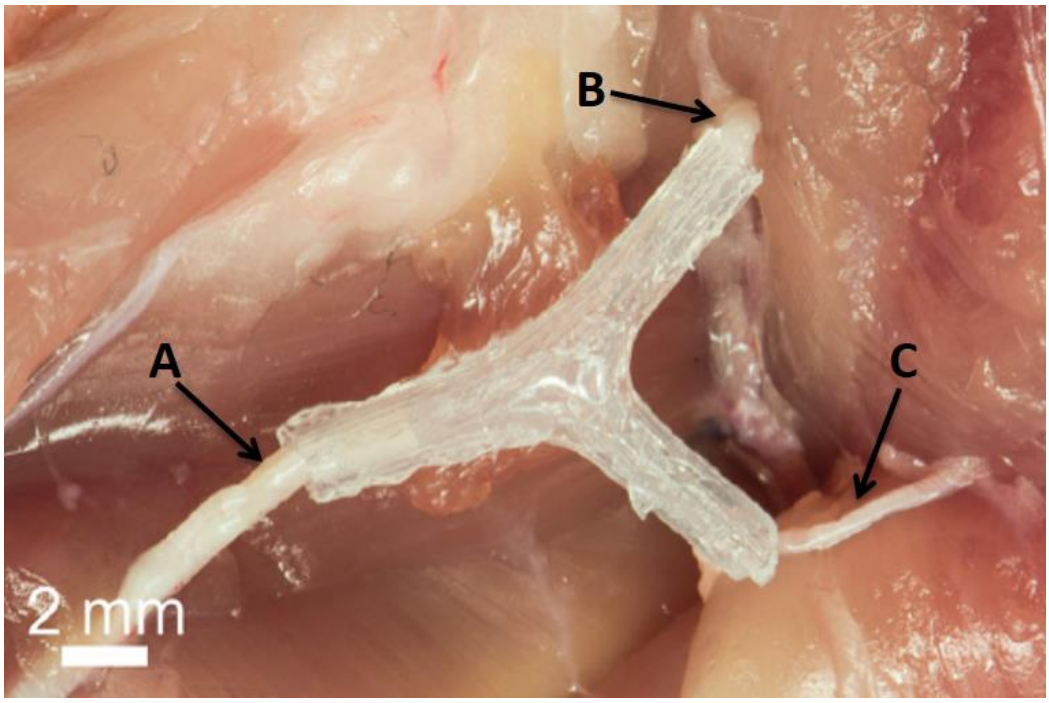

Figure 7.2: 3D bifurcate conduit placed between A) Sciatic nerve, B) Tibial nerve and C) Common fibular nerve (Johnson et al., 2015).

7.3 CONCLUSION

The studies described in this thesis showed that nerve guide conduit can be used as an alternative method to bridge a gap of injured nerves. Moreover, the use of etanercept reduces the level of inflammation and therefore enhances the nerve regeneration. The Common fibular nerve injury model offers a good method for assessing nerve regeneration. The use of YFP mice and axon counting and tracing methods gives more detail about the injury repair such as detecting the decrease of axon disruption in etanercept treated repairs. In addition, it helps to observe the organisation of regenerated axons.

In summary, autografting remains the clinical gold standard for nerve gap repair; however, promising advances have been reported in the development of artificial nerve guides, suggesting that with further work conduits that can fully replace the use of nerve grafts may be developed.

REFERENCES

Abd-El-Basset, E. M. (2013). Pro-inflammatory cytokine; tumor-necrosis factoralpha (TNF-a&RPKT; inhibits astrocytic support of neuronal survival and neurites outgrowth. *Advances in Bioscience and Biotechnology***.** 4, 73-80.

Acheson, A., et al. (1991). Detection of brain- derived neurotrophic factor- like activity in fibroblasts and Schwann cells: Inhibition by antibodies to NGF. *Neuron* 7(2) 265-275.

Aebischer, P., et al. (1988). Blind- ended semipermeable guidance channels support peripheral nerve regeneration in the absence of a distal nerve stump. *Brain Research* 454(1) 179-187.

Aguayo, A.et al. (1982). Axonal elongation in peripheral and central nervous system transplants. *Fedoroff, S. and L. Hertz (Ed.). Advances in Cellular Neurobiology, Vol. 3. Academic Press, Inc.: New York, N.Y., USA: London, England. Illus*, P215-234.

AlSalihi, M. O., et al. (2017). Tumor necrosis factor-α antagonist suppresses local inflammatory reaction and facilitates olfactory nerve recovery following injury. *Auris Nasus Larynx* 44(1) 70-78.

Alovskaya A, et al. (2007) Chapter 12: Fibronectin, Collagen, Fibrin - Components of Extracellular Matrix for Nerve regeneration. Topics in Tissue Engineering. Ashammakhi, Reis RL, Chiellini E (Eds). Expertissues E-book, Vol. 3, University of Oulu, Oulu, Finland.

Andrews, K. (1993). The effect of changes in temperature and humidity on the accuracy of von Frey hairs. *Journal of Neuroscience Methods* 50(1) 91-93.

Ängeby Möller, K., B. Johansson and O.-G. Berge (1998). Assessing mechanical allodynia in the rat paw with a new electronic algometer. *Journal of Neuroscience Methods* 84(1) 41-47.

Annadora, J. B., et al. (1996). Altered neuronal and microglial responses to excitotoxic and ischemic brain injury in mice lacking TNF receptors. *Nature Medicine* 2(7) 788.

Archibald, S., et al. (1995). Monkey median nerve repaired by nerve graft or collagen nerve guide tube. *Journal of Neuroscience* 15(5) art II-4123.

Archibald, S. J., et al. (1991). A collagen-based nerve guide conduit for peripheral nerve repair: An electrophysiological study of nerve regeneration in rodents and nonhuman primates. *Journal of Comparative Neurology.* 306(4) 685-696.

Arslantunali, D., et al. (2014). Peripheral nerve conduits: technology update. *Medical Devices (Auckland, N.Z.)* 7 405-424.

Artico, M., et al. (1996). Birthday of peripheral nervous system surgery: The contribution of Gabriele Ferrara (1543-1627). *Neurosurgery* 39(2) 380-383.

Ashley Jr, W. W., T. Weatherly and S. P. Tae (2006). Collagen nerve guides for surgical repair of brachial plexus birth injury. *Journal of Neurosurgery* 105(6) 452-456.

Ashur, H. et al. (1987). Extent of fibre regeneration after peripheral nerve repair: silicone splint vs suture, gap repair v graft. *Experimental Neurology*. 97, 365-374.

Atkins, S., et al. (2007). Interleukin- 10 reduces scarring and enhances regeneration at a site of sciatic nerve repair. *Journal of the peripheral nervous system: JPNS* 12(4) 269.

Atkins, S., et al. (2006a). The effect of antibodies to TGF-beta 1 and TGF-beta 2 at a site of sciatic nerve repair. *Journal of the peripheral nervous system.* 11(4) 286-293.

Atkins S. et al. (2006b). Scarring impedes regeneration at sites of peripheral nerve repair. *Neuroreport,* 17, 1245-1249.

Bailey, R., et al. (2009). Effect of Upper Extremity Nerve Damage on Activity Participation, Pain, Depression, and Quality of Life. *Journal of Hand Surgery* 34(9) 1682-1688.

Bastien, D. and S. Lacroix (2014). Cytokine pathways regulating glial and leukocyte function after spinal cord and peripheral nerve injury. *Experimental Neurology.* 62-77.

Battiston, B., et al. (2005). Nerve repair by means of tubulization: Literature review and personal clinical experience comparing biological and synthetic conduits for sensory nerve repair. *Microsurgery* 25(4) 258-267.

Bayrakli, F., et al. (2012). Etanercept treatment enhances clinical and neuroelectrophysiological recovery in partial spinal cord injury. *European Spine Journal* 21(12) 2588-2593.

Beggs, S. and M. W. Salter (2007). Stereological and somatotopic analysis of the spinal microglial response to peripheral nerve injury. *Brain Behavior and Immunity* 21(5) 624-633.

Beggs, S. and M. W. Salter (2013). The known knowns of microglia– neuronal signalling in neuropathic pain. *Neuroscience Letters* 557 37-42.

Beirowski, B., et al. (2004). Quantitative and qualitative analysis of Wallerian degeneration using restricted axonal labelling in YFP- H mice. *Journal of Neuroscience Methods* 134(1) 23-35.

Bell-Krotoski, J. and E. Tomancik (1987). The repeatability of testing with Semmes- Weinstein monofilaments. *Journal of Hand Surgery* 12(1) 155-161.

Benson, M. D., et al. (2005). Ephrin- B3 is a myelin- based inhibitor of neurite outgrowth. *Proceedings of the National Academy of Sciences of the United States of America* 102(30) 10694.

Beuche, W. and R. Friede (1984). The role of non- resident cells in Wallerian degeneration. *Journal of Neurocytology* 13(5) 767-796.

Bhandari, P. S. (2013). Use of fibrin glue in the repair of brachial plexus and peripheral nerve injuries. *The Indian Journal of Neurotrauma* 10(1) 30-32.

Bla**c**kburn, J. L. et al. (2008). A comparison of functional recovery indices following sciatic nerve repair in mice (Poster). European Winter Conference on Brain Research, France.

Bozkurt, A., et al. (2008). CatWalk gait analysis in assessment of functional recovery after sciatic nerve injury. *Journal of Neuroscience Methods* 173(1) 91-98.

Bozkurt, A., et al. (2011). Aspects of static and dynamic motor function in peripheral nerve regeneration: SSI and CatWalk gait analysis. *Behavioural Brain Research* 219(1) 55-62.

Breen, A., et al. (2009). Fibrin scaffold promotes adenoviral gene transfer and controlled vector delivery. *Journal of Biomedical Materials Research Part A* 89(4) 876-884.

Brennan, M., (1991). Fibrin glue. *Blood reviews*. 5(4), 240-244.

Brushart, T. M. (1993). Motor axons preferentially reinnervate motor pathways. *The Journal of neuroscience : the official journal of the Society for Neuroscience* 13(6) 2730.

Bruce, A.J. et al. (1996). Altered neuronal and microglial responses to excitotoxic and ischemic brain injury in mice lacking TNF receptors. *Nature medicine.* 2(7), 788-794.

Brück, W. (1997). The Role of Macrophages in Wallerian Degeneration. Oxford, UK. 741-752.

Burnett, M. G. and E. L. Zager (2004). Pathophysiology of peripheral nerve injury: a brief review. *Neurosurgical focus* 16(5) E1.

Burry, R. W. (2011). Controls for Immunocytochemistry: An Update. *journal of histochemistry and cytochemistry.* 6-12.

Bushnell, B. D., et al. (2008). Early Clinical Experience with Collagen Nerve Tubes in Digital Nerve Repair. *Journal of Hand Surgery* 33(7) 1081-1087.

Chang C.J. (2009a). Effects of nerve growth factor from genipin-crosslinked gelatin in polycaprolactone conduit on peripheral nerve regeneration-in vitro and in vivo. *Journal of Biomedical Materials Research* Part A 91A, 586-596.

Chang C.J. (2009b). The Effect of Pulse-Released Nerve Growth Factor from Genipin-Crosslinked Gelatin in Schwann Cell-Seeded Polycaprolactone Conduits on Large-Gap Peripheral Nerve Regeneration. *Tissue Engineering* Part A 15, 547-557.

Cajal, S.R. (1991). Cajal's Degeneration and Regeneration of the Nervous System. Oxford: Oxford University Press Inc.

Calder, J. and Green C. (1995). Nerve- muscle sandwich grafts: The importance of schwann cells in peripheral nerve regeneration through muscle basal lamina conduits. *Journal of Hand Surgery* 20(4) 423-428.

Campbell, P. G., et al. (1999). Insulin- like growth factor- binding protein- 3 binds fibrinogen and fibrin. *Journal of Biological Chemistry* 274(42) 30215-30221.

Campbell, W. W. (2008). Evaluation and management of peripheral nerve injury. *Clinical Neurophysiology* 119(9) 1951-1965.

Caroni, P. (1997). Overexpression of growth- associated proteins in the neurons of adult transgenic mice. *Journal of Neuroscience Methods* 71(1) 3-9.

Catelas, I., J. F. Dwyer and S. Helgerson (2011). Controlled Release of Bioactive Transforming Growth Factor Beta- 1 from Fibrin Gels In Vitro. *Tissue Engineering Part C: Methods* 110306233138079.

Chan, F. K.-M., R. M. Siegel and M. J. Lenardo (2000). Signaling by the TNF Receptor Superfamily and T Cell Homeostasis. *Immunity* 13(4) 419-422.

Chandross, K., et al. (1996). TNF alpha inhibits Schwann cell proliferation, Connexin46 expression, and gap junctional communication. *Molecular and Cellular Neuroscience.* 7(6) 479-500.

Chang, C. J. (2009a). Effects of nerve growth factor from genipin-crosslinked gelatin in polycaprolactone conduit on peripheral nerve regeneration-in vitro and in vivo. *Journal of Biomedical Materials Research.* Part A 91A, 586-596.

Chang, C. J. (2009b) The Effect of Pulse-Released Nerve Growth Factor from Genipin-Crosslinked Gelatin in Schwann Cell-Seeded Polycaprolactone Conduits on Large-Gap Peripheral Nerve. Regeneration. *Tissue Engineering* Part A 15, 547-557.

Chen, R. K.-B., et al. (2011). Tumor Necrosis Factor-α Antagonist Reduces Apoptosis of Neurons and Oligodendroglia in Rat Spinal Cord Injury. *Spine.* 36(17) 1350-1358.

Chen, Z.-L., W.-M. Yu and S. Strickland (2007). *Peripheral Regeneration*. 30 209-233.

Chiono, V. et al. (2008). Enzymatically-modified melt-extruded guides for peripheral nerve repair. *Engineering in Life Sciences.* 8,226-237.

Choi, J. S. et al. (2015). Regeneration of recurrent laryngeal nerve using polycaprolactone (PCL) nerve guide conduit coated with conductive materials. *Journal of Korean Thyroid Association. 8*(1) 88-97.

Clemence, A., R. Mirsky and K. Jessen (1989). Non- myelin- forming Schwann cells proliferate rapidly during Wallerian degeneration in the rat sciatic nerve. *Journal of Neurocytology* 18(2) 185-192.

Coderre, T., R. Grimes and R. Melzack (1986). Deafferentation and chronic pain in animals: An evaluation of evidence suggesting autotomy is related to pain. *Pain*. 26, 61-84.

Cohen, S.P. and Mao, J. (2014). Neuropathic pain: mechanisms and their clinical implications. *British Medical Journal (Online)*, 348.

Colburn, R. W., A. J. Rickman and J. A. Deleo (1999). The Effect of Site and Type of Nerve Injury on Spinal Glial Activation and Neuropathic Pain Behavior. *Experimental Neurology* 157(2) 289-304.

Cornwall, R. and T. Radomisli (2000). Nerve injury in traumatic dislocation of the hip. *Clinical Orthopaedics and Related Research.* (377) 84-91.

Coyle, D. E. (1998). Partial peripheral nerve injury leads to activation of astroglia and microglia which parallels the development of allodynic behavior. *Glia* 23(1) 75-83.

Crang, A. and W. Blakemore (1987). Observations on the migratory behaviour of Schwann cells from adult peripheral nerve expiant cultures. *Journal of Neurocytology* 16(3) 423-431.

Cruz, N. I., N. Debs and R. E. Fiol (1986). Evaluation of fibrin glue in rat sciatic nerve repairs. *Plastic and Reconstructive Surgery* 78(3) 369-373.

Cui, Y. et al. (2018). Functional collagen conduits combined with human mesenchymal stem cells promote regeneration after sciatic nerve transection in dogs. *Journal of tissue engineering and regenerative medicine*, 12(5) 1285-1296.

D'Mello, R. and Dickenson, A. H. (2008). Spinal cord mechanisms of pain. *British journal of anaesthesia*, *101*(1), 8-16.

Dagum, A. B. (1998). Peripheral nerve regeneration, repair, and grafting. *Journal of Hand Therapy* 11(2) 111-117.

Dahlin, L. B. (2008). (ii) Nerve injuries. *Current Orthopaedics* 22(1) 9-16.

Dahlin, L. B., Anagnostaki, L. and Lundborg, G. (2001) Tissue response to silicone tubes used to repair human median and ulnar nerves. *Scandinavian journal of plastic and reconstructive surgery and hand surgery.* 35(1) 29-34.

Davison, S.P. et al. (1999). Improved Nerve Regeneration With Neutralization of Transforming Growth Factor-β1. *The Laryngoscope*, 109(4), 631-635.

Daly, T. J. and W. L. Weston (1986). Retinoid effects on fibroblast proliferation and collagen synthesis in vitro and on fibrotic disease in vivo. *Journal of the American Academy of Dermatology* 15(4) 900-902.

De Medinaceli, L., W. J. Freed and R. J. Wyatt (1982). An index of the functional condition of rat sciatic nerve based on measurements made from walking tracks. *Experimental Neurology* 77(3) 634-643.

De Ruiter, G., et al. (2008). Accuracy of motor axon regeneration across autograft, single- lumen, and multichannel poly(lactic- co- glycolic acid) nerve tubes. *Neurosurgery* 63(1) 144-153.

De Ruiter, G. C., et al. (2008). Methods for in vitro characterization of multichannel nerve tubes. *Journal of Biomedical Materials Research Part A* 84(3) 643-651.

De Ruiter, G. C. W., et al. (2009). Designing ideal conduits for peripheral nerve repair. *Neurosurgical focus* 26(2) E5.

Dellon, A. L. and S. E. Mackinnon (1988). An alternative to the classical nerve graft for the management of the short nerve gap. *Plastic and reconstructive surgery* 82(5) 849.

Dellon, A. L. and C. T. Maloney (2006). Salvage of Sensation in a Hallux-to- Thumb Transfer by Nerve Tube Reconstruction. *Journal of Hand Surgery* 31(9) 1495-1498.

Den Dunnen, W., et al. (1998). Peripheral nerve regeneration through P (DLLA- epsilon- CL) nerve guides. *Journal of Materials Science: Materials in Medicine.* 9(12) 811-814.

Dennis, P. A. and D. B. Rifkin (1991). Cellular activation of latent transforming growth factor beta requires binding to the cation- independent Mannose 6- phosphate/ insulin- like growth factor type II receptor. *Proceedings of the National Academy of Sciences of the United States of America* 88(2) 580.

Deumens, R., et al. (2007). The CatWalk gait analysis in assessment of both dynamic and static gait changes after adult rat sciatic nerve resection. *Journal of Neuroscience Methods* 164(1) 120-130.

Donoghoe, N., G. Rosson and A. L. Dellon (2007). Reconstruction of the human median nerve in the forearm with the neurotube (TM). *Microsurgery* 27(7) 595-600.

Dotchev, K. and Yusoff, W. (2009). Recycling of polyamide 12 based powders in the laser sintering process. *Rapid Prototyping Journal.* 15, 192-203.

Ducker, T. B. and G. J. Hayes (1968). Experimental improvements in the use of Silastic cuff for peripheral nerve repair. *Journal of neurosurgery* 28(6) 582.

Dworkin, R. H., et al. (2010). Recommendations for the Pharmacological Management of Neuropathic Pain: An Overview and Literature Update. *Mayo Clinic Proceedings* 85(3) S3-S14.

Edshage, S. (1964). Peripheral nerve suture. Techniques for improved intraneural topography evaluation of some suture materials. *Acta chirurgica Scandinavica. Supplementum*, *15*, 331

Einheber, S., et al. (1995). Transforming growth factor-β1 regulates axon/ Schwann cell interactions. *Journal of Cell Biology* 129(2) 443-458.

Elizabeth, J. B., et al. (2002). Chondroitinase ABC promotes functional recovery after spinal cord injury. *Nature* 416(6881) 636.

Eriksson, N., et al. (1993). A quantitative analysis of the microglial cell reaction in central primary sensory projection territories following peripheral nerve injury in the adult rat. *Experimental Brain Research* 96(1) 19-27.

Evans, G. R. D., et al. (2002). Bioactive poly(l-lactic acid) conduits seeded with Schwann cells for peripheral nerve regeneration. *Biomaterials* 23(3) 841-848.

Evans, G. R. D., et al. (1999). In vivo evaluation of poly(l-lactic acid) porous conduits for peripheral nerve regeneration. *Biomaterials* 20(12) 1109-1115.

Evans, P. J., R. Midha and S. E. Mackinnon (1994). The peripheral nerve allograft: A comprehensive review of regeneration and neuroimmunology. *Progress in Neurobiology* 43(3) 187-233.

Farole, A. and B. T. Jamal (2008). A Bioabsorbable Collagen Nerve Cuff (NeuraGen) for Repair of Lingual and Inferior Alveolar Nerve Injuries: A Case Series. *Journal of Oral and Maxillofacial Surgery* 66(10) 2058-2062.

Faweett, J. W. and R. J. Keynes (1990). Peripheral Nerve Regeneration. *Annual Review of Neuroscience.* 13(1) 43-60.

Feng, G., et al. (2000). Imaging Neuronal Subsets in Transgenic Mice Expressing Multiple Spectral Variants of GFP. *Neuron* 28(1) 41-51.

Ferguson, M. W. J. and S. Kane (2004). Scarfree healing: from embryonic mechanisms to adult therapeutic intervention. *Philosophical Transactions of the Royal Society B: Biological Sciences* 359(1445) 839-850.

Fischer, D. W., et al. (1985). Comparative study of microepineurial anastomoses with the use of CO 2 laser and suture techniques in rat sciatic nerves: Part 1. Surgical technique, nerve action potentials, and morphological studies. *Neurosurgery* 17(2) 300-308.

Flores, A. J., Lavemia, C. J. and Owens, P. W. (2000). Anatomy and physiology of peripheral nerve injury and repair. *The American Journal of Orthopedics, 29*(3) 167-178.

Foltán, R., et al. (2008). Mechanism of traumatic neuroma development. *Medical Hypotheses* 71(4) 572-576.

Forman, D. S., et al. (1980). Time course of the conditioning lesion effect on axonal regeneration. *Brain Research* 182(1) 180-185.

Friede, R. L. and R. Bischhausen (1980). The fine structure of stumps of transected nerve fibers in subserial sections. *Journal of the Neurological Sciences* 44(2) 181-203.

Friedlander, D. R., M. Grumet and G. M. Edelman (1986). Nerve growth factor enhances expression of neuron-glia cell adhesion molecule in PC12 cells. *Journal of Cell Biology* 102(2) 413-419.

Gabriel, A. F., et al. (2007). The CatWalk method: A detailed analysis of behavioral changes after acute inflammatory pain in the rat. *Journal of Neuroscience Methods* 163(1) 9-16.

Garrison, C. J., et al. (1991). Staining of glial fibrillary acidic protein (GFAP) in lumbar spinal cord increases following a sciatic nerve constriction injury. *Brain Research* 565(1) 1-7.

Gaudin, R., et al. (2016). Approaches to Peripheral Nerve Repair: Generations of Biomaterial Conduits Yielding to Replacing Autologous Nerve Grafts in Craniomaxillofacial Surgery. *BioMed Research International* 2016.

Genovese, T. et al. (2008). TNF-alpha blockage in a mouse model of SCI: evidence for improved outcome. *Shock.* 29, 32–41.

George, E. B., Glass J. and Griffin J. (1995). Axotomy- induced axonal degeneration is mediated by calcium influx through ion- specific channels. *The Journal of neuroscience: the official journal of the Society for Neuroscience* 15(10) 6445.

Gerecht, S. et al. (2007). A porous photocurable elastomer for cell encapsulation and culture. *Biomaterials.* 28(32), 4826-4835.

Geuna, S. et al. (2009). Histology of the Peripheral Nerve and Changes Occurring During Nerve Regeneration. *Essays on Peripheral Nerve Repair and Regeneration.* 87, 27-46.

Ghosh P., Dahms N. M., Kornfeld S. (2003) Mannose 6-phosphate receptors: new twists in the tale. *Nature reviews Molecular cell biology*, *4*(3) 202-213.

Gibson, K. L. et al. (1991). Comparison of nerve regeneration through different types of neural prostheses. *Microsurgery*. *12*(2), 80-85.

Gilron, I., et al. (2006). Neuropathic pain: a practical guide for the clinician. *The Canadian Medical Association Journal.* 265-275.

Glasby, M. (1991). Interposed muscle grafts in nerve repair in the hand: An experimental basis for future clinical use. *World Journal of Surgery* 15(4) 501-510.

Gomez, N. et al. (1996). Histologic assessment of sciatic nerve regeneration following resection and graft or tube repair in the mouse. *Restorative neurology and neuroscience,* 10(4) 187−196.

Gonzalez-Perez, F. et al. (2017). Schwann cells and mesenchymal stem cells in laminin-or fibronectin-aligned matrices and regeneration across a critical size defect of 15 mm in the rat sciatic nerve. *Journal of Neurosurgery: Spine*, 1-10.

Goraltchouk A, Freier T, Shoichet MS (2005) Synthesis of degradable poly(L-lactide-co-ethylene glycol) porous tubes by liquid-liquid centrifugal casting for use as nerve guidance channels. *Biomaterials*. 26,7555-7563.

Gordon, T. and G. H. Borschel (2017). The use of the rat as a model for studying peripheral nerve regeneration and sprouting after complete and partial nerve injuries. *Experimental Neurology* 287 331-347.

Goulart, C. O., et al. (2016). Evaluation of biodegradable polymer conduits – poly(l- lactic acid) – for guiding sciatic nerve regeneration in mice. *Methods* 99 28-36.

Graham W. P. et al. (1973). Enhancement of peripheral nerve regeneration withtriamcinolone after neurorrhaphy. *Surgery Forum*. 24, 457-459.

Grados-Munro, E. M. and A. E. Fournier (2003). Myelin- associated inhibitors of axon regeneration. *Hoboken*. 479-485.

Griffin, J. W. and W. J. Thompson (2008). Biology and pathology of nonmyelinating Schwann cells. *In* K. R. Jessen, R. Mirsky and J. Salzer eds. Hoboken. 1518-1531.

Groves, M. L., et al. (2005). Axon regeneration in peripheral nerves is enhanced by proteoglycan degradation. *Experimental neurology* 195(2) 278.

Hadlock, T., et al. (2000). A Polymer Foam Conduit Seeded with Schwann Cells Promotes Guided Peripheral Nerve Regeneration. *Tissue Engineering* 6(2) 119-127.

Hall, S. (1997). Axonal regeneration through acellular muscle grafts. *Journal of anatomy* 190 (Pt1) 57.

Hamers, F. P. et al. (2001). Automated quantitative gait analysis during overground locomotion in the rat: its application to spinal cord contusion and transection injuries. *Journal of neurotrauma*, 18(2) 187-201.

Harding, A. 2014. The use of the *thy-1-yfp-h* transgenic mouse strain in studies of peripheral nerve injury (Doctoral dissertation, University of Sheffield).

Harding, A. J., et al. (2014). Mannose- 6- phosphate facilitates early peripheral nerve regeneration in thy- 1- YFP- H mice. *Neuroscience* 279 23-32.

Harris R. and Matthews, B. (1978) Amplifiers for electrophysiology. *Journal of Physiology*. 277, 34P-35P.

Hausamen, J. E. and Schmelzeisen, R. (1996). Current principles in microsurgical nerve repair. *British Journal of Oral and Maxillofacial Surgery*. 34(2), 143-157.

Heath, C. A. and G. E. Rutkowski (1998). The development of bioartificial nerve grafts for peripheral-nerve regeneration. *Trends in Biotechnology* 16(4) 163-168.

Hellal, F., et al. (2011). Microtubule stabilization reduces scarring and causes axon regeneration after spinal cord injury. *Science (New York, N.Y.)* 331(6019) 928.

Herx, L. and V. Yong (2001). Interleukin- 1[beta] is Required for the Early Evolution of Reactive Astrogliosis Following CNS Lesion. *Journal of Neuropathology & Experimental Neurology* 60(10) 961-971.

Hoenig, L. J. (1997). Jacob's limp. *Seminars in Arthritis and Rheumatism* 26(4) 684-688.

Holland GR, Robinson PP (1998) Peripheral Nerve Damage and Repair. In: Clinical Oral Science (Harris, M. et al., eds), 279-280 Oxford, UK: John Wright.

Ichihara, S., Y. Inada and T. Nakamura (2008). Artificial nerve tubes and their application for repair of peripheral nerve injury: an update of current concepts. *Injury* 39 29-39.

Ide, C. (1996). Peripheral nerve regeneration. *Neuroscience Research* 25(2) 101-121.

Imamoto, N., et al. (2013). [11C] PK11195 PET imaging of spinal glial activation after nerve injury in rats. *NeuroImage* 79 121-128.

Jackson, S.J. et al. (2017). Does age matter? The impact of rodent age on study outcomes. *Laboratory animals*. 51(2), 160-169.

Jaggi, A. S. and N. Singh (2011). Role of different brain areas in peripheral nerve injury- induced neuropathic pain. *Brain Research* 1381 187-201.

James, L. S. and P. B. Richard (1980a). Studies of Schwann cell proliferation. I. An analysis in tissue culture of proliferation during development, Wallerian degeneration, and direct injury. *The Journal of Cell Biology* 84(3) 739-752.

Jang, C. H., et al. (2016). Effect of polycaprolactone/collagen/hUCS microfiber nerve conduit on facial nerve regeneration. *International Journal of Biological Macromolecules* 93 1575-1582.

Jansen, K., et al. (2004). Long- term regeneration of the rat sciatic nerve through a biodegradable poly(DL- lactide- epsilon- caprolactone) nerve guide: Tissue reactions with focus on collagen III/ IV reformation. *Journal of Biomedical Materials Research Part A.* 69A(2) 334-341.

Jernigan, W. T., et al. (2004). Small Intestinal Submucosa for Vascular Reconstruction in the Presence of Gastrointestinal Contamination. *Annals of Surgery* 239(5) 733-740.

Jiang, X., et al. Nanofibrous nerve conduit-enhanced peripheral nerve regeneration. *Journal of tissue engineering and regenerative medicine*. *8*(5) 377-385.

Johansson, C. B., et al. (1999). Identification of a Neural Stem Cell in the Adult Mammalian Central Nervous System. *Cell* 96(1) 25-34.

Johnson, A., Bingham, G. and Wimpenny, D. (2013). Additive manufactured textiles for high-performance stab resistant applications. *Rapid Prototyping Journal.* 19, 199-207.

Kato, K., et al. (2010). Immediate anti- tumor necrosis factor-α (etanercept) therapy enhances axonal regeneration after sciatic nerve crush. *Journal of Neuroscience Research* 88(2) 360-368.

Kehoe, S., X. F. Zhang and D. Boyd (2012). FDA approved guidance conduits and wraps for peripheral nerve injury: A review of materials and efficacy. *Injury* 43(5) 553-572.

Kelley, K. A. et al. (1994). Expression of Thy-1/lacZ fusion genes in the CNS of transgenic mice. *Molecular brain research*. 24(1), 261-274.

Khan, S.B. et al. (2005). Antibody blockade of TNF-α reduces inflammation and scarring in experimental crescentic glomerulonephritis. *Kidney international*, 67(5), 1812-1820.

Kim, D.H. et al. (1993). Comparison of macropore, semipermeable, and nonpermeable collagen conduits in nerve repair. *Journal of reconstructive microsurgery,* 9(6) 415−420.

Kim, Y.-T., et al. (2008). The role of aligned polymer fiber- based constructs in the bridging of long peripheral nerve gaps. *Biomaterials* 29(21) 3117-3127.

Kizilay, Z., et al. (2016). Effect of Etanercept on the Formation of Epidural Fibrosis in an Experimental Model. *Turkish neurosurgery*.

Kobayashi, M. and R. M. Costanzo (2009). Olfactory Nerve Recovery Following Mild and Severe Injury and the Efficacy of Dexamethasone Treatment. *Chemical Senses* 34(7) 573-580.

Kobayashi, M., et al. (2013). Blockade of interleukin- 6 receptor suppresses inflammatory reaction and facilitates functional recovery following olfactory system injury. *Neuroscience Research* 76(3) 125-132.

Kohta, M., E. Kohmura and T. Yamashita (2009). Inhibition of TGF-β1 promotes functional recovery after spinal cord injury. *Neuroscience Research* 65(4) 393-401.

Koopman**s,** G. C. et al. (2005). The assessment of locomotor function in spinal cord injured rats: the importance of objective analysis of coordination. *Journal of neurotrauma*. 22(2) 214-225.

Kottis, V., et al. (2002). Oligodendrocyte- myelin glycoprotein (OMgp) is an inhibitor of neurite outgrowth. *Journal of Neurochemistry* 82(6) 1566-1569.

Kouyoumdjian, J. A. (2006). Peripheral nerve injuries: A retrospective survey of 456 cases. *Muscle & Nerve* 34(6) 785-788.

Krekoski, C. A., et al. (2001). Axonal regeneration into acellular nerve grafts is enhanced by degradation of chondroitin sulfate proteoglycan. *The Journal of neuroscience: the official journal of the Society for Neuroscience* 21(16) 6206.

Kuffler, D.P. (2009). Enhancement of nerve regeneration and recovery by immunosuppressive agents. *International review of neurobiology*, *87*, 347-362.

LaBanc, J.P. (1992). Classification of nerve injuries. *Oral and Maxillofacial Surgery Clinics of North America.*, 4, 285-296.

Lambertsen, K. L., et al. (2009). Microglia protect neurons against ischemia by synthesis of tumor necrosis factor. *The Journal of neuroscience: the official journal of the Society for Neuroscience* 29(5) 1319.

Landis, S. C. (1983). Neuronal growth cones. *Annual review of physiology* 45 567.

Lane, M. J., Bora, W. F. and Pleasure, W. D. (1978). Neuroma scar formation in rats following peripheral nerve transection. *The Journal of Bone & Joint Surgery* 60(2) 197-203.

Lee, J. Y., et al. (2009). Polypyrrole- coated electrospun PLGA nanofibers for neural tissue applications. *Biomaterials* 30(26) 4325-4335.

Legnani, F.G. et al. (2006). Lactacystin exhibits potent anti-tumor activity in an animal model of malignant glioma when administered via controlled-release polymers. *Journal of neuro-oncology*. 77(3), 225-232.

Li, H., Terenghi, G. & Hall, S.M. (1997). Effects of delayed reinnervation on the expression of c-erbB receptors by chronically denervated rat Schwann cells in vivo. *Glia*, 20, 333-347.

Li, J. and R. Shi (2007). Fabrication of patterned multi- walled poly- l-lactic acid conduits for nerve regeneration. *Journal of Neuroscience Methods* 165(2) 257-264.

Li, R., et al. (2014). Peripheral Nerve Injuries Treatment: a Systematic Review. *Cell Biochemistry and Biophysics* 68(3) 449-454.

Liebl, D. J. et al. (1997). Absence of sensory neurons before target innervation in brain-derived neurotrophic factor-, neurotrophin 3-, and TrkC-deficient embryonic mice. *Journal of Neuroscience,* 17, 9113-9121.

Liu,F. and Yuan,H. (2014). Role of Glia in neuropathic pain. *Frontiers in Bioscience*, 19, pp.798-807.

Liu, I. H., et al. (2010). Matrix Metalloproteinase Inhibition Enhances the Rate of Nerve Regeneration In Vivo by Promoting Dedifferentiation and Mitosis of Supporting Schwann Cells. *Journal of Neuropathology and Experimental Neurology* 69(4) 386-395.

Liu, W., Y. Tang and J. Feng (2011). Cross talk between activation of microglia and astrocytes in pathological conditions in the central nervous system. *Life Sciences* 89(5) 141-146.

Luis, A. L., et al. (2007). PLGA 90/ 10 and caprolactone biodegradable nerve guides for the reconstruction of the rat sciatic nerve. *Microsurgery* 27(2) 125-137.

Logan, A.et al. (1994). Effects of transforming growth factor beta 1 on scar production in the injured central nervous system of the rat. *European Journal of Neuroscience*. 6(3) 355-363.

Lohmeyer, J.A. et al. (2009). The clinical use of artificial nerve conduits for digital nerve repair: a prospective cohort study and literature review. *Journal of Reconstructive Microsurgery*, 25(01) 55-61.

Ludwin, S.K. (1988). Remyelination in the central nervous system and the peripheral nervous system. *Advances in neurology*, 47, 215-254

Lundborg, G. R. and H.-A. Hansson (1979). Regeneration of peripheral nerve through a preformed tissue space. Preliminary observations on the reorganization of regenerating nerve fibres and perineurium. *Brain Research* 178(2) 573-576.

Lundborg, G., et al. (1982). Nerve regeneration across an extended gap: A neurobiological view of nerve repair and the possible involvement of neuronotrophic factors. *Journal of Hand Surgery* 7(6) 580-587.

Lundborg, G. and Sweden, M. (2000). A 25- year perspective of peripheral nerve surgery: Evolving neuroscientific concepts and clinical significance. *Journal of Hand Surgery* 25(3) 391-414.

Lundborg, G. et al. (2004). Tubular repair of the median or ulnar nerve in the human forearm: a 5-year follow-up. *Journal of hand surgery.* 29(2) 100-107.

Lunn, E. R. et al. (1989). Absence of Wallerian degeneration does not hinder regeneration in peripheral nerve. *European Journal of Neuroscience*, *1*(1) 27-33.

Mackinnon, S.E. (1988). Surgery of the peripheral nerve. *Carpal tunnel syndrome*. 146-169.

Martini, R., M. Schachner and T. M. Brushart (1994). The L2/ HNK- 1 carbohydrate is preferentially expressed by previously motor axon- associated Schwann cells in reinnervated peripheral nerves. *The Journal of neuroscience: the official journal of the Society for Neuroscience* 14(11 Pt 2) 7180.

Martins, R. S. et al. (2005). Overall assessment of regeneration in peripheral nerve lesion repair using fibrin glue, suture, or a combination of the 2 techniques in a rat model. Which is the ideal choice? *Surgical neurology*. 64, S10-S16.

Mathur, A., Merrell, J. C., Russell, R. C. and Zook, E. G., (1983). A scanning electron microscopy evaluation of peripheral nerve regeneration. *Scanning electron microscopy*, (Pt 2), 975-981.

Matsumoto, K., et al. (2000). Peripheral nerve regeneration across an 80- mm gap bridged by a polyglycolic acid (PGA)– collagen tube filled with laminin- coated collagen fibers: a histological and electrophysiological evaluation of regenerated nerves. *Brain Research* 868(2) 315-328.

Matsuyama, T., M. Mackay and R. Midha (2000). Peripheral nerve repair and grafting techniques: a review. *Neurologia medico-chirurgica* 40(4) 187.

McCallion R. and Ferguson M. (1996). Fetal Wound Healing. In: The Molecular and Cellular Biology of Wound Repair (Clarke, R. A. F., ed) New York: Plenum Press.

McKerracher, L., et al. (1994). Identification of myelin- associated glycoprotein as a major myelin-derived inhibitor of neurite growth. *Neuron* 13(4) 805-811.

Mease, P. J., et al. (2000). Etanercept in the treatment of psoriatic arthritis and psoriasis: a randomised trial. *The Lancet* 356(9227) 385-390.

Meek, M.F. et al. (2003). Gramsbergen A. Functional nerve recovery after bridging a 15 mm gap in rat sciatic nerve with a biodegradable nerve guide. *Scandinavian Journal of Plastic and Reconstructive Surgery and Hand Surgery,* 37(5) 258-265.

Meek, M. F. and J. H. Coert (2008). US Food and Drug Administration / Conformit Europe- approved absorbable nerve conduits for clinical repair of peripheral and cranial nerves. *Annals of plastic surgery* 60(4) 466-472.

Meek, M. F. and W. F. A. Den Dunnen (2009). Porosity of the wall of a Neurolac® nerve conduit hampers nerve regeneration. *Microsurgery* 29(6) 473-478.

Meek, M. F. and K. Jansen (2009). Two years after in vivo implantation of poly(DL -lactide-ε-caprolactone) nerve guides: Has the material finally resorbed? *Journal of Biomedical Materials Research Part A* 89(3) 734-738.

Meller, K. (1987). Early structural changes in the axoplasmic cytoskeleton after axotomy studied by cryofixation. *Cell and Tissue Research* 250(3) 663-672.

Mello, R. and A. H. Dickenson (2008). Spinal cord mechanisms of pain. *British Journal of Anaesthesia* 101(1) 8-16.

Menovsky, T. and J. F. Beek (2001). Laser, fibrin glue, or suture repair of peripheral nerves: a comparative functional, histological, and morphometric study in the rat sciatic nerve. *Journal of neurosurgery* 95(4) 694.

Mika, J., et al. (2009). Differential activation of spinal microglial and astroglial cells in a mouse model of peripheral neuropathic pain. *European Journal of Pharmacology* 623(1) 65-72.

Mika, J., et al. (2013). Importance of glial activation in neuropathic pain. *European Journal of Pharmacology* 716(1-3) 106-119.

Molander, c., Xu, Q. and Grant, G. (1984). The Cytoarchitectonic Organization of the Spinal Cord in the Rat. I. The Lower Thoracic and Lurnbosacral Cord. *Journal of Comparative Neurology*, 230(1) 133-141.

Monkhouse, A. and Ali, T. (2013). InnovAiT : Education and inspiration for general practice Neuropathic pain.

Moore, A. M., et al. (2009). Limitations of Conduits in Peripheral Nerve Repairs. *HAND* 4(2) 180-186.

Moreland, L. W. et al. (1997). Treatment of Rheumatoid Arthritis with a Recombinant Human Tumor Necrosis Factor Receptor (p75)– Fc Fusion Protein. *The New England Journal of Medicine* 337(3) 141-147.

Moreland, L. W. et al. (1998). Phase III trial of DMARD failing rheumatoid arthritis patients with TNF receptor p75 Fc fusion protein (TNFR:Fc, ENBREL). *Journal of Investigative Medicine.* 46(3) 228-228.

Morris, R. (1985). Thy-1 in Developing Nervous Tissue (Part 1 of 2). *Developmental neuroscience*, *7*(3), 133-146.

Nagata, M. et al. (1999). Synthesis, characterization, and enzymatic degradation of network aliphatic copolyesters. *Journal of Polymer Science Part A: Polymer Chemistry*. 37(13), 2005-2011.

Navissano, M. 2005. Neurotubeo1 for facial nerve repair. *Microsurgery*, 25, 268-271.

Neumann, M., et al. (2009). Assessing gait impairment following experimental traumatic brain injury in mice. *Journal of Neuroscience Methods* 176(1) 34-44.

Ngeow, W. (2010). Scar less: a review of methods of scar reduction at sites of peripheral nerve repair. *Oral Surgery, Oral Medicine, Oral Pathology, Oral Radiology, and Endodontology.* 357-366.

Ngeow, W. C., et al. (2011a). A comparison between the effects of three potential scar- reducing agents applied at a site of sciatic nerve repair. *Neuroscience* 181 271-277.

Ngeow, W. C., et al. (2011b). The effect of Mannose- 6- Phosphate on recovery after sciatic nerve repair. *Brain Research* 1394 40-48.

Nickel, F.T. *et al*., 2012. Mechanisms of neuropathic pain. *European Neuropsychopharmacology*, 22(2), 81-91.

Nie, X., et al. (2014). Axonal Regeneration and Remyelination Evaluation of Chitosan/ Gelatin-Based Nerve Guide Combined with Transforming Growth Factor-β1 and Schwann Cells. *Cell Biochemistry and Biophysics* 68(1) 163-172.

Nijst, C. L. et al. (2007). Synthesis and characterization of photocurable elastomers from poly (glycerol-co-sebacate). *Biomacromolecules*. 8(10), 3067-3073.

Noble, J. (1998). Analysis of upper and lower extremity peripheral nerve injuries in a population of patients with multiple injuries. *Journal of Trauma and Acute Care Surgery*. *45*(1), 116-122.

Norimoto, M., et al. (2008). Direct application of the TNF- alpha inhibitor, etanercept, does not affect CGRP expression and phenotypic change of DRG neurons following application of nucleus pulposus onto injured sciatic nerves in rats. *Spine* 33(22) 2403.

Novakovic, S., et al. (1998). Distribution of the Tetrodotoxin- Resistant Sodium Channel PN3 in Rat Sensory Neurons in Normal and Neuropathic Conditions. *Journal of Neuroscience* 18(6) 2174-2187.

Oh, S.H. et al. (2018). Enhanced peripheral nerve regeneration through asymmetrically porous nerve guide conduit with nerve growth factor gradient. *Journal of Biomedical Materials Research Part A*, 106(1) 52-64.

Ogawa, A. (1998). Effect of tazarotene, an acetylenic retinoid, on human dermal fibroblast. *Japanese Journal of Pharmacology*. 76, 317-319.

Ornelas, L, et al. (2006). Fibrin glue: an alternative technique for nerve coaptation--Part I. Wave amplitude, conduction velocity, and plantar-length factors. *Journal of Reconstructive Microsurgery*, 22(2) 19-122.

Osbourne, A. (2007). Peripheral Nerve Injury and Repair Reviews : Surgery. *Jundishapur Scientific Medical* Journal*.* 8, 29-33Pabari, M. A., et al. (2014). Nerve Conduits for Peripheral Nerve Surgery. *Plastic and Reconstructive Surgery* 133(6) 1420-1430.

Pabari, A. et al. (2014). Nerve conduits for peripheral nerve surgery. *Plastic and reconstructive surgery*. 133(6), 1420-1430.

Pagnussat, A., et al. (2012). Effect of skilled and unskilled training on nerve regeneration and functional recovery. *Brazilian Journal of Medical and Biological Research* 45(8) 753-762.

Pan, H.-L., et al. (2008). Modulation of pain transmission by G- protein- coupled receptors. *Pharmacology and Therapeutics* 117(1) 141-161.

Pasparakis, M. et al. (1996). Immune and inflammatory responses in TNF alpha-deficient mice: a critical requirement for TNF alpha in the formation of primary B cell follicles, follicular dendritic cell networks and germinal centers, and in the maturation of the humoral immune response. *Journal of Experimental Medicine*. 184(4), 1397-1411.

Patel, R. and Dickenson, A.H., 2016. Mechanisms of the gabapentinoids and α2δ-1 calcium channel subunit in neuropathic pain. *Pharmacology research & perspectives*, 4(2).

Pateman, C. J., et al. (2015). Nerve guides manufactured from photocurable polymers to aid peripheral nerve repair. *Biomaterials* 49 77-89.

Perry, G. W., Kryanek, S. R. and Wilson, D. L. (1981). Protein synthesis and fast axonal transport during regeneration of dorsal roots. *Journal of neurochemistry*. 37(5) 1203-1217.

Pradipta, G., M. D. Nancy and K. Stuart (2003). Mannose 6- phosphate receptors: new twists in the tale. *Nature Reviews Molecular Cell Biology* 4(3) 202.

Pritchard, C. D. et al. (2010). The use of surface modified poly (glycerol-co-sebacic acid) in retinal transplantation. *Biomaterials*. 31(8), 2153-2162.

Qui, S. H., S. J. Dai and H. X. Wu (1984). The segmental and regional projections of the sciatic, tibial and common peroneal nerves to the substantia gelatinosa of the spinal cord in rats--an experimental study by means of an acid phosphatase (ACP) method. *Okajimas folia anatomica Japonica* 61(4) 245.

Rabinder, P., et al. (2000). Neurobiology: Inhibitor of neurite outgrowth in humans. *Nature* 403(6768) 383.

Radosevich, M., Goubran, H.A. and Burnouf, T. (1997). Fibrin sealant: scientific rationale, production methods, properties, and current clinical use. *Vox sanguinis*, 72, 133-143.

Rai, R. et al. (2012). Synthesis, properties and biomedical applications of poly (glycerol sebacate) (PGS): a review. *Progress in polymer science*. 37(8), 1051-1078.

Rath, S. and C. J. Green (1991). Selectivity of distal reinnervation of regenerating mixed motor and sensory nerve fibres across muscle grafts in rats. *British Journal of Plastic Surgery* 44(3) 215-218.

Ray, W. Z. and S. E. Mackinnon (2010). Management of nerve gaps: Autografts, allografts, nerve transfers, and end-to- side neurorrhaphy. *Experimental Neurology* 223(1) 77-85.

Reid, A. J., et al. (2013). Long term peripheral nerve regeneration using a novel PCL nerve conduit. *Neuroscience Letters* 544 125-130.

Reynolds, M. L. and Woolf, C. J. (1993). Reciprocal Schwann cellaxon interaction. *Current Opinion in Neurobiology,* 3(5) 683-693.

Rhodes, K. E. and J. W. Fawcett (2004). Chondroitin sulphate proteoglycans: preventing plasticity or protecting the CNS? Oxford, UK. 33-48.

Richardson, P. M., McGuinness, U. M. and Aguayo, A. J. (1980). Axons from CNS neurones regenerate into PNS grafts. *Nature*, *284*(5753) 264-265.

Rigaud, I. M., et al. (2008). Species and strain differences in rodent sciatic nerve anatomy: Implications for studies of neuropathic pain. *Pain* 136(12) 188-201.

Roberts A. B. and Sporn M. B. (1996) Transforming Growth Factor-β. New York: Plenum Press.

Robinson, L. R. (2000). Traumatic injury to peripheral nerves. *Muscle & Nerve* 23(6) 863-873.

Robinson, L. R. (2004). Traumatic injury to peripheral nerves. *Supplements to Clinical neurophysiology*, *57*, 173-186.

Rodríguez, F., Valero-Cabré, A. and Navarro, X. (2004). Regeneration and functional recovery following peripheral nerve injury. *Drug Discovery Today: Disease Models*. 1(2) 177-185.

Roganovic, Z. and S. Petkovic (2004). Missile severances of the radial nerve. Results of 131 repairs. *The European Journal of Neurosurgery* 146(11) 1185-1192.

Romero-Sandoval, A., et al. (2008). A comparison of spinal Iba1 and GFAP expression in rodent models of acute and chronic pain. *Brain Research* 1219 116-126.

Rosson, G. D., E. H. Williams and A. L. Dellon (2009). Motor nerve regeneration across a conduit. *Microsurgery* 29(2) 107-114.

Rudge, J. S. and J. Silver (1990). Inhibition of neurite outgrowth on astroglial scars in vitro. *The Journal of neuroscience : the official journal of the Society for Neuroscience* 10(11) 3594.

Rufer, M., Flanders, K. and Unsicker, K. (1994). Presence and regulation of transforming growth factor beta mRNA and protein in the normal and lesioned rat sciatic nerve. *Journal of neuroscience research*, *39*(4) 412-423.

Rutishauser, U. (1993). Adhesion molecules of the nervous system. *Current Opinion in Neurobiology* 3(5) 709-715.

Sabatier, M. J., et al. (2008). Treadmill training promotes axon regeneration in injured peripheral nerves. *Experimental Neurology* 211(2) 489-493.

Sahni, A. and C. W. Francis (2000). Vascular endothelial growth factor binds to fibrinogen and fibrin and stimulates endothelial cell proliferation. *Blood* 96(12) 3772.

Salzer, J. L., et al. (1980). Studies of Schwann cell proliferation. II. Characterization of the stimulation and specificity of the response to a neurite membrane fraction. *The Journal of Cell Biology* 84(3) 753-766.

Saper, C. B. and P. E. Sawchenko (2003). Magic peptides, magic antibodies: Guidelines for appropriate controls for immunohistochemistry. *Journal of Comparative Neurology* 465(2) 161-163.

Sarah, B. K., et al. (2005). Antibody blockade of TNF-α reduces inflammation and scarring in experimental crescentic glomerulonephritis. *Kidney International* 67(5) 1812.

Sasaki, R., et al. (2008). Neurosphere generation from dental pulp of adult rat incisor. *European Journal of Neuroscience* 27(3) 538-548.

Sasaki, R. et al. (2011). PLGA artificial nerve conduits with dental pulp cells promote facial nerve regeneration. *Journal of tissue engineering and regenerative medicine*, *5*(10) 823-830.

Scheidt, P. and R. Friede (1987). Myelin phagocytosis in Wallerian degeneration. *Acta Neuropathologica* 75(1) 77-84.

Scherer, S., Kamholz, J. and Jakowlew, S. (1993). Axons modulate the expression of transforming growth factor-betas in Schwann cells. *Glia*. 8(4) 265-276.

Schmalfeldt, M., et al. (2000). Brain derived versican V2 is a potent inhibitor of axonal growth. *Journal of Cell Science* 113(5) 807-816.

Schmauss, D. et al. (2014). Is nerve regeneration after reconstruction with collagen nerve conduits terminated after 12 months? The long-term follow-up of two prospective clinical studies. *Journal of reconstructive microsurgery*, 30(08), 561-568.

Schmidt, C. E. and J. B. Leach (2003). Neural tissue engineering: strategies for repair and regeneration. *Annual review of biomedical engineering* 5 293.

Schmidt, C. E., Shastri, V. R., Vacanti, J. P. and Langer, R. (1997). Stimulation of neurite outgrowth using an electrically conducting polymer. *Proceedings of the National Academy of Sciences*. 94(17) 8948-8953.

Schneider-Schaulies, J., et al. (1991). Down- regulation of myelin- associated glycoprotein on Schwann cells by interferon-γ and tumor necrosis factor-α affects neurite outgrowth. *Neuron* 7(6) 995-1005.

Seddon, H. J. (1943). Three types of nerve injury. *Brain* 66(4) 237-288.

Seijffers, R., C. D. Mills and C. J. Woolf (2007). ATF3 increases the intrinsic growth state of DRG neurons to enhance peripheral nerve regeneration. *The Journal of neuroscience: the official journal of the Society for Neuroscience* 27(30) 7911.

Selmaj, K., et al. (1990). Proliferation of astrocytes invitro in response to cytokines - a primary role for tumor necrosis factor. *Journal of Immunology.* 144(1) 129-135.

Shah, M., D. M. Foreman and M. Ferguson (1994). Neutralizing antibody to tgf- beta (1,2) reduces cutaneous scarring in adult rodents. *Journal of Cell Science.* 107 1137-1157.

Shah, M., D. M. Foreman and M. Ferguson (1995). Neutralization of tgf- beta(1) and tgf- beta(2) or exogenous addition of tgf- beta(3) to cutaneous rat wounds reduces scarring. *Journal of Cell Science.* 108 985-1002.

Shah, M., D. M. Foreman and M. W. J. Ferguson (1992). Control of scarring in adult wounds by neutralising antibody to transforming growth factor β. *The Lancet* 339(8787) 213-214.

Shanti, R. M. and V. B. Ziccardi (2011). Use of Decellularized Nerve Allograft for Inferior Alveolar Nerve Reconstruction: A Case Report. *Journal of Oral and Maxillofacial Surgery* 69(2) 550-553.

Shin, H. R., et al. (2009). Treatment of a Segmental Nerve Defect in the Rat with Use of Bioabsorbable Synthetic Nerve Conduits: A Comparison of Commercially Available Conduits. *The Journal of Bone & Joint Surgery* 91(9) 2194-2204.

Shuhua, Q., Shiji, D. and Haixia, W. (1984). The Segmental and Regional Projections of the Sciatic. Tibial and Common Peroneal Nerves to the Substantia Gelatinosa of the Spinal Cord in Rats - An Experimental Study by Means of an Acid Phosphatase (ACP) Method. *Okajimas Folia Anatomica Japonica.* 61(4), 245 252.

Siemionow, M. and Brzezicki, G. (2009). Current techniques and concepts in peripheral nerve repair. *Essays on Peripheral Nerve Repair and Regeneration,* 87, 141-172.

Sivak, W.N. et al. (2017). Delivery of chondroitinase ABC and glial cell line-derived neurotrophic factor from silk fibroin conduits enhances peripheral nerve regeneration. *Journal of tissue engineering and regenerative medicine*, 11(3), 733-742.

Šmahel, J., Meyer, V. and Bachem, U., (1987). Glueing of peripheral nerves with fibrin: experimental studies. *Journal of reconstructive microsurgery. 3*(03), 211-218.

Smith, R.M. et al. (2004). Role of small intestine submucosa (SIS) as a nerve conduit: preliminary report. *Journal of Investigative Surgery*.,17(6) 339–444.

Son, Y.-J. and W. J. Thompson (1995). Schwann cell processes guide regeneration of peripheral axons. *Neuron* 14(1) 125-132.

Spicer, P. P. and A. G. Mikos (2010). Fibrin glue as a drug delivery system. *Journal of Controlled Release* 148(1) 49-55.

Stoll, G., et al. (1989). Wallerian degeneration in the peripheral nervous system: participation of both Schwann cells and macrophages in myelin degradation. *Journal of Neurocytology* 18(5) 671-683.

Stoll, G. and H. W. Müller (1999). Nerve Injury, Axonal Degeneration and Neural Regeneration: Basic Insights. *Brain Pathology* 9(2) 313-325.

Strittmatter, S. (2010). Spinal Cord Regeneration: *Ready, Set, Nogo. Eukaryon*, 6, 55-60.

Stuesse, S. L., et al. (2001). Neuropathic pain in aged rats: behavioral responses and astrocytic activation. *Experimental Brain Research* 137(2) 219-227.

Sun, M., et al. (2010). In vitro and in vivo testing of novel ultrathin PCL and PCL/ PLA blend films as peripheral nerve conduit. *Journal of Biomedical Materials Research Part A* 93(4) 1470-1481.

Sundback, C. A. et al. (2005). Biocompatibility analysis of poly(glycerol sebacate) as a nerve guide material. *Biomaterials.* 26, 5454-5464.

Sundback, C. A. et al. (2012). Behavior of poly(glycerol sebacate) plugs in chronic tympanic membrane perforations. *Journal of Biomedical Materials Research Part B.* 100, 19431954.

Sunderland, S. (1973). The internal anatomy of nerve trunks in relation to the neural lesions of leprosy: Observations on pathology, symptomatology and treatment. *Brain* 96(4) 865-888.

Sunderland, S., (1990). The Anatomy and Physiology. *Muscle and Nerve,* 13(9) 771-784.

Suri, A., V. S. Mehta and C. Sarkar (2002). Microneural anastomosis with fibrin glue: An experimental study. *Neurology India* 50(1) 23-26.

Taha, M. O., et al. (2004). Effect of retinoic acid on tibial nerve regeneration after anastomosis in rats: histological and functional analyses. *Transplantation Proceedings* 36(2) 404-408.

Tam, S. and T. Gordon (2003). Mechanisms controlling axonal sprouting at the neuromuscular junction. *Journal of Neurocytology* 32(5) 961-974.

Tam, S. L. and Gordon, T. (2008). Axonal sprouting in health and disease. In *Encyclopedia of Neuroscience,* 322-328.

Tanga, F. Y., V. Raghavendra and J. A. Deleo (2004). Quantitative real- time RT- PCR assessment of spinal microglial and astrocytic activation markers in a rat model of neuropathic pain. *Neurochemistry International* 45(2) 397-407.

Taras, J. S., V. Nanavati and P. Steelman (2005). Nerve Conduits. *Journal of Hand Therapy* 18(2) 191-197.

Taskinen, H. S., et al. (2000). Peripheral nerve injury induces endoneurial expression of IFN-γ, IL- 10 and TNF-α mRNA. *Journal of Neuroimmunology* 102(1) 17-25.

Terenghi, G. (1999). Peripheral nerve regeneration and neurotrophic factors. *Journal of anatomy* 194 (Pt 1) 1.

Terenghi, G. and S. Hall (1997). Effects of delayed re-innervation on the expression of c- erbB receptors by chronically denervated rat Schwann cells in vivo. *Glia* 20(4) 333-347.

Trang, T., S. Beggs and M. W. Salter (2012). ATP receptors gate microglia signaling in neuropathic pain. *Experimental Neurology* 234(2) 354-361.

Treede, D. R., et al. (2008). Neuropathic pain: Redefinition and a grading system for clinical and research purposes. *Neurology* 70(18) 1630-1635.

Tsuda, M. et al. (2003). P2X4 receptors induced in spinal microglia gate tactile allodynia after nerve injury. *Nature*, 424(6950) 778-783.

Tsuda, M. et al. (2017). Neuronal and microglial mechanisms for neuropathic pain in the spinal dorsal horn and anterior cingulate cortex. *Journal of neurochemistry*. 141(4):486-498

Tyner, T. R., et al. (2007). Effects of collagen nerve guide on neuroma formation and neuropathic pain in a rat model. *The American Journal of Surgery* 193(1) e1-e6.

Unezaki, S., et al. (2009). Effects of neurotrophic factors on nerve regeneration monitored by in vivo imaging in thy1- YFP transgenic mice. *Journal of Neuroscience Methods* 178(2) 308-315.

Vega-Avelaira, D., A. Moss and M. Fitzgerald (2007). Age- related changes in the spinal cord microglial and astrocytic response profile to nerve injury. *Brain, behavior, and immunity* 21(5) 617.

Vidal, M. et al. (1990). Tissue-specific control elements of the Thy-1 gene. *The EMBO journal*, 9(3), 833-840.

Vrinten, H. D. and F. T. F. Hamers (2003). 'CatWalk' automated quantitative gait analysis as a novel method to assess mechanical allodynia in the rat; a comparison with von Frey testing. *Pain* 102(12) 203-209.

Wade, N. J. (2004). Visual Neuroscience before the Neuron. *Perception* 33(7) 869-889.

Waitayawinyu, T., et al. (2007). A Comparison of Polyglycolic Acid Versus Type 1 Collagen Bioabsorbable Nerve Conduits in a Rat Model: An Alternative to Autografting. *Journal of Hand Surgery* 32(10) 1521-1529.

Walker, J. L., et al. (1994). Gait- stance duration as a measure of injury and recovery in the rat sciatic nerve model. *Journal of Neuroscience Methods* 52(1) 47-52.

Wall, D. P., et al. (1979). Autotomy following peripheral nerve lesions: experimental anesthesia dolorosa. *Pain* 7(2) 103-113.

Waller, A. (1850). Experiments on the Section of the Glossopharyngeal and Hypoglossal Nerves of the Frog, and Observations of the Alterations Produced Thereby in the Structure of Their Primitive Fibres. *Philosophical Transactions of the Royal Society of London* 140 423-429.

Wang, Y. et al. (2002). A tough biodegradable elastomer. *Nature biotechnology*. 20(6), 602-610.

Wang, J., et al. (2010). Biodegradable microfluidic scaffolds for tissue engineering from amino alcohol- based poly(ester amide) elastomers. *Organogenesis* 6(4) 212-216.

Wang, G.W. et al. (2017). Design and optimization of a biodegradable porous zein conduit using microtubes as a guide for rat sciatic nerve defect repair. *Biomaterials*, 131, 145-159.

Wangensteen, K. J. and L. K. Kalliainen (2010). Collagen Tube Conduits in Peripheral Nerve Repair: A Retrospective Analysis. *HAND* 5(3) 273-277.

Weber, R. A. and Dellon A. L. (2004) Nerve Lacerations: Repair of Acute Injuries. In: Hand Injury (Berger, R. A. and Weiss, A.-P. C., eds), pp 819-845 Philadelphia, USA: Lippincott Williams & Wilkinson.

Weinblatt, M. E., et al. (1999). A Trial of Etanercept, a Recombinant Tumor Necrosis Factor Receptor:Fc Fusion Protein, in Patients with Rheumatoid Arthritis Receiving Methotrexate. *The New England Journal of Medicine* 340(4) 253-259.

Whitlock, E. L. et al. (2009). Processed allografts and type I collagen conduits for repair of peripheral nerve gaps. *Muscle & nerve*. *39*(6), 787-799.

Whitby, D. J. and M. W. J. Ferguson (1991). The extracellular matrix of lip wounds in fetal, neonatal and adult mice. *Development* 112(2) 651-668.

Williams, K. R. and Blayney, A. W. (1987). Tissue response of several polymeric materials implanted in the rat middle ear. *Biomaterials*. 8(4), 254-258.

Williams, R. S., et al. (1992). Effect of transforming growth factor β on postoperative adhesion formation and intact peritoneum. *Journal of Surgical Research* 52(1) 65-70.

Witzel, C., Rohde, C. and Brushart, T. M. (2005). Pathway sampling by regenerating peripheral axons. *Journal of Comparative Neurology,* 485:183-190.

Wong, C., et al. (2003). Fibrin- based biomaterials to deliver human growth factors. *Thrombosis and haemostasis* 89(3) 573.

Wong, J.K. et al. (2014). Reduction of tendon adhesions following administration of Adaprev, a hypertonic solution of mannose-6-phosphate: mechanism of action studies. *PloS one*, 9(11): 112672.

Wood, M. D., et al. (2014). Rat- derived processed nerve allografts support more axon regeneration in rat than human- derived processed nerve xenografts. *Journal of Biomedical Materials Research Part A* 102(4) 1085-1091.

Woodruff, M., et al. (2007). Sustained release and osteogenic potential of heparan sulfate- doped fibrin glue scaffolds within a rat cranial model. *Journal of Molecular Histology* 38(5) 425-433.

Woolf, C. and M. Salter (2000). Neuronal plasticity: Increasing the gain in pain. *In* C. Woolf ed. 1765-1768.

Woolf, C. J. and R. J. Mannion (1999). Neuropathic pain: aetiology, symptoms, mechanisms, and management. *The Lancet* 353(9168) 1959-1964.

Xu, F., et al. (2016). Microglial polarization dynamics in dorsal spinal cord in the early stages following chronic sciatic nerve damage. *Neuroscience Letters* 617 6-13.

Xu, Q. G., et al. (2008). Facilitated sprouting in a peripheral nerve injury. *Neuroscience* 152(4) 877-887.

Yan, Y., et al. (2011). Evaluation of peripheral nerve regeneration via in vivo serial transcutaneous imaging using transgenic Thy1- YFP mice. *Experimental Neurology* 232(1) 7-14.

Yao, L. and A. Pandit (2010). Controlling dispersion of axonal regeneration using a multichannel collagen nerve conduit.

Yoshida, H., et al. (2000). Novel drug delivery system using autologous fibrin glue - Release properties of anti- cancer drugs. *Biological and Pharmaceutical Bulletin* 23(3) 371-374.

Zhang, J., et al. (2003). Induction of CB2 receptor expression in the rat spinal cord of neuropathic but not inflammatory chronic pain models. *European Journal of Neuroscience* 17(12) 2750-2754.

Zhang, J. and Y. Koninck (2006). Spatial and temporal relationship between monocyte chemoattractant protein- 1 expression and spinal glial activation following peripheral nerve injury. *Journal of Neurochemistry* 97(3) 772-783.

Zhang, J. et al., (2015). A cationic-independent mannose 6-phosphate receptor inhibitor (PXS64) ameliorates kidney fibrosis by inhibiting activation of transforming growth factor-β1. *Public Library of Science one*, *10*(2), 1-15.

Zochodne, D. W. (2008). *Neurobiology of Peripheral Nerve Regeneration,* Cambridge, Cambridge University Press.

Zhu, Y., et al. (2011). Engineering Bi- Layer Nanofibrous Conduits for Peripheral Nerve Regeneration. *Tissue Engineering Part C: Methods* 17(7) 75-715.

Zuniga, J. and Radwan, A. (2013). Classification of Nerve Injuries. *Trigeminal Nerve Injuries*, 17-25.